membranes

MDPI

Review

Electrodialysis Applications in Wastewater Treatment for Environmental Protection and Resources Recovery: A Systematic Review on Progress and Perspectives

Luigi Gurreri, Alessandro Tamburini *, Andrea Cipollina and Giorgio Micale

Dipartimento di Ingegneria, Università degli Studi di Palermo, viale delle Scienze Ed. 6, 90128 Palermo, Italy; luigi.gurreri@unipa.it (L.G.); andrea.cipollina@unipa.it (A.C.); giorgiod.maria.micale@unipa.it (G.M.)

* Correspondence: alessandro.tamburini@unipa.it; Tel.: +39-091-2386-3780

Received: 31 May 2020; Accepted: 4 July 2020; Published: 9 July 2020

Abstract: This paper presents a comprehensive review of studies on electrodialysis (ED) applications in wastewater treatment, outlining the current status and the future prospect. ED is a membrane process of separation under the action of an electric field, where ions are selectively transported across ion-exchange membranes. ED of both conventional or unconventional fashion has been tested to treat several waste or spent aqueous solutions, including effluents from various industrial processes, municipal wastewater or salt water treatment plants, and animal farms. Properties such as selectivity, high separation efficiency, and chemical-free treatment make ED methods adequate for desalination and other treatments with significant environmental benefits. ED technologies can be used in operations of concentration, dilution, desalination, regeneration, and valorisation to reclaim wastewater and recover water and/or other products, e.g., heavy metal ions, salts, acids/bases, nutrients, and organics, or electrical energy. Intense research activity has been directed towards developing enhanced or novel systems, showing that zero or minimal liquid discharge approaches can be techno-economically affordable and competitive. Despite few real plants having been installed, recent developments are opening new routes for the large-scale use of ED techniques in a plethora of treatment processes for wastewater.

Keywords: electro-membrane process; electrodialysis reversal; bipolar membrane electrodialysis; selectrodialysis; electrodialysis metathesis; electrodeionisation; reverse electrodialysis; monovalent selective membranes; water reuse; brine valorisation

1. Introduction

The growing water demand in urban, rural and industrial sites poses serious ecological and economic concerns in water management linked to resources depletion and wastes disposal. Several industrial processes use large water volumes, thus producing high quantities of wastewater or spent streams with contaminants and valuable components. In addition, municipal wastewater treatment plants effluents are not directly reusable.

Water recovery offers the possibility of sustainable development. On the other hand, it requires the design and implementation of advanced treatment methods, which represent a techno-economic challenge. In this framework, the zero liquid discharge (ZLD) concept aims at developing strategies to close the material loop, thus minimizing the liquid waste [1–3]. This approach is a specific accomplishment of circular economy [4,5], which proposes "business models based on reducing, alternatively reusing,

recycling and recovering materials in production/distribution and consumption processes", by replacing the old perspective of *end of life* [6].

Membrane processes are attracting a great deal of interest, and several studies have led to significant advances [7]. Among them, electro-membrane technologies separate ions by the selective transport through ion-exchange membranes (IEMs) under the influence of an electric field. A large variety of electro-membrane processes has been developed [8–14].

In particular, electrodialysis (ED) produces two streams with different concentrations flowing in alternate compartments separated alternatively by cation-exchange membranes (CEMs) and anion-exchange membranes (AEMs). ED may be cost-effective thanks to properties favourable to the attainment of large selectivity and product recovery, and to the avoided, or limited, need for chemicals [8,9,15–17]. At industrial scale, ED is mainly applied to desalinate brackish water for drinking water production. There have been installed also some ED plants to produce table salt from seawater desalination. However, many studies have focused on application of ED techniques in the (bio)chemistry, food processing, and pharmaceutical industries [8–11,13,17–21], encompassing wastewater treatment, recovery of chemicals or other valuable products, and removal of toxic components [8,9,13,17,20,22,23].

In regard to wastewater treatment via ED, the research exhibits an exponential growth in the last 20 years (Figure 1). More than 75% of the 879 scientific documents published since 1969 up until now fall in this period.

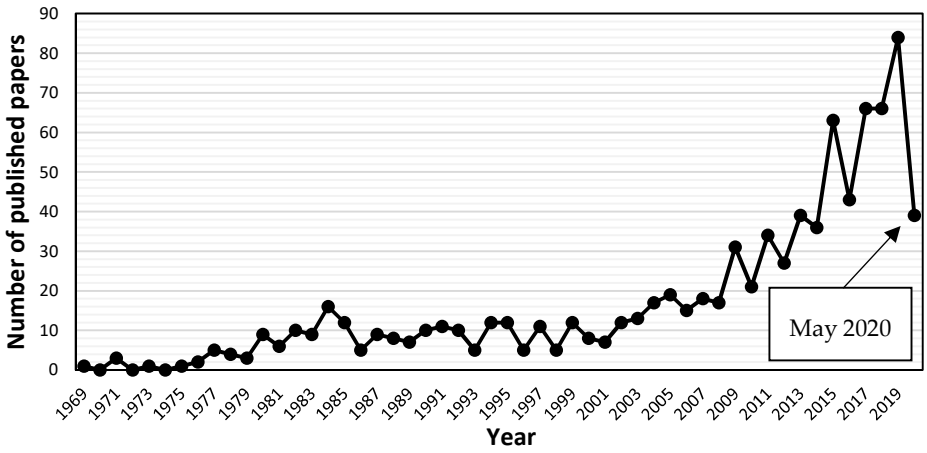

Figure 1. Scientific documents chronology reported on Scopus with "electrodialysis" and "wastewater" search words (article title, abstract or keywords). Source: www.scopus.com, accessed on 7 May 2020.

Many industrial effluents (e.g., from metal finishing, tanning, pulp and paper processing) have a complex composition with contaminants and/or valuable components, e.g., heavy metal ions, acids, organic matter, etc. Similarly, treated effluents from municipal or animal farming sources contain, for example, nutrients, as well as water. Finally, desalination plants' reject brines may provide water and/or salt. Thanks to its ability in separating charged particles, ED methods can effectively recover water and/or other products from these effluents, including electrical energy.

Despite the fact that ED has a long history over more than 120 years, and that intense research activity has been developed, especially in recent years, only a few review articles have been published so far. In 2010, Strathmann [15] described the principle of ED, its operating conditions, and its design features, focusing on water desalination and recent advancements (profiled membranes). ED-related processes were included, by highlighting advantages and limitations. In 2018, our research group published a review paper on ED updated with the most recent developments for water desalination [16]. The main topics

were IEMs progress and characterisation, hydrodynamics and transport phenomena, process models, other modelling tools, and ED-related technologies. Recently, Sajjad et al. [17] provided an overview on (waste)water treatment via ED, by discussing the main technological limitations.

The lack of an organic review on ED for wastewater treatment motivated the present work. For the first time, to the best of the authors' knowledge, this paper presents a comprehensive and systematic review of studies on ED applications in wastewater treatment for environmental protection and recovery of resources, outlining the current status and the future prospect. The large variety of uses of conventional ED and similar technologies is discussed by analysing experimental results, process performance, strengths and drawbacks, and techno-economic competitiveness. Recent advances and emerging applications are reviewed, along with examples among the few well-established implementations in real environments.

2. Research Method, Rationale and Structure of the Review

The investigation of the review topic was based on a literature search in the Scopus electronic database. The search words listed in Table 1 were used without limits of date and by excluding only conference papers among the document types. This search found a total number of studies amounting approximatively to 1000, by excluding duplicate results. For the selection process, the eligibility criteria were relevance/consistency for/with the review topic, full text availability and accessibility, number of citations (except for most recent results), and journal metrics. The selected papers were organised in a bibliography on *Mendeley desktop*. The screening by full-text analysis filtered about 400 relevant higher-quality scientific papers to be reviewed and discussed (excluding those used for the fundamentals, Section 3).

Table 1. Search words used in the literature exploration on Scopus.

Search Word		Search Word
Electrodialysis		Wastewater
Bipolar membrane electrodialysis		Effluent
Selective electrodialysis		Spent solution
Selectrodialysis		Recovery
Electrodialysis metathesis	AND	Reclamation
Electrodeionisation		Reuse
Continuous electrodeionisation		Valorisation
Reverse electrodialysis		Regeneration
		Zero liquid discharge

The selected articles were classified into three main categories according to the wastewater origin, and into sub-categories based on the treatment aim, as shown in Figure 2. A third level of sub-classification was used in some cases in order to distinguish among different waste effluents. Sections and sub-sections of the paper will reflect exactly this classification. Therefore, the paper is structured as follows. After a brief description of the process fundamentals (Section 3), Sections 4–6, which are the core of the review, correspond to the three main categories of the classification, and their sub-sections to the sub-categories. Where not specified, the data reported in the review will refer to lab-scale experiments. Otherwise, pilot plants and installations in real environments will be explicitly indicated throughout the paper. Finally, Section 7 provides discussion, conclusions and outlook, highlighting the main technical challenges, the current status of the process scale in the various applications, and the key points for future R&D.

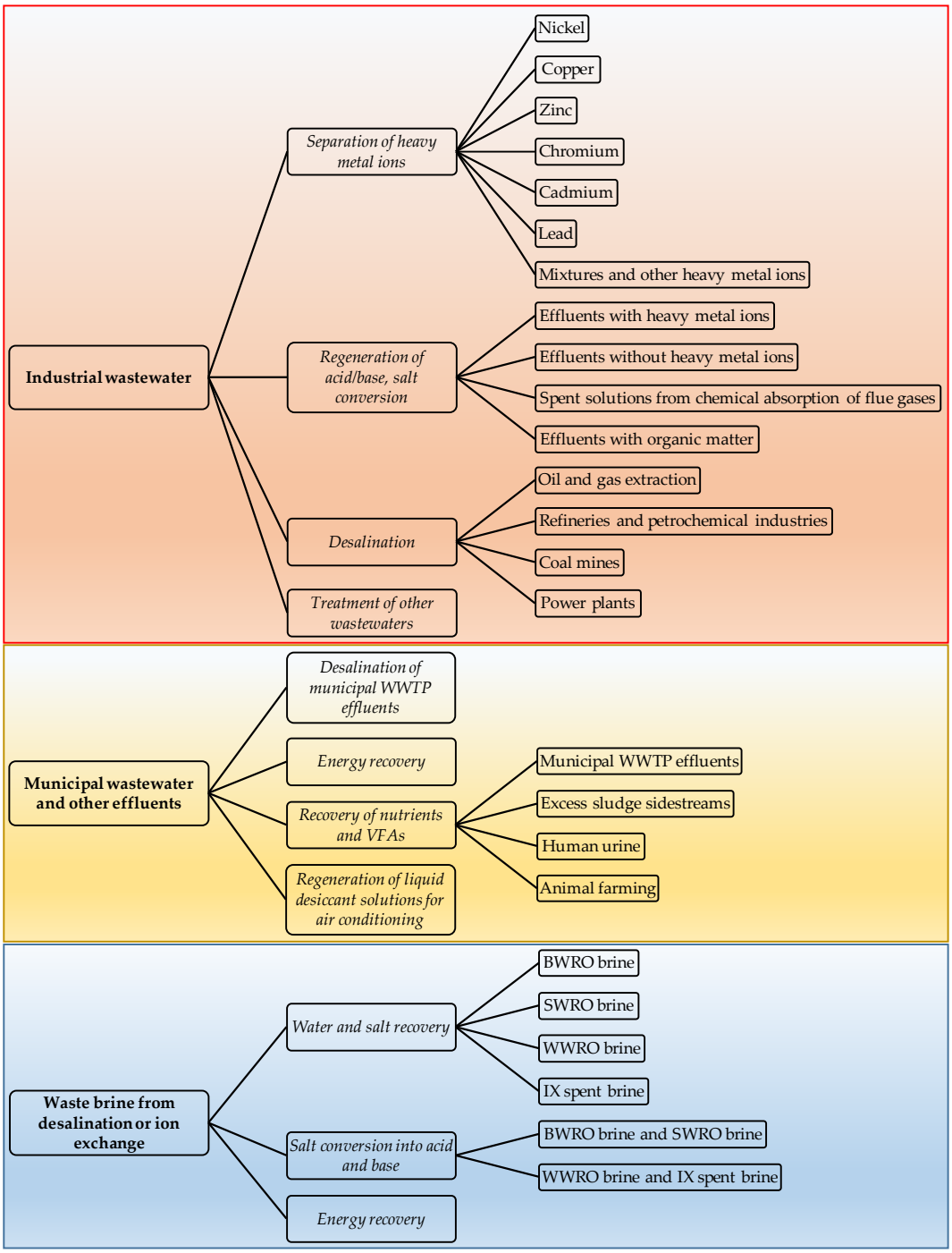

Figure 2. Classification of the selected papers, reflected in the review structure (Sections 4–6 and their sub-sections).

3. Electrodialysis Process Fundamentals

3.1. Working Principle and Design/Operating Features of ED Processes

Figure 3a depicts a scheme of conventional ED. A pile of alternating AEMs and CEMs is arranged with alternating diluate and concentrate channels. At the extreme sides, the ED stack is completed by electrode compartments. Here, the external power supply establishes an electric potential difference, which causes redox reactions. A direct electric current flows through the external circuit as electronic current, and through the stack as ionic current, with cations and anions migrating towards the cathode and the anode, respectively. The co-ion block by the IEMs leads to a selective transport with a resulting salt concentration reduction/increase in the diluate/concentrate channels, respectively. The repetitive unit in a conventional stack, namely the "cell pair", includes an AEM, a diluate, a CEM, and a concentrate. The two inlet feeds may differ each other.

The number of cell pairs in electrodialyzers ranges from few or some tens at bench- or pilot-scale up to hundreds in commercial stacks for real applications. The active area spans roughly from 0.01 to 1 m^2 for the single membrane.

The plate-and-frame configuration is by far the most used. Net spacers (with typical thickness of ~300 μm to ~2 mm [16]) equipped with gaskets are placed between the IEMs in order to create the feed compartments (Figure 3b). The two main designs of the spacer-filled channels are sheet flow and tortuous path [15,16]. In the former pattern, the fluid flows roughly straight along a rectangular channel (Figure 3b). In the latter pattern, the feed moves along a serpentine. U-shaped channels with halfway features are almost common in large units, similarly to tortuous path layouts, while sheet flow channels are more used for small stacks. Membranes with built-in profiles avoid the use of net spacers [15,16], but they have been used only for theoretical or experimental studies [24–28].

The typical range of fluid velocity is 1–10 cm/s. However, along tortuous path layouts, the velocity may be increased to ~50 cm/s to counteract the poorer mixing. In most cases, flow regimes are steady, but turbulence may occur at higher velocities [16].

Batch operations with solution recirculation are typical for lab-scale studies, while continuous processes are basically limited to industrial plants. The "feed and bleed" operation (partial continuous recirculation) is commonly practiced to control water recovery and outlet concentrations [8]. Multi-stage schemes can be devised with several configurations (e.g., multiple hydraulic and/or electrical steps) in order to attain the wanted product features.

IEMs suffer from fouling phenomena less than semi-permeable membranes (e.g., for reverse osmosis). However, depending on the solutions treated, IEMs may experience serious deterioration, resulting in a higher electrical resistance and even in a physical damage. Both suspended and dissolved solids (organic and inorganic) can cause membrane fouling. Organic anions and inorganic compounds can often imply fouling of AEMs and CEMs, respectively [29]. Fouling caused by sparingly soluble salt precipitates is called scaling. Electrodialysis reversal (EDR) is commonly practiced for fouling mitigation. It is applied by periodic switching (cycles of minutes/hours) of electrode polarity (with simultaneous switch of feed solutions). As a result, charged components are removed from the IEM surface by migration in the contrary direction. In addition, feed pre-treatment and stack cleaning-in-place methods (acidic and/or alkaline solutions) can prevent and remove fouling, respectively.

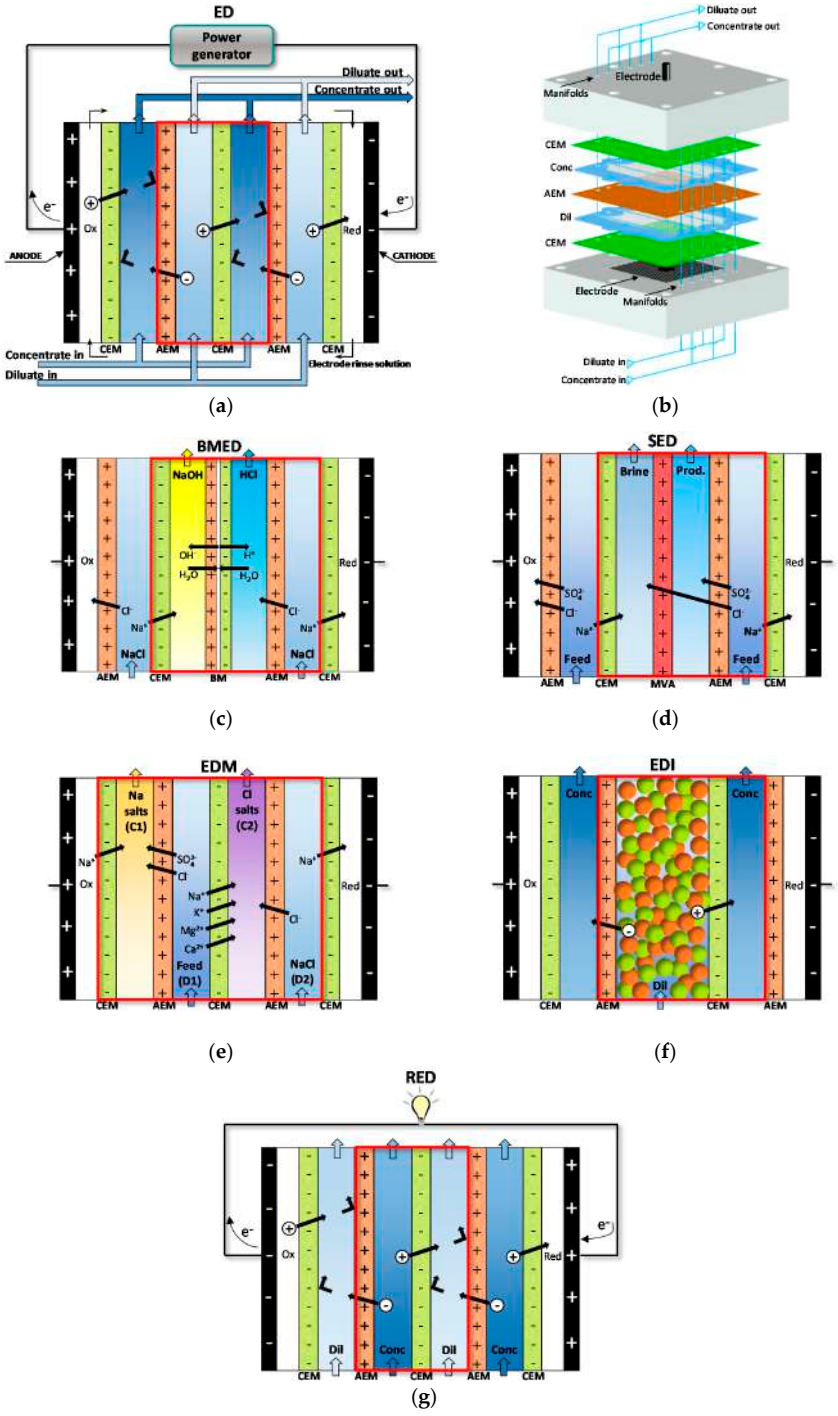

Figure 3. Schematics of ED techniques: (**a**) Conventional electrodialysis (ED); (**b**) Lab-scale ED stack with sheet-flow design (exploded view of one cell pair with an additional CEM); (**c**) Three-compartment bipolar membrane electrodialysis (BMED); (**d**) Selectrodialysis (SED) with MVA (the illustration refers to the fractionation of SO_4^{2-} from Cl^-); (**e**) Electrodialysis metathesis (EDM); (**f**) Electrodeionisation (EDI) with ion-exchange resins filling the diluate; (**g**) Reverse electrodialysis (RED). Red rectangles indicate the repeating units. Panels (**a**,**b**,**g**) are reproduced (adapted) with permission from [16], published by Elsevier, 2018.

Bipolar membrane electrodialysis (BMED) uses both monopolar membranes and bipolar membranes (BMs) to generate acid and base by water dissociation (Figure 3c). A BM consists of the overlapping of a cation-exchange layer (CEL) and an anion-exchange layer (AEL), whose inter-layer (thinner than 10 nm [8,30]) promotes water dissociation when a voltage (>0.83 V) is applied, thus releasing H^+ and OH^- [8,10,12,30] at a rate that is six (or more) orders of magnitude larger than in solution [8,12]. This is caused by the catalytic role of the functional groups and/or of the catalyst in the bipolar region, and to the strong electric field (second Wien effect) [31]. The mechanisms of ion transfer and water dissociation are still under study via theoretical approaches and numerical models [31]. Novel preparation techniques based on electrospinning methods can produce high-performing BMs [32,33].

Figure 3c depicts the three-compartment BMED arrangement, which converts salt into acid and base. The repeating cell consists of: AEM, acid compartment, BM, base compartment, CEM, and diluate salt compartment. Protons and hydroxyl ions, generated in the bipolar region by the electric field, cross the CEL and the AEL and migrate to the acid and base channel, respectively, while salt anions and cations (e.g., Cl^- and Na^+) in the salt channel cross the monopolar IEMs and migrate to the acid and base compartment, respectively. Nevertheless, other BMED arrangements have been developed with two-compartment repetitive units, with either BM-AEM or BM-CEM membranes for either acid or base production (and salt feed alkalisation or acidification). These configurations are used when it is possible or desired to obtain only one solution at high purity, with applications in regeneration processes [34–38]. Further BMED configurations include cell triplets with two monopolar IEMs of the same type. The outlet salt stream is sent to the acidic or alkaline channel to attain higher recovery rates [34,35].

Selective ED occurs within electrodialyzers containing monovalent selective membranes (MVMs), which may be anionic (MVAs) and/or cationic (MVCs) and segregate monovalent and multivalent ions. Specifically, the selectrodialysis (SED) process has a three-compartment configuration with an MVM and two conventional IEMs, and fractionates ions by using three different streams [39]. Figure 3d provides a sketch of SED fractionation of SO_4^{2-} from Cl^- contained in a feed solution. The results of the process are the mixture desalination, the product enrichment in divalent anions, and the brine concentration in monovalent ions.

ED stacks may be arranged to perform a metathesis of salts, known also as "double decomposition" (interchange of cations and anions between salts). With a couple of salts, one has:

$$MX + M'X' \rightarrow M'X + MX'. \quad (1)$$

Electrodialysis metathesis (EDM) [40,41] has a four-compartment repeating unit which includes two diluate and two concentrate channels, all being different from each other, divided by two AEMs and two CEMs (Figure 3e). The feed (D1) contains a salt or a salts mixture, while a substitution solution flows along the other diluate channel (D2). From the D1 solution, anions move to the C1 concentrate, and cations move to the C2 concentrate; while from the D2 substitution solution, anions are transferred to the C2 concentrate, and cations are transferred to the C1 concentrate. As a result, the metathesis of salts between feed and substitution solution occurs in the concentrate products. In the example of Figure 3e, Na^+ salts and Cl^- salts are generated inside compartments C1 and C2, respectively.

To boost the ED performance, ion-exchange resins (IXRs) can be inserted inside the channels. The hybridisation of ED and ion exchange (IX) is referred to as electrodeionisation (EDI) or continuous electrodeionisation (CEDI) [8,9,42,43] (Figure 3f). In EDI units, continuously regenerated IXRs beds within the diluate (sometimes also within the concentrate) cause a conductivity increment and a concentration polarisation reduction. Improved ion transport is obtained, thus making it possible to effectively treat very diluted solutions thanks to lower electrical resistances and higher limiting currents. The regeneration in situ of IXRs is carried out by H^+ and/or OH^- from water dissociation occurring at bipolar contacts of

IXRs particles or between IXRs and IEMs [42,43]. EDI is more suitable than its source technologies for producing industrial ultra-pure water [44] and for treating some kinds of wastewater, e.g., wastewater containing metal ions [42]. Moreover, fully regenerated IXRs can ionize and remove weakly ionized species (SiO_2, CO_2, boron, and NH_3) [9,43]. The complex transport mechanism has been argued for several years through various models [42]. It involves the following steps [8,42,43]: ion diffusion through the solution (controlling step), IX, migration across the IXR bed and the IEM, and regeneration of the IXR.

EDI units are arranged with several configurations [8,9,42] by changing the IXRs bed composition and structure (mixed, separate or layered) and the IEMs number, placement and type, also including the employment of BMs as locations for water dissociation. EDI modules may be assembled with several repeating units between the electrodes, similarly to ED stacks. However, other arrangements with few compartments (three or some more) in total, including the electrode ones, were developed. Among them, some units exploit electrode water electrolysis to deliver H^+ ad OH^- for the IXRs electro-regeneration [45–50], thus differing considerably from conventional ED. Limitations in EDI performance may derive from small current efficiencies in operations with high water dissociation [9], and from inhomogeneous flow distributions [42]. The former issue can be solved by identifying optimal values of the applied voltage, thus resulting in the co-existence of water dissociation and electroconvection in the overlimiting regime, which can enhance the process efficiency [51]. The latter issue can be addressed by adopting fixed resin wafers [52].

Reverse electrodialysis (RED) is the opposite process with respect to ED. RED produces electricity by converting the mixing free energy of two streams with different salt concentration (salinity gradient energy, or blue energy or osmotic energy), and is carried out with stacks equivalent to ED units [53–57] (Figure 3g). A high-salinity solution (concentrate, which is actually diluted along the channel) and a low-salinity solution (diluate, which is actually concentrated along the channel) flow through the two compartments of an RED cell pair. The most conventional solutions are seawater and river water, which would provide a maximum theoretical energy density of ~880 kJ/m^3 (equal amounts of both solutions). However, recent studies have assessed the use of waste effluents.

The working principle of RED relies on the electrochemical equilibrium of the co-ion exclusion theorized by Donnan (see Section 3.2), which generates an electrical potential over IEMs immersed between two solutions at different concentration (i.e., different chemical potential). The sum of all membrane potentials of a stack is its electromotive force. It can be measured as the electric potential difference under open circuit conditions (open circuit voltage). When the circuit is closed with an external load, redox reactions at the electrode compartments convert the internal ions flux into the external electrons current. This implies that the voltage over the stack, which corresponds to the voltage over the external load, is reduced when the circuit is closed. Please note that in RED (generator), the cathode and anode are positive and negative, respectively, i.e., with the opposite charge with respect to ED (user). In addition to provide electricity, RED units may produce H_2 via cathode reduction.

The power output depends on electromotive force and stack resistance. Therefore, a trade-off between them, maximizing the power supplied, is due to the effects of the diluate concentration. The RED performance may be significantly affected by the presence of divalent ions, which increase the membrane resistance and reduce the membrane permselectivity [58].

RED stacks are often operated with single pass (once-through), even in lab-scale experiments.

3.2. Ion Exchange Membranes and Mass Transfer

IEMs are dense membranes made by polymeric material with fixed charged groups and movable ions of opposite charge (counter-ions) [12]. IEMs allow counter-ions to pass, while blocking co-ions, which have the same sign of fixed charges. Cation-exchange membranes (CEMs) contain negative fixed

groups such as SO_3^-, COO^-, PO_3^{2-}, PO_3H^-, and $C_6H_4O^-$; anion-exchange membranes (AEMs) contain positive fixed groups such as NH_3^+, NRH_2^+, NR_2H^+, NR_3^+, PR_3^+, and SR_2^+ [10]. As mentioned above, bipolar membranes (BMs) consist of an anion-exchange layer (AEL) overlapped to a cation-exchange layer (CEL). Monovalent selective membranes (MVMs) allow monovalent counter-ions to pass, whereas retain multivalent counter-ions [19,28–30]. IEM categories are distinguished on the basis of materials, functional groups, and microstructure [9]. For details on IEM features and methods of preparation, see [8–12,59,60].

The theorisation of co-ion exclusion by IEMs was introduced by Donnan equilibrium [8,61], which implies an electric double layer (EDL) at the membrane–solution boundary [8,9,59,61]. A membrane between two salt solutions with different concentration generates a voltage difference (Teorell-Meyer-Sievers) [9,59]:

$$\Delta\varphi^{IEM} = \frac{RT}{F}\int \sum \frac{t_i^{IEM}}{z_i} d\ln a_i, \tag{2}$$

where $\Delta\varphi^{IEM}$ is the "membrane potential", R is the universal gas constant, T is the absolute temperature, F is Faraday's constant, z_i is the valence, t_i^{IEM} is the transport number in the IEM, a_i is the ion activity. Transport numbers are usually assumed constant [62], and, for a single salt, the following well-known expression is obtained [8,9,59,61]

$$\Delta\varphi^{IEM} = \left(2\, t_{counter}^{IEM} - 1\right)\frac{RT}{z_i F} ln \frac{a^{SOL,R}}{a^{SOL,L}}, \tag{3}$$

where $a^{SOL,R}$ and $a^{SOL,L}$ are the salt activities at the right and left solution, respectively. Transport phenomena in IEMs and electrolyte solutions are often described through the Nernst–Planck equation, which encompasses the ion flux with three contributions (diffusion, migration and convection):

$$\vec{J}_i = -D_i\vec{\nabla}C_i - z_i F D_i C_i\vec{\nabla}\varphi + C_i\vec{u}, \tag{4}$$

where D_i is the ion diffusivity, C_i is the ion concentration, φ is the electric potential and $\vec{u}$ is the velocity. For strong binary electrolytes, it can become [61]

$$\vec{J}_i = -D_{el}\vec{\nabla}C_i + \frac{t_i\vec{i}}{z_i F} + C_i\vec{u}, \tag{5}$$

where D_{el} is the electrolyte diffusivity, t_i is the ion transport number and $\vec{i}$ is the current density. The Nernst–Planck formalism assumes negligible interactions among ions, thus being strictly valid for dilute solutions. Nevertheless, the Maxwell–Stefan and other rigorous, but more complex, approaches are less used [63–65].

From Faraday's law, the electric current is

$$\vec{i} = F\sum_i z_i\vec{J}_i. \tag{6}$$

The transport number of an ionic species is the relative portion of electric current that it carries [8,9,59,60]:

$$t_i = \frac{z_i J_i}{\sum_i z_i J_i}. \tag{7}$$

The IEM permselectivity for a counter-ion is [8,11,60]:

$$P = \frac{t_i^{IEM} - t_i^{SOL}}{1 - t_i^{SOL}}. \quad (8)$$

The IEM permselectivity between two ions (A and B) is [9,59,60,66]:

$$P_B^A = \frac{t_A^{IEM}/t_B^{IEM}}{N_A^{DIL-IEM}/N_B^{DIL-IEM}}, \quad (9)$$

where $N^{DIL-IEM}$ is the equivalent concentration (of A or B) at the membrane–solution interface in the diluted side.

Several methods can evaluate permselectivity and transport numbers. Static techniques measure the membrane potential, while dynamic methods consist of electrodialysis experiments (current efficiency) [11,59,60] or chronopotentiometric measurements [11,60,67,68].

Electrical resistance is another important membrane property. It may be measured by either direct current [11,68–70] or alternating current [11,69,71–75] techniques. The last ones (electrochemical impedance spectroscopy) are more complex, but make it possible to separate EDL and polarisation contributions. At lower solution concentration, membrane resistance exhibits an increasing vertical asymptote [69,72,75]. This behaviour was associated with the IEM morphology by following the micro-heterogeneous model [75,76], which represents the membrane with multi-phase structure [77], also containing the solution from outside. There are various physical models, and also phenomenological models for membrane resistance [78]. Moreover, a diverse behaviour was found by some measurements [74], thus this topic could deserve further investigation.

Salt and water permeabilities are other IEM properties [9,59,79–83] that affect the ED efficiency. The diffusive fluxes of salt and water (from concentrate to diluate and vice versa, respectively) are driven by gradients of concentration and osmotic pressure, respectively. An additional water flux originates from electro-osmosis (water molecules in the salt ions solvation shell).

Concentration polarisation in ED is caused by the difference in the transport numbers between membrane and solution, so that a diffusive transport in solution maintains a constant overall flux [15,16,84]. In particular, salt depletion occurs at the IEM-diluted side, and salt enrichment takes place at the IEM-concentrated side. The Nernst model (film theory) can be used to study transport phenomena in IEM-solution systems [85,86]. As the electric current increases, the salt depletion is possible until reaching a null interface concentration, corresponding to the condition of diffusion-limited current. The theoretical diffusion-limited current density may be related to the mass transfer characteristics in the fluid channel, i.e., to the Sherwood number.

However, current–voltage curves exhibit three regions, including the manifestation of overlimiting currents [87–92]. The first region starts following a linear trend, but more and more pronounced polarisation effects (and larger Ohmic resistances in ED stacks) cause a reduced slope at higher currents. The second region is a low-slope transition step indicating the limiting current achievement (high resistance). In the third region, a secondary current growth occurs. When the change in slope is not evident, Cowan's method (apparent resistance) can identify the limiting current [16,93,94].

The current that is carried by H^+ and OH^- generated through water dissociation can partially explain the appearance of overlimiting currents [84,95–99]. Instead, other overlimiting mechanisms involve counter-ions by current-induced convection [67,88,91,100–108]. Electroconvection is the primary process that alters the depleted region for dilute solutions. An extended space charge region develops near the IEM, where the solution is not electroneutral, and inhomogeneous electric

fields cause dynamic vortices [87–89,109–116]. The conductive and geometrical heterogeneity in the IEM surface [67,105,111–113,117–121] and other features, e.g., roughness, grade of hydrophobicity, and superficial charge density [102,103,122–125], affect overlimiting mechanisms and current–voltage curve. Another overlimiting mechanism is gravitational convection, which is caused by temperature or concentration gradients [96,111,114,119,126].

Overlimiting regimes may lead to an enhancement of mass transfer [127], and surface modifications can improve IEMs performance [102]. Therefore, ED operations at overlimiting conditions may be considered to enhance the process efficiency. Nevertheless, maintaining ED stacks below the limiting current is a traditional practice [8,103,128] for avoiding dangerous pH values posing risks of fouling and IEM damage [84,95,129,130].

Despite the actual limiting conditions depend significantly on the membrane properties, experimental correlations of the Sherwood number [63,128,131–134] or of the limiting current density [90,131,135–137] are given by similar expressions:

$$\mathrm{Sh} = a\mathrm{Re}^{b}\mathrm{Sc}^{c}, \tag{10}$$

$$i_{lim} = dC_{i}^{bulke}u^{b}, \tag{11}$$

where Re and Sc are the Reynolds and Schmidt number, respectively, u is the solution velocity, and a–e are coefficients. Many experiments show b values around 0.5, but it can span in a broader range. Actually, power laws fit experimental data well in narrow Reynolds number ranges [128,135], while more complex trends develop at wider ranges (a similar behaviour is exhibited by the friction factor [138–140]). The coefficient c was found to be equal to 1/3 [141,142], but it can assume different values [139,143,144].

Please note that the current–voltage curve of a BM exhibits two limiting zones. At low currents, the first limit is due to salt ions transport. Then, water dissociation occurs. At high currents, the second limit is due to water transport, eventually implying membrane damage.

3.3. Performance Parameters

The performance of ED processes is governed by membrane selectivity and transport properties, non-Ohmic voltage drop given by the membrane potential ("back" electromotive force in most cases, electromotive force in RED), Ohmic voltage drop, and pumping power consumption. The voltage drop over the stack can be computed as [16,145,146]:

$$V_{stack} = V_{ru}N_{ru} + Ir_{el} = \left(\pm r_{Ohm,\,ru}I + V_{non-Ohm,ru}\right)N_{ru} + Ir_{el}, \tag{12}$$

where V_{ru} is the voltage drop over a single repeating unit (e.g., cell pair or triplet), N_{ru} is the number of repeating units, I is the electric current, r_{el} is the resistance of the electrode compartments (negligible in stacks with many repetitive units), $r_{Ohm,ru}$ and $V_{non-Ohm,ru}$ are the Ohmic resistance and non-Ohmic voltage drop in the repeating unit, respectively, the sign "+" applies for ED methods using an electric current provided by an external power supply, i.e., all ED methods except for RED, where the sign "−" applies. The Ohmic resistance encompasses the contributions from all compartments and IEMs (counting also spacer shadow effects [71,147]). $V_{non-Ohm,ru}$ consists of membrane potentials, including polarisation effects. The electric power consumption (or production in RED) can be simply calculated by multiplying the stack voltage drop by the electric current. Actually, the overall power would include the pumping power [16] (it has to be added to the power consumption in most cases, and has to be subtracted to the power production only in RED). The specific energy consumption expresses the energy consumed per product unit volume (e.g., kWh/m^3):

$$E_{spec} = \frac{V_{stack}\, I}{Q_{prod}}, \text{ for continuous operations} \tag{13}$$

$$E_{spec} = \frac{\int_0^\tau V_{stack}\, I\, dt}{v_{prod}}, \text{ for batch operations} \tag{14}$$

where Q_{prod} is the product volume flow rate exiting the module, t is the time, v_{prod} is the product volume at time τ. E_{spec} can be expressed with reference to the transported mass of electrolyte (e.g., kWh/kg):

$$E_{spec} = \frac{V_{stack}\, I}{\left|C_{el,prod,\,in} Q_{prod,\,in} - C_{el,prod} Q_{prod}\right| M_{el}}, \text{ for continuous operations,} \tag{15}$$

$$E_{spec} = \frac{\int_0^\tau V_{stack}\, I\, dt}{\left|C_{el,prod,\,in} v_{prod,\,in} - C_{el,prod} v_{prod}\right| M_{el}}, \text{ for batch operations,} \tag{16}$$

where $C_{el,prod,\,in}$, $Q_{prod,\,in}$ and $v_{prod,\,in}$ are the inlet or initial product concentration, flow rate and volume, respectively, $C_{el,prod}$ is the concentration in the product outgoing from the stack or at time τ, and M_{el} is the molar mass of electrolyte.

The current efficiency quantifies the utilization of the applied current by an ion species:

$$\eta_i = \frac{z_i F \left|C_{i,prod,\,in} Q_{prod,\,in} - C_{i,prod} Q_{prod}\right|}{N_{ru} I}, \text{ for continuous operations,} \tag{17}$$

$$\eta_i = \frac{z_i F \left|C_{i,prod,\,in} v_{prod,\,in} - C_{i,prod} v_{prod}\right|}{N_{ru} \int_0^\tau I\, dt}, \text{ for batch operations ,} \tag{18}$$

where $C_{i,prod,\,in}$ is the inlet or initial concentration of i in the product, $C_{i,prod}$ is the outlet or final (at time τ) concentration of i in the product. The total η for ion mixtures is the sum over all anions or cations. The current efficiency is less than 100% because of unwanted salt and water transport phenomena, water splitting, and current leakage (parasitic or shunt currents through manifolds [146]) [8]. Further performance parameters such as removal efficiency, concentration factor and water recovery, result from easy calculations.

In the special case of RED, an important performance parameter is the electromotive force, given by the open circuit voltage of the stack, which can be estimated as:

$$V_{OC} = N_{ru}(\alpha_{CEM} + \alpha_{AEM}) \frac{RT}{zF} ln \frac{a^{CONC}}{a^{DIL}}, \tag{19}$$

where α_{CEM} and α_{AEM} are the apparent permselectivity of CEM and AEM, respectively, and a^{CONC} and a^{DIL} are the salt activity in the concentrate and diluate, respectively. As V_{OC} is usually estimated with the inlet concentrations, it may differ from the actual (local or average) non-Ohmic voltage drop used in Equation (12). When V_{OC} is measured, the average permselectivity can be obtained from Equation (19).

The power density in RED is defined as the power divided by the total membrane area:

$$P_d = \frac{V_{stack} I}{2 N_{ru} A}, \tag{20}$$

where A is the active area of one membrane. The voltage over the external load, and thus over the stack, depends on the external resistance ($V_{stack} = I \cdot r_{ext}$). By reducing the external resistance, the stack voltage decreases and the current increases up to short-circuit conditions, where the electromotive force is completely consumed inside the stack. The power $V_{stack} \cdot I$ theoretically follows a parabolic trend as

a function of I or V_{stack}, exhibiting a maximum under conditions halfway between open-circuit and short-circuit, in which the external resistance is equal to the stack resistance. The theoretical maximum power density is given by:

$$P_{d,max} = \frac{E_{OCV}^2}{8 r_{stack} N_{ru} A}, \quad (21)$$

where r_{stack} is the stack resistance (including cell pairs and electrode chambers). With the conventional couple seawater-river water at ambient temperature, $P_{d,max}$ is in the order of ~1 W/m^2, with the highest measured value being 2.4 W/m^2 [54,148]. As the power density produced by RED units is modest, the pumping power consumption cannot be neglected. Therefore, the net power $P_{d,net}$ (and, more specifically, the net power corresponding to the maximum gross power, $P_{d,max,net}$) is an important performance parameter [149]. As a function of the fluid velocity, the net power (both $P_{d,net}$ and $P_{d,max,net}$) first exhibits an increasing trend, then reaches a maximum, and finally decreases. Similarly to Equation (13), the specific energy production, or energy density, may be calculated for RED operations.

4. Industrial Wastewater

Waste effluents from industry may have different compositions. However, they often contain dissolved ions. Electrodialytic treatments for industrial wastewater can be classified in: separation of heavy metal ions (Section 4.1); regeneration of acid/base, salt conversion (Section 4.2); desalination (Section 4.3). The applications studied for the main types of industrial wastewater are examined first. Then, further studies on other waste effluents are collected in Section 4.4.

4.1. Separation of Heavy Metal Ions

Heavy metals are harmful pollutants characterized by toxicity, carcinogenicity, non-biodegradability, and persistence in the environment and in living beings. Among the treatment processes proposed for wastewater containing heavy metal ions [150], electrodialytic methods have been tested for industrial effluents from several processes (metal finishing, leather industry, etc.) aiming at reuse. For instance, ED can recuperate water and metals from spent baths or rinse waters of plating processes [151], and different EDI configurations offer several alternatives to ED [42,152].

Several studies have focussed on transport phenomena by assessing IEMs properties, pH effect, complexes formation and ions competition, and by developing modified or novel IEMs. Among them, experiments with aqueous solutions of Ni [153–157], Cu [158–162], Zn [157,163,164], Cr [154,156,165–170], Fe [154,156] and Pb [155,157] have been conducted, as well as with mixtures (e.g., Ni, Cu and Pb, or Cu and Zn) [171,172], thus providing important insights on basic phenomena and ED processes. Another crucial aspect is the identification of optimal operative conditions. With this aim, Taguchi's method was adopted for experiments with metal ions present as single salts or salt mixtures [173,174]. It is a powerful method of design of experiments with optimisation of control parameters, and is based on orthogonal arrays that reduce the number of tests. The statistical analysis of the experimental results was performed by analysis of variance, evaluating error variance and relative importance of the various factors. Moreover, validated models can be adopted for sensitivity analyses and optimisation studies [173].

Each of the next sections, from Sections 4.1.1–4.1.6, focuses on main wastewaters with a single heavy metal ion. Finally, Section 4.1.7 focuses on mixtures of metal ions and waste effluents with other metal ions.

4.1.1. Nickel

Nickel is used for the plating processes of metal pieces with a galvanic bath, which is followed by multiple rinse stages with water. ED can be used to treat the first rinse solution, thus recovering a Ni^{2+}

concentrate recycled to the galvanic bath, and a diluate recycled to the rinse stages (Figure 4). In an early study with pilot ED testing, Ni was recovered by 90% (5 g/L rinse wastewater) [175].

Recent experiments with artificial solutions of electroplating Watts' bath (65 g/L $NiCl_2$, 275 g/L $NiSO_4$, 45g/L H_3BO_3, organic additives) recovered ~95–99% of ions and exhibited an acceptable quality of plated pieces [176]. A scale-up was then performed [177], by operating an ED plant introduced within an industrial plating process for 30 days (Figure 4), demonstrating techno-economic feasibility (saving of 3800 US$/y with E_{spec} of 2.8 kWh/m^3 for treating 480 L/day).

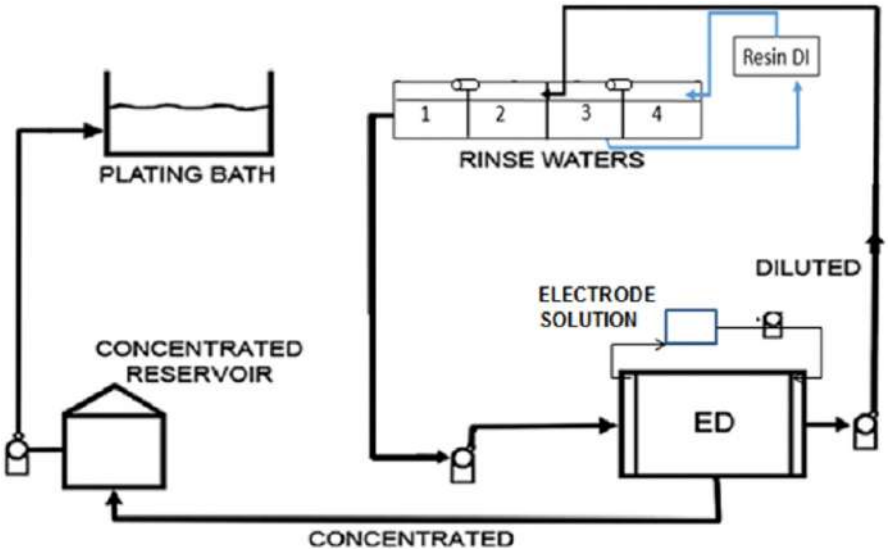

Figure 4. Flow-chart of the ED treatment for Ni electroplating rinse wastewater (the IXR extended the water cycle within the third and fourth tank). Reproduced with permission from [177], published by Elsevier, 2017.

An interesting alternative for ED units with enhanced current efficiencies is given by corrugated membranes [178]. ED was also tested with electroless plating spent solutions, removing harmful ions (HPO_3^{2-}, SO_4^{2-}, and Na^+), and maintaining useful ions (Ni^{2+}, $H_2PO_2^-$, and organic acids) at high concentration [179].

An electrolysis-ED-EDI combined system (13-cell-pair EDI equipped with mixed IXRs in all channels) yielded ~99.8% of Ni^{2+} recovery with 93.9% of purity from a synthetic solution [180]. A simpler two-stage EDI was developed to mitigate the back diffusion [181]. By using a model Ni electroplating rinse solution at 50 mg/L, the first stack diluate effluent (~3 mg/L) was the initial feed of both compartments of the second stack. Mixed beds in the concentrate channels minimized the metal hydroxide precipitation in the 1st stage by limiting the contact probability of OH^- with Ni^{2+} (the lower concentration did not require this measure in the 2nd stage concentrate). Concentration and enhanced purification were accomplished. Ni^{2+} was separated by over 99.8% with E_{spec} of 0.64 kWh/m^3, and the solutions produced were suitable for use in plating and rinsing operations. An economic analysis prospected significant savings compared to chemical precipitation.

Numerous EDI configurations deviating from ED stacks have been tested. They include three-compartment electro-regenerated devices [45,49,50,182], among which there are a hybrid system coupling EDI with capacitive deionisation [183], and a unit without membranes and with electrostatic shielding regions made of graphite powder filling the concentrate compartments [184].

4.1.2. Copper

The ED efficacy in Cu^{2+} separation has been proved. For example, removal percentages of ~97% were attained under optimal conditions [185]. ED can treat and recycle rinsing water from electroless plating [186], and baths and rinse solutions from cyanide electroplating (flowing through concentrate and diluate compartments, respectively) [187].

Non-toxic cyanide-free electroplating baths can be reclaimed by ED. Model rinse waters with 683–1281 mg/L 1-hydroxyethane 1,1-diphosphonic acid and 32–48 mg/L Cu^{2+} (from Cu alkaline strike bath) were used [188]. Despite various ionic complexes formed as the pH was changed, diluate and concentrate products were suitable for recycle in the bath and rinsing processes, respectively (maximum recovery of 99.7% for Cu, 94.4% for organic acid). Further experiments again achieved high recoveries, and pieces of electroplated Zamak alloy exhibited good-quality coatings [189]. However, AEMs properties were worsened (electrical resistance and limiting current), likely because of interactions between organic acids or their chelates and fixed groups. Transport properties were restored only in part by cleaning procedures.

Overlimiting regimes were shown to lead to high values of separation percentage and η [159]. However, copper hydroxide may precipitate causing scaling [190].

An integrated electrochemical process was developed by a pilot system with ED and electrolysis (Figure 5), recovering over 99% of Cu^{2+} and all the water from synthetic solutions (165–504 mg/L), with E_{spec} of ~2 kWh/m^3 in the ED stage [191].

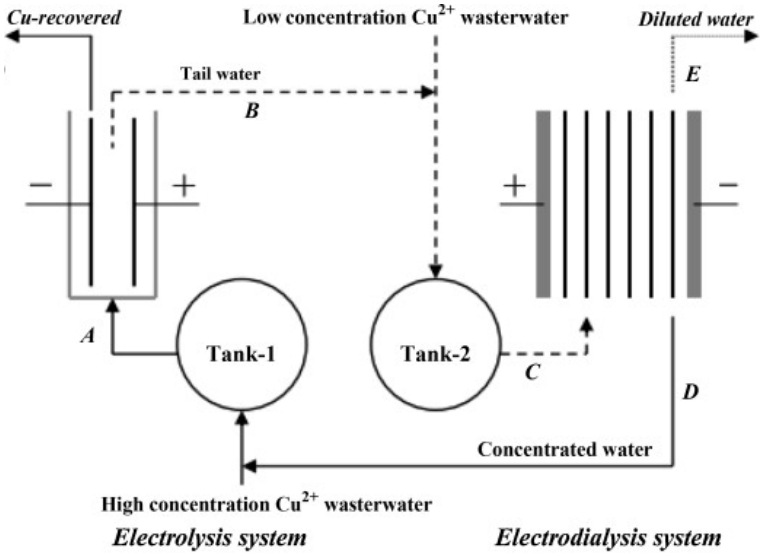

Figure 5. Electrolysis-ED integrated system treating $CuSO_4$ solutions. Reproduced with permission from [191], published by Elsevier, 2011.

Further combined systems aim at treating multiple wastewaters. For example, a process integrating microbial desalination cell, precipitation and ED was developed to treat simultaneously domestic wastewater, Cu wastewater and salt water [192]. In particular, ED finalized the removal of Cu residues and the desalination.

Metal–organic complexes can be separated by ED, which, for example, showed higher efficiencies with Cu–EDTA complexes compared to other electrochemical technologies [193].

EDI processes are suitable for Cu diluted wastewaters, such as plating rinse solutions, as shown, e.g., by a three-compartment device equipped with electro-regenerated layered IXR bed [47].

4.1.3. Zinc

Different plating processes are performed with zinc. Among them, $Zn_3(PO_4)_2$ coating layers are produced via phosphate plating baths with H_3PO_4. Rinse solutions contaminated by different ions (Zn^{2+}, Fe^{2+}, PO_4^{3-}, NO_3^-, etc.) can be treated by ED. For example, 6.5 ppm Zn^{2+} were reduced to ~0.5 ppm, with E_{spec} of ~3.5 kWh/m^3 [186]. ED can also be carried out for Zn cyanide electroplating solutions [187].

4.1.4. Chromium

Hexavalent chromium is another heavy metal commonly used in electroplating. It can exist in the form of several ion species ($Cr_2O_7^{2-}$, $HCr_2O_7^-$, $HCrO_4^-$, CrO_4^{2-}) affected by concentration and pH, and is characterized by high toxicity and carcinogenicity.

In ED experiments with Cr(VI) model solutions, operating conditions (i.e., flow rate, initial concentration, pH, and voltage) were varied, attaining removal percentages of ~79% and ~99% for 50 ppm and 10 ppm as initial concentration, respectively, with $E_{spec} \approx$ 2–4 kWh/m^3 [194]. Therefore, the diluted water can be reclaimed. However, the concentrate has to be cleaned from impurities in order to be recycled.

With this aim, a two-stage selective ED with MVAs was developed [195]. The real wastewater contained Cr(VI) as $HCrO_4^-$ at pH of 2.2, so that it was possible to concentrate it in the first stage along with other ions. By adjusting the pH of the concentrate at 8.5, the most stable form of chromate was the divalent CrO_4^{2-}. MVAs of the second stage retained this in the diluate, while letting monovalent ions to pass (Figure 6). From a 418 mg/L Cr(VI) feed, the first stage achieved a maximum concentration factor of ~1.9, while the second one removed Cl^- by ~45%.

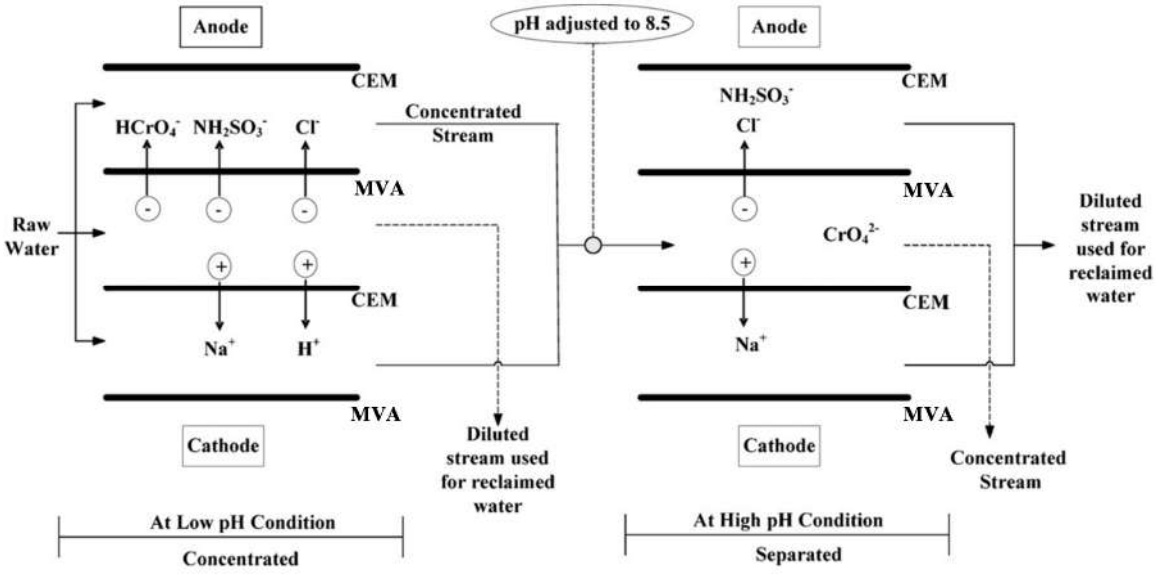

Figure 6. Two-stage selective ED with MVAs for recovering water and concentrate solution from Cr(VI) electroplating wastewater. Reproduced (adapted) with permission from [195], published by Elsevier, 2009.

ED was proposed as a post-concentration step of Cr(VI) diluted solutions after biological treatment [196]. The maximum initial concentration was 100 ppm, simulating the residual concentration of an anaerobic degradation process. A large Cr(VI) retention in the membranes was observed. However, some metal ions were transported to the concentrate channels, leading to a maximum concentration of

570 ppm. The Cr(VI) removal from the feed solution was ~99%, and the volume of concentrate was only ~5.3% of that of the feed. These results suggested the possible reuse of the diluate and concentrate streams.

Cr(VI) separation by EDI processes was studied [197–201]. For example, EDI (four-compartment device, Figure 7a) was combined with IX [198]. After mixed IXRs saturation, electric current was applied by exceeding by 10% the limiting value, removing 98.5% of 100 ppm Cr(VI) with $E_{spec} \approx 0.07$ kWh/m^3.

Cr(III) is less hazardous than Cr(VI). However, it is used in various industrial processes, including plating, and thus can be present in waste effluents. Complexation ED removed simultaneously Cr(III) from a synthetic electroplating wastewater and acetylacetone from a model pharmaceutical waste [202]. The two solutions were mixed, obtaining clathrates formation. These charged chelates were concentrated with removal efficiencies of 99.4–99.5% for Cr and 97.8–99.9% for acetylacetone. The proposed strategy of joint treatment was very promising, but further studies should focus on fouling.

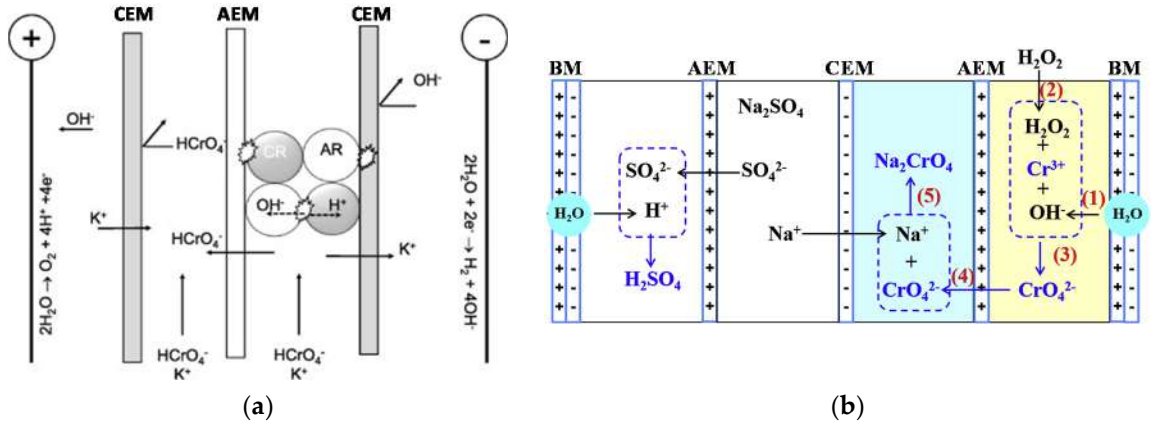

(**a**) (**b**)

Figure 7. Treatment processes for Cr wastewater: (**a**) EDI with diluate compartment filled by mixed IXRs for separating Cr(VI), water dissociation is highlighted at the bipolar contacts; (**b**) BMED for recovering Cr(III) after oxidation to Cr(VI). Panel (**a**) is reproduced (adapted) with permission from [198], published by Elsevier, 2013. Panel (**b**) is reproduced (adapted) with permission from [203], published by Elsevier, 2020.

Cr(III) was oxidized and recovered as Cr(VI) by BMED [203] (Figure 7b). $Cr_2(SO_4)_3$ synthetic wastewater (50–1000 mg/L Cr(III)) received OH^- from the BM (1), forming CrO_2^-. By adding H_2O_2 (2), it was oxidized to CrO_4^{2-} (3), which migrated to the recovery chamber (4), where Na^+ came from the buffer chamber (5). H_2SO_4 in the acid chamber was an additional product. Under optimal conditions (e.g., 5.0 g/L Na_2SO_4 in 100–1000 mg/L Cr(III) solution) ~70% of Cr was recovered. At 500 mg/L Cr(III), η was 67.6% and E_{spec} was 730 kWh/kg Cr in a stack with three repetitive units. By repeating the experiment three times, the recovery increased to ~88%, because of Cr adsorption and release in/by the AEM (removal decreased from ~98% to ~92%).

Cr(VI) and Cr(III) coexisting in wastewater can be removed by electrodialytic techniques. For example, EDI was able to remove both Cr^{3+} and $HCrO_4^-$ from a model solution with 100 ppm of both contaminants, but with higher removal for the latter [204]. The separation from salt mixtures with monovalent or divalent ions is more difficult [205].

Industrial treatments of hides and skins require massive consumption of process water containing chemicals for several manufacturing steps. In particular, salts of Cr(III) are used for tanning processes, which produce wastewater at large volumes and with different contaminants (organics, tannins, and salts). Tanning effluent treatment for recycling purposes has to separate Cr(III) from other ions. ED has been used to recover salt water and Cr(III)-solution by taking advantage of the different selectivity of the membranes towards different ions. For instance, filtered spent tanning effluents flowed through ED

diluate, where the membranes retained most of Cr(III), which was present in different ionic and non-ionic forms (total concentration of ~0.27%), while removing other ions (Cl^- by ~91% and SO_4^{2-} by ~51% from concentrations of 3.4% and 3.3% as NaCl and Na_2SO_4, respectively) [206]. Fouling and chromium leakage were alleviated by dosing EDTA in small quantities and applying EDR. The overall process economics was promising, as the chromium load was lowered by ~33% and the concentrate salt water was usable in pickling operations.

Another strategy for recovering Cr tanning solutions was developed in two steps with (i) monovalent selective ED and (ii) conventional ED [207]. From model tanning wastewaters with concentrations in the order of ~0.1 eq/L, MVCs retained Cr(III) in the diluate and separated NaCl in the concentrate. Then, chromium was concentrated by conventional ED. Optimal pH was around 3, avoiding precipitation and also the competing transfer of H^+. Thus, η approached 100% at the second stage. Further experiments on the first step with salt mixtures (Na_2SO_4, $MgCl_2$ and $CaCl_2$) showed that most of Na^+ could be removed ($\eta \approx 70\%$), with a global η of ~97% [208].

Treatment of tannery wastewaters has been based on integrated processes for water recycling where the first operation degraded organics. Photoelectrochemical oxidation [209] or electrocoagulation [210] have been proposed for this purpose, followed by ED or BMED, respectively. The former combined process removed 87.3% of COD and more than 98.5% of ions (Cr was present only in traces in the raw effluent, i.e., with concentration < 0.01 mg/L); the latter combined process removed ~90% of COD and almost all Cr (from 570 mg/L), ammonium and colour, with E_{spec} of 14–30 kWh/m^3.

4.1.5. Cadmium

Cadmium electroplating is a galvanic process performed via alkaline baths with cyanide, and ED represents again an option as recovery process from waste effluents [211]. A simulated wastewater (CdO, NaCN and NaOH at 0.0089, 0.081 and 0.018 mol/L, respectively) flowed through the diluate of a five-compartment ED module. Maximum removals of 86% of $CdCN_4^{2-}$ (which was the predominant complex) and 95% of CN^- were achieved. However, the process efficiency was affected by $Cd(OH)_2$ precipitation on the CEM at the diluate side.

Solutions with similar composition simulating diluted baths (Cd concentration between 1 and 3 g/L) were used in further experiments [212]. No precipitation was observed, with removals of 21.6% and 46.1% for $CdCN_4^{2-}$ and CN^-, respectively (η of 13.2% and 59.6%). The process was performed in the same way when feeding the model wastewater in both diluate and concentrate channel, i.e., in a configuration more similar to conventional ED. To recycle the concentrate into electroplating baths, while avoiding efficiency losses and risks of membrane damage, the diluate feed was changed four times. This led to a concentrate concentration increase by 56% for cadmium and 250% for cyanide.

The selective separation between metal ions by EDI, referred to as electropermutation, was achieved in a solution containing Cd^{2+} and Na^+ [213]. A cation-exchange resin, modified by natural polyelectrolyte, fixed selectively Cd^{2+} in the central channel of a five-compartment electro-regenerated unit.

4.1.6. Lead

ED has been tested for wastewater containing lead, which originates from industrial processes (regarding, for example, batteries, electronics, printing pigments, explosives, metallurgical processes). With a $Pb(NO_3)_2$ model solution, experiments assisted by analysis of variance assessed the effect of concentration (100–1000 ppm), flow rate, voltage and temperature [214]. The separation was affected mostly by the flow rate, and reached ~95% under optimal conditions. Modelling tools validated against experiments showed that the artificial neural network model was more accurate than the simplified model, the former being able to predict the non-linearity of transport phenomena and thus of ED [215].

Another important operating parameter is the pH. Optimal values of 3–5 were found in experiments with a solution at 800 mg/L Pb^{2+} performed with an ED pilot stack [216]. Lower voltages were effective in increasing η (up to ~35%) and maintaining low E_{spec} values (~0.1 kWh/m^3), while higher voltages could regenerate the membranes from the adsorbed ions. The same ED stack was used in a combined treatment process developed with electrolysis and a further ED unit for adsorption in CEMs [217]. The initial concentration had the most significant effects on the ED performance. With optimized parameters (Taguchi method), ED reduced the initial Pb^{2+} concentration of 600 mg/L to ~16 mg/L in the ED diluate. This was further reduced by adsorption to ~1 mg/L, reaching the target required by the Chinese regulation. The electrolysis process recovered ~90% of Pb via cathode deposition from the ED concentrate. Other ED experiments reduced the concentration from 500–1000 mg/L to 1–2 mg/L [218]. Under optimal operating conditions, high values of η were obtained (82.8–72.4%) with E_{spec} of 0.16–0.36 kWh/m^3. Despite several promising results, the feasibility for real Pb-wastewaters has still to be demonstrated.

4.1.7. Mixtures and Other Heavy Metal Ions

Real industrial wastewaters often contain mixtures of metal ions (either ions with similar concentration or impurities), and ED processes can effectively recover water, concentrate ions, and, in some cases, separate different ion species from each other.

Brass (Cu and Zn) electroplating was evaluated by cyanide-free baths with EDTA, by using ED for treating the rinsing water [219]. By adjusting the ED concentrate concentration to that of the original bath, good deposits were obtained. In the overlimiting regime, the recovery of metals and EDTA was more advantageous [220]. The rinse water was prepared with 0.0006 M $CuSO_4$, 0.0014 M $ZnSO_4$, 0.0015 M EDTA, 0.03 M NaOH (conductivity of 5.3 mS/cm), corresponding to 1% of the concentrations in the bath. The diluate solution was replaced once reached the conductivity of ~0.2 mS/cm, and the concentrate solution was not replaced to maximise its concentration. Cu, Zn and EDTA were concentrated more with overlimiting operation (concentration factor of ~3.45 against ~2.94 with underlimiting operation), likely due (i) to water dissociation generating protons that reacted with complexes and insoluble species, and (ii) to electroconvective mass transfer enhancement. Moreover, fouling and scaling were reduced.

High removals were achieved by ED from a real electroplating effluent containing Ni^{2+} and Cu^{2+} (~23 mg/L for both) [221]. A tertiary treatment line was developed for reclaiming a plating wastewater effluent with a mixture of heavy metal ions at low concentration (~1 mg/L) [222]. Microfiltration (MF) and ultrafiltration (UF) removed organics and suspended solids, then ED desalination was conducted, and finally, the concentrate was treated by nanofiltration (NF) or reverse osmosis (RO) to increase water recovery. The ED step removed 97% of Cr^{3+}, Cu^{2+}, and Zn^{2+}, 95% of SO_4^{2-} and Cl^- (from initial concentration of 1000 mg/L), and 85% of COD (300 mg/L initial concentration). In another study, ED was conducted after chemical precipitation of a real Cr(VI) electroplating wastewater (19 mg/L) with minor concentrations of Cu^{2+}, Zn^{2+} and Cd^{2+} [223]. Cr(VI) was reduced to Cr^{3+} by Na_2S and $FeCl_2$, and then precipitated with other metal ions by NaOH dosage (pH = 9). Then, ED diminished the Cr(VI) concentration in the effluent (1–8 mg/L) by up to more than 95%, thus producing a water reusable for rinsing operations. By treating synthetic rinse waters of Cd cyanide electroplating (1000 mg/L Cd) contaminated by either Cu (50 mg/L), Fe (50 mg/L) or Cr (100 mg/L), the non-selective transport made the ED concentrate not reusable for electroplating baths [212].

However, metals from a mixture can be selectively separated in different channels by complexation–ED. A simulated Zn electroplating bath was prepared with 48.9 g/L Zn^{2+} and 1 g/L Fe^{3+}, and treated by testing different chelating agents [224]. These solutions were circulated through the diluate of a five-compartment ED stack with two concentrate channels (Figure 8a), obtaining the separation between Zn^{2+} and Fe complexes. The process was more efficient when heterogeneous IEMs and citric acid were used. A high

retention of Fe (~92%) in the feed channel was caused by the generation of an electrically neutral citrate complex, while ~87% of Zn^{2+} was removed with $\eta \approx 85\%$. These results suggest that recovering concentrate solutions from contaminated baths can be feasible in conventional ED with one diluate and one concentrate. Further experiments confirmed these results [225], while finding problematic the selective separation for a Zn^{2+} solution contaminated by Cu^{2+}. This occurred due to a partial formation (~65%) of Cu–citric acid anions.

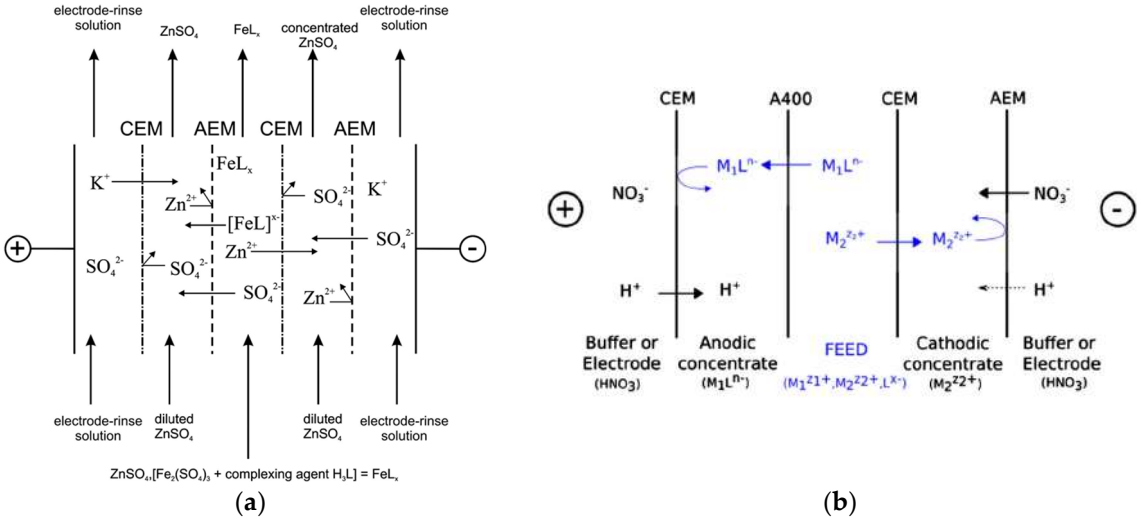

Figure 8. Schemes of complexation-enhanced ED: (**a**) Zn^{2+} recovery from a model Fe^{3+}-contaminated electroplating bath by Fe-citrate neutral complex retention; (**b**) selective separation of metal cations (Ag^{+}/Zn^{2+} or Cu^{2+}/Cd^{2+}). The feed solution contains initially the two metal ions $M_1^{z_1+}$ and $M_2^{z_2+}$, and the ligand L^{x-}, which forms complexes only with $M_1^{z_1+}$ (i.e., M_1L^{n-}) in situ. The A400 AEM allows for the transport of anion complexes of ~400D without fouling. Panel (**a**) is reproduced (adapted) with permission from [224], published by Elsevier, 2018. Panel (**b**) is reproduced with permission from [226], published by Elsevier, 2017.

By taking advantage of the actual formation of anion chelates, complexation–ED was carried out by a three-compartment configuration (Figure 8b) in order to separate metals from mixtures of Ag^{+}/Zn^{2+} or Cu^{2+}/Cd^{2+} [226]. The two ions of each mixture were transported to two different concentrate compartments. In fact, Zn or Cd formed anion complexes, instead Ag^{+} or Cu^{2+} persisted as free ions. EDTA was found to be the best among various complexing agents, allowing for removal percentages higher than 99% from initial concentrations of 0.1–1 meq/L with E_{spec} between 0.28 and 0.55 kWh/m^3, thus enhancing the process compared to previous results reported in [227]. BMED was suggested for separating the complexed cation and regenerating the ligand.

Ni and Co were separated by complexation with EDTA [178]. A Ni-EDTA negative complex was preferentially formed and retained, while Co^{2+} ions migrated through the CEM.

Waste mixtures with heavy metal ions can be purified by EDI processes. A five-compartment EDI device with electro-regenerated cation and anion IXRs in separated beds was tested with a real electroplating waste rinse with Ni^{2+}, Cu^{2+}, Zn^{2+}, Cd^{2+} and Cr^{3+} [46]. A similar unit was tested with a waste solution from a Zn electrolysis process containing Zn^{2+} and other metals [48].

Electrodialytic technologies have been studied for treating various other industrial waste effluents containing metal ions. H_2SO_4-$CuSO_4$ solutions with impurities (As(III), As(V) and Sb(III)) typical of Cu-electrorefining electrolytes were reclaimed via ED by separating and concentrating metal ions [228]. Similarly, a Cu–electrowinning model solution containing 50 g/L H_2SO_4 and 9 g/L Cu^{2+} (as $CuSO_4$

salt) with 0.5 g/L Fe^{2+} impurities was reclaimed by removing 96.6% of copper and 99.5% of iron with $E_{spec} \approx 1$ kWh/kg [229]. Cr(VI) was recovered as H_2CrO_4 by BMED from chromite ore processing residue (chromate production byproduct) [230]. The waste effluent contained a mixture of ~3728 mg/kg Cr(VI) and ~2650 mg/kg Cr(III), along with other metal ions (Fe, Al, As, etc.). The BM-AEM configuration was used, and MF membranes were placed in the wastewater compartment to protect the BM and the AEM from clogging. Recoveries of ~90% were obtained with η of 2.3% E_{spec} of 395 kWh/kg.

Selectrodialysis (SED) with MVC was used with synthetic solutions simulating an acidic metallurgical wastewater (pH = 2.3) with 47 mM $CuSO_4$, 146.8 mM $ZnSO_4$, and 31.6 mM Na_2HAsO_4 [231] (Figure 9). The process recovered 80% of Cu^{2+} and 87% of Zn^{2+} in a solution, and 95% of As(V) in another solution, at η of ~38% for Cu^{2+} and Zn^{2+} and E_{spec} of ~2.6 kWh/kg for their salts. The solution rich in Cu^{2+} and Zn^{2+} was pure by 99.8% (over 80% due to Zn^{2+}), while the product rich in As(V) contained a comparable concentration of Zn^{2+}. To solve this problem, the authors suggested recirculating the As(V) product to the feed.

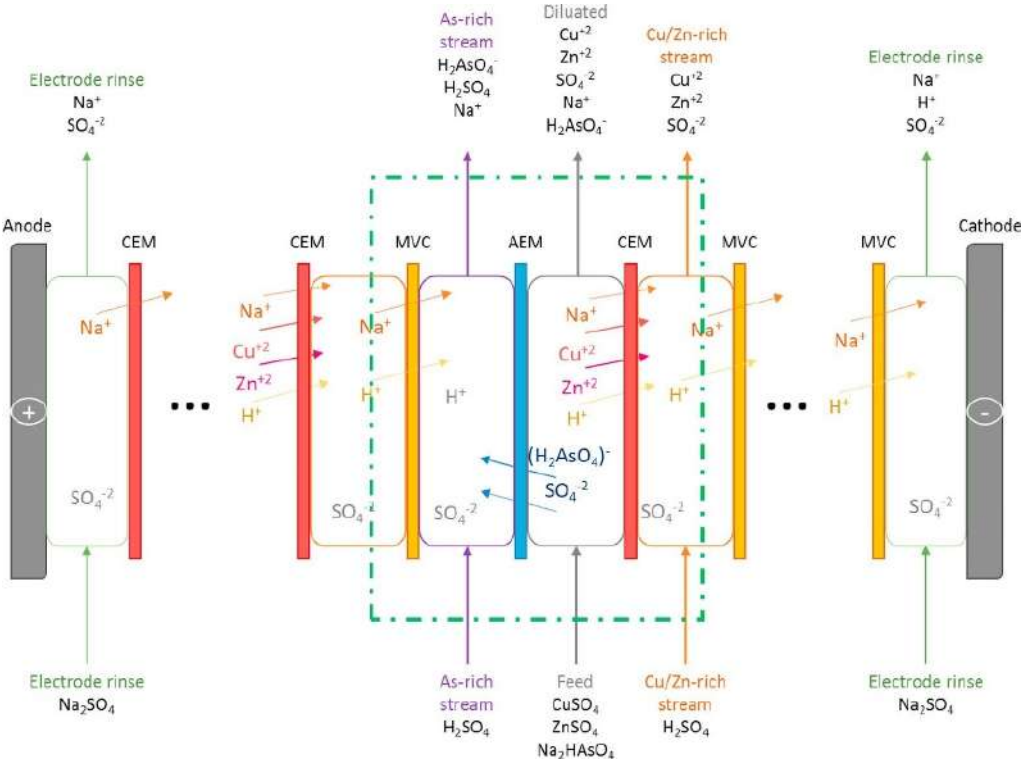

Figure 9. SED configuration for recovering Cu^{2+} and Zn^{2+} from acidic metallurgical wastewater containing As(VI). Reproduced (adapted) with permission from [231], published by Elsevier, 2018.

ED arrangements either with or without MVAs were proposed for reclaiming alkaline gold mine wastewater containing heavy metals (copper and zinc), sodium and cyanide [232].

EDI is suitable for purifying nuclear power plants' primary coolants, which contain low concentrations of Co^{2+} [233,234]. Among several arrangements tested with model solutions (e.g., 0.34 mM), a five-compartment EDI module was developed by using a layered bed within the diluate to prevent the precipitation of metal hydroxide, remove both anions and cations, and control the pH (Figure 10a) [233]. Starting from this EDI arrangement, a stack with four-compartment repetitive units was assembled (Figure 10b). Removals of over 99% at $\eta \approx 30\%$ and $E_{spec} = 14$ kWh/m^3 were obtained. Other experiments

conducted with a four-compartment EDI device removed up to ~99.9% of Cs^+ from model waste solutions (e.g., 50 mg/L) [235]. Different radionuclides (Cs^+, Sr^{2+} and Co^{2+}) in traces were removed by 77.1–99.7% [236]. Th^{4+} was removed at rates of up to ~99% (from 30–90 mg/L) in experiments optimized by response surface methodology [237]. Overall, EDI processes are very promising for treating low radioactive effluents.

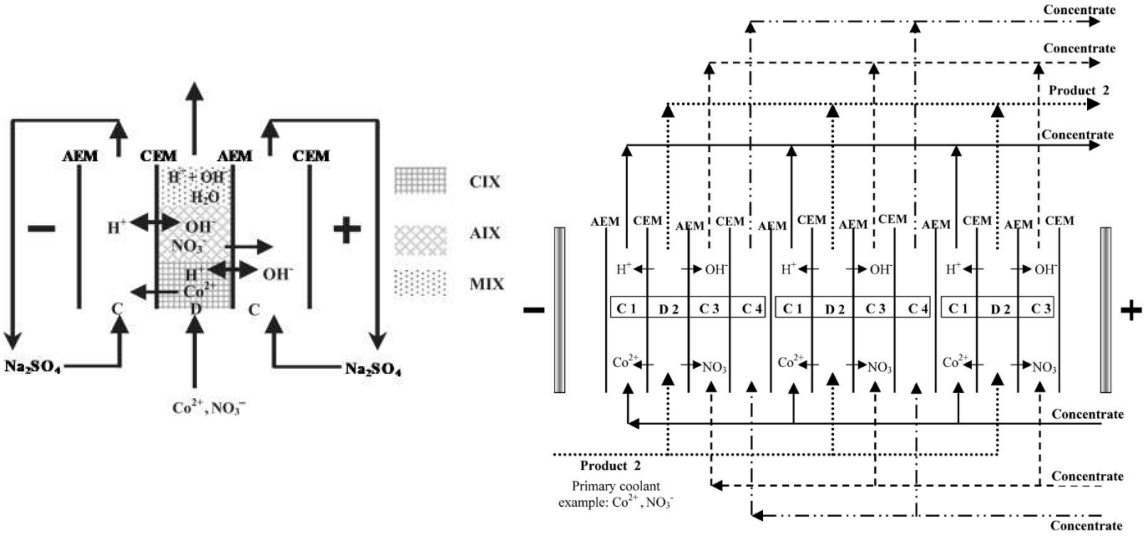

(**a**) (**b**)

Figure 10. EDI configuration with diluate compartment filled by layered bed for the treatment of a Co^{2+} solution simulating the primary coolant from nuclear power plants: (**a**) sketch of the bed packing; (**b**) stack with three repetitive units with four channels each. Reproduced (adapted) with permission from [233], published by Elsevier, 2004.

4.2. Regeneration of Acid/Base, Salt Conversion

Many manufacturing processes produce large quantities of acidic/alkaline waste streams, and their neutralisation is commonly practiced for disposal. In other cases, spent alkaline/acidic solutions result in waste salt streams. In all cases, economic and environmental benefits can be drawn from reuse/recycling approaches. From this perspective, electrodialytic processes (mainly ED and BMED) can be used for treating different industrial effluents, such as acidic wastewaters with heavy metal ions from pickling ant other processes (Section 4.2.1), waste solutions without heavy metal ions (Section 4.2.2), spent alkaline solutions from flue gases chemical absorption (Section 4.2.3), and wastewaters with organic matter, including organic acids (Section 4.2.4).

4.2.1. Effluents with Heavy Metal Ions

Waste acidic effluents are produced form pickling and other processes of metal manufacturing and metallurgical industry. In particular, pickling is a surface treatment that removes impurities (oxides, rust, and others) before metal pieces go through painting, plating, etc. The main application is steel acid pickling. Pickle liquors contain sulphuric, hydrochloric, nitric or hydrofluoric acid, which react with oxides, thus dissolving metal ions. They are regarded as being spent once the acid concentration diminishes by 75–80%, and the metal concentration rises to 150–250 g/L [238]. Pickling processes produce large quantities of spent solutions. For instance, steelwork plants generate ~3×10^5 m^3/y waste pickle liquors in the only Europe.

The regeneration (recovery and purification) of pickling operations effluents can be accomplished by several methods, including ED for acid concentration and metal separation [238,239]. For example, 60–70% of H_2SO_4 was recovered from a pickling rinse water (9100 ppm) with a ten times increased acid/iron concentration ratio (from 7.4:1 to 74.6:1) [186]. Optimal operating conditions and selective membranes are crucial [240]. Proton leakage through AEMs, which limits the acid concentration [241], can be alleviated by purposely developed proton-blocking membranes [240,242–248]. On the other hand, the passage of metal ions across the membranes may impair the concentrate purity [249] and cause fouling [240]. However, using MVCs that retain multivalent metal cations allows for the acid recovery with high purity [250].

After neutralisation of the spent pickling solution and precipitation of metals, BMED can regenerate the acid stream in combination with an ED salt concentration step [251]. A BMED-ED integrated pilot has been used since 1987 [34] in an industrial treatment plant at the Washington Steel Corporation facilities (Pennsylvania) [37], where a pickling solution with mixed acids (8–15 wt% HNO_3 and 2–5 wt% HF) was used. The process scheme is depicted in Figure 11, and can be described as follows [37]. Metals in the spent liquor were removed by neutralisation/precipitation (KOH dosage) and filtration. The KF/KNO_3 solution obtained (1.1–1.5 M, with metal ions at concentration < 1 ppm) went through the salt compartment of BMED, which produced the base used for neutralisation, and the mixed acids (HF + HNO_3) recycled into the pickling bath. ED recovered water (for filter cake washing) and salt from the BMED diluate (0.3–0.5 M) stream. The base was diluted with a fraction of the BMED diluate. The BMED and ED stacks were assembled with 25 and 15 cell units, respectively, totalling 2.33 m^2 and 1.4 m^2 of membrane area. During a long-term run with 240 L/day waste acid, η was ~80% for acid and base, and remained quite stable over time, while E_{spec} was ~0.25 kWh/L acid product (180 L/day). 93% of F^-, 99% of NO_3^-, and 96% of K^+ were recovered. The economic analysis for a scaled-up system (6×10^6 L/y) found high investment costs, but with a 4-year payback period.

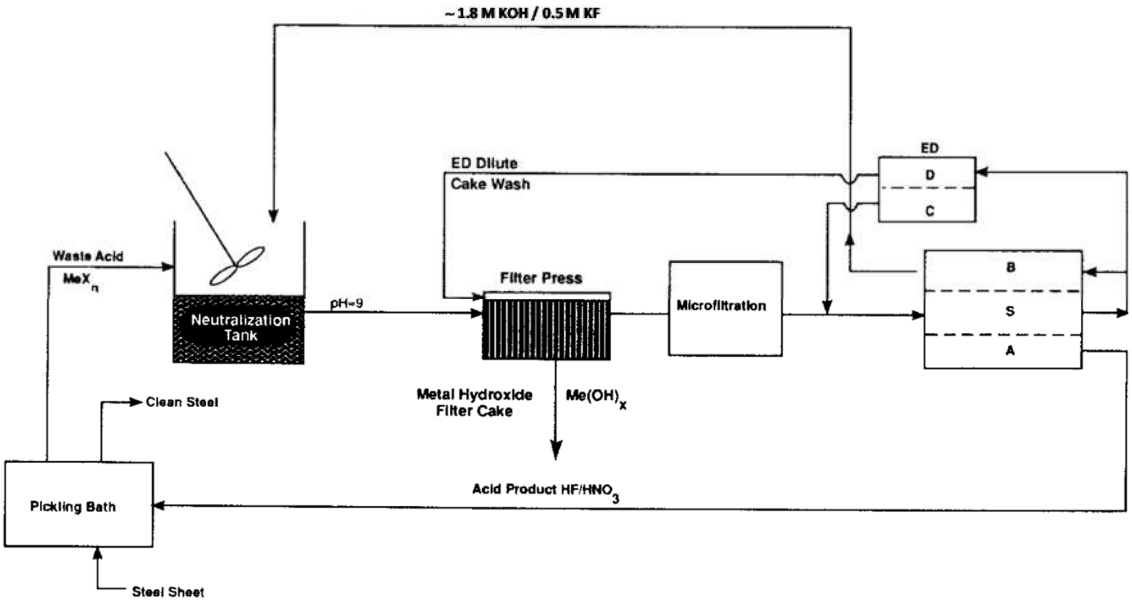

Figure 11. Flowsheet of the pickling liquor recovery by BMED-ED coupling. Reproduced (adapted) with permission from [38], published by Elsevier, 1991.

Several metallurgical processes produce spent acidic solutions with metal ions, and the reclamation via ED or BMED has been tested. ED concentration of a spent solution from a metallurgical industry, containing Ni^{2+}, Cu^{2+} and other ions, recovered more than 80% of H_2SO_4, showing the impact of the

membranes (MVMs, proton-blocking AEMs) [252]. Similarly to the example previously reported for waste pickling effluents, BMED can produce acid and base from waste mixtures of heavy metals and salts, after pre-treatment removing metals. From a Ni washing wastewater, crystallisation (fluidized pellet reactor) removed up to 74% and 94.4% of Ni^{2+} and Ca^{2+}, respectively (with filtration), thus minimizing scaling in the BMED [253]. The feed salt solution of BMED contained ~45 g/L Na^+ and ~80 g/L SO_4^{2-} as main ions, with ~10 mg/L Ni^{2+}, ~16 mg/L Ca^{2+}, and other minor components. η was 69% and 80% for acid (H_2SO_4) and base (NaOH), respectively, while E_{spec} was 5.5 kWh/kg acid and 4.8 kWh/kg base. In a long-term test, acid and base at 1.76 N and 2.41 N, respectively, were obtained starting from 0.2 N, with small scaling.

An alternative way for reclaiming acidic streams from metal finishing is the conversion to organic acid via ion substitution ED [254]. The wastewater feed maintains metal ions retained by an MVC, and releases protons and anions to the organic salt stream and the inorganic salt stream, respectively (Figure 12). From a model waste acid (0.4 M HCl, 0.1 M $FeCl_2$) and a 0.3 M sodium acetate solution, acetic acid at high purity was produced (0.2 mM Fe^{2+}) with average η of 91%. A proton selective composite CEM was then developed, showing a possible process enhancement [255].

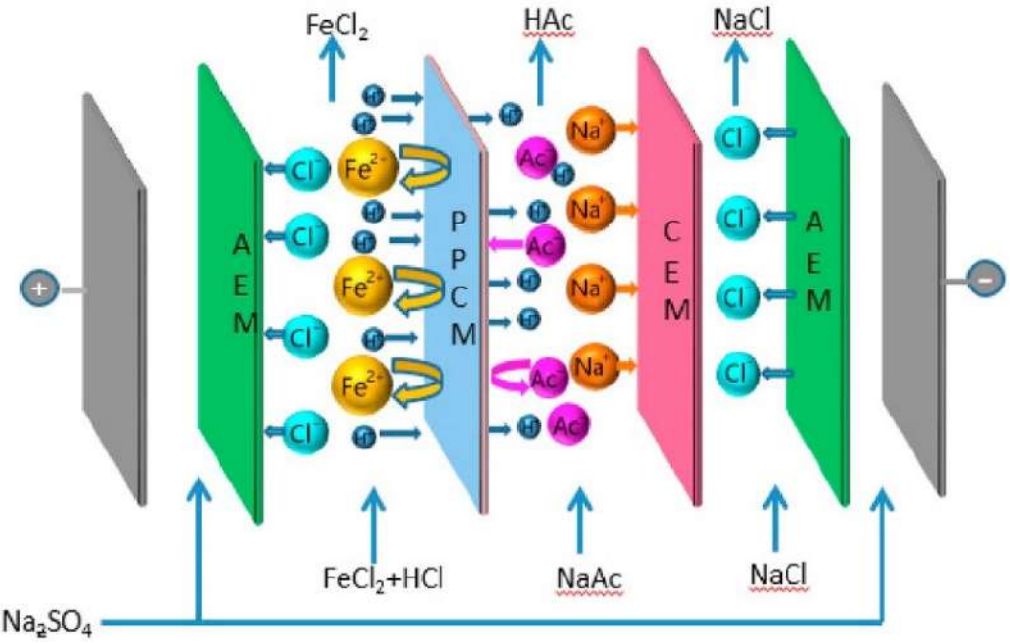

Figure 12. Schematics of ion substitution ED with three-compartment repeating units for the conversion of metal finishing waste acid into organic acid. Reproduced with permission from [255], published by Elsevier, 2019.

Other ED applications regard spent acids produced by Zn hydrometallurgy [256–258]. Again, in order to prevent acid and metal leakage, proton-blocking AEMs and MVCs are crucial elements for performing feasible recovery processes via ED [256]. MVCs were prepared by different methods [259,260], reaching $P_{Zn^{2+}}^{H^+}$ of 34.4 [260]. An interesting alternative is provided by replacing CEMs with NF membranes (Figure 13) [261]. Homemade NF membranes were used for acid recovery from a Zn^{2+}-containing synthetic solution (diluate feed with 0.5 mol/L H_2SO_4 and 0.23 mol/L $ZnSO_4$, concentrate with 0.05 mol/L H_2SO_4). The modified ED system exhibited better performance compared to the stack equipped with MVCs, increasing the permselectivity $P_{Zn^{2+}}^{H^+}$ from 15 to 354.

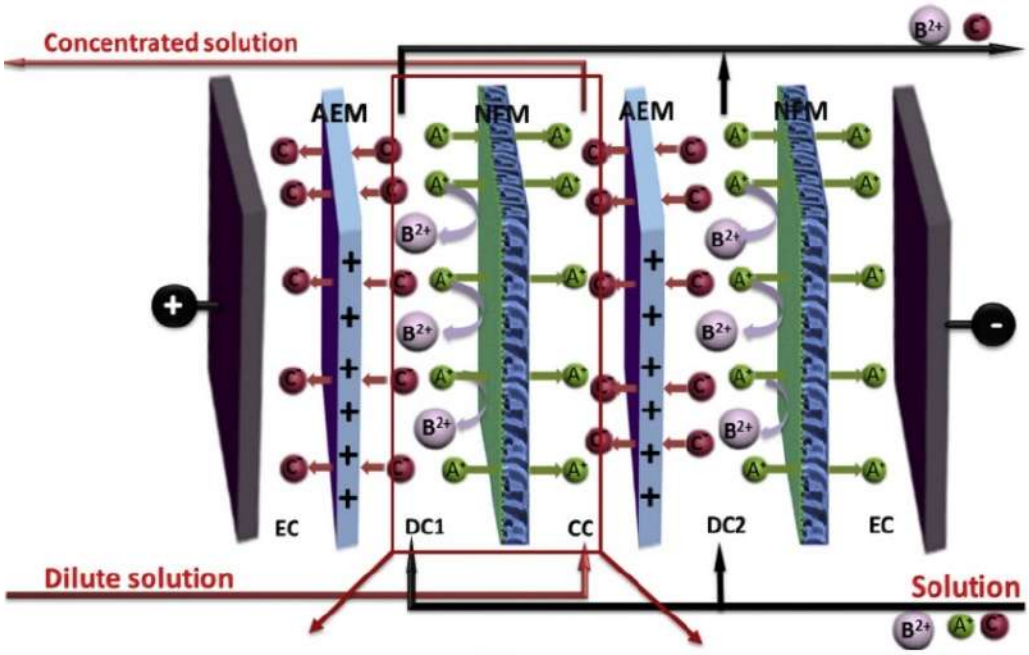

Figure 13. Modified ED equipped with NF membrane in place of CEM. Monovalent cations A^+ (e.g., H^+) can move across the NF membrane, while divalent cations B^{2+} (e.g., Zn^{2+}) are retained. Reproduced with permission from [261], published by Elsevier, 2016.

BMED of acidic raffinate from Cu ore hydrometallurgical processing was proposed [262]. From the raffinate (11,800 mg/L Fe, 336 mg/L Zn, 135 mg/L Cu, etc.) heavy metals were separated (from ~70% to ~99%) as precipitates in the base, and SO_4^{2-} (45.2 g/L) was transported to the acid (by ~86%), thus recovering H_2SO_4, albeit with some impurities. With E_{spec} below 0.1 kWh/L and high values of η, the treated raffinate reached a metal concentration below 100 mg/L, thus being reusable as leachate.

ED tests were performed to recover nitric acid from rinsing-wastewater from aluminium anodizing industry (acidity of 4085 mg/L $CaCO_3$) [263]. Despite some issues of Al precipitation and leakage, most of the waste acid was recovered with a conductivity removal of ~86–91% and E_{spec} values of ~0.11–0.3 kWh/mol acid. Acid recovery can be obtained also by combined membrane processes. HCl from acidic wastewater produced by aluminium foil industry was recovered by integrating diffusion dialysis and ED (model solution with 1.35 mol/L HCl and 0.15 mol/L $AlCl_3$) [264] or BMED (model solution with 4.7 mol/L HCl and 0.59 mol/L $AlCl_3$) [265], showing that cost-effective schemes can be devised. In the former combined process, up to ~75% of HCl was recovered with a metal leakage of ~12%. In the latter, after acid recovery by diffusion dialysis, the dialysate was fed to the base compartment of the BMED, thus allowing for the aluminium recovery.

Experiments showed the ED effectiveness for acidic wastewater with various metal ions (including Cu, Fe, Zn, Cd and As) from the chalcopyrite ($CuFeS_2$) mining industry [266]. An effluent from the SO_2 wet purification process was cleansed from metal ions by IX, then was fed into the ED diluate to concentrate H_2SO_4 in the concentrate (95–98% recovery from a feed concentration of ~17 g/L) and to provide reusable water.

Sulphuric acid and sodium hydroxide were produced by BMED from IX spent regenerant (containing ~0.75 M H_2SO_4, ~0.55 M Na_2SO_4, and metal ions) coming from hydroxy acids liberation from alkaline kraft black liquor [267]. Feeding acid and base compartments with initial concentrations of 0.1 M, the BMED provided a solution with 1 mol/L H_2SO_4 at 95% purity, and a solution with 0.79 mol/L

NaOH at 93% purity, thus presenting a promising perspective to reduce the chemicals consumption in the overall process.

A rare example of ED application for base recovery from an alkaline solution was reported in a study on a synthetic wastewater of 0.1 mol/L Na_2WO_4 and 1 mol/L NaOH [268]. Composite AEMs were prepared and tested, showing OH^- recovery ratios up to ~65%, E_{spec} of ~7 kWh/kg, and low tungstate leakages (5–14%).

4.2.2. Effluents without Heavy Metal Ions

BMED can recover acidic/alkaline solutions from several saline wastewaters produced in industrial processes. In rayon production plants, BMED can restore the acidity of spin baths by converting part of the Na_2SO_4 from spent baths into H_2SO_4, and produce NaOH reusable in cellulose dissolution [37,38] (Figure 14). The crystallisation of Na_2SO_4 produced Glauber salt. After purification and dissolution in water, the solution passed through the acid compartment of a two-cell BMED unit or through the salt compartment of a three-cell BMED unit (receiving a spent bath portion in the acid compartment). η values of 80–95% were reported. For a production of 10,000 Mt/y NaOH, a payback period of 2–5 years was estimated.

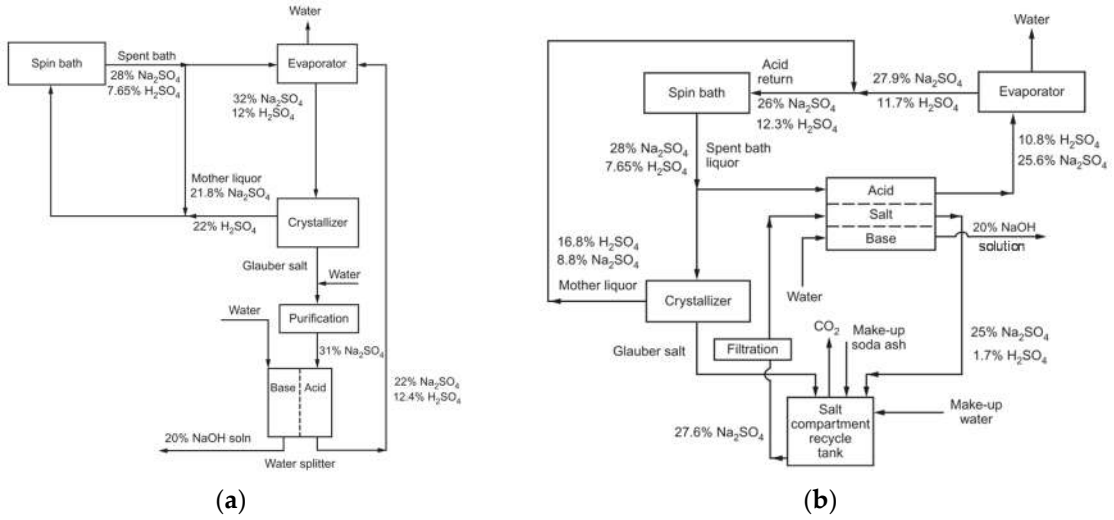

Figure 14. Rayon process flowsheet with BMED: (**a**) Two-compartment configuration (BM-CEM); (**b**) Three-compartment configuration. Panel (**a**) is reproduced with permission from [37], published by Elsevier, 1988. Panel (**b**) is reproduced with permission from [38], published by Elsevier, 1991.

BMED was cost-effective for desalinating cooling tower blowdown and producing acid and base, which could be reused on-site, e.g., for IXRs regeneration [269]. From NaCl synthetic solutions (48–390 mM, with the lower part of the range being representative of cooling tower blowdown), 73–81% of salt was converted into acid/base, at η higher than 75% and E_{spec} of 0.02–0.09 kWh/mol. The maximum estimated cost (12.6 $/kmol, under the assumption that the total cost is 1.7 times the energy cost) was less than the minimum cost of purchase (21 $/kmol).

The technical feasibility of BMED was proven for recycling several other saline wastewaters. Tests on BMED stacks were performed with NH_4NO_3 nuclear fuel processing effluents [270,271] or $NaNO_3$ dying industry effluents [272] to produce HNO_3 and NaOH. Wastewaters from UF_6 production can be recycled as HF and KOH [251]. Phosphogypsum ($CaSO_4$) by-product from phosphoric acid production can be converted by NaOH into $Ca(OH)_2$ and Na_2SO_4, thus splitting the salt into base and sulphuric acid via

BMED [273]. Other applications were proposed to convert NH_4Cl into HCl and NH_3 [274,275], NH_4HCO_3 into NH_3 and CO_2 [276], Na_3PO_4 into H_3PO_4 and NaOH [277], NaBr into HBr and NaOH [278,279], $Na_2SO_4/(NH_4)_2SO_4$ into H_2SO_4 and $NaOH/NH_3$ [280], NaCl/KCl into HCl and NaOH/KOH [281], boron into boric acid [282–284].

A SED-BMED coupled process was developed for waste salt mixtures (NaCl and Na_2SO_4, originated from dye synthesis) conversion into NaOH and separated acids (HCl and H_2SO_4) [285] (Figure 15). Different feed solutions were used, with sulphate concentration from 26 to 840 mM and chloride concentration from 63 to 497 mM. SED with MVAs fractionated the salts into two product streams at purity of ~90% for Cl^- and over 90% for SO_4^{2-}. From these solutions, the BMED processes yielded pure NaOH and acid solutions rich in HCl or H_2SO_4 by 87% or 93%, respectively. E_{spec} was ~6.4 kWh/kg product on average for the SED with solutions at medium to high concentration, while it was ~5 kWh/kg NaOH for the BMED.

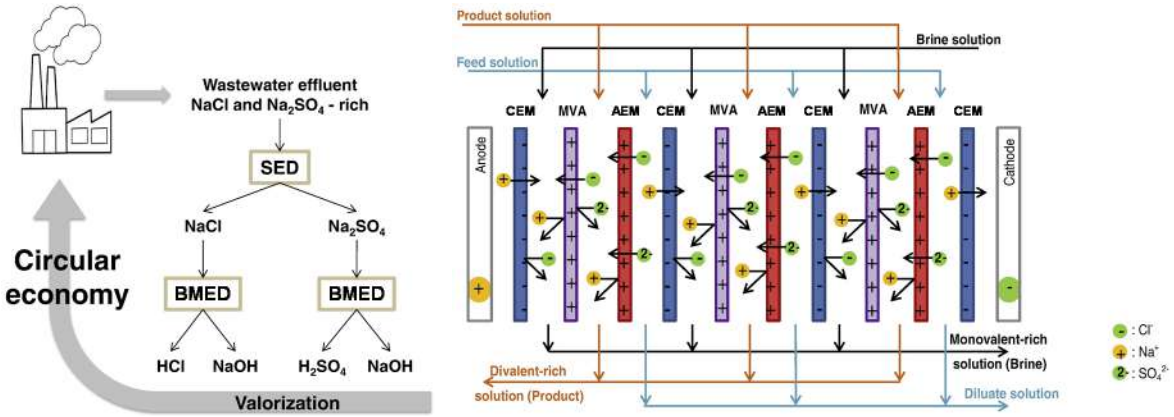

Figure 15. Valorisation of salt mixture wastewater by SED-BMED integration: (**a**) Scheme of the process; (**b**) Sketch of SED with MVAs. Reproduced (adapted) with permission from [285], published by Elsevier, 2016.

4.2.3. Spent Solutions from Chemical Absorption of Flue Gases

Chemical absorption through wet scrubbers is used in treatment lines for waste gases produced by combustion at power plants (e.g., coal-fired) and by other processes. BMED or ED can be adopted for regenerating spent alkaline or acidic solutions from flue gases chemical absorption, thus recycling the absorbent for the scrubbing tower. Two different processes were developed to recover spent alkaline absorbents for SO_2. One of them was based on the three-compartment BMED fed by the Na_2SO_4 solution from the stripper to produce NaOH, which is reused for absorption [8,286]. The other process was developed by the two-compartment BMED unit with BM and CEM [286,287], and took the name of Soxal^{TM} as an industrial process [38] (Figure 16). The spent solution is an $NaHSO_3/Na_2SO_4$ mixture that is converted into a regenerated stream of Na_2SO_3 (in the base channel), and into a stream with SO_2 (in the acid channel) that is then stripped. These regeneration processes led to significant economic advantages, exhibiting $\eta \approx 90\%$ and $E_{spec} \approx 1.3$ kWh/kg base [9].

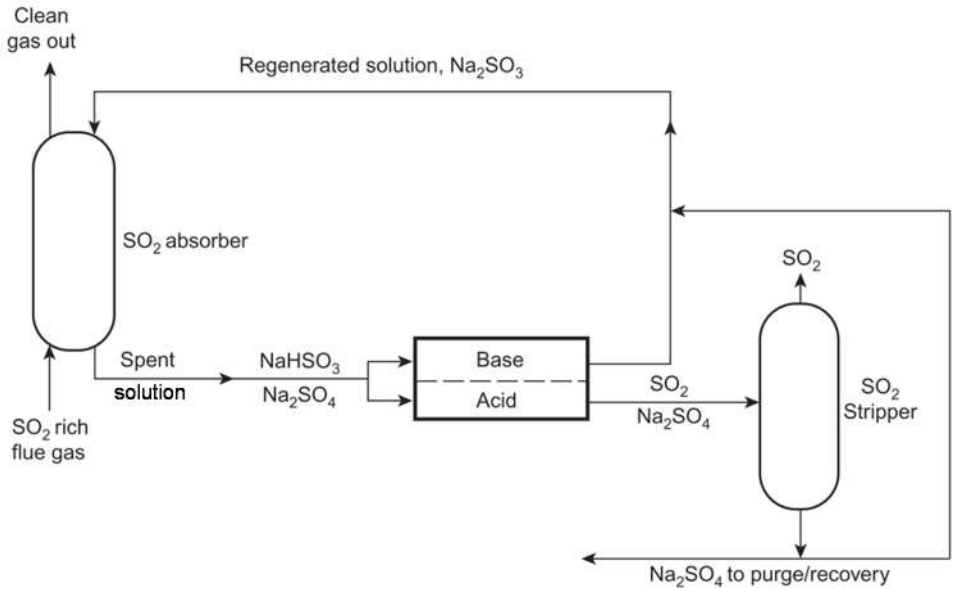

Figure 16. BMED Soxal^{TM} process for flue gas desulfurisation. Reproduced (adapted) with permission from [38], published by Elsevier, 1991.

The coupling of IX with BMED was tested to treat limestone-gypsum wet flue gas desulfurisation wastewater after chemical precipitation of Ca^{2+} and Mg^{2+} [288]. A synthetic wastewater (35–140 g/L NaCl and Na_2SO_4 mixed salts at mass ratio of 2:1, and 40–250 mg/L Ca^{2+} or Mg^{2+}) was softened by chelating IXRs to remove residual hardness, thus preventing scaling. The BMED obtained 99.3% pure acid and 99.0% pure base. The former will regenerate the saturated IXRs, and the latter will be dosed for the precipitation step.

BMED powered by solar organic Rankine cycle was tested with saline wastewater from flue gas desulfurisation in fluid catalytic cracking [289]. Experimentally assisted simulations were performed for a process in which the NaOH absorption spent solution contains HSO_3^- and SO_3^{2-} that are oxidized (in an aeration tank) to SO_4^{2-}. Thus, the Na_2SO_4 solution was treated by BMED. Simulation results showed that the salt solution was converted into H_2SO_4 (7.6 wt%) and NaOH (6.4 wt%), by reducing the salt content in the wastewater from 8.0 wt% to 0.37 wt% with $\eta \approx 52\%$ and $E_{spec} \approx 2.7$ kWh/kg salt.

A two-step ED treatment removed fluoride and chloride from ammonia-based flue gas desulfurisation slurry [290]. The slurry was pre-treated by MF and IX to remove fly ash and metals. A synthetic solution (10,000 mg/L F^-, 20,000 mg/L Cl^-, and 50% $(NH_4)_2SO_4$, by dissolving NH_4F, NH_4Cl, and $(NH_4)_2SO_4$) was also used for comparison purposes. After the first stage, Cl^- was almost completely transported to the concentrate (tap water) with $\eta \approx 54\%$ and $E_{spec} \approx 0.9$ kWh/kg, while a small amount of F^- was removed, mainly remaining with ammonium and sulphate in the slurry (diluate). A double second stage was then carried out to treat the two outlet solutions from the first stage. One was fed with the previous concentrate in the diluate channels to further separate Cl^-, another was fed with the previous diluate in the diluate channels to separate F^- and purify the slurry. The MVAs were crucial for SO_4^{2-} retention. A solution with Cl^- purity larger than 95% and a solution with F^- maximum purity of 51.4% were obtained.

ED can be cost-effective for regenerating spent alkanolamine effluents used for H_2S absorption, by removing inorganic and organic degradation by-products that form heat stable salts [291,292]. The estimated cost was 14.6 $/ton with E_{spec} of 39.4 kWh/ton for a spent amine wastewater from the H_2S desulfurisation stripper of a thermoelectric factory (20.38 wt% N-methyldiethanolamine and 2.54 wt% salts, 36 L/day [291]). The selective removal of heat stable salts along with the

minimisation of N-methyldiethanolamine loss was attained by developing ED or EDI stacks equipped with three-compartment repeating units [293]. This configuration comprised: CEM, concentrate, AEM, diluate (with or without anion-exchange resin), AEM, NaOH solution. Hydroxyl ions of the base compartment migrated to the diluate and reacted with binding amine, and thus neutral amine was regenerated. Moreover, the hydrolysed (cationic) amine was retained in the diluate. This solution was depleted in anions migrating to the concentrate. The spent solution coming from an H_2S desulfurisation stripper in an integrated gasification combined cycle power plant contained 21.06 wt% N-methyldiethanolamine and 5.19 wt% heat stable salts, at pH of 9.4 and conductivity of 12.32 mS/cm. Salts were removed by ~94%, 86% and 65% in the three-compartment EDI, three-compartment ED, and conventional ED, respectively, which exhibited losses of amine of ~3.8%, 5.6% and 21.1%, with E_{spec} of 71.7, 66.6, and 56.25 kWh/m^3 wastewater and estimated total cost of 0.88, 0.92, and 1.04 US$/kg heat stable salt (treatment of 48 L/h). Moreover, AEM fouling was reduced in the EDI.

Similarly, ED can regenerate spent alkanolamine absorbents for CO_2. Pilot-scale studies were conducted with a spent solution at 30 wt% monoethanolamine, showing stable performances during long-term operations [294]. The effect of CO_2 loading (from 0 to 0.2 mole/mole amine) on heat stable salts (48 meq/L) removal from monoethanolamine-based solvent (30 wt%) was studied by two-stage ED [295] (Figure 17). An increase in recovery of salts was observed as the CO_2 concentration decreased, due to the smaller content of amine charged species and their lower competitive transport. An optimum CO_2 loading of 0.1 mole/mole amine and the associated E_{spec} of 25.9 MJ/kg solvent were estimated, considering that the change in CO_2 loading would require additional power for further solvent regeneration in the stripping column.

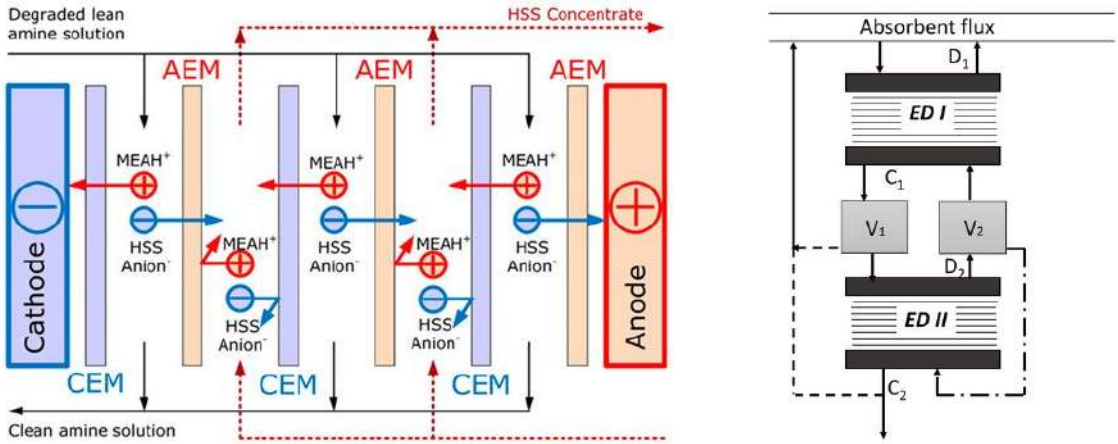

(**a**) (**b**)

Figure 17. ED for heat stable salt removal from monoethanolamine solvent: (**a**) principle of the process; (**b**) flow scheme of the two-stage ED, where the concentrate stream after the first stage goes to the second stage to reduce monoethanolamine loss. Reproduced from [295].

A BMED stack with BM-CEM configuration recovered CO_2 and regenerated NaOH from model carbonate solutions [296], recording η values of 46–80% and E_{spec} values of 1–3 kWh/kg CO_2. The economic analysis highlighted the importance of the membrane cost for the process competitiveness. A coupled system was developed with the BM-AM two-cell BMED configuration and a hollow fibre membrane contactor aiming at regenerating spent absorbers (1 M monoethanolamine, piperazine or $NaHCO_3$), removing heat stable salts and separating CO_2 [297]. From BMED, the alkaline stream was recirculated

into the flue gas absorber, while the acidic stream was recirculated into the membrane module for CO_2 separation. The developed mathematical model predicted E_{spec} = 2 MJ/kg CO_2, but the actual consumption in the experiments was 3–4 times higher due to the low η (~40%).

4.2.4. Effluents with Organic Matter

Salt or acidic wastewaters may have organic compounds. BMED or ED have been studied for acid/base recovery and organic matter separation, despite such solutions are complex and bring possible issues of organic fouling.

In a BMED stack used to regenerate NH_4^+ and H_2SO_4 from glutamate wastewater, CEM scaling at the base side was caused by Ca^{2+} and Mg^{2+}, along with minor fouling on the other surface [298]. However, acid–ultrasound cleaning restored the membrane properties. Glyphosate recovery and HCl/NaOH production were obtained by BMED of alkaline glyphosate (12.8 g/L, with ~175 g/L NaCl) neutralisation liquor from pesticide industry [299,300]. Glyphosate was recovered by 98.2%, and the NaOH solution (~1.45 M with ~96.5% purity) was produced with maximum η of 80.8% and minimum E_{spec} of 2.15 kWh/kg [300]. Prospecting the base reuse for CO_2 sequestration, the overall balance estimation was positive only if employing renewable energies.

A three-stage BMED process was developed to remove aniline (1000–3000 ppm) and salt (0.1 M NaCl) from a model wastewater and to simultaneously capture CO_2, through the reaction of the amine group with carbon dioxide that results in positively charged amine [301]. Aniline was completely transported to the base compartment (at η up to 80% and E_{spec} of ~3 kWh/kg), and the desalination exceeded 94% (at η = 90% and $E_{spec} \approx$ 1 kWh/kg). The possible use of conventional ED for aniline-H_2SO_4 wastewater was suggested by performing an analysis of mass transfer and current–voltage characteristics [302].

Measures for counteracting the adverse effects of leakage currents (parasitic currents flowing through the manifolds) were suggested in a BMED process fed by high ammonium chloride organic wastewater (2.46 M NH_4^+, 1.95 M Cl^-, 6 g/L carbocystein) [303]. Experiments and simulations showed that, to enhance the process efficiency and reduce overheating phenomena, a proper stack design should be devised, increasing the relative resistance of the parasitic pathways. In particular, using low-resistance membranes, thin spacers, sufficiently long slots in the spacer gasket, and implementing a two-stage scheme can be fruitful to this aim.

BMED with BM-CEM configuration reclaimed waste solutions with polymeric bonding agents and sorbed heavy metals from, e.g., polymer-enhanced UF [304]. Bonding agents were regenerated (84–95%) in the acid compartment by protonation, while heavy metals (Cu^{2+}, Ni^{2+}, Co^{2+} and Pb^{2+}) were transported to the base compartment and separated by formation of hydroxides.

Spent caustic reclamation for NaOH regeneration via BMED was demonstrated by testing a BM-CEM unit [305]. From a spent caustic with 0.44 M NaOH, 0.29 M Na_2CO_3, and 0.048 M Na_2SO_4, optimal conditions yielded a 0.11 M base at η approaching 100%, E_{spec} of ~8 kWh/kg NaOH, and an estimated cost of 0.97 US$/kg (process capacity of 18.9 kg/year), without observing effects due to oil.

ED concentration was reported for HCl from waste effluents originating from hydrolysis of palm oil by-products [306], and for NaOH from cellulose mercerisation wastewater [307].

ED technologies have been widely studied for production of organic acids, with development for some industrial applications [19,308]. New opportunities are derived from the recovery of organic acids from wastewaters via ED [309–315], or BMED [316–318] or both [319,320], including systems combined with biotechnologies.

Naphthenic acids were recovered by BMED from sodium naphtenate solutions [321]. Naphthenic acids are valuable chemical raw materials, which negatively affect the quality of petroleum distillates. They are removed by alkaline extraction, thus generating a solution with salts of naphthenic acids. The BMED with

BM-CEM-CEM three-chamber unit cell formed insoluble naphthenic acids (salt compartment fed with 18 wt% sodium naphtenate, 24 wt% NaOH, 1.5 wt% oil), which are separated in a sodium naphthenate reservoir filled with Raschig rings (Figure 18). The same process was conducted by introducing a cation-exchange resin (EDI) and sodium sulphate in the salt chamber, obtaining (i) a reduction in the electrical resistance, (ii) gains in limiting current density, η (up to ~80%) and E_{spec} (0.38 kWh/L), and (iii) a total conversion.

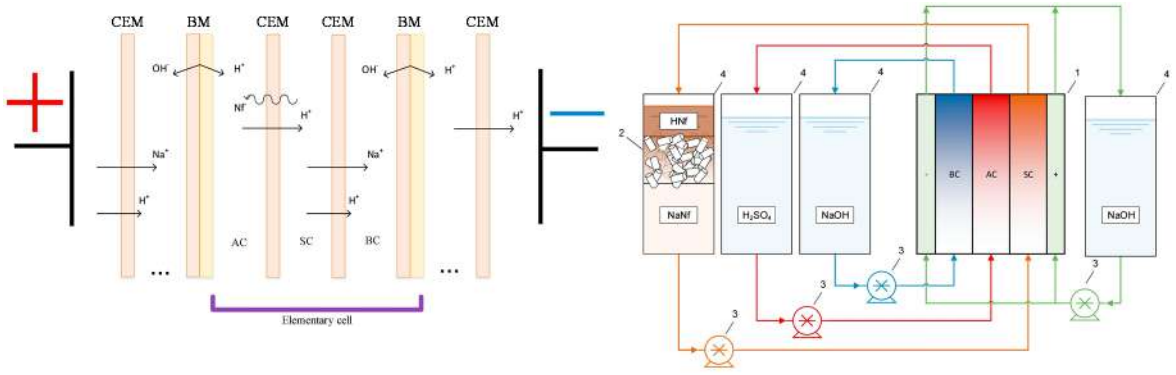

(**a**) (**b**)

Figure 18. BMED recovering naphthenic acids from sodium naphtenates: (**a**) BM-CEM-CEM configuration; (**b**) flow scheme with electrodialyzer (1), Raschig rings (2), pumps (3) and tanks (4). Reproduced (adapted) with permission from [321], published by Elsevier, 2019.

4.3. Desalination

Several industrial processes originate salty wastewater, which needs to be desalinated before its reuse or discharge. To this end, the use of ED has been studied for the following main types of wastewater from industrial activities: produced water from oil and gas extraction (Section 4.3.1), wastewater from refineries and petrochemical industries (Section 4.3.2), drainage wastewaters from coal mining (Section 4.3.3), and wastewater from power plants (Section 4.3.4).

4.3.1. Oil and Gas Extraction

Operations of oil and gas extraction produce large volumes of effluents. The amount of water produced worldwide as a by-product of oil and gas production is ~250 × 10^6 barrels/day, i.e., approximatively triple the produced oil [322]. During some extractions of oil and gas, water can be brought to the surface, as present in (or nearby) the hydrocarbons reservoir, or because intentionally injected with additives to enable the withdrawal. Water is pumped during extraction of unconventional gases, such as coal seam gas and shale gas. The former (known also as coal bed methane), which is adsorbed to the coal surface, is released up to ~1 km underground by effect of a depressurisation applied by wells pumping water from the seams. The latter is extracted from greater depths via hydraulic fracturing, i.e., rocks fracturing by injecting a high-pressure liquid (water with chemicals) from vertical or horizontal wells, thus producing flow-back water. The produced water is also generated during oil recovery enhanced by the polymer flooding technique, which consists of injecting a high-viscosity aqueous solution with soluble polymers that improves the oil sweep efficiency by a less mobile phase.

The produced water composition is strongly site-specific. Total Dissolved Solids (TDS) may amount from some to ~300,000 mg/L [322], being 200–40,000 mg/L in coal seam gas produced water [323] and more in shale gas produced water [324,325]. Polymer flooding produced water falls in the lower part of this range.

Additionally, produced waters contain oil, organic compounds, suspended solids, heavy metals and natural radioactive materials. Therefore, treatments (e.g., biological and physico-chemical processes) are needed before reuse/discharge. Membrane processes [322–327], including ED for desalination, can be adopted.

Two ED applications are documented in [328]. After de-oiling and removal of dissolved organics (floatation and fluidized bed reactors), the produced water from a conventional well was desalinated, attaining a TDS removal of ~89% from 9100 ppm. Coalbed methane produced water (TDS up to 27,000 ppm) was recovered by 80–90% by mobile ED units, and was reused for fracturing.

ED experiments with simulated produced waters (TDS from ~4400 mg/L to ~97,600 mg/L through the diluate, 25 g/L NaCl through the concentrate) were carried out in order to evaluate the attainment of standards for different reuses (targets of 500–5000 mg/L TDS) [329]. At low feed concentrations, regardless of the composition, it was possible to attain the concentration targets with E_{spec} of ~1.2 kWh/m^3, while at high concentrations it was not feasible due to exaggerated E_{spec} values (more than 20 times higher) or even to unattainable targets. Several lab-scale tests exhibited promising results, even for hypersaline solutions [330–332]. Cost analyses (based on experiments with NaCl solutions) and models showed that ED is a cost-effective method for brackish water [333], but, if optimized, it can be competitive also for high salinity feeds [331]. However, the system behaviour should be characterized by tests with real feeds, where other ions are present.

With simulated produced waters from shale gas fracking (3% or 6% NaCl with 1000 or 4000 mg/L Ca^{2+}), scaling at the cathode chamber was mitigated by an MVC end-membrane (Ca^{2+} flux decreased by 47–73%), thus obtaining a current density increase of ~40% [334]. Both simulated and real produced waters from shales were then used [335]. After pre-treatment (NaOH dosage, settlement and MF) and, in some cases, dilution, the field samples were partially desalinated by ED (feeds with 25,000–44,600 mg/L TDS, removals up to ~60%) showing similar performance compared to simulated effluents. Operations with a periodic pulse polarity-reversal enhanced the ion migration by temporarily disrupting the stagnant layer of Ca^{2+}, Mg^{2+} and Ba^{2+} retained by the MVC. Nevertheless, the occurrence of some precipitation of $Fe(OH)_3$ on any IEM suggested to boost the pre-treatment.

For reusing polymer flooding produced water, TDS must be reduced at 500–1000 ppm because higher concentrations could lessen the viscosity of the solution. ED desalination can be applied (Figure 19), and has been demonstrated by pilot-/large-scale plants [336,337]. Serious fouling issues occur, and its mechanisms were investigated along with fouled membranes characterisation [338–341], proposing chemical cleaning strategies [337,342]. Synthetic solutions at 5000 mg/L (brackish water) or 32,000 mg/L (seawater) TDS and with 1.0 g/L partially hydrolysed polyacrylamide (HPAM) were reusable after ED desalination (concentrate feed with 5 g/L NaCl) with small replenishment of polymer (~25% was withhold in the stack) [343]. η was 85–99% and E_{spec} was 0.5–6 kWh/m^3. Moreover, a preferential removal of divalent ions was feasible, especially at low current densities [344]. Separating multivalent ions is desirable to allow polymer-flooding produced water to be reused, since they have the most significant effects in reducing the solution viscosity (calcium and magnesium) and could lead to scaling and reservoir souring. Tests with different solution compositions showed that fouling issues were associated mostly to HPAM adsorption on AEM and formation of a gel layer favoured by divalent cations [345]. However, the gel layer was significantly removed by application of current reversal and use of foulant-free solution. The minimisation of the gel layer formation was then obtained by applying pulsed electric fields [346]. Oily compounds (synthetic solution with 53.3 mM NaCl plus HCO_3^-, SO_4^{2-}, Ca^{2+} and Mg^{2+}, 250 mg/L HPAM and 2 mg/L crude oil) increased slightly membrane fouling, but made the HPAM gel layer less stable. The best condition (1 s/1 s of pulse/pause) led to a reduction of ~35% in E_{spec} (~0.6 kWh/m^3).

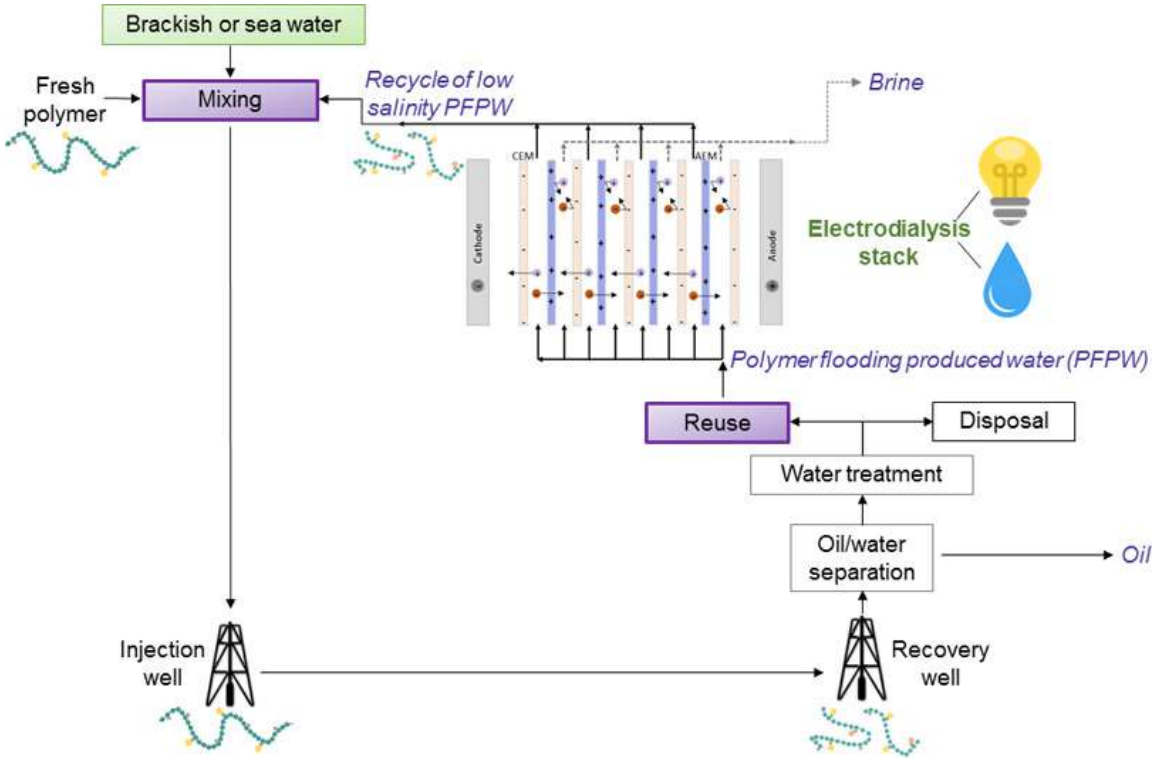

Figure 19. Scheme of ED desalination of polymer flooding produced water. Reproduced from [343], published by Elsevier, 2018.

One study proposed reverse electrodeionisation (REDI) for simultaneous energy recovery and water reuse by controlled mixing between treated fracturing produced water and fresh water (needed for replenishment) [347]. The REDI diluate contained IXR-wafers to lessen the electrical resistance. The highest P_d was 0.9 W/m^2 along with a $P_{d,net}$ of 0.79 W/m^2 by using produced water at 162 mS/cm (~130 g/L, after NF) coupled with fresh water at 1 g/L, without observing fouling. Assuming the use of 5×10^6 gallons and 60% water recovery from drilling, rough economic calculations show an average increase in revenue over 300,000 $/(year·well). However, the profit will depend strongly on the process (mainly capital) cost.

4.3.2. Refineries and Petrochemical Industries

Petroleum refineries use water for many processes [348,349]. However, cooling processes are responsible for ~90% of overall water consumption [349]. Refinery wastewaters, including cooling tower blowdown, are sent to treatment plants [350], and ED can be adopted for desalination.

A pilot EDR was installed (late 1980s) at STANIC Industria Petrolifera (Livorno, Italy) [351]. The effluent from the biological treatment (~1500 ppm TDS) was desalinated by ~90%, thus providing cooling tower makeup and boiler feeding, along with a concentrate suitable for discharge, and kicking off the construction of a 180 m^3/h full-scale plant.

A pilot EDR was used as pre-desalination step followed by RO for a tertiary effluent (~1150 mg/L TDS) from petrochemical industry [352]. Two ED modules (75 cell pairs per each, with a total area of 28.8 m^2) were used either in series or in parallel mode. The EDR step removed up to ~90% of TDS, while the EDR-RO hybrid system achieved overall removals above 90% for several physico-chemical parameters, with 41% water recovery (75% in EDR, and 50% in RO). Water recovery can be boosted by hybrid schemes in which ED treats the RO brine retentate (see Section 6.1.3).

4.3.3. Coal Mines

Coal mining drainage waters are brines with high salt content that must be reduced to allow water reuse. An industrial EDR application at Tutuka power station (South Africa) was upgraded to a more than doubled capacity (13,200 m^3/day) to desalinate mine water as well (2500 mg/L TDS) [353] (see Section 4.3.4).

EDR tests with coal mine effluent at low concentration (~2100 mg/L TDS) were performed at single pass with a diluate velocity ten times the concentrate velocity [354]. Despite the high super-saturation level of calcium sulphate and calcium carbonate in the concentrate, crystallisation was avoided by the insufficient residence time, thus preventing scaling. Water recovery of ~90% and salts removal of ~70% were obtained. ED brine valorisation by salt production via two-stage ED (prior to evaporation-crystallisation) was studied with a coal mine solution with 32.8 g/L Cl^-, finding E_{spec} values in the order of 10 kWh/m^3, and producing a sufficiently pure concentrate [355]. Then, a combined NF-ED-RO system was proposed [356], supported by additional experiments [357]. An alternative way of coal mine brine valorisation could be represented by energy recovery through RED [358]. Artificial solutions simulating coal mine brine (111 g/L NaCl) and fresh water (0.56 g/L NaCl) produced a $P_{d,max}$ of 0.87 W/m^2 and a corresponding $P_{d,max,net}$ of 0.71 W/m^2. An investment cost of 3 $/kWh was estimated by assuming a peak power of ~1 W/m^2 (low-resistance membranes), showing that the economic feasibility is strongly dependent on the membrane cost.

Sulfide minerals (pyrite, FeS_2) can be oxidized when in contact with water and oxygen, thus resulting in acid mine drainage that contains sulphate, iron and other (heavy) metals. Samples collected from different locations in a carboniferous, with pH < 3 in most cases and different compositions (conductivity from 1155 to 15,300 µS/cm, SO_4^{2-} from ~500 to ~8000 mg/L, various cations) were desalinated by ED (after settling and MF) achieving removals of 97–99%, thus recovering the diluate [359]. Iron precipitation was observed on CEMs, thus long-term operations could require pre-treatment to prevent scaling. A reduction in membrane resistance was found at higher current densities with solutions of $Fe_2(SO_4)_3$, attributing this behaviour to the $FeSO_4^+$ dissociation into more mobile Fe^{3+} and SO_4^{2-} ions at the boundary layer [360]. Moreover, a significantly different selectivity was observed between homogeneous and heterogeneous CEMs immersed in mixtures with Na_2SO_4.

4.3.4. Power Plants

Power plants' cooling tower blowdown can be desalinated by ED. The industrial EDR with 7-year operation at Tutuka power station cited in Section 4.3.3 was accomplished in ZLD approach [353]. The plant, upgraded (13,200 m^3/day) also to treat mine water, received a feed with 2500 mg/L TDS with ~50% $CaSO_4$ saturation. After pre-treatment with HCl dosage for scaling inhibition, chlorine dosage against organics, and coagulation–filtration for suspended solids removal, the EDR plant recovered water by 75% at η of 86%, with attractive costs and long membrane life.

Cooling tower blowdown (conductivity from 2.3 to 3.5 mS/cm, flow rate of 2.3 m^3/h) was treated by including EDR desalination in the pilot facility (lamella separator, UF, MF, EDR) in Terneuzen, The Netherlands [361]. The ED stack comprised four hydraulic stages and two electrical stages. Normalized parameters were introduced for pressure drop, IEM resistance and η to control, monitor and optimize the process. In a 2-month operation, η was stable.

4.4. Treatment of Other Wastewaters

This section reports studies on ED methods (for separation, desalination, concentration, regeneration or energy recovery) applied to other industrial wastewaters that have not been presented above. Tables 2 and 3 regard effluents with and without organic matter, respectively.

Table 2. Other studies on industrial wastewaters without organic matter (adapted from [23]).

Wastewater	Treatment Process	Main Remarks	Ref.
NaCl + Na_2SO_4 solution, 0.01 M each	ED with MVAs	Layer-by-layer composite AEM, $P^{Cl^-}_{SO_4^{2-}} = 11.5$	[312]
NaCl + Na_2SO_4 solution, 0.05 M each	ED with MVAs	MVAs with hydrophobic alkyl side chain, max $P^{Cl^-}_{SO_4^{2-}} = 13.1$, long-term stability	[362]
NaCl + $MgCl_2$ or LiCl + $MgCl_2$ solutions, 0.1 M each	ED with MVCs	Zwitterion structure MVCs, $P^{Na^+}_{Mg^{2+}} = 58.4$ and $P^{Li^+}_{Mg^{2+}} = 6.5$	[363]
NaCl+$MgCl_2$ solution, 0.1 M each	ED with MVCs	Zwitterion structure MVCs with hydrophobic alkyl side chain, max $P^{Na^+}_{Mg^{2+}} = 25.3$	[364]
Model solutions with two salts with the same counter-ion among NaCl, Na_2SO_4, $MgCl_2$, $MgSO_4$ and $NaNO_3$, 0.01 M each	ED or ED with MVMs	Max separation efficiency ~68% for cations by MVMs (comparable to NF), but lower for anions	[365]
NaCl + Na_2SO_4 solution, 8 mM each	SED	SO_4^{2-} purity > 85%, $\eta \approx 50\%$	[39]
$MgCI_2$ + Na_2SO_4 solutions, 0.3–0.5 M each	EDM	$\eta > 100\%$, $E_{spec} \approx 0.9$–1.6 kWh/kg, $MgSO_4$ purity ~98%	[40]
Na_2SO_4 solutions, 0.01 M/0.3 M	RED-alkaline polymer electrolyte water electrolysis	$V_{OC} \approx 12$ V (200 cell pairs), $P_{d,max} = 0.04$–0.11 W/m^2 by changing solutions velocity and temperature, H_2 production 50 cm^3/(h·cm^2)	[366]
Catalyst plant model wastewater $\left(Na^+, Cl^-, Mg^{2+}, Ca^{2+}, SO_4^{2-}\right)$, 25.8 g/L TDS	Two-stage ED with MVCs	On-line membrane modification, $P^{Ca^{2+}}_{Na^+}$ reduced from 0.36 to 0.11, $P^{Mg^{2+}}_{Na^+}$ from 0.81 to 0.12, η = 75–92%, 1 g/L diluate, stable long-run, but larger water transport, membrane resistance, and E_{spec} (up to ~35% more)	[367]
Photovoltaic industry simulated wastewater, 120–180 mg/L NaF and/or 750–2000 mg/L $NaNO_3$	ED	With single salt, max removal efficiency ~60% and 75% for F^- and NO_3^- in 6 min, under optimal conditions E_{spec} = 0.25–0.36 kWh/m^3; with mixture, ion competition affected only F^- removal	[368]
F^- solutions: single salt at 25–200 mg/L, binary and ternary mixtures with 100 mg/L $F^- + Cl^-$ and/or SO_4^{2-} at same equivalent concentration	ED	High removal efficiencies, E_{spec} = 0.02–0.49 kWh/m^3, Cl^- affected F^- separation, SO_4^{2-} did not	[369]
Synthetic secondary effluent of graphite industry, 10–30 mg/L NaF, 6 g/L NaCl	ED	Response surface methodology, F^- removal 99.69% with E_{spec} = 0.76 kWh/m^3 under optimal conditions	[370]
B artificial wastewater, 25–100 mg/L; binary or ternary mixtures with 100 mg/L B + Cl^- and/or SO_4^{2-} at same or doubled equivalent concentration	ED	Max removal of B ~80%, enhanced at high pH (10.5) due to a predominance of $B(OH)_4^-$, hindered by Cl^- and not by SO_4^{2-}, E_{spec} = 0.02–1.24 kWh/m^3	[371]
Acidic model solution from B-selective sorbents regeneration, 0.2 M HCl or 0.1 M H_2SO_4 + 1.0 or 5.2 g/L H_3BO_3	Two-stage ED with pH increase	Regenerating acid (HCl or H_2SO_4) recovered in the concentrate ~90%, ~93% of H_3BO_3 (non-ionic) retained within the diluate and concentrated in the 2nd stage after alkalinisation, reusable solutions	[372]
B-containing industrial landfill leachate, 62.8–76.5 mg/L B (+ SO_4^{2-}, Cl^-, Ca^{2+} and Mg^{2+})	Two-stage ED with pH increase	Desalination in the 1st stage 80%, $B(OH)_4^-$ removal in the 2nd stage 97% under alkaline conditions, max η = 25–28%, estimated cost 1.27 \$/m^3	[373,374]
Model nuclear power plant effluent, 60–400 mg/L H_3BO_3	Three-compartment EDI	Max removal ~45%, optimal pH = 10	[375]
NH_4NO_3 model wastewater from fertilizer production, 0.012 M	ED	Thin heterogeneous IEMs vs. commercial ones: higher limiting current density due to larger back-diffusion and electroconvection; lower alkalisation due to lower water dissociation	[376]
Synthetic solutions with single acid or salt: H_2SO_4, HNO_3, NH_4NO_3, NaCl, LiCl, Na_2SO_4, 0.06–0.3 M	ED or BMED-ED	ED concentrator without flow through concentrate chambers, acid concentration 1.16 M at η = 89% for BMED and 26% for ED, E_{spec} = 0.83 kWh/mol SO_4^{2-}	[377]
Alkaline liquid from bauxite solid residue (Bayer process) washing (2.4 g/L Al^{3+}, $+K^+$, Na^+, F^-, SO_4^{2-} …)	ED with aeration	NaOH recovery, $NaAl(OH)_4$ separation, TDS and OH^- removal 61.3% and 76.6%, η = 60%, E_{spec} = 11.15 kWh/kg	[378]
Synthetic or real wastewater from mineral carbonation for CO_2 sequestration, 0.05–1.0 M $(NH_4)_2SO_4$, 0.05–0.54 M $(NH_4)HSO_4$, (+$MgSO_4$, NH_3, Fe(II), Fe(III) …)	BMED	Different setups for regenerating rock-derived solutions after leaching or after carbonation, E_{spec} = 1.7–350 MJ/kg NH_4^+	[379]
Model solution from Li-ion waste batteries, Li^+ and Co^{2+} 0.02 M each	BMED with complexation	Co-EDTA chelated anions and Li^+ separated in the acid and base compartments, respectively, removals 99%, but Co absorption in AEM; metal recovery enhanced in semi-batch operation for the feed	[380]

Table 3. Other studies on industrial wastewaters with organic matter (adapted from [23]).

Wastewater	Treatment Process/Exp. Device	Main Remarks	Ref.
Solutions with octanoic acid or anionic surfactants; alkaline bleach plant filtrate from sulphate pulp mill, 1370 mg/L COD	IEM resistance measurement cell	Slight inorganic fouling on CEM by bleach plant filtrate, significant organic fouling on AEM by all solutes	[29]
Solutions with carboxylic acids (propanoic, octanoic and decanoic acid); alkaline bleach plant filtrate from sulphate pulp mill, 1850 mg/L COD	IEM resistance measurement cell, ED	No CEM fouling, AEM fouling due to organic anions, especially compounds with longer chain, and at higher currents	[381]
Solutions with 16 charged or neutral trace organic contaminants, 0.1 mg/L with 100 g/L NaCl	ED	Adsorption governed by electrostatic interactions, transport mostly diffusion driven, migration of charged components only at very low NaCl concentration	[382]
Solutions with NaCl, Na_2SO_4 or $MgCl_2$ and acetic acid, phenol or glucose, 0.8 eq/L salts and 0.1 M organics	ED	Phenomenological model: convection-diffusion of neutral organics affected by steric effects and ion hydration	[383]
Solutions with NaCl, Na_2SO_4 or $MgCl_2$ and acetic acid, phenol, glucose or acetate	ED	Phenomenological model: transport of several organics larger with SO_4^{2-} than with Cl^-, opposite trend for phenol	[384]
Wastewater from bisphenol A diphenyl phosphate production, 4.5–4.8% total salt (NaCl and sodium phenolate), pH = 13.2–13.5, diluted with pure water	RED-ED	Ultrapure water fed into the RED diluate, V_{OC} up to 1.65 V (10 cell pairs) and $P_{d,max,net}$ up to 1.12 W/m^2 in RED at dilution ratio 1.0:0.5, E_{spec} lower than that of standalone ED (17.65 vs. 25.32 kWh/m^3) with 27.4% pre-desalination in RED	[385]
NaCl-glycerol solution, 1.11–1.67 M NaCl and 0.06–0.6 M glycerol	ED	7 membrane pairs tested, phenomenological model: $C_3H_8O_3$ electro-osmotic co-transport 38–64%, osmotic co-transport 16–41%, diffusion 9–28%, low glycerol/NaCl flux at low glycerol/NaCl and NaCl concentrations	[386]
Simulated dairy wastewater, 10 mM citrate, 1 mM lactate, 30 mM NaCl …	ED	Guanidinium groups in AEM as functional moiety binding oxyanions, enhanced transport of phosphate and citrate	[387]
Diluted effluent from sodium dithionate processing, 35 g/L HCOONa, 30 g/L $Na_2S_2O_3$ …	ED with MVAs	Recovery of HCOONa 69%, with 87% purity, η = 70%, E_{spec} = 96 kWh/m^3	[388]
Steel manufacturing wastewater (Cl^-, SO_4^{2-}, Na^+, Mg^{2+}, Ca^{2+}), 2.8–4.0 mS/cm, 36–72 mg/L COD	Sand filtration-EDR	Water recovery 75%, desalination 92%, concentrate COD below discharge limit, E_{spec} = 0.85 kWh/m^3, operation cost 0.146 \$/m^3	[389]
Secondary effluent from spinning processes, chemical industries, and metal processors (Cl^-, SO_4^{2-}, Mg^{2+}, Ca^{2+}, NO_3^-, PO_4^{3-} …), 7.3 mS/cm, 41.5 g/L COD	Sand filtration-EDR	Lower techno-economic efficiency compared to fiber filtration-UF-RO	[390]
ZnO washing wastewater (Na^+, K^+, Cl^-, Ca^{2+} and SO_4^{2-}), ~0.35 M, 1.2 mM TOC	ED with MVMs	Overall $\eta \approx$ 80%, divalent ions retained, thus scaling prevented, stable long-term performance of pilot plant with removal target of 50% (before evaporation)	[281]
Kraft pulp mill dissolved electrostatic precipitator dust (Cl^-, CO_3^{2-}, SO_4^{2-}, Na^+, K^+), 137 g/L TDS (0.1 wt% TOC in the dust)	ED with MVMs	Selective removal of Cl^- at η = 60–78% and $E_{spec} \approx$ 1 kWh/kg, organics in the dust recycled with the sulphate-rich diluate, no fouling, accumulated dust simply flushed, successful long-term operation, operation saving of 800 \$/1000 ton Kraft pulp	[391]
Paper mill effluent, 6046 mg/L TDS, 390 mg/L COD	MF-ED	Max TDS removal ~90%, water recovery 80%, $E_{spec} \approx$ 0.5 kWh/m^3, concentrate usable as biomass	[392]
Primary textile effluent, 2,980 mg/L TDS, 220 mg/L COD	UF-ED	Desalination ~96%, E_{spec} = 0.9 kWh/m^3, reusable water	[393]
Model textile effluent with 1 g/L reactive blue 194 and 40 g/L Na_2SO_4	Tight UF-based diafiltration-BMED	Pre-concentration at a factor of 8 and diafiltration with 8 diavolumes, UF permeate with low dye content (2.7 mg/L) and 21.06 g/L Na_2SO_4, 99.5% dye recovery, ~99% salt conversion into 99% pure 0.29 M acid and 0.4 M base without fouling, E_{spec} = 4.2 kWh/kg	[394]
Model textile effluent with 0.25 g/L Remazol Brilliant Blue R and 50 g/L Na_2SO_4	BMED	Effect of zeta potential of dye molecule on fouling, fouling controlled by the identification of a "critical salt concentration" below which desalination cannot proceed due to fouling, η =39%, desalination 74%, 72% of Na^+ and 66.9% of SO_4^{2-} converted into base and acid, respectively	[395]
Tannery unhairing effluent, pH = 12, 576 mg/L S^{2-}, 23,289 mg/L COD, 436 mg/L Ca^{2+}, 429.6 mg/L Cl^-	ED with protective UF membrane on AEM	Anti-fouling solution against proteins and peptides, desalination 56%, 90% of organics retained within the diluate, thus water recycling	[396]

Table 3. *Cont.*

Wastewater	Treatment Process/Exp. Device	Main Remarks	Ref.
Almond processing treated wastewater (electrocoagulation and electrooxidation), 7.2 mS/cm, 296 mg/L TOC	ED	Concentration factor of 10 in the concentrate, diluate target 0.5 mS/cm, TOC removal ~70%, water recovery 94%, no fouling, scale-up at pre-industrial scale, E_{spec} = 1.1–2.9 kWh/m^3	[397]
Waste brine from olive pickling process, 103.3 mS/cm, pH = 3.5, 8033 mg/L dissolved organic carbon; coupled with storm water, 3.6 mS/cm	RED	V_{OC} = 1.37 V (~70% of the ideal one, 10 cell pairs), $P_{d,max}$ = 0.59 W/m^2 enhanced (with respect to NaCl solutions at the same conductivities, 0.44 W/m^2) by pH gradient and organic acids (lower resistance)	[398]
Lysine fermentation effluent, 152 mS/cm, 17,800 g/L $NH4_4^+$, 71,000 mg/L SO_4^{2-}, 102,300 ppm TOC	MF-ED	Separation of 73.1% NH_4^+ and 83.5% SO_4^{2-}, E_{spec} = 106 kWh/m^3, pulsed electric field effective against fouling, demineralized waste usable as animal feed, concentrate as fertilizer	[399]
Bio-refinery effluents: molasses effluents, lignocellulosic stream, sugar cane juice, 3.2–72.4 mS/cm, 38–380 g/L COD	ED	Salt removal 96% and 63% from lignocellulosic and molasses effluents, lower from sugar cane juice, low COD loss (< 6.3%), η = 69–104%, E_{spec} = 0.44–1.59 kWh/kg salt	[400]
Bio-refinery effluents: synthetic salt mixtures with sorbitol, molasses effluent	ED	Simplified process model, predictions in good agreement with experimental results	[401]
Vinasse from a distillery producing ethanol from sugar can juice, 30,500 mg/L COD, 11.5 mS/cm	UF-ED with MVMs	K^+ recovery 72%, E_{spec} = 9 kWh/m^3, η = 54%, concentrated stream for fertigation, diluate stream for fertigation or biogas production (anaerobic digestion)	[402]
Solutions of 3-chloro-1,2-propanediol (α-monochlorohydrin or 3-MCH) (model effluent from biodiesel production or other sources), 10 or 30% wt + 0.1 M KCl	BMED	Recovery of glycidol by dehydrohalogenation caused by OH^- in the base compartment, selectivity 96%, η = 64%, glycidol distilled with 75.6% yield	[403]
Model antibiotic effluent with 0.95 g/L penicillin, 1 g/L SO_4^{2-} and 1 g/L bovine serum albumin	ED with UF membrane, 3-comp. (AEM-UF-CEM)	Penicillin recovery ~20%, removal of SO_4^{2-} from feed and antibiotic product 90%, no fouling, E_{spec} = 0.058–0.082 kWh/g, estimated profit 6850 $/ton produced penicillin (8 L/day wastewater)	[404]
Effluent from anaerobic digester–decanter, 13,800 mg/L COD, 1700 mg/kg total N, 1800 mg/kg Cl^-, 2,900 mg/kg Na^+ …	ED	Separation 70–96% for monovalent ions, < 50% for divalent ions, E_{spec} = 6–11 kWh/m^3 for water recovery 50–95%	[405]
Simulated supernatant of excess sludge mixed with influent from anaerobic-aerobic biological treatment, 100 mg/L P *	ED or ED-BMED	ED : PO_4^{3-} recovery 95.8%, ED-BMED: 0.075 M H_3PO_4 recovered, $\eta \approx$ 70–80%, E_{spec} = 5.3–29.3 kWh/kg	[406]
Effluent of upflow anaerobic sludge blanket reactor from potato processing, 2.5 mM phosphate $\left(+K^+, NH_4^+, Cl^- \ldots\right)$*	SED-struvite precipitator	6.8 mM phosphate in SED product (from 0.8 mM initial product, struvite effluent), average overall $\eta \approx$ 70%, desalination 95%, phosphate recovery 93%, E_{spec} = 16.7 kWh/kg phosphate	[407]

* These effluents did not contain organic matter; however, as they come from biological treatment, they could have, in general, residual organics.

5. Municipal Wastewater and Other Effluents

Desalination via ED can make treated municipal wastewater reusable, as shown by several field plant applications (Section 5.1). As an alternative, it could be used as a low-salinity solution coupled with seawater for recovering salinity gradient energy (Section 5.2). Additionally, ED methods are under study to recover nutrients (as well as water) and, in some cases, volatile fatty acids (VFAs) from treated wastewater and related/similar effluents (Section 5.3). Another ED application studied is the regeneration of liquid desiccant solutions for air conditioning (Section 5.4).

In addition, ED methods have been proposed for desalinating drainage wastewaters for agricultural reuse [408], and the experimental screening/optimisation has been studied [409].

5.1. Desalination of Municipal WWTP Effluents

Secondary or even tertiary effluents from wastewater treatment plants (WWTPs) are normally not reusable in irrigation, aquifer recharge, or industrial processes. When the salinity of treated effluents is relatively high, it can be suitably reduced by ED. MF is often used before ED to remove suspended solids

and microorganisms. Pre-treatments, EDR operation and cleaning procedures against fouling can maintain or restore, at least partially, IEMs properties.

A rapid sand filtration-activated carbon-EDR plant of ~1100 m^3/day capacity supplied treated wastewater to Moody Gardens plants and fishponds (Galveston, Texas) [410]. Other EDR plants (Middle East) were cited in the same paper. In Gran Canaria, a pilot MF-EDR plant was tested for irrigation water reuse [411]. The EDR achieved reductions of conductivity and TDS of 89% and 74%, respectively, from a feed with 2.7 mS/cm average conductivity and 1565 mg/L average TDS. Among the other physico-chemical parameters, the following removals were obtained: 79% ammonia, 88% nitrate, 59% phosphate, 83% BOD_5, 40% COD, 50% faecal coliforms, from feed concentrations of 24 mg/L, 50 mg/L, 56 mg/L, 18 mg/L, 65 mg/L, 4 colonies/100 mL, respectively. The chance of slightly reducing capital costs compared to RO (by ~6%) was shown.

In another plant with UF and RO for irrigation reuse (Las Palmas, Gran Canaria), the pilot EDR produced 100–140 m^3/day of desalted water (<500 mg/L) with 82–90% recovery [412]. Metal membrane MF and ED provided a stable effluent quality over a 6-month testing, reducing by more than 90% most physico-chemical parameters, including nutrients [413]. A pilot plant with 144 m^3/day capacity consisted of 500 μm pre-filtration, coagulation-disinfection ($Fe_2(SO_4)_3$ and NaClO), 15 μm multimedia filtration and EDR [414]. EDR performed a desalination of ~70% (1104 mg/L TDS in the EDR feed), thus providing an effluent for horticultural reuse with TDS below the 375 mg/L target identified by guidelines. E_{spec} was 1 kWh/m^3 (60% of which was in EDR) and 82% of wastewater was recovered with an estimated operating cost of 18 $cents/$m^3$. A further benefit from ED is the hypochlorite production in the anolyte, to be used then for disinfection [415]. Pilot MF-RO and MF-EDR plants were compared for a tertiary effluent containing endocrine disrupting chemicals, and pharmaceuticals and personal care products, showing that only RO was capable of removing them, as expected [416]. The same conclusion was drawn from another study, which exhibited moderate removals of some compounds (48–58%) and low removals for other compounds [417].

ED desalination was tested for 930 h during one year with a macrophytes pilot system effluent [418]. The conductivity reduced from ~0.67 mS/cm to 0.2 mS/cm, obtaining an effluent appropriate for reuse (e.g., in cooling towers) with only slight fouling. Further tests were conducted with the secondary effluent from a small WWTP for a university campus sewage [419]. The conductivity of ~1 mS/cm reduced to 0.05–0.1 mS/cm, with removals above 80% for cations and 70% for anions, and with E_{spec} values of 0.104 kWh/m^3 increased by fouling to 0.119 kWh/m^3. Other physico-chemical features (colour, turbidity, COD, BOD, etc.) were mildly cut down, thus providing an effluent suitable for fish farming after simple pH correction, but requiring some further treatment to reduce BOD and turbidity in case of urban and agricultural reuse.

Different schemes coupled ED and forward osmosis (FO). For example, FO extracted water from a secondary effluent (0.05 M salt concentration) to provide it to a draw NaCl solution then sent to the ED stage [420] (Figure 20). Ions, organic and inorganic substances were rejected in the FO retentate, while the draw stream enriched in water (diluted from 0.5 M to 0.2 M) by osmosis went to the ED. This yielded high-quality water (0.81–0.88 mS/cm) and the draw solution for the FO. ED driven by photovoltaic energy exhibited E_{spec} of 4.98–5.57 kWh/m^3 and η of 78.2–100%, while the estimated cost for a system producing 130 L/day potable water was ~3–5 €/m^3.

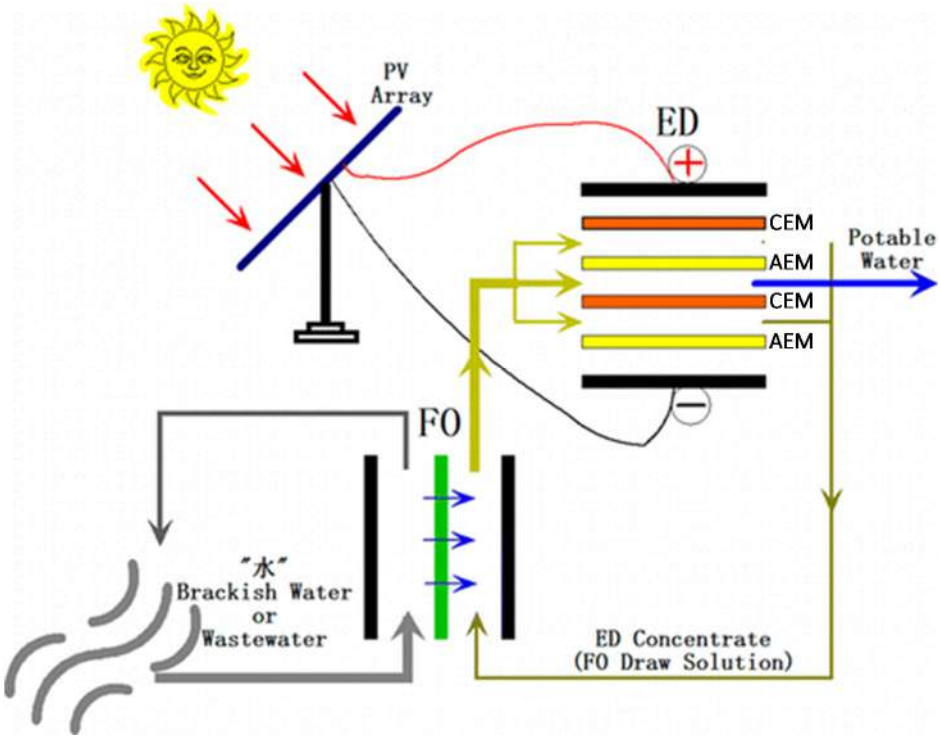

Figure 20. Scheme of FO–ED integrated process for wastewater (or brackish water) reclamation. Reproduced (adapted) with permission from [420], published by American Chemical Society, 2013.

An osmotic membrane bioreactor–ED system treated a synthetic primary effluent (300 mg/L COD, 0.51 g/L salts, 1.1 mS/cm) [421]. FO and biological degradation by activated sludge occur in the bioreactor, which thus suffers from salt accumulation caused by osmosis to the draw side and contrary solute flux. This would result in increased costs for draw replenishment, as well as in discharge issues and microbial growth inhibition. In this study, ED desalted the treated wastewater, by achieving a salinity build-up mitigation (conductivity maintained at 8 mS/cm), which allowed for (i) an increase by 6 times of the biological treatment duration (24 days), and (ii) the waste salt recovery, thus providing the concentrate draw solution. η was 41.6–76.2% and E_{spec} 1.88–4.01 kWh/m^3. In another hybrid process, ED mitigated the salinity build-up in the FO (submerged module) feed (secondary wastewater with 29.3 mg/L COD, ~0.5 mS/cm) by using a fertilizer draw solution with 0.5–2 M $(NH_4)_2HPO_4$ [422]. A diluted fertilizer was recovered by FO from wastewater, while 96.6% of the fertilizer lost by reverse flux (63 mg/L ammonium and 83 mg/L phosphate) to the feed was recovered through ED, which also returned the desalinated feed to the FO module. E_{spec} of the system was 0.72–1.49 kWh/m^3.

5.2. Energy Recovery

WWTP effluents can be used as diluate coupled with salty waters as concentrate in RED stacks recovering energy. The most abundant high-salinity solution is represented by seawater, thereby implying possible applications in coastal areas.

RED experiments with artificial NaCl solutions (diluate 0.002–0.08 M, concentrate 0.6 M) showed that the optimal diluate concentration maximizing the power output ($P_{d,max}$ of 0.39 W/m^2) was in the range 0.01–0.02 M [423], which often corresponds to the concentration range of WWTP effluents from biological treatment. By increasing the temperature from 25 °C to 60 °C, $P_{d,max}$ increased by 60%, suggesting that

co-locating RED with a thermal power plant where the solutions are pre-heated (e.g., cooling tower seawater) can boost the energy recovery. Moreover, the seawater–WWTP effluent RED process may be used as a pre-desalination step before RO, by providing great potential of reducing the energy consumption of seawater desalination plants [424]. The RED unit may also be operated under "assisted" conditions, in which the applied electrical current overcomes the short-circuit current, thus requiring a lower membrane area [425]. Simulation results showed that hybrid RED-RO systems either with assisted or conventional RED yielded cost savings compared to standalone SWRO [426]. However, a critical issue affecting these RED-RO systems is the potential contamination of the seawater by organic micropollutants that may be adsorbed and transported from the impaired water [427]. In contrast, this problem is less important in RO-RED schemes (Section 6.3), where the RED process is fed by the RO reject brine and the WWTP effluent.

Several studies tested RED with real WWTP effluents and seawater. After filtration by a 10 μm filter, a treated wastewater at conductivity of 0.44 mS/cm (~0.002 M) coupled with seawater (46.2 mS/cm) produced a $P_{d,max}$ of 0.15 W/m^2 [398]. The low concentration of the diluate led to a high electromotive force (V_{OC} of 1.66 V with 10 cell pairs, 70% permselectivity), but limited the power density due to the high electrical resistance. The presence of natural organic matter (NOM) in the WWTP effluent (16.3 mg/L dissolved organic carbon) increased the resistance, causing a reduction in $P_{d,max}$ of ~17% with respect to a model solution lacking NOM.

Higher values of $P_{d,max}$, i.e., up to 0.38 W/m^2, were obtained by testing a pilot plant [428]. The WWTP effluent was treated by dual-media filtration, bag filter (50 μm) and cartridge filters (5 μm), while the seawater underwent only the 5 μm filtration. The RED feed solutions had conductivity of 1.3–5.7 mS/cm and 52.9–53.8 mS/cm, respectively. The transport of inorganic solutes and NOM (4.3 mg/L dissolved organic carbon in the treated wastewater) was investigated. Over 12 days, the power density was on average ~20% lower than the highest one. It was observed a slight increase of the IEMs resistance, which can be attributed to fouling and effects of divalent ions. However, the reduction of P_d was mainly caused by precipitates clogging the cathode chamber, where the wastewater was used as electrolyte (high pH due to the hydrogen evolution reaction). Organics at low molecular weight were transported towards the seawater compartments. Therefore, attention should be paid to this aspect in case RED is followed by RO. Pressure drops increased continuously over 12 days up to almost 3 and 1.5 times in the wastewater and seawater compartment, respectively, due to spacer-filled channels clogging at the inlet regions. This may affect significantly the net power (not calculated). Therefore, suitable pre-treatments and cleaning procedures should be adopted.

The same $P_{d,max}$ (~0.38 W/m^2) was recorded by another pilot RED fed with treated water (anaerobic-oxix activated sludge process) at conductivity of 1.0–2.5 mS/cm and seawater at 50 mS/cm [429]. Actually, the seawater solution was obtained by mixing a desalination brine with the treated water. Suspended particles were removed from both streams by cartridge filter and fibre filter (10 μm pore size). V_{OC} was 28.6 V (200 cell pairs), 20% lower than the theoretical one due to effects of divalent ions and reduction of driving force along the channels. A 5 wt% Na_2SO_4 electrolyte was fed to the electrode compartments, obtaining 0.9 L/h H_2 with ~100% efficiency by cathode reduction. Without pre-filtration, the performance was stable over 300 h, but a subsequent reduction of power density was observed (up to 80% after 800 h). Cleaning without chemicals removed clogging from the disassembled stack and restored its performance. However, cleaning in place methods should be developed with short interruptions of the RED process.

Filtration pre-treatments of a domestic WWTP effluent (1.13 mS/cm) were compared, i.e., 100 μm filtration, rapid sand filtration or river bank filtration [430]. Seawater (48.35–58.38 mS/cm) was pre-treated with sand filtration, bead filtration and UV. During 40-day RED testing, the pressure drop increased by only 0.09–0.18 bar from the initial value of 0.03–0.04 bar when using 100 μm filtration and rapid sand filtration, respectively. With an almost stable $P_{d,max}$ of ~0.25 W/m^2, $P_{d,max,net}$ was 0.23 and 0.22 W/m^2, respectively. Instead, the RED operation with river bank filtration or without pre-treatment exhibited high

pressure drops (~0.6 bar on average) and low $P_{d,max,net}$ (~0.06 W/m^2), despite alkaline and acidic cleanings. Inlet and outlet regions of spacer-filled channels were critical points of biofilm development even at the seawater side (biological growth during storage).

The pre-treatment with polyaluminium chloride coagulant (and 0.45 μm filtration) was tested for reclaimed water (~0.5 mS/cm) [431]. Filtered seawater (~48.5 mS/cm) was the RED concentrate. Polyaluminium chloride residue affected the RED performance by increasing the CEM resistance and, thus, by reducing the power density. However, the optimized dosage removed up to 50% of the organic matter (from ~6.5 ppm TOC) and resulted in a $P_{d,max}$ of ~0.42 W/m^2, increased by 20% with respect to that obtained with filtration only. Multivalent ions and NOM, instead, reduced $P_{d,max}$ by ~20% with respect to that produced by model solutions. The long-term operation should be tested.

A secondary effluent was treated by coagulation-flocculation, decantation and 10 μm filtration [432]. The treated stream (1.8 mS/cm, ~0.008 M NaCl) was used with 1 μm-filtered and UV-disinfected seawater (54.7 mS/cm, ~0.5 M NaCl) for RED energy recovery, showing a stable performance over 480 h. The treatment before RED and the slight increase of salinity after RED provided a water quality acceptable for reuse. V_{OC} was 3.45 V (20 cell pairs) and $P_{d,max}$ was 1.43 W/m^2 without observed fouling. This is the highest value of P_d recorded so far with this kind of streams. However, no data on pressure drop nor on $P_{d,net}$ were provided.

RED was performed with both compartments fed by treated wastewater [433]. Similarly to the previous cases, the low-salinity solution was a reclaimed urban WWTP effluent (from membrane bio-reactor pilot plant) at conductivity of 0.6–1.8 mS/cm (corresponding to ~0.004–0.016 M NaCl). Instead of seawater, the concentrate stream was a fish canning factory wastewater, treated by a pilot aerobic granular sludge sequence batch air-lift reactor, 5 μm MF, and acidification at 4 < pH < 5, which had a conductivity of 47.0 or 87.5 mS/cm. During long-term experiments of 29 days, fouling and increase of pressure drops (clogging) were observed. Backwashing with short pulses (1–2 s) at high fluid velocity (10 cm/s) was performed. An alkaline solution through the compartment of the fish wastewater was more effective than other solutions, while distilled water through the compartment of the reclaimed WWTP effluent was sufficient. Periodic ED pulses reduced the absorption of foulants, maintaining almost constant the stack resistance. However, fouling issues did not vanish, especially those involving AEMs. Under the best conditions tested, V_{OC} was almost constant around 1.6 V (10 cell pairs), while $P_{d,max}$ declined from ~0.9 to ~0.6 W/m^2. $P_{d,max,net}$ corrected by excluding the effect of the blank resistance declined from ~1.3 to 0.1 W/m^2. Therefore, measures against fouling and clogging should be further studied. Some detrimental effects of divalent ions were observed.

The integration between membrane distillation (MD) and RED was proposed to recover water and energy from urine in off-grid applications [434]. From real urine feed (12.65 mS/cm, 207 mg/L NH_4^+ – N, 6.33 g/L COD), the MD produced a retentate with doubled conductivity (24.1 mS/cm) and a permeate at 0.21 mS/cm. These streams were then used as feeds for an RED unit for partial remixing with energy recovery. $P_{d,max}$ (~0.2 W/m^2) was comparable to that produced by NaCl solutions (0.32 W/m^2). By increasing the temperature from 22 to 50 °C, $P_{d,max}$ could be increased by 70%, as shown by experiments with synthetic solutions, thus prospecting the use of waste heat. In RED tests with recirculation, ~47% of the Gibbs free energy was extracted. In optimized systems, the energy efficiency could be enhanced even compatibly with a good quality of the final diluate.

5.3. Recovery of Nutrients and VFAs

ED methods can recover nutrients from wastewater, thus lowering the ecological impact of discharge (eutrophication) and producing fertilizers. In some cases, VFAs are other valuable components that can be recovered along with nutrients. Studies have been performed on treated municipal wastewater

(Section 5.3.1), excess sludge sidestreams (Section 5.3.2), separately collected human urine (Section 5.3.3), and waste effluents from animal farming (Section 5.3.4).

5.3.1. Municipal WWTP Effluents

Municipal WWTP effluents can provide nutrients, i.e., ammonia, phosphate, nitrate, and potassium, thus producing fertilizers. To this aim, ED systems can concentrate P-based nutrients before precipitation/crystallisation of struvite, i.e., $(NH_4)MgPO_4{\cdot}6(H_2O)$, or calcium phosphates [435].

Several studies have tested SED units with MVAs to fractionate and concentrate phosphate (Figure 21). Experiments with synthetic wastewater (3–7 mM KH_2PO_4 and 13–17 mM NaCl) achieved a phosphate removal of 62.3% with a product concentration of 16 mM at 44% purity, and a Cl^- removal of 87% [436]. Values of η for $H_2PO_4^-$ through the AEM and for Cl^- through the MVA were 26.6% and 63%, respectively. These outcomes were obtained at pH = 12 in the product, as multivalent phosphates (HPO_4^{2-} and PO_4^{3-}) predominate under alkaline conditions. Crystallisation with $CaCl_2$ in a pellet reactor produced hydroxyapatite and brushite with 82.7% efficiency, thus demonstrating the feasibility of the integrated process.

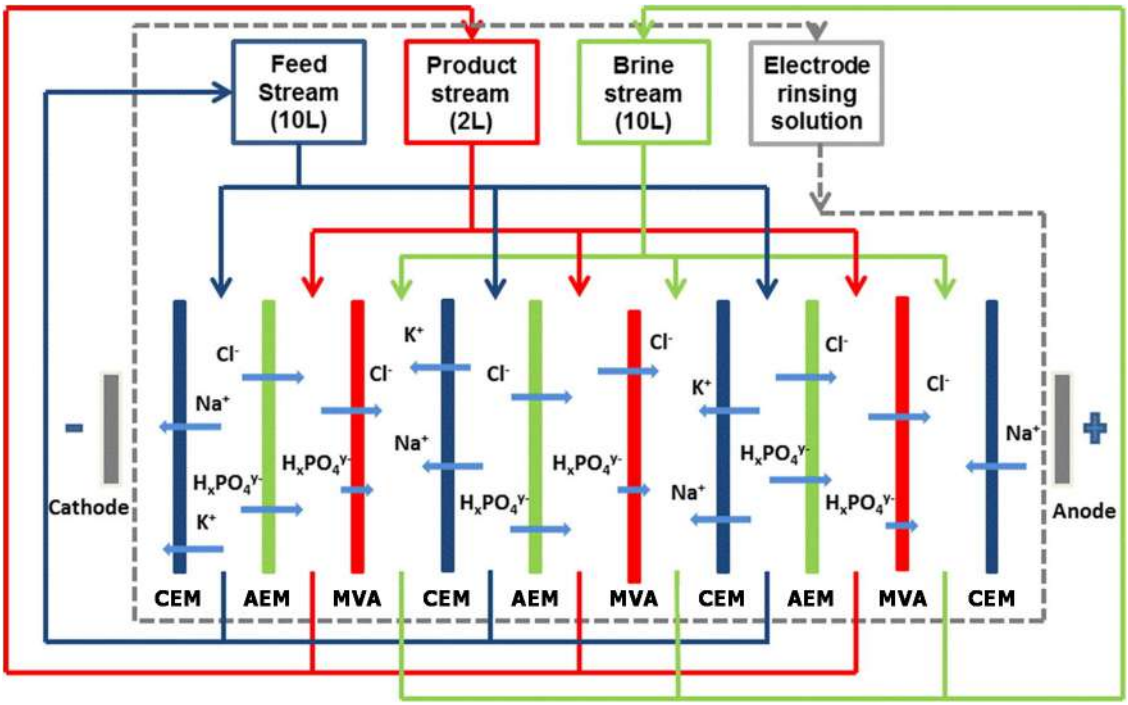

Figure 21. SED stack equipped with MVAs to fractionate and concentrate phosphate. Reproduced (adapted) with permission from [437], published by Elsevier, 2015.

With a more realistic synthetic municipal effluent containing an ion mixture (1 mM KH_2PO_4, and 2 mM NO_3^-, HCO_3^-, SO_4^{2-}, Ca^{2+} and Mg^{2+}), although the process required a longer operation, 41.9% of phosphate was removed and concentrated by 161% in the product, and acid cleaning removed scaling [437]. Other experiments with a synthetic secondary effluent (NaCl, $NaNO_3$ and Na_2HPO_4 with 355 mg/L Cl^-, 30 mg/L N, 10 mg/L P) exhibited recovery efficiencies of 56.97–64.28% for N in the brine and 67.42–73.67% for P in the product, with overall η of 56.7–61% and E_{spec} of 1.63–2.92 kWh/m^3 [438]. The pH in the tank with

the product was adjusted at 10.2–10.5. However, at high values of applied voltage, lower concentration rates of P suggested water dissociation as a likely cause of pH reduction.

Even conventional ED is able to recuperate nutrients [439]. To accomplish a selective separation, a two-stage underlimiting/overlimiting ED was proposed [440]. A model macrophyte-treated wastewater (0.022 g/L $Na_2HPO_4{\cdot}7H_2O$, 0.011 g/L $NaH_2PO_4{\cdot}H_2O$, 0.481 g/L Na_2SO_4) was circulated through both compartments. In the first stage, ions were concentrated by cycles where the diluate was changed once reached 50% desalination (49.8% Na^+, 46.7% $H_xPO_4^{3-x}$, 42.6% SO_4^{2-}) to avoid pH reduction that would occur at higher desalination percentages. $H_xPO_4^{3-x}$ reached 0.118 g/L (concentration factor of ~10), which is satisfactory for an efficient precipitation/crystallisation. To segregate phosphate, a concentrated solution was treated with a second stage at overlimiting currents promoting water dissociation and phosphate protonation-deprotonation. Na^+ and SO_4^{2-} were removed by 97.7% and 94.2%, respectively, while phosphate transfer was significantly hampered, by retaining it by 81.3% in the diluate. Studies for membrane characterisation and transport mechanisms elucidation can help to enhance such ED applications [441,442].

A pilot ED was assembled with Mg anode to provide Mg^{2+} to the concentrate and precipitate struvite [443]. Synthetic wastewater with 34.6 mg/L NH_4^+ – N, 10 mg/L PO_4^{3-} – P and 300 mg/L NaCl was used as initial solution for concentrate, anode and diluate. The concentrate chambers were connected with the anode, so that the product solution exiting the concentrate flowed through the anode and vice versa. At the optimal pH of 8.8 and with multiple cycles in the diluate, 65% of phosphate was removed as struvite, the diluate had on average less than 4 mg/L PO_4^{3-} – P (below 0.5 mg/L at the end of several cycles), and the concentrate had 30 mg/L PO_4^{3-} – P. The cost of the Mg anode was 31.27 $/kg P.

5.3.2. Excess Sludge Sidestreams

ED techniques were proposed also for recovery of fertilizers from excess sludge sidestreams (supernatant, centrate, filtrate) of municipal WWTPs. An economic analysis based on an ED simulator estimated a total cost of 0.392 $/kg N (29.5 m^3/day capacity), 65% of which due to operation cost (E_{spec} of 2.36 kWh/kg), showing the convenience of ED compared to other conventional or novel processes [444]. As Table 3 reports, either ED or ED-BMED recovered phosphate or phosphoric acid from a synthetic solution modelling the supernatant of excess sludge mixed with the influent [406], and these treatment processes may be intended also for municipal effluents. In other experiments, an integrated system with ED, struvite precipitation and ammonia stripping was developed by testing synthetic sludge anaerobic digestion sidestreams (dewatering by, e.g., centrifuge or belt filter press) [445]. The feed contained 200 mg/L P and 600 mg/L N. After concentration via ED, nutrients were recovered by the struvite reactor, while the ammonia excess was recovered via gas stripping at 40 °C. Overall removal percentages were ~86% for P and ~92% for N.

Lab-scale [446] and pilot-scale [447] ED experiments were conducted with a real anaerobic digester supernatant (centrifuge centrate) to concentrate NH_4^+ and K^+. A crystallisation/precipitation pre-treatment was performed to recover struvite and prevent scaling (Figure 22). The ED feed (232 mg/L K^+, 1003 mg/L Na^+, 768 mg/L Cl^-, 835 mg/L NH_4^+ – N, etc., 351 mg/L COD) was pumped with single pass through the diluate (23% reduction of conductivity) and with recirculation through the concentrate, reaching concentration factors of ~8 for NH_4^+ – N and K^+ with average overall η of 76% and E_{spec} of 4.9 kWh/kg NH_4^+ – N [447]. The treatment was competitive and provided a product usable as fertilizer. However, improvements were needed, especially in terms of increase of product recovery (affected by water flux and ions back diffusion) and elimination of unwanted ions like Cl^-. The transport of pharmaceuticals (10 or 100 µg/L) was then studied [448]. Nutrients were concentrated by a maximum factor of ~5, while less than 8% of pharmaceuticals were transported to the concentrate product. However, the lower concentrations usually present in real effluents do not hinder the product use as fertilizer.

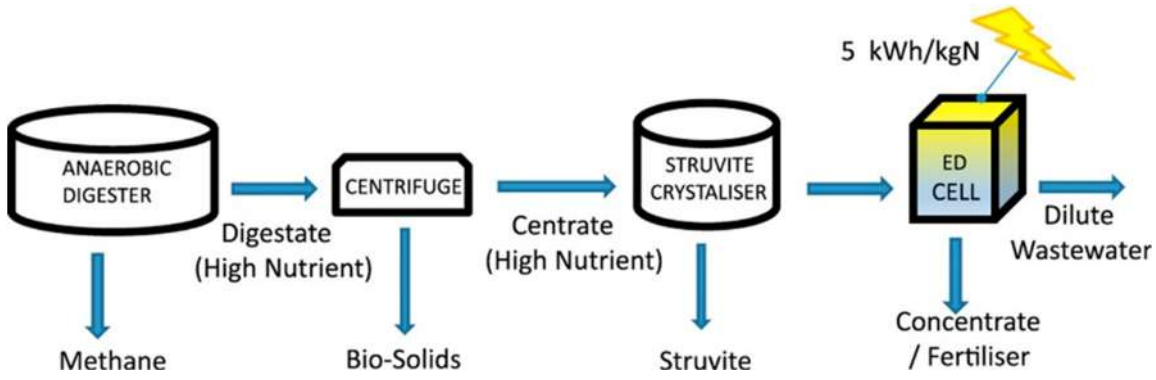

Figure 22. Conceptual scheme of the recovery of materials from anaerobic digestion of WWTP excess sludge, including ED concentration of nutrients from centrate after struvite precipitation for fertilizer production. Reproduced (adapted) with permission from [447], published by Elsevier, 2018.

A solution prepared with 6.6 g/L NH_4HCO_3 (1.5 g/L NH_4^+), simulating sludge reject water, was concentrated by ED with dynamic current [449]. The current density was controlled during the batch process by applying values equal to a fraction of the instantaneous limiting current density (related to the diluate electrical conductivity). This reduced the operational run time by 75% compared to the operation with fixed current, thanks to reduced effects of osmosis and back-diffusion. A more efficient separation was thus obtained: the concentration factor increased from 4.5 to 6.7, while E_{spec} remained unchanged at 5.4 MJ/kg N removing 90% of NH_4^+ at η = 83–96%.

Dissolved ammonia (1.7 or 4.0 g/L) in anaerobic digestion centrate solutions was converted by acid stripping through a liquid–liquid hollow fibre membrane contactor into ammonium salts (NH_4NO_3 or $NH_4H_2PO_4$ at 5.1 wt% or 10.1 wt% in nitrogen), which were then concentrated by ED [450]. Under optimal conditions (10.1 wt%), the ED produced a liquid fertilizer at 15.6 wt% NH_4NO_3-N, with E_{spec} of 0.21 kWh/kg and η of ~93%.

A treatment integrating BMED, struvite precipitation, and multi-stage membrane capacitive deionisation (MCDI) was demonstrated for recovering phosphorus and ammonium from a synthetic supernatant (12.5 mM NH_4^+ and 2.5 mM PO_4^{3-}) [451]. BMED was used only to alkalify the wastewater, thus facilitating struvite precipitation, while MCDI was employed to separate excess ammonia in a small volume. E_{spec} of the BMED was ~1 kWh/m^3. The integrated process removed ~100% of phosphorous and ~77% of ammonia, recovering ~81% of high-quality effluent and ~19% of concentrated stream meeting reuse standards.

VFAs are other products extractable from excess sludge. To recover them, as well as nutrients, thermally hydrolysed waste activated sludge was fermented anaerobically, and after screening and MF, the permeate was concentrated by ED [452]. The 6.15 g/L total VFAs present in the MF permeate were concentrated by ED to 19.82 g/L, corresponding to 92% of transferred mass, while 0.92 g/L NH_4^+ and 0.16 g/L PO_4^{3-} were concentrated to 3.02 and 0.45 g/L, respectively. After that, struvite precipitation was performed to remove the excess ammonium and phosphate, and fermentation was conducted to produce polyhydroxyalkanoates. ED and precipitation significantly enhanced their accumulation in the fermentation broth (from 24 mg/L to 165 mg/L), thus offering a cost-effective valorisation process.

ED techniques can also recover lactic acid from the organic fraction of municipal solid waste hydrolysate [453].

5.3.3. Human Urine

Human urine comprises up to 91–96% water, with urea ($CO(NH_2)_2$) being the major solute fraction (50% of TOC) and with other organic and inorganic components, including P and K [454]. Anthropogenic urine represents a small fraction of domestic wastewater. Nevertheless, nutrients are present in it, along with micropollutants (endocrine disrupting compounds and pharmaceuticals). Therefore, suitable treatment processes have been proposed for separately collected urine to separate and concentrate nutrients (fertilizers) from micropollutants, including ED [455]. IEMs enable ion passage, while retaining neutral organics, proteins and microorganisms. Therefore, ED produces a nutrient-enriched concentrate stream (starting from water with or without salt), and a waste urine stream (diluate).

After MF, in experiments with lab-scale [456] and pilot-scale [457] ED units, maximum concentration factors of nutrients were 3.3 and 4.1, respectively, with urine desalination of 85–99%. The urine contained 4.85 g/L NH_4^+ – N, 0.23 g/L PO_4^{3-} – P, 1.96 g/L Na^+, 3.83 g/L Cl^-, 1.72 g/L K^+, 0.67 g/L SO_4^{2-}, and 4.36 g/L COD in the former study, while it contained 2.9 g/L NH_4^+ – N, 0.18 g/L PO_4^{3-} – P, 1.6 g/L Na^+, 3.0 g/L Cl^-, 1.4 g/L K^+, 0.7 g/L SO_4^{2-}, and 3.6 g/L COD in the latter study. The compartments of concentrate were filled at the start of the experiment; then, the concentrate flow was generated only by water transport. η values up to 50% were observed for ions, suggesting that part of the current was transferred by charged fractions of COD [456]. During a 90-day operation, spiked micropollutants (mixture of pharmaceuticals and hormones) were adsorbed and, after saturation, partially permeated the membranes, reaching the concentrate [456]. However, natural levels of micropollutants (e.g., ~100 µg/L ibuprofen) in the feed would allow much longer operations (e.g., 400 days) without permeation [457]. Membranes cleaned after 195 operating days exhibited a desalination rate enhancement of 35%. Ozonation removed completely micropollutants. Fertilisation by the concentrate showed good performances [457]. However, the ED method would be economically feasible only for large-scale plants, while other processes are affordable for developing countries [458].

A system with precipitation, anaerobic nitrification and ED concentration was developed and operated for ~7 months [459] (Figure 23). The first two treatment processes minimized scaling and biofouling in the ED step. The influent was with 20% or 40% urine in water (151 mg/L NH_4^+ – N, 0.4 mg/L NO_3^- – N, 42 mg/L PO_4^{3-} – P, 449 mg/L Na^+, 753 g/L Cl^-, 401 mg/L K^+, 31 mg/L Ca^{2+}, 11 mg/L Mg^{2+}, 14 mg/L SO_4^{2-} in the 20% solution). After precipitation by NaOH dosage for Ca^{2+} and Mg^{2+} removal, the biological treatment (moving bed biofilm) oxidised organics and stabilised N via ammonification–nitrification, which converts urea (volatile and thermally unstable) into nitrate. The ED transferred 70%/80% of ions in 15%/20% of the starting volume by treating an influent with 20%/40% of urine, respectively (concentration factors of 3–5), with E_{spec} of 4.3 kWh/m^3. The P-rich solids from precipitation and the ED concentrate produced fertilizers; the ED diluate could allow water recovery.

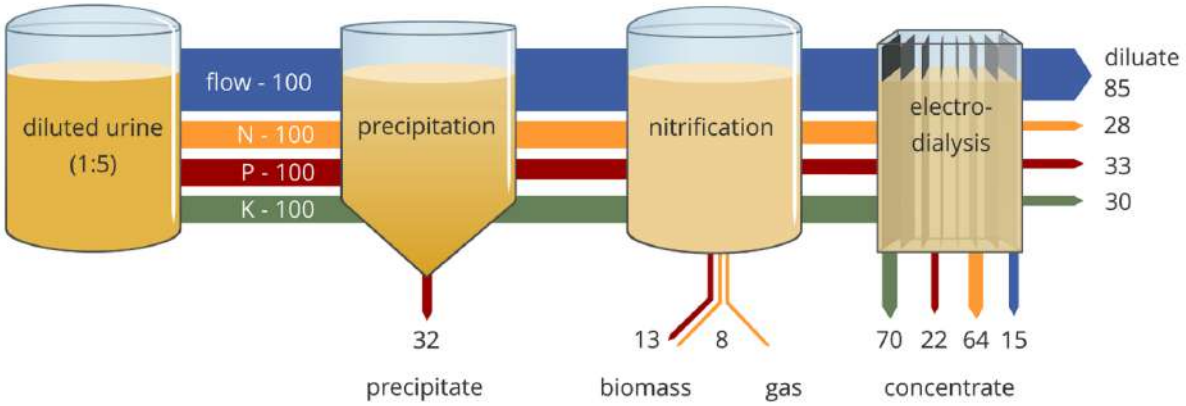

Figure 23. Flowsheet with mass balances of the pilot plant for urine-water solution treatment. Reproduced with permission from [459], published by Elsevier, 2018.

5.3.4. Animal Farming

The augmentation of intensive livestock production caused by massive meat consumption implies several environmental impacts, including those associated with inappropriate disposal of raw or digested animal manure (e.g., eutrophication). Animal manure is a slurry which contains faeces, straw, urine, and water, but sometimes the solid fraction is separately collected [460]. The nutrient content (P, K, N) could allow fertilisation by animal manure. Additionally, biogas can be produced via anaerobic digestion [461]. Unfortunately, the direct agricultural use is limited by transportation costs and foul odours release. However, separation and concentration of nutrients from raw or digestate manure can solve these problems, and ED techniques (after solid–liquid separation) have been studied to this aim, especially for effluents from pig farms, which account for ~36% of the meat market [462].

After vacuum filtration, ammonium contained in liquid swine manures (3.29 or 5.14 g/L NH_3-N, 2.09 or 2.52 g/L K^+, 0.2 or 0.24 g/L P, 20.66 or 40.32 g/L soluble COD, VFAs, solids, etc.) was concentrated into a 1 g/L KCl feed concentrate, by testing different IEMs [463]. Total ammonia reached ~14.4 g/L (of which free ammonia, NH_3, represented ~6%) with $\eta \approx 75\%$. Most of the remaining current was used for K^+ transport (3.8 concentration factor), while a small quantity of phosphorus was transferred (0.45 concentration factor). Volatilisation of free ammonia caused a 17% loss of total ammonia, whose concentration was also limited by water transport. Coupling RO with ED did not bring improvements. Fouling phenomena impaired the IEMs properties resulting in a decline of ED performance [464]. An alkaline–acidic cleaning was fully successful for the CEMs, but restored 80% of conductivity of AEMs, which were likely affected by permanent organic fouling (dark coloration). After cleaning, current density and desalination rate were 95% and 91% of the values measured with new IEMs. To limit losses of ammonia by volatilisation, its transfer to an acid solution by air stripping of the concentrate was tested [465]. Total ammonia nitrogen was concentrated by ~7 times (from a feed at 3.2 g/L) with η = 64–71%. However, the acidic trap recuperated only 14.5% of NH_3 present in the concentrate. Since the residual total ammonia in the swine manure was 1.2 g/L, the NH_3 recovery could be enhanced at higher pH values.

Nutrients were recovered by EDR treatment of pig manure digestate [466]. The raw manure was completely digested. Then, pre-treatments prior to ED included: acidification for P extraction from solids, 0.4 mm sieving, flocculation, centrifugation. The generated effluent (2637 mg/L NH_4^+ – N, 492 mg/L PO_4^{3-} – P, 3259 mg/L K^+, 8894 mg/L Cl^-, 691 mg/L Na^+, 1021 mg/L Ca^{2+}, 555 mg/L Mg^{2+}, 2.8 g/L soluble COD, VFAs, solids, etc.) was the diluate feed. All ammonium and most of phosphate (84%) were removed, obtaining a concentrate product at 4.2 g/L NH_4^+ – N and 0.7 g/L PO_4^{3-} – N, with overall η of 46.8–61.3% and

E_{spec} of 0.13 kWh/L. At every polarity reversal (15 min), acidic cleaning was performed. Reversible fouling was removed, but irreversible effects of organic fouling were observed as well. However, they became stable, likely because the foulants transport inside the membrane was hindered by superficial fouling, thus suggesting the feasibility of long-term operations. The antibiotics fate in the EDR process was studied with spiked (from 50 µg/L to 5 mg/L) pre-treated pig manure, by investigating sorption and migration mechanisms and fouling formation [467]. The main conclusion was that antibiotics can be transported to the concentrate, thus presenting the possible need for further treatment.

The ED stack with Mg anode for struvite precipitation discussed at the end of Section 5.3.1 was also tested with a solution that was 10 times more concentrated (100 mg/L PO_4^{3-} – P) simulating swine wastewater digestate [443]. The final diluate had on average ~20 mg/L PO_4^{3-} – P, the concentrate product had ~100 mg/L PO_4^{3-} – P.

The simultaneous fractionation of cations and anions into several streams by SED offers an interesting approach to recover nutrients from digested swine manure [468]. The tested SED stack (Figure 24a) was built with repeating units of four membranes, i.e., AEM, CEM, MVC and MVA, and four channels, i.e., feed, cationic product (Mg^{2+} and Ca^{2+}), brine (K^+ and NH_4^+) and anionic product (PO_4^{3-} and SO_4^{2-}). The initial feed was prepared with NaH_2PO_4 (40 mg/L P), NH_4Cl (500 mg/L N) Na_2SO_4 (100 mg/L SO_4), KCl (400 mg/L K), $MgCl_2$ (60 mg/L Mg), $CaCl_2$ (100 mg/L Ca) and NaCl (3.192 mM). The other initial solutions were with 0.1 M NaCl. The feed conductivity was practically reduced to zero, obtaining fractionations from ~33% (K^+) to ~90% (PO_4^{3-}), η from ~2% (SO_4^{2-}) to ~30% for NH_4^+, and E_{spec} from ~1 kWh/kg NH_4Cl to ~0 kWh/kg NaH_2PO_4. The two divalent ion products were mixed, obtaining phosphate precipitation by NaOH dosage.

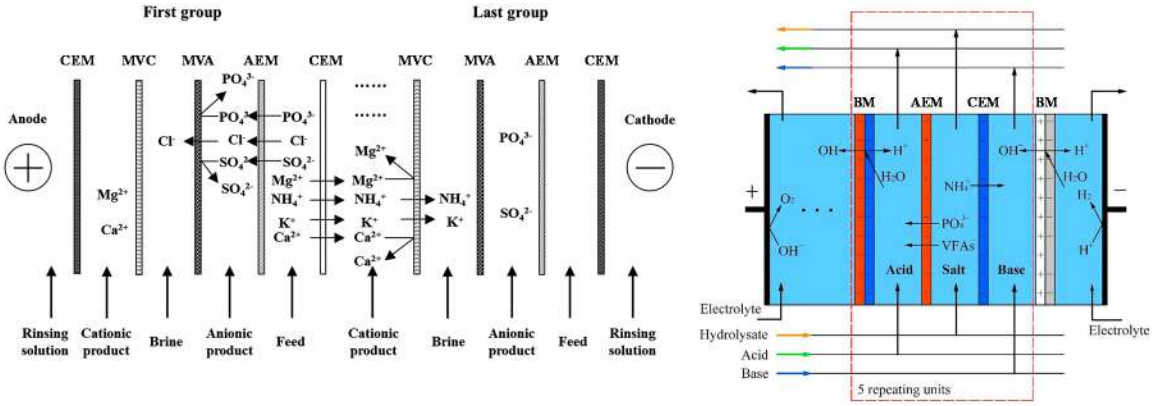

(**a**) (**b**)

Figure 24. Schematics of ED methods for animal farming effluents: (**a**) four-compartment SED of swine manure digestate; (**b**) BMED of pig manure hydrolysate. Panel (**a**) is reproduced (adapted) with permission from [468] published by Elsevier, 2019. Panel (**b**) is reproduced (adapted) with permission from [469], published by Elsevier, 2018.

BMED recovered nutrients and VFAs from pig manure hydrolysate (after acidification and solid−liquid separation, the effluent contained ~4.0 g/L NH_4^+ – N, ~1.8 g/L PO_4^{3-} – P, 9.54 g/L VFAs, 52.68 g/L COD, residual solids, etc.) [469]. The salt tank was filled with the effluent, while the acid and base tanks with deionized water (Figure 24b). Preliminary experiments with model solutions exhibited low values of recovery efficiency, η and purity, due to ion diffusion. The migration of Cl^- and SO_4^{2-} (as well as NH_4^+) was faster than other ions and constant until reaching low concentrations in the feed compartment. Instead, PO_4^{3-} and acetate remained in the feed compartment until that time, and then started to migrate. Therefore,

a two-stage process enhanced significantly the performance. Once reached the inflection point of voltage (galvanostatic mode) corresponding to the start of PO_4^{3-} and VFAs transport, the produced acid and base were substituted with demi water. Two acid and two base products with higher purity were thus generated: acid I contained mainly strong acidic ions (~30 g/L Cl^-), acid II had high concentrations of acetate and PO_4^{3-} (~15 and 5 g/L, respectively, with recovery efficiency of 87% and 77%), base I and II contained mainly NH_4^+ (~10.5 and 3.2 g/L, respectively, with recovery efficiency of 60%) with Cl^- impurity. Air stripping of base I recovered NH_3, while acid I acidified the pig manure. P and VFAs may be extracted from acid II by further processes.

5.4. Regeneration of Liquid Desiccant Solutions for Air Conditioning

Liquid desiccant air conditioning has emerged as an efficient and energy-saving alternative to vapor compression air conditioners in buildings. In particular, liquid desiccant can dehumidify air by absorption. Membrane processes can replace conventional thermally driven evaporation methods in the regeneration (concentration) of hypersaline liquid desiccant solutions, by avoiding droplet carry-over and by lowering energy consumption [470]. Several studies have addressed the ED regeneration of LiCl or LiBr liquid desiccant solutions.

The application potential and the benefits over thermal regeneration were first shown by theoretical studies, where ED was powered by photovoltaic energy [471]. A two-stage ED was more advantageous, by saving more than 50% of energy compared to a single stage under optimized conditions [472,473]. An experimental setup was then developed, obtaining a maximum difference in LiCl mass concentration in the regenerated desiccant solution between start and end of ED of 0.03 wt% (experiments conducted with initial regenerate concentration of ~21–23 wt%) [474]. Low η values were observed (<55%), which is not surprising, given the hard conditions where the IEMs have to work, i.e., high concentrations and high concentration gradient. η values spanned over a large range (21–65%) in other experiments, showing the important role played by the concentrate (regenerate) −diluate concentration difference [475]. The same occurred towards E_{spec} and the overall coefficient of performance of the liquid desiccant air-conditioning system with ED regeneration, COP, defined as the refrigerating capacity divided by the power consumption ($E_{spec} \approx$ 1.4–16 kWh/m^3, COP ≈ 0.3–4). However, at high current densities and concentration differences, η and COP were governed by liquid desiccant concentration and flow rate, membrane properties and stack design. Experiments and simulations showed that higher values of concentration difference, initial regenerate concentration and applied current, reduced η (20–70%) [476]. However, the concentration difference had lower effects on the COP and energy efficiency. In contrast, the increase of the initial concentration from 27 wt% to 35 wt% reduced η, but enhanced the COP from 4 to 6.2 ($E_{spec} \approx$ 8.3–8.7 kWh/m^3).

In other experiments, η values between 55.17% and 73.54% were found [477]. With initial concentrations of 23.96 wt% and 28.77 wt% for spent and regenerate solution, respectively, when a concentration difference of 5.86 wt% was reached, a concentration decrease in the regenerate was even observed. Negative effects derived from osmosis and electro-osmosis from diluate to concentrate, and salt back diffusion. Further tests and simulations showed that water transport was more significant than salt transport, and increased as the applied current increased and the initial solution concentration decreased [478]. It was concluded that minimizing the concentration difference between the two solutions can improve the ED regeneration. Its performance was then investigated and optimized by the Taguchi method, and the percentage contribution of each factor was evaluated by analysis of variance [479]. The optimal initial concentration was 27.5 wt% (without concentration difference, as expected). The applied current was the main parameter affecting the energy consumption, but had mild effects on the concentration increase. Instead, it was mostly affected by the concentration difference between the two solutions (accounting for ~78% of the effects) and,

at a lesser extent, by the initial regenerate concentration. Compared to average values, optimal conditions led to an energy saving of 31.7% (E_{spec} ≈ 25 kWh/m^3) and to a concentrative effect increased by 9.4% (regenerate at 36.22% wt).

A hybrid method combining continuous ED and thermal regeneration of the spent solution by a low-temperature heat source was developed [480] (Figure 25). The technical feasibility of the system was assessed by modelling validated by ED experiments. Simulations of one week's summertime weather in Darwin, Australia, showed that the two outlet concentrations from the ED regenerator were maintained at 29.93–30.17 wt% and 26.70–26.85 wt%, respectively (from inlet concentrations of 29.80–30.05 wt% and 26.80–26.95 wt%). The computed water removal in the low-temperature thermal regenerator and water absorption in the dehumidifier amounted at 128.6 kg and 126.6 kg, respectively. The largest part of energy for desiccant regeneration was consumed by ED (85%, corresponding to E_{spec} of 22 kWh/m^3), while the COP was on average equal to 0.5, thus suggesting that high-performance IEMs are crucial for the system efficiency. Experiments were designed by Taguchi's method, and results were analysed by analysis of variance, showing that increasing inlet temperatures from 30 to 45 °C and from 20 to 30 °C for the spent and regenerate solutions, respectively, resulted in an enhancement of regenerate concentration increase of 19% and to a similar energy saving [481]. These tests confirmed that a higher initial concentration of the regenerate causes higher E_{spec} and a lower concentration increase, which is considerably affected also by the initial concentration difference.

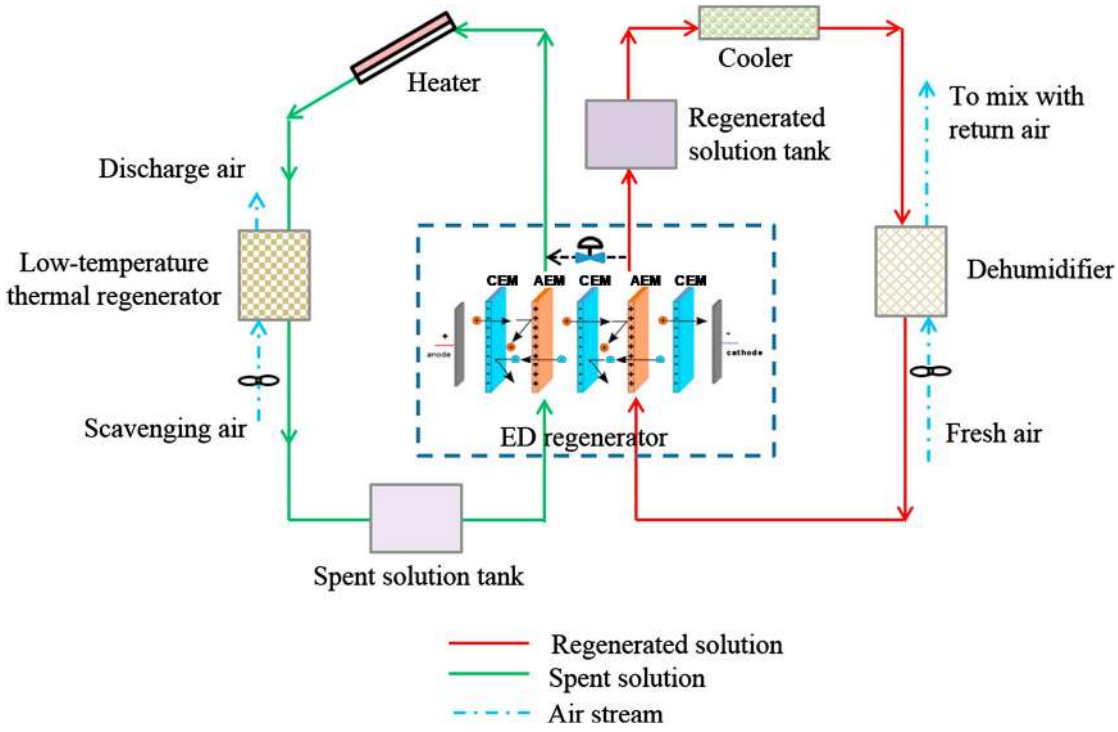

Figure 25. Scheme continuous ED regeneration integrated into a liquid desiccant dehumidification system. Reproduced (adapted) with permission from [480], published by Elsevier, 2019.

The ED regeneration of LiBr solutions showed lower values of η (9–31%) compared to LiCl solutions, because of the higher concentration (~45 wt%) [482]. As the operating conditions were let to vary, η and the COP changed significantly. However, a maximum COP of 4.26 was reached. A mathematical model simulated LiCl, LiBr and $CaCl_2$ solutions regeneration, confirming that initial concentration and applied

current are important factors in all cases [483]. Concentrations of 15, 25 and 15 wt% were suggested for LiCl, LiBr and $CaCl_2$ solutions, respectively ($\eta \approx 70\%$ and $E_{spec} \approx 0.1$ kWh/mol).

6. Waste Brine from Desalination or Ion Exchange

Desalination technologies provide an important contribution in response to water scarcity. The global desalination capacity reached ~100×10^6 m^3/day [484,485], by producing ~142×10^6 m^3/day waste brine [485]. Therefore, brine management is a critical issue facing the desalination industry. RO holds ~60–70% of the desalination market share [485,486] and has several applications. About 50% of RO plants produces potable water from brackish or sea water, ~40% provides ultrapure water to industries, and some installations reclaim polluted or waste effluents, or process food [487]. Brackish water RO (BWRO) has water recoveries of 85–90%, while seawater RO (SWRO) of 35–50%, limited by high osmotic pressure [487]. RO retentate is usually discharged or evaporated. Similarly, environmental impacts are related to the disposal of IXRs regeneration spent brines and ED desalination brines. However, novel brine management methods at low environmental impact are oriented by (near) ZLD strategies towards waste disposal minimisation and resources (water and others) recovery [488–490]. Membrane processes are under study for this aim [1,488–490]. In particular, ED techniques may recover water and salt (Section 6.1), acid and base (Section 6.2), or energy (Section 6.3).

6.1. Water and Salt Recovery

ED has been studied to recover water and salt (diluate and concentrate, respectively) from BWRO brine (Section 6.1.1), SWRO brine (Section 6.1.2) or wastewater RO (WWRO) brine (Section 6.1.3) in ZLD approaches. Moreover, ED has been proposed for the regeneration of spent NaCl brines from IX (Section 6.1.4).

6.1.1. BWRO Brine

ED of BWRO brine can boost water recovery (diluate product) and facilitate the salts separation (concentrate product) in ZLD desalination.

A pilot EDR treated BWRO brine, and a gypsum precipitator for the ED concentrate protected the stack, since $CaSO_4$ was near to saturation [491]. The diluate salt concentration decreased from ~340 mN to ~20 mN, allowing for a total water recovery of 97–98%. Other performances were: concentrate concentration increase to 10% (from 1.5%), η = 60–75%, E_{spec} = 7–8 kWh/m^3. Despite the slow transport, the attainment of silica saturation level limited the brine concentration. Concentration and water recovery were similar for the BWRO-ED system depicted in Figure 26 (feed concentration ~0.3%, retentate ~1%) [492]. Scaling was minimized by acidification, EDR operation, and alleviation of sparingly soluble salts super-saturation via crystallisation, settling and MF or UF. Wind-aided intensified evaporation increased finally the TDS concentration over 30%. η was of 81%, E_{spec} was of 5–6 kWh/m^3, and the estimated cost was 0.408 €/m^3 for treating 100 m^3/h feed with 98% water recovery, thus showing the process competitiveness.

Pilot tests were conducted with a commercial-size ED unit (two electrical stages and four hydraulic stages) fed by BWRO brine (~10 g/L TDS, water recovery of 82.5%) [493]. ED recovered 55% of its feed, raising the overall recovery to 92.1%. MVMs obtained by modification of commercial IEMs changed the product composition. Compared to original IEMs, the MVMs ED achieved the same conductivity reduction (up to 60% of 19.5 mS/cm), while requiring higher E_{spec} (up to ~70% more, ~4 kWh/m^3). Efficient concentrative ED operations are designed by multi-stage configurations within more complex schemes. For example, two- or three-stage batch ED with concentrate split concentrated a 3.5 wt% NaCl solution to 17.9 or 20.6 wt%, with average η = 82.9% or 84.8%, and E_{spec} = 0.31 or 0.45 kWh/kg salt (18.83 and 27.06 kWh/m^3), respectively [494].

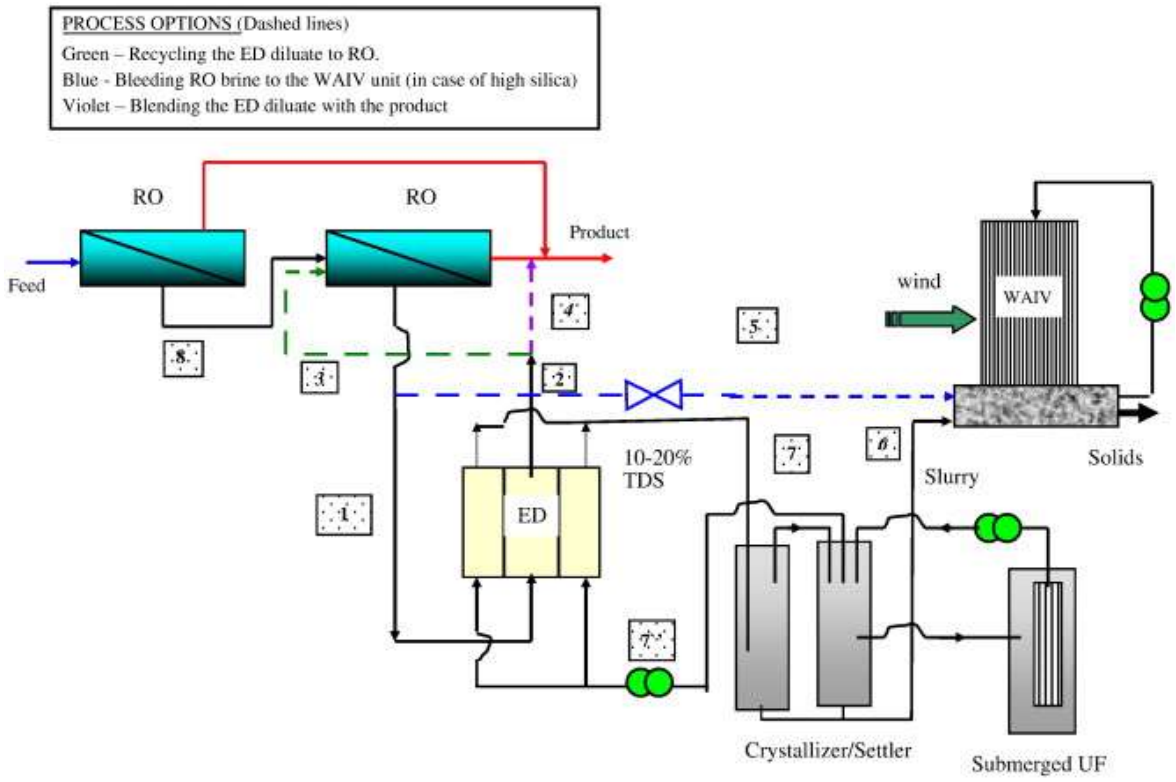

Figure 26. BWRO-ED desalination process. EDR treats the RO retentate (1). The EDR diluate product (2) can go through the second RO step (3) or, if it is sufficiently desalted, is conveyed with the permeate (4). The EDR concentrate (7) is sent to the seeded crystallizer/settler, and to the submerged UF module, thus the crystal-free concentrated stream (7′) recirculates to the EDR. The bleed stream (6) is evaporated by the WAIV unit. Reproduced with permission from [492], published by Elsevier, 2010.

6.1.2. SWRO Brine

SWRO brine treatment via ED recovers water and/or a high-concentration NaCl stream usable to produce coarse salt (via evaporation-crystallisation) or for other purposes, e.g., as raw material for the chlor-alkali industry.

ED stacks assembled with different IEMs were used with a simulated SWRO brine (10.5% TDS) [495]. A multi-stage operation (Figure 27a) produced two solutions with concentrations of up to 27.13% and 470 mg/L. The concentrated brine was suitable for producing edible salt, the diluate (water recovery of ~68%) was suitable more for industrial use than for drinking.

A real SWRO brine (70 g/L TDS) was concentrated through a pilot ED unit (single-pass diluate) equipped with MVMs, tested for 24 months to produce a feed for the chlor-alkali industry [496]. η ranged from 80% to 92% for Cl^-. The concentrate stream was even depleted in most multivalent ions because of water transport. Instead, the Cu and Ni concentration increased due to the transported monovalent Cl-complexes. Better performances were observed at higher temperatures (27 °C), which led the salt concentration to a maximum of 245 g/L. E_{spec} values comparable with the target of ED plants producing edible salt from seawater (0.12 kWh/kg salt, > 200 g/L) were obtained at lower concentrations (185 g/L). Instead, a process enhancement would be needed to meet the requirements of electrolysis for chlorine production (300 g/L, high purity) along with competitive costs. Experimental data from the same pilot plant validated a modelling tool [497]. Model predictions highlighted again that the RO-ED system was

competitive in the edible salt market, but did not reach the targets for industrial use. Among different synthetized MVCs, the best permselectivities measured with a model SWRO brine were $P_{Na^+}^{Mg^{2+}} = 0.09$ and $P_{Na^+}^{Ca^{2+}} = 0.8$, which can provide concentrates at purity sufficient for the chlor-alkali process [498].

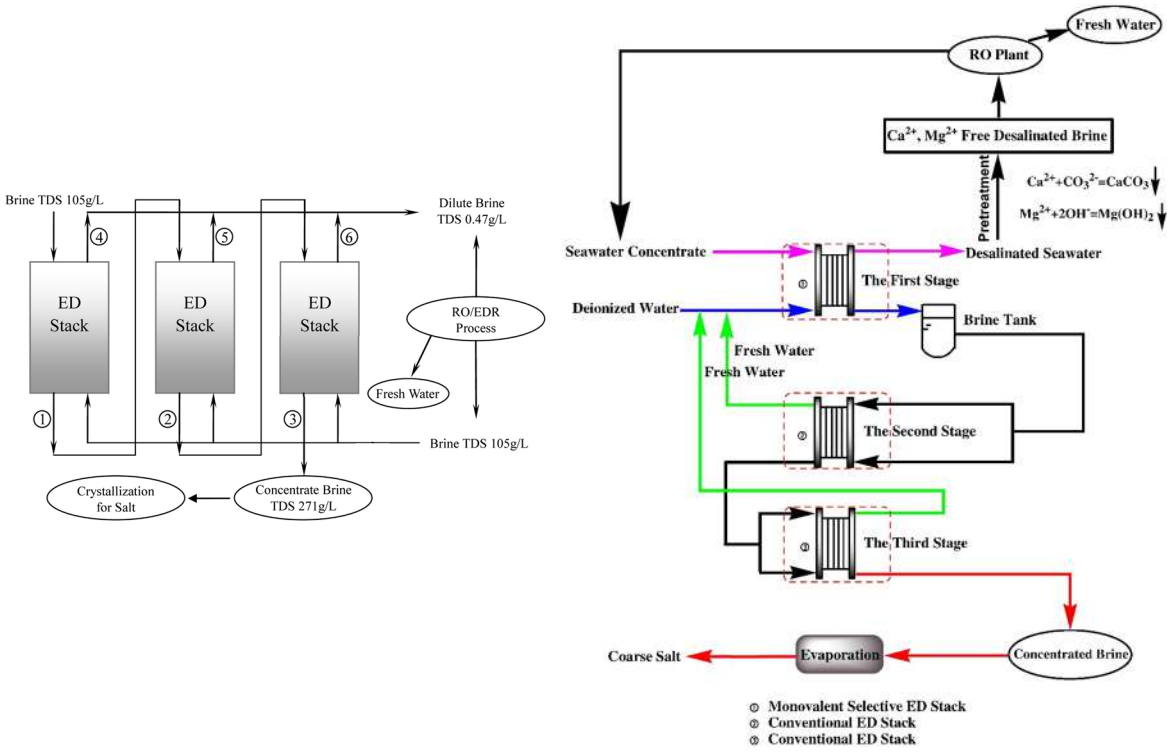

(**a**) (**b**)

Figure 27. Flowcharts of three-stage ED systems for water reclamation and salt production from SWRO brine: (**a**) conventional ED; (**b**) ED with MVMs in the first stage, followed by conventional ED in the second and third stage. Panel (**a**) is reproduced (adapted) with permission from [495], published by Elsevier, 2014. Panel (**b**) is reproduced (adapted) with permission from [499], published by Elsevier, 2017.

A three-stage ED was developed for recovering water and salt from SWRO brine (~45 g/L TDS, 60 mS/cm) [499] (Figure 27b). The first ED was performed with MVMs to retain divalent ions in the diluate feed and transfer NaCl to the concentrate (deionized water). The produced diluate (70% desalination) can return to RO after removal of divalent ions, while the concentrate went through two concentrative steps with conventional IEMs. The conductivities of the concentrate products were 42.4, 73.2 and 105 mS/cm, and coarse salt 85% pure in NaCl was produced by final brine evaporation. The water recoveries relative to the initial diluate of each stage were 90%, 86% and 82%, obtaining fresh water from the last two stages. The total E_{spec} was of 2.3–2.4 kWh/kg NaCl.

Another strategy for enhancing the salt purity consists of using an NF pre-treatment, reducing the divalent ions concentration [500]. From an artificial SWRO brine (66.8 g/L TDS), the NF rejected Ca^{2+}, Mg^{2+} and SO_4^{2-} by 40, 87 and 100%, respectively, recovering water by 54.3% as permeate (58.7 g/L TDS). The ED tests achieved a maximum concentration of 160 g/L NaCl with some impurities (5 g/L) at E_{spec} of 1.4 kWh/kg NaCl. The final ED diluate (~95% of the NF permeate) had a minimum concentration of 25.25 g/L TDS, hence it could go to the RO. Similarly, the NF retentate could go to further recovery processes.

Theoretical approaches, including process simulators, techno-economic estimations and thermodynamic evaluations, can drive the design of optimized systems. Several hybrid schemes and multi-stage operations are viable, prospecting promising developments [501–504]. A techno-economic analysis found that the salt production costs of an SWRO-ED-crystallizer plant (RO feed at 50 m^3/h) may be competitive (61–111 $/ton salt), i.e., lower by 19–55% than those of conventional standalone ED-crystallizer systems [505]. However, the process main aim (brine minimisation or salt production) and the site-specific features (water, salt and electricity prices) may require different strategies. For example, in another analysis, feeding the ED diluate with SWRO brine instead of seawater reduced the water production costs by 87% (i.e., from 27 to 3.5 $/$m^3$), but increased the salt production costs by 26% (i.e., from 135 to 170 $/ton salt), by considering an SWRO plant capacity of 150,000 m^3/day [506]. Optimal currents further reduced the water costs (3.0 $/$m^3$), but increased E_{spec} by 26% to 12.7 kWh/m^3. The complete salt production scheme (SWRO-ED-crystallizer) was competitive with the SWRO desalination only in some Middle-East countries, where the salt price is higher than 104.5 $/ton.

EDM of BWRO [507] or SWRO [41] brine was proposed. The complete conceptual scheme of SWRO-EDM is depicted in Figure 28. EDM separates ions from SWRO brine (diluate 1) into two high-solubility salt solutions products (the initial feed is SWRO permeate), one with Na^+ salts (concentrate 1) and another one with Cl^- salts (concentrate 2), following the metathesis MX + NaCl → NaX + MCl, where NaCl is supplied by the substitution solution (diluate 2). The diluates recirculation to RO increases water recovery, crystallizer I recovers Na_2SO_4 and NaCl from concentrate 1, crystallizer II recovers NaCl from concentrate 2 after Ca^{2+} and Mg^{2+} precipitation. In the EDM experiments, initial solutions were an SWRO retentate at 50 g/L TDS, an NaCl substitution solution with the same conductivity, and deionized water (concentrates). To find optimal operating conditions, preliminary experiments with partial concentration were performed, exhibiting E_{spec} values lower than 1 kWh/kg salt. Then, a maximum concentrates concentration of ~200 g/L TDS was attained (while desalinating the diluate products at 5 mS/cm) with negligible co-ion leakages and scaling. However, 170 g/L was the concentration recommended to preserve the process efficiency. The feasibility of the overall process scheme should be assessed by further studies.

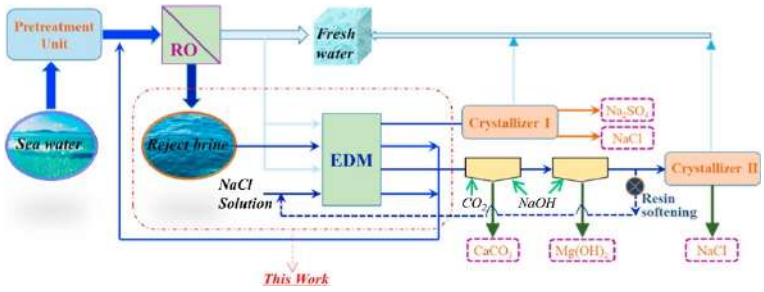

Figure 28. Conceptual scheme of SWRO-EDM for water and salts recovery. Reproduced with permission from [41], published by Elsevier, 2019.

6.1.3. WWRO Brine

ED was studied to recover further water from RO brines produced in industrial/municipal WWTPs (WWRO brine).

At an industrial WWTP of ~1900 L/min (heavy metal clarification, settling UF, RO), a six-stack EDR plant treated ~265 L/min WWRO retentate with TDS at 3000–5000 ppm [508]. The EDR was designed for E_{spec} of 4 kWh/m^3 and a cost of 0.33 $/$m^3$. It reclaimed 85% of the WWRO reject brine as diluate (550 ppm),

which recirculated to the treatment line, while the remaining 15% waste concentrate (45,000 ppm) went to evaporation ponds.

A WWTP receiving mainly a domestic effluent was endowed with UF and RO tertiary treatment to reuse water in groundwater recharge [509]. A pilot ED stack was tested to desalinate the WWRO retentate and recirculate it into the biological step (after ozonation preventing organics accumulation), while discharging the ED concentrate (Figure 29). The WWRO retentate had ~4.8 mS/cm conductivity, with high scaling potential (Ca^{2+}, Mg^{2+} and carbonates), which was lowered by acidification-decarbonation with HCl. Batch or feed and bleed experiments provided a diluate with 75% desalination (average overall $\eta \approx 70$–85%), while a long-run test (42 h) attained a 69% desalination, thus the effluent could be recirculated, though it needed a TOC reduction. The ED addition enhanced water recovery from 75% (standalone RO) to 95%. An ED operational cost of 0.19 €/m^3 was estimated, 20% of which went from E_{spec} of 0.9 kWh/m^3 [510]. The capital cost was actually prohibitive (~15 €/m^3) for a plant capacity of 300 L/h, but the significant abatement with a full-sized plant could make the system feasible. The membrane processes produced significant CO_2 emissions, but if they were driven by renewable energy, the total emissions could be lower than those from conventional methods. The precipitation/crystallisation in a pellet reactor with fluidized bed showed that 80% of Ca^{2+} removal made the ED operation stable ($\eta \approx 70\%$) without any scaling [511]. The integration of a phytoremediation pre-treatment (willow field for nutrients and organics removal) with ED recycled effectively the treated WWRO concentrate in the WWTP [512]. However, again, an oxidation step after ED was needed.

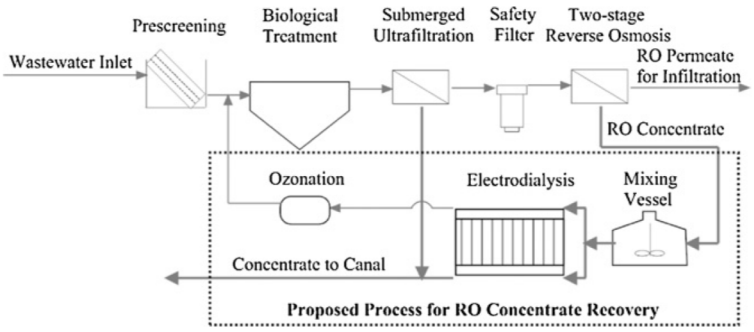

Figure 29. Scheme of the WWTP with RO-ED water recovery. Reproduced with permission from [509], published by Elsevier, 2011.

A pilot plant integrating a membrane bioreactor with RO and EDR was developed for treating municipal landfill leachate (15 mS/cm, 2250 mg/L COD) [513]. The RO had a water recovery of 84% and a rejection > 95% for most components. The EDR produced a diluate product at 30–65 mS/cm and recovered 67% of water, leading to an overall water recovery over 93%.

Recovery of nutrients and/or organics via ED from RO concentrate of food industry wastewater was assessed [514]. Experiments with model solutions (salts mixture, ~20 mM as total concentration) without or with organic compounds (120 g/L TOC) showed that monovalent ions and multivalent ions can be separated from each other under suitable operating conditions (low currents, for example), especially by using MVAs. However, separating nutrients (NO_3^- and $H_xPO_4^{y-}$) from other ions (Cl^- and SO_4^{2-}) was not feasible. The organics fate was strongly affected by molecular weight and charge, as the transport was slower for larger molecules and even slower for zwitterions and uncharged compounds. With a real WWRO retentate (90 mM Cl^-, 4.5 mM SO_4^{2-}, 70 ppm TOC), ions were almost completely removed, while more than 85% of the organics was retained within the diluate.

When RO treats wastewater, organic micropollutants (e.g., pesticides) may interact with the IEMs functional groups and may by adsorbed by the IEMs, with important implications such as fouling/poisoning and release during cleaning [515].

Some ED applications were studied for desalinating RO brine from petrochemical industry wastewater treatment, showing interesting results despite the scaling and fouling potential. A pilot EDR exhibited removal efficiencies above 90% for Cl^- and alkalinity, and of 76% for TDS, from a WWRO brine with 1104 mg/L TDS, and this RO-EDR process enhanced significantly the water recovery (87.3%) [516] compared to the EDR-RO scheme [352] (41%, see Section 4.3.2), thus offering the chance of reuse (cooling towers). Another EDR study achieved TDS removal of 50% (from 8663 mg/L TDS in the feed) with 85% of water recovery that reduced the brine volume by ~6.5 times [517]. No organic fouling was observed; however, the stack resistance increased during operation due to scaling at the concentrate side. A comparison among ED, NF and IX assessed the separation of NaCl and natural organic matter (NOM) [518]. The WWRO retentate had 6.9 g/L TDS and 35 mg/L NOM. ED removed ~90% of NaCl and recovered ~97% of water, retaining more NOM (e.g., TOC by 65%) when using MVMs. All the tested technologies exhibited results opening new opportunities to recover solid NaCl from brines in ZLD perspective.

The response surface methodology modelled and optimized the ED for RO concentrate (1950 mS/cm) reclamation in coal-fired power plants, finding a reduction in conductivity of 75.3% with E_{spec} of 0.11 kWh/m^3 and ~50% of water recovery with optimized conditions [519].

An IX-RO-ED treatment process for industrial Li-containing wastewater was developed [520] (Figure 30). The effluent (1268.9 mg/L Li^+, 17.87 mS/cm) from a Li-ion batteries production plant was softened to prevent scaling. Then, it was concentrated by RO and a two-stage ED, thus obtaining fresh water (RO permeate) with increased recovery (ED diluate recycle) and a concentrate solution suitable for Li_2CO_3 precipitation by Na_2CO_3 addition. Under optimal conditions, the RO retentate (60 mS/cm) was split into diluate/concentrate ED feed solutions with 3:1 volume ratio, obtaining water recoveries of 67.51%, 78.73%, and 69.44% in the RO step, the first and the second ED, respectively (E_{spec} in ED of ~30 and 50 kWh/m^3). A final LiCl concentration of ~87 g/L was reached with average η of 67.52%, total E_{spec} of 0.772 kWh/kg and a total cost of 0.47 $/kg (process capacity of 282 kg/year).

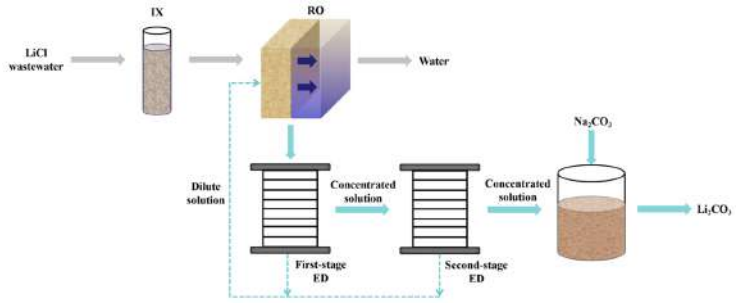

Figure 30. Scheme of the IX-RO-ED system for concentrating LiCl from industrial lithium-containing wastewater. Reproduced with permission from [520], published by American Chemical Society, 2019.

6.1.4. IX Spent Brine

Studies on ED regeneration of spent brines from IX treatment of surface water have exhibited promising results. A two-stage pilot ED treated an NOM-containing spent brine from anion exchange resin regeneration [521] (Figure 31). Electrostatic interactions and formation of metal-organic complexes caused the NOM removal by IX and the transfer of these compounds to the regeneration brine. The spent NaCl brine (8530 mg/L Na^+, 9050 mg/L Cl^-) contained NOM at 700 mg/L as dissolved organic carbon, but also NO_3^- (113 mg/L), SO_4^{2-} (3350 mg/L) and HCO_3^- (2660 mg/L). The first ED step was conducted

with MVAs, while the second one was with standard membranes. Both the ED steps used fresh water (RO permeate) in the concentrate, while the spent brine flowed through the diluate of both stages. As a result, with a removal of 85% for Cl^- and 65% for Na^+, the ED stage 1 produced a monovalent salt solution (concentrate) with sufficient quality to be reused for IX regeneration, while the ED stage 2 produced a multivalent salts solution (concentrate, with predominance of Na_2SO_4) and a 470 mg/L NOM solution (diluate). The potential reuse of the NOM solution should be further studied, since its quality was impaired by heavy metals.

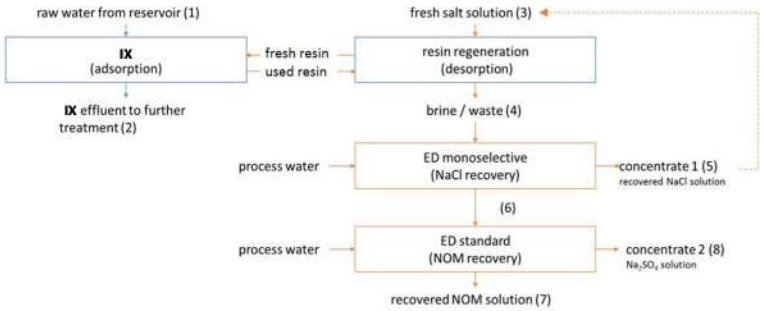

Figure 31. Process scheme of IX water production and two-stage ED treatment of brine. (1) Surface water from IJssel lake (the Netherlands), (2) ceramic MF and advanced oxidation, (3) NaCl regenerating solution, (4) spent regeneration brine, (5) concentrate from monovalent selective ED, (6) diluate from monovalent selective ED, (7) NOM-containing diluate from conventional ED, (8) multivalent salts-containing concentrate from conventional ED. Reproduced (adapted) from [521], published by Elsevier, 2019.

A simpler process was adopted for an IX spent brine with NaCl, sulphate and NOM concentrations of 90, 1, and 1 g/L (as dissolved organic carbon), respectively [522]. A single ED step (spent brine as diluate, 2 g/L NaCl solution as concentrate) with MVMs was effective, yielding a pure NaCl solution with 88.8% removal, negligible membrane fouling, and E_{spec} of 2 kWh/kg salt.

6.2. Salt Conversion into Acid and Base

BMED can valorise brines by salt transformation into acid and base. Moreover, the desalted feed may improve water recovery (ZLD approach). Studies on this application are presented for BWRO brine and SWRO brine in Section 6.2.1, and for WWRO brine and IX spent brine in Section 6.2.2.

6.2.1. BWRO Brine and SWRO Brine

The cost-effectiveness of acid/base production was demonstrated with artificial solutions (up to 390 mM NaCl) representing also BWRO concentrates [269] (see Section 4.2.2).

Several studies have been devoted to concentrated solutions from seawater desalination. A model SWRO brine was prepared with a salts mixture (~61 g/L) without Ca^{2+} and Mg^{2+}, and BMED produced mixed acids and bases up to 1 M [523]. The feed was desalinated up to 80% (from 70 to 12 mS/cm), but its pH decreased to ~2 due to proton leakage. η values between 50% and 80% indicated co-ion leakages as well, and impurities (e.g., SO_4^{2-} in the acid) made the products unsuitable to reach commercial chemicals quality standards. However, they could be intended for uses not requiring high purity. The employment of nanocomposite MVAs synthetized by commercial AEMs coating, led only to a 10% reduction of SO_4^{2-} in the acid compared to the original AEMs (~6 mM) [524]. However, the MVA was stable over more than 90 h operation ($P_{Cl^-}^{SO_4^{2-}} \approx 0.8$ = constant, against ~1.08 for the AEM). By using a 1 M NaCl feed and a photovoltaic solar array simulator, a BMED process powered by photovoltaic energy was characterized [525].

In overflow configuration, the manipulation of flow rate for pH control resulted in a drop in E_{spec} from 7.3 kWh/kg acid (reference case at constant current) to 4.4 kWh/kg at variable current. An acid stream at a constant concentration of ~1 M HCl was produced for 30 h. Other BMED experiments produced up to 3.31 M HCl and 3.65 NaOH (from 1 M NaCl feed) [526]. E_{spec} was in the range 21.8–41.0 kWh/kg HCl at constant currents, and 26.7–43.5 kWh/kg HCl at variable currents. Azeotropic distillation was simulated as post-concentration step, producing 11.4 M HCl (35 wt%, commercial level) with overall E_{spec} of ~40–60 kWh/kg HCl. A life cycle assessment included environmental burdens associated with brine disposal and carbon footprint [527]. It was shown that renewable energies can be crucial for an overall process sustainability. However, though photovoltaic energy reduced the carbon footprint of the BMED-distillation process, it was still higher than that of industrial production from H_2-Cl_2 reaction, excluding the contribution of the transportation [526].

A real brine from seawater desalination (~42 g/L) pre-treated for Ca^{2+} and Mg^{2+} removal (precipitation by NaOH and CO_2) was used [528]. Preliminary tests were conducted with model solutions for optimisation purposes, finding η = 50–74% and $E_{spec} \approx$ 7.5 kWh/kg. With the real effluent, the BMED produced continuously ~1 M acid and base without visible fouling. These products were usable at the desalination plant. For other industrial uses necessitating high quality standards, they would require purification. The low-salinity diluate product enhanced water recovery (direct reuse or recirculation to RO).

An SWRO brine (~60 g/L) was cleaned from Ca^{2+} and Mg^{2+} by NF and chemical precipitation, then the effluent (52 g/L) went to BMED [529]. The feed was almost fully desalted, and the NaCl conversion into HCl and NaOH was over 70%, obtaining ~1 M products at η of ~77% and E_{spec} of ~2.6 kWh/kg NaOH. Improvements were achieved with a combined process where an SWRO brine (~70 g/L) was purified and concentrated (~100 or ~200 g/L) by ED with MVMs, and then was converted (1.6 or 2 M acid, 1.2 or 2 M base) by BMED [530]. The diluate produced by BMED was at ~20 mg/L, the conversion was between 46% and 84%. The ED E_{spec} was 0.055–0.217 kWh/kg NaCl, the BMED one was 1.82–3.62 kWh/kg NaOH (η = 55–88%). The associated operating cost exceeded the market prices of the products. Therefore, in situ uses and/or stringent brine management regulations could justify the process.

BMED equipped with MVMs (bipolar membrane selectrodialysis, BMSED) was used with SWRO model brines at 70 or 105 g/L [531] (Figure 32). The process, which used commercial membranes, was highly selective ($P^{Na^+}_{Ca^{2+}}$ = 3.6–10.6, $P^{Cl^-}_{SO_4^{2-}}$ = 31.0–67.5) and thus produced high purity (approaching 99.99%) HCl and NaOH solutions at concentration up to 1.9 and 2.2 M, respectively. The final salt water was still at high concentration (~50 g/L) and could return to RO.

6.2.2. WWRO Brine and IX Spent Brine

BMED for RO concentrates was actually first proposed for a WWTP effluent (2590 mg/L TDS, 9 mS/cm) softened by IX [532]. Mixed acids and mixed bases at ~0.2 N concentration were produced, along with a diluate at conductivity below 2 mS/cm. For an RO capacity of 37,850 m^3/day, the estimated process cost of ~0.7 \$/m^3 was lower than those of conventional disposal (e.g., evaporation pond) or thermal ZLD processes.

BMED was proposed for waste neutralisation brine (20.4 mS/cm) from acid and base effluents regenerating IXRs used for surface water desalination [533]. The process concept included an ED step with MVCs followed by IX to concentrate and soften the brine and increase water recovery (ED diluate recycle) before BMED. Acid and base products from BMED were reusable for IXRs regeneration, and the produced diluate could recirculate to the ED concentrate. The saline water conductivity increased to 40 mS/cm by ED. BMED desalinated this solution up to ~5–10 mS/cm, and produced 0.9 M acid and base at η of 47% and E_{spec} of 6.25 kWh/kg HCl. Higher concentrations were reached with worse performance, due to co-ion leakage and current leakage (shunt currents).

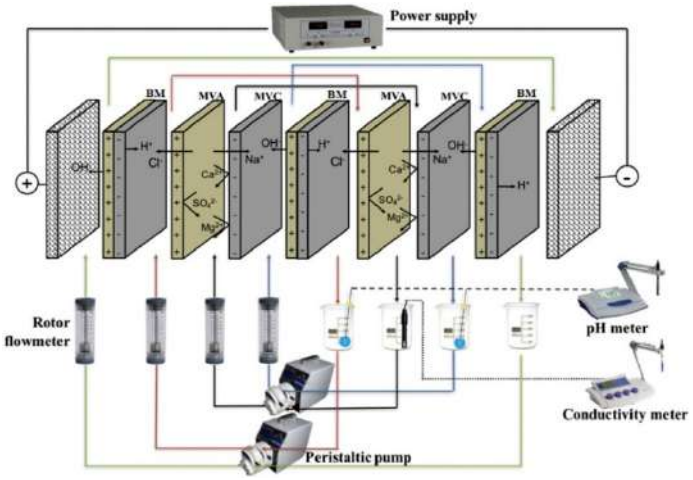

Figure 32. Scheme and experimental set-up of BMSED for acid/base recovery from SWRO brine. Reproduced with permission from [531], published by Elsevier, 2018.

6.3. Energy Recovery

The valorisation of desalination waste brines can be done in the form of energy recovery through salinity gradient power technologies [534,535]. Brines from RO desalination (of seawater, typically) can be employed as high-salinity feed (concentrate) for RED to produce electrical energy, reducing the overall energy consumption of desalination. Moreover, the RO brine is partially desalted prior to discharge. RED units require also a low-salinity feed; thus, using reclaimed wastewater as RED diluate can enhance the energy recovery compared to that achievable when using the desalination plant influent, e.g., seawater. Figure 33a shows the RO-RED scheme in which seawater is desalinated by RO, and RED receives the SWRO brine and a secondary effluent [424]. This scheme avoids issues of seawater contamination by organic micropollutants that, instead, may occur in the opposite scheme, i.e., RED-RO (Section 5.2). However, the overall energy balance may be less favourable in the RO-RED configuration, despite the higher power produced by RED due to the higher-concentration concentrate. For example, model predictions of the energy consumption are ~1 kWh/m^3 for RO-RED and ~0.5 kWh/m^3 for RED-RO [424]. More complex schemes were assessed, i.e., with RED pre- and post-treatment or with brine recirculation, but similar energy performances were predicted. In all cases, the costs should be evaluated.

Using desalination brines as concentrate, energy recovery by RED has been evaluated with different feed solutions and within different desalination schemes. Figure 33 depicts some of them.

Some integrated schemes involve a third process, e.g., membrane distillation (MD, Figure 33b) or membrane capacitive deionisation (MCDI, Figure 33c), between RO and RED, enhancing water recovery and/or energy saving. In the ED-RED coupling shown in Figure 33d, RED uses the ED brine (seawater desalination) and treated wastewater. ED and RED offer the possibility of internal integration in one stack with four-compartment repeating units (Figure 33e) and could by coupled with other desalination processes (e.g., RO) by using their brines as high-concentration streams boosting the energy recovery.

Table 4 reports several studies on energy recovery via RED using desalination brines, including those illustrated in Figure 33. As shown in Table 4, $P_{d,max}$ spans in a wide range in the order of ~1 W/m^2. It was shown that the addition of RED can reduce the energy consumption of desalination. Promising results were exhibited by ED-RED couplings, thus posing the bases for the development of self-sufficient or low-energy consuming systems. In all cases, however, a critical issue is represented by the capital costs.

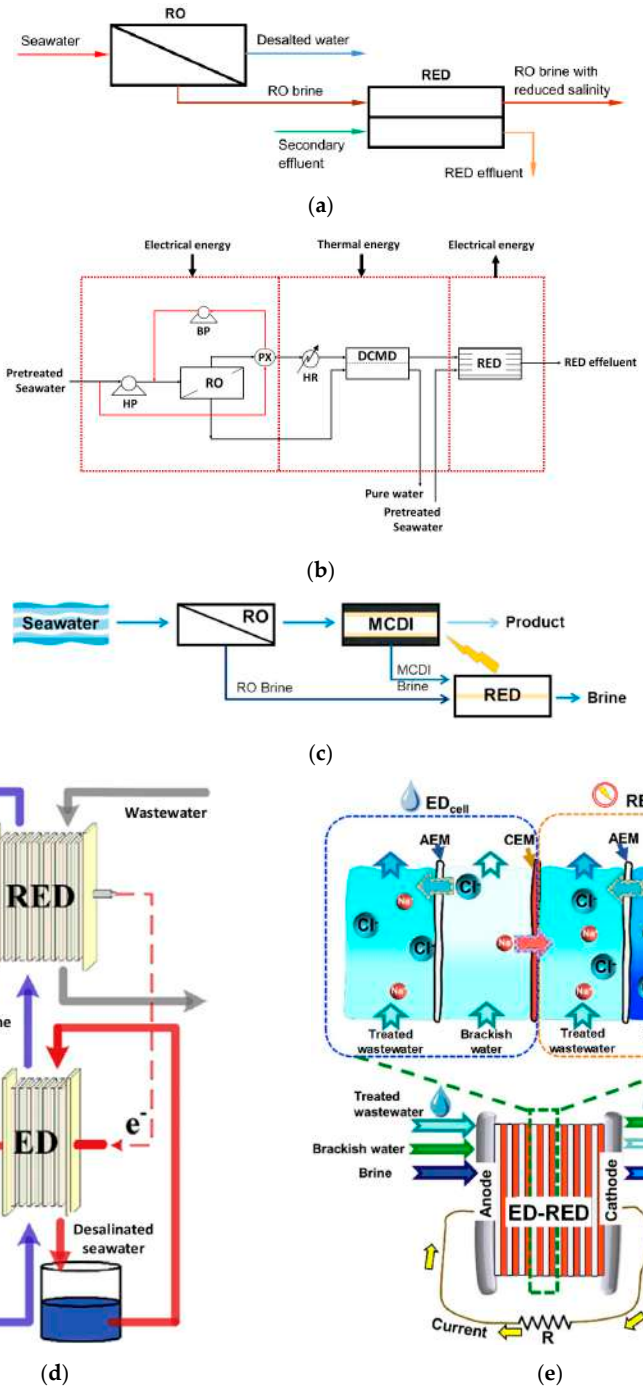

Figure 33. Desalination systems with RED using desalination brine for recovering energy: (**a**) RO-RED scheme in which RED receives the SWRO brine and a secondary effluent; (**b**) RO-MD-RED scheme; (**c**) RO-MCDI-RED scheme; (**d**) ED-RED scheme; (**e**) ED-RED process integrated in single stack (four-channel repetitive unit, coupling an ED cell with an RED cell). Panels (**a**–**e**) are reproduced with permission from [424,536–539] (adapted), respectively, all published by Elsevier, 2013, 2019, 2019, 2017 and 2020, respectively.

Table 4. Recent experimental studies on energy recovery via RED from desalination brines.

High-Salinity Sol.	Low-Salinity Sol.	Performance	Ref.
SWRO brine 1 or 2 M NaCl	Secondary effluent 0.02 M NaCl	V_{OC} (5 cell pairs), $P_{d,max}$: 1 M–0.02 M → 0.90 V, ~0.48 W/m^2 2 M–0.02 M → 1.02 V, ~0.57 W/m^2	[423] Figure 33a
• SWRO brine 1.2 M NaCl • FO brine 2.4 M NaCl	• River water 0.01 M NaCl • Seawater 0.6 M NaCl	$P_{d,max}$, estimated maximum reduction of E_{spec}: 1.2 M–0.01 M → 1.48 W/m^2, 7.8%; 2.4 M–0.01 M → 1.86 W/m^2, 13.5%; 1.2 M–0.6 M → 0.09 W/m^2, 0.5%; 2.4 M–0.6 M → 0.37 W/m^2, 2.2%	[540]
BWRO brine 31.3 mS/cm (~0.4 M), 19.5 mg/L dissolved organic carbon	Brackish groundwater 8.3 mS/cm (~0.095 M), 4.1 mg/L dissolved organic carbon	V_{OC} = 0.53 V (10 cell pairs, 78% permselectivity), $P_{d,max}$ = 0.07 W/m^2; with NaCl solutions at the same conductivity, $P_{d,max}$ = 0.09 W/m^2 indicated effects of NOM and divalent ions	[398]
MD brine 4, 5 or 5.4 M NaCl (from 1 M feed, i.e., SWRO retentate)	Seawater 0.5 M NaCl	At 20 °C and 0.7 cm/s, V_{OC} = 1.23–2.1 V (25 cell pairs), $P_{d,max}$ = 0.45–1.1 W/m^2, water recovery 92%; at 10–50 °C, 5 M and 0.7 cm/s, V_{OC} ≈ 1.7 and $P_{d,max}$ ≈ 0.5–1.05 W/m^2; at 20 °C, 5 M and 1.1 cm/s, $P_{d,max}$ ≈ 1.1 W/m^2 and $P_{d,max,net}$ ≈ 0.67 W/m^2	[541] Figure 33b
• SWRO brine 1 M NaCl • MD brine 5 M NaCl	• Brackish water 0.1 M NaCl • Seawater 0.5 M NaCl	V_{OC} (25 cell pairs), $P_{d,max}$: 1 M–0.1 M → 2.1 V, 0.39 W/m^2; 5 M–0.1 M → 3.4 V, 1.5 W/m^2 ($P_{d,max,net}$ ≈ 1.2 W/m^2, H_2 production by alkaline polymer electrolyte water electrolysis cell 44 cm^3/(h·cm^2)); 1 M–0.5 M → 0.71 V, 0.05 W/m^2; 5 M–0.5 M → 1.9 V, 0.55 W/m^2	[542]
MD brine 2–5 M NaCl (from 1 M feed, i.e., SWRO retentate)	Seawater 0.5 M NaCl	At 20–60 °C, water recovery 75–95%, V_{OC} = 1.26–1.95 V (25 cell pairs), $P_{d,max}$ ≈ 0.22–1.1 W/m^2, exergetic efficiency 49% under best conditions, electrical energy consumption (1.3 kWh/m^3) reduced by 23% and E_{spec} (4.4 kWh/m^3) reduced by 16.6% through RED inclusion	[536] Figure 33b
SWRO brine 1.1–1.5 M NaCl (RO with 30–50% water recovery from 43 g/L feed, i.e., high salinity seawater)	MCDI brine ~0.023 M NaCl (MCDI with 50–80% water recovery from ~0.85 g/L feed, i.e., SWRO permeate)	$P_{d,max}$ ≈ 2.45–2.83 W/m^2, E_{spec} = 2.0 kWh/m^3 reduced by ~39% compared to RO-RO and by ~17% compared to RO-RO-RED	[537] Figure 33c
• ED diluate 38.1 mS/cm (from ED of real seawater in salt production plant) • Seawater 48.7 mS/cm	Distilled water 0.2 mS/cm (from evaporation of ED brine in salt production plant)	V_{OC} (10 cell pairs), $P_{d,max}$: 38.1–0.2 mS/cm → 2.02 V, ~0.23 W/m^2; 48.7–0.2 mS/cm → 2.1 V, ~0.26 W/m^2	[543]
ED brine (from ED of simulated seawater at 30 g/L sea crystal)	Simulated wastewater 0.8 g/L NaCl, 0.1 g/L KH_2PO_4, 0.1 g/L NH_4Cl, 0.5 g/L glucose	Partial desalination of seawater (~60%) by consuming only the electrical energy produced by RED	[538] Figure 33d
Desalination brine 1.2 M NaCl	• Brackish water 0.02 M NaCl • Seawater 0.6 M NaCl	Partial desalination of brackish water (~75%) or seawater (~50%) by consuming only the self-produced electrical energy, the developed model predicted enhanced desalination by changing the operating conditions	[539] Figure 33e

7. Discussion, Conclusions and Outlook

ED and unconventional configurations of ED, i.e., BMED, SED, EDM and EDI, have great potential in desalination and valorisation strategies of wastewater for a broad range of applications to recover water and/or other valuable components. The main ones are metals, salts, acids and bases, nutrients, and organics. Energy recovery via RED is another possibility.

ED methods can be applied for effluents originating from various industrial processes (Section 4). In the separation of heavy metal ions (Section 4.1), such as Ni, Cu, Zn, Cr, Cd, and Pb, ED can provide solutions suitable for reuse, e.g., plating baths and rinse waters, including solutions with complexing agents (cyanide or organic acids), and tanning solutions. Two-stage operations (either both or one with MVMs) can improve purity, while EDI can reduce the energy consumption when treating diluted solutions

(including low radioactive effluents). ED techniques (including complexation-enhanced ED) can also produce reusable solutions from heavy metal ions mixtures. BMED and SED have been poorly studied so far, but have exhibited promising results. Future research should be focused on experiments with real effluents, by assessing long-term operations, and should aim at scaling up the systems. Cost analyses are needed to assess the techno-economic feasibility.

For the regeneration of acid/base and salt conversion (Section 4.2), ED methods have been studied with a variety of industrial wastewaters. In the presence of heavy metal ions (waste solutions from pickling and other metallurgical processes), the use of proton-blocking AEMs and proton-selective CEMs is crucial for recovering acids by ED concentration. Interestingly, NF membranes instead of CEMs can increase significantly the proton/metal permselectivity. Further studies on the development and testing of special membranes would be beneficial. BMED is a valid alternative and can also convert salts into acids and bases, either with or without previous precipitation of heavy metals, if present. The regeneration of spent solutions from chemical absorption of flue gases (SO_2, H_2S, CO_2) is an interesting application of ED techniques, which may offer economic advantages. Various effluents containing organic matter were treated as well, finding only minor fouling issues in many cases. There are some commercialized systems and pilot plants. The scaling up should be extended to a wider range of applications.

Desalination (Section 4.3) via ED enables water reuse by treating salty wastewater from different industrial sources. Produced water of oil and gas extraction poses challenges related to high energy consumptions in the case of high-salinity feeds. Preliminary studies show that optimized systems can be competitive even for these solutions, but significant efforts are still needed in this direction. Dealing with fouling, cleaning procedures and EDR operation may have a partial effectiveness, as also shown by pilot plants. However, pulsed electric fields can minimize fouling phenomena. Therefore, this technique deserves further studies. Pilot installations have reclaimed wastewater of refineries and petrochemical industries, drainage water of coal mines, and wastewater of power plants. The treatment costs were shown to be attractive in some cases, but further economic analyses are needed. Energy recovery via RED is an interesting option, thus it should be explored more deeply in the future, by paying attention to the investment costs.

ED methods may be effective for various other industrial wastewaters (Section 4.4). Single salts or mixtures, waste effluents from pulp and paper manufacturing, textile processing, and bio-refining are just some examples. However, only a small number of studies have been conducted so far for each application. Therefore, further research is required to improve the performance (e.g., in terms of selectivity and energy consumption/recovery) and to develop techno-economically competitive systems for the various types of industrial wastewater.

There are several possible applications for municipal wastewater and other effluents (Section 5). In the desalination of municipal WWTP effluents (Section 5.1), ED can be a cost-effective treatment enabling water reuse (e.g., irrigation), as shown by several field plant applications. Interesting results were shown by some studies on ED coupled with FO for recovering high-quality water or for controlling salinity build-up, thus this coupling is deserving of more attention in the future.

Treated wastewater may be used as a low-salinity stream coupled with seawater or other waste effluents as high-salinity stream in order to recover energy via RED (Section 5.2). The presence of organics requires the development of cost-effective pre-treatments and cleaning methods against fouling and clogging, enabling long-term operations with stable net power. Some pilot installations have been tested, but techno-economic analyses are needed. The integration of membrane distillation with RED has been proposed to recover water and energy from urine, but further studies are needed to assess the process feasibility.

The recovery of nutrients (Section 5.3) via SED or ED is another option, but energy consumptions and costs still need to be evaluated. Fertilizers can be produced also by ED treatment of excess sludge

sidestreams, human urine and animal farming effluents. Pilot installations were operated, and the processes may be competitive. Pre-treatments (in the case of human urine) or cleaning and polarity reversal (in the case of digested swine manure) minimized fouling phenomena, and thus long-term operations may be feasible. In a couple of studies, VFAs were recovered along with nutrients by ED (from excess sludge) or BMED (from pig manure). Promising results were obtained in a study on SED for the simultaneous fractionation of cations and anions into several streams from digested swine manure. These emerging applications deserve further studies.

A possible application of ED in the buildings sector is the regeneration of liquid desiccant solutions for air conditioning (Section 5.4). The high-concentration solutions (for example ~30 wt% LiCl) used for this process require the development of high-performance IEMs and a delicate process optimisation in order to limit detrimental effects due to undesired transport phenomena.

Resources can also be recuperated by treating waste brine from desalination or ion exchange (Section 6). Water and salt recovery (Section 6.1) has been demonstrated at pilot scale in various zero brine discharge systems. Scaling and/or fouling were controlled in all cases, without particular problems. ED exhibited competitive costs in recovering water from BWRO brine. The same applies for ED with MVMs recovering concentrated brines for edible salt production (evaporation–crystallisation) and diluted solutions (fresh or brackish water) from SWRO retentate, as shown also by long-term testing. However, the competitiveness with respect to a standalone SWRO depends on the local water, salt and electricity prices. Instead, NaCl recovery for industrial use (e.g., in the chlor-alkali industry) is not yet feasible. EDM has been proposed to separate salts, and it was found to be efficient. However, the overall process should be assessed. Some studies showed that water recovery by ED may be feasible also from WWRO brine (either municipal effluents or industrial effluents, e.g., from petrochemical sites). In the presence of organics (e.g., food industry wastewater), attention should be paid to their molecular weight and charge, which affect their transport. Water and salt (LiCl concentrated solution) were recovered from the effluent of a Li-ion batteries production plant, thus deserving further research to promote the industrial application. A couple of studies have investigated the treatment of surface water IX spent regeneration brines containing NOM. NaCl solutions that were reusable for IX regeneration were obtained via ED with MVMs, thus minimizing waste brine disposal. Further studies should be focused on the potential reuse of the NOM solution, the process sustainability and the long-term operation.

Salt conversion into acid and base from waste brines (Section 6.2) is a recovery method that can be performed by BMED. Moreover, the desalted solution may improve water recovery. In most cases, the treatment was tested with SWRO brine. Acid and base recovered have not reached the quality standards of commercial chemicals. This, in conjunction with the high energy consumptions, does not yet allow market entry. However, in situ use at the desalination plant is possible. The use of MVMs significantly enhanced the purity of the products. Future research should be intensified in this direction, as well as in the development of highly selective membranes, in the process optimisation, in the evaluation of post-concentration systems and in the scaling up.

Waste brines from desalination plants are suitable as concentrated solutions for energy recovery via RED (Section 6.3). Low-energy consuming systems were demonstrated in a few recent studies. However, capital costs may increase significantly, and thus economic analyses should reveal the actual feasibility. Other critical points for further research are the development of scaled-up systems, the testing with real solutions, and the evaluation of the net power density. Addressing all these aspects is necessary in order to attempt the implementation of integrated methodologies in real systems.

The application of ED techniques in wastewater treatment offers new opportunities for environmental protection and recovery of resources. Techno-economic challenges are still present, but great efforts have been made, mainly in the last 20 years, opening promising perspectives within efficient ZLD systems.

Some commercial applications and several pilot installations are accompanied by hundreds of studies with laboratory tests.

Some process limitations can be alleviated or even remediated. EDR operation, pulsed electric fields, pre-treatment and cleaning procedures against fouling can maintain or restore, at least partially, IEM properties. However, permanent fouling and poisoning of membranes may occur. Special membranes, e.g., proton-blocking AEMs, proton-selective CEMs, monovalent selective membranes, and even UF or NF membranes, can improve process selectivity and products purity. Nevertheless, energy consumptions may be high. Therefore, in addition to developing high-performing membranes (low resistance, high selectivity, low osmotic transport), optimizing system design and operation is essential to implement competitive processes. In this regard, novel concepts based on multi-stage ED configurations or integrated (electro-)membrane processes provide interesting technological solutions. Performance with real effluents, scaling up, long-term operation, overall sustainability, and techno-economic analysis have still to be assessed for several applications. An abatement in the membrane cost will be important to improving the process economics.

Please note that studies on similar or hybrid processes have been growing, i.e., EDI with configurations deviating from conventional ED stacks (important role of electrode chambers) [42,45–47,183], RED and fuel cell (Fenton)-RED with wastewater treatment at the electrode compartments [53,57,544–547], concentration gradient or pH gradient flow batteries [548–550], membrane electrolysis and electro-electrodialysis [551–560], hybrid liquid membrane-ED [561–563], decoupled ED [564], shock ED [565], (membrane) capacitive deionisation [566–574], membrane electrode redox transistor ED [575], bio-electrochemical systems [576–579] including microbial desalination cell [580–583], microbial desalination and chemical-production cell [584], and (Fenton) microbial RED [585–587]. Hence, knowledge acquired on common aspects will likely promote substantial advances in ED.

In light of all of the above considerations, a realistic scenario where ED techniques will conquer a wider market share for real applications can be prospected for a not far future.

Author Contributions: All the authors contributed to the writing and editing of this work. All authors have read and agreed to the published version of the manuscript.

Funding: This work was performed within the framework of the REvivED project (Low energy solutions for drinking water production by a REvival of ElectroDialysis systems) and the BAoBaB project (Blue Acid/Base Battery: Storage and recovery of renewable electrical energy by reversible salt water dissociation). These projects have received funding from the European Union's Horizon 2020 Research and Innovation program under Grant Agreements no. 685579 (www.revivedwater.eu) and 731187 (www.baobabproject.eu).

Conflicts of Interest: The authors declare no conflict of interest. The funders had no role in the design of the study; in the collection, analyses, or interpretation of data; in the writing of the manuscript, or in the decision to publish the results.

Abbreviations

AEL	Anion exchange layer
AEM	Anion exchange membrane
BM	Bipolar membrane
BMED	Bipolar membrane electrodialysis
BMSED	Bipolar membrane selectrodialysis
BWRO	Brackish water reverse osmosis
CEDI	Continuous electrodeionisation
CEL	Cation exchange layer
CEM	Cation exchange membrane
COP	Coefficient of performance
ED	Electrodialysis

EDI	Electrodeionisation
EDL	Electrical double layer
EDM	Electrodialysis metathesis
EDR	Electrodialysis reversal
EDTA	Ethylenediaminetetraacetic acid
FO	Forward osmosis
HPAM	Partially hydrolysed polyacrylamide
IEM	Ion exchange membrane
IX	Ion-exchange
IXR	Ion-exchange resin
MCDI	Membrane capacitive deionisation
MD	Membrane distillation
MF	Microfiltration
MVA	Monovalent selective anion exchange membrane
MVC	Monovalent selective cation exchange membrane
MVM	Monovalent selective ion exchange membrane
NF	Nanofiltration
NOM	Natural organic matter
RED	Reverse electrodialysis
REDI	Reverse electrodeionisation
RO	Reverse osmosis
SED	Selectrodialysis
SWRO	Seawater reverse osmosis
TDS	Total Dissolved Solids
UF	Ultrafiltration
VFA	Volatile fatty acid
WWRO	Wastewater reverse osmosis
WWTP	Wastewater treatment plant
ZLD	Zero liquid discharge

References

1. Tong, T.; Elimelech, M. The Global Rise of Zero Liquid Discharge for Wastewater Management: Drivers, Technologies, and Future Directions. *Environ. Sci. Technol.* **2016**, *50*, 6846–6855. [CrossRef]
2. Ahirrao, S. Zero Liquid Discharge Solutions. In *Industrial Wastewater Treatment, Recycling and Reuse*; Butterworth-Heinemann: Oxford, UK, 2014; pp. 489–520. ISBN 9780444634030.
3. Yaqub, M.; Lee, W. Zero-liquid discharge (ZLD) technology for resource recovery from wastewater: A review. *Sci. Total Environ.* **2019**, *681*, 551–563. [CrossRef] [PubMed]
4. Voulvoulis, N. Water reuse from a circular economy perspective and potential risks from an unregulated approach. *Curr. Opin. Environ. Sci. Health* **2018**, *2*, 32–45. [CrossRef]
5. European Comission. *Report from the Commission to the European Parliament, the Council, the European Economic and Social Committee and the Committee of the Regions on the Implementation of the Circular Economy Action Plan*; European Comission: Brusselles, Belgium, 2019.
6. Kirchherr, J.; Reike, D.; Hekkert, M. Conceptualizing the circular economy: An analysis of 114 definitions. *Resour. Conserv. Recycl.* **2017**, *127*, 221–232. [CrossRef]
7. Obotey Ezugbe, E.; Rathilal, S. Membrane Technologies in Wastewater Treatment: A Review. *Membranes* **2020**, *10*, 89. [CrossRef] [PubMed]
8. Strathmann, H. *Ion.-Exchange Membrane Separation Processes*, 1st ed.; Elsevier: Amsterdam, The Netherlands, 2004; ISBN 044450236X.

9. Tanaka, Y. *Ion. Exchange Membranes: Fundamentals and Applications*; Elsevier: Amsterdam, The Netherlands, 2007; Volume 12, ISBN 0927-5193.
10. Xu, T. Ion exchange membranes: State of their development and perspective. *J. Membr. Sci.* **2005**, *263*, 1–29. [CrossRef]
11. Nagarale, R.K.; Gohil, G.S.; Shahi, V.K. Recent developments on ion-exchange membranes and electro-membrane processes. *Adv. Colloid Interface Sci.* **2006**, *119*, 97–130. [CrossRef]
12. Ran, J.; Wu, L.; He, Y.; Yang, Z.; Wang, Y.; Jiang, C.; Ge, L.; Bakangura, E.; Xu, T. Ion exchange membranes: New developments and applications. *J. Membr. Sci.* **2017**, *522*, 267–291. [CrossRef]
13. Xu, T.; Huang, C. Electrodialysis-Based separation technologies: A critical review. *AiCHE J.* **2008**, *54*, 3147–3159. [CrossRef]
14. Zhao, W.Y.; Zhou, M.; Yan, B.; Sun, X.; Liu, Y.; Wang, Y.; Xu, T.; Zhang, Y. Waste conversion and resource recovery from wastewater by ion exchange membranes: State-of-the-art and perspective. *Ind. Eng. Chem. Res.* **2018**, *57*, 6025–6039. [CrossRef]
15. Strathmann, H. Electrodialysis, a mature technology with a multitude of new applications. *Desalination* **2010**, *264*, 268–288. [CrossRef]
16. Campione, A.; Gurreri, L.; Ciofalo, M.; Micale, G.; Tamburini, A.; Cipollina, A. Electrodialysis for water desalination: A critical assessment of recent developments on process fundamentals, models and applications. *Desalination* **2018**, *434*, 121–160. [CrossRef]
17. Sajjad, A.-A.; Yunus, M.Y.B.M.; Azoddein, A.A.M.; Hassell, D.G.; Dakhil, I.H.; Hasan, H.A. Electrodialysis Desalination for Water and Wastewater: A Review. *Chem. Eng. J.* **2020**, *380*, 122231.
18. Fidaleo, M.; Moresi, M. Electrodialysis Applications in The Food Industry. *Adv. Food Nutr. Res.* **2006**, *51*, 265–360.
19. Huang, C.; Xu, T.; Zhang, Y.; Xue, Y.; Chen, G. Application of electrodialysis to the production of organic acids: State-of-the-art and recent developments. *J. Membr. Sci.* **2007**, *288*, 1–12. [CrossRef]
20. *Electrodialysis and Water Reuse: Novel Approaches*; Moura Bernardes, A.; Zoppas Ferreira, J.; Siqueira Rodrigues, M.A. (Eds.) Springer: Berlin/Heidelberg, Germany, 2014; ISBN 9783642402494.
21. López-Garzón, C.S.; Straathof, A.J.J. Recovery of carboxylic acids produced by fermentation. *Biotechnol. Adv.* **2014**, *32*, 873–904. [CrossRef] [PubMed]
22. Gurreri, L.; Cipollina, A.; Tamburini, A.; Micale, G. Electrodialysis for wastewater treatment—Part I: Fundamentals and municipal effluents. In *Current Trends and Future Developments on (Bio-) Membranes-Membrane Technology for Water and Wastewater Treatment-Advances and Emerging Processes*; Basile, A., Comite, A., Eds.; Elsevier: Amsterdam, The Netherlands, 2020; pp. 141–192. ISBN 9780128168233.
23. Gurreri, L.; Cipollina, A.; Tamburini, A.; Micale, G. Electrodialysis for wastewater treatment—Part II: Industrial effluents. In *Current Trends and Future Developments on (Bio-) Membranes-Membrane Technology for Water and Wastewater Treatment-Advances and Emerging Processes*; Basile, A., Comite, A., Eds.; Elsevier: Amsterdam, The Netherlands, 2020; pp. 195–241. ISBN 9780128168233.
24. Gurreri, L.; Battaglia, G.; Tamburini, A.; Cipollina, A.; Micale, G.; Ciofalo, M. Multi-physical modelling of reverse electrodialysis. *Desalination* **2017**, *423*, 52–64. [CrossRef]
25. Battaglia, G.; Gurreri, L.; Airò Farulla, G.; Cipollina, A.; Pirrotta, A.; Micale, G.; Ciofalo, M. Membrane Deformation and Its Effects on Flow and Mass Transfer in the Electromembrane Processes. *Int. J. Mol. Sci.* **2019**, *20*, 1840. [CrossRef]
26. Battaglia, G.; Gurreri, L.; Airò Farulla, G.; Cipollina, A.; Pirrotta, A.; Micale, G.; Ciofalo, M. Pressure-Induced Deformation of Pillar-Type Profiled Membranes and Its Effects on Flow and Mass Transfer. *Computation* **2019**, *7*, 32. [CrossRef]
27. Battaglia, G.; Gurreri, L.; Cipollina, A.; Pirrotta, A.; Velizarov, S.; Ciofalo, M.; Micale, G. Fluid–Structure Interaction and Flow Redistribution in Membrane-Bounded Channels. *Energies* **2019**, *12*, 4259. [CrossRef]
28. Pawlowski, S.; Crespo, J.; Velizarov, S. Profiled Ion Exchange Membranes: A Comprehensible Review. *Int. J. Mol. Sci.* **2019**, *20*, 165. [CrossRef]
29. Lindstrand, V.; Sundström, G.; Jönsson, A.S. Fouling of electrodialysis membranes by organic substances. *Desalination* **2000**, *128*, 91–102. [CrossRef]

30. Strathmann, H.; Krol, J.J.; Rapp, H.J.; Eigenberger, G. Limiting current density and water dissociation in bipolar membranes. *J. Membr. Sci.* **1997**, *125*, 123–142. [CrossRef]
31. Mareev, S.A.; Evdochenko, E.; Wessling, M.; Kozaderova, O.A.; Niftaliev, S.I.; Pismenskaya, N.D.; Nikonenko, V.V. A comprehensive mathematical model of water splitting in bipolar membranes: Impact of the spatial distribution of fixed charges and catalyst at bipolar junction. *J. Membr. Sci.* **2020**, *603*, 118010. [CrossRef]
32. Pan, J.; Hou, L.; Wang, Q.; He, Y.; Wu, L.; Mondal, A.N.; Xu, T. Preparation of bipolar membranes by electrospinning. *Mater. Chem. Phys.* **2017**, *186*, 484–491. [CrossRef]
33. Shen, C.; Wycisk, R.; Pintauro, P.N. High performance electrospun bipolar membrane with a 3D junction. *Energy Environ. Sci.* **2017**, *10*, 1435–1442. [CrossRef]
34. Pourcelly, G. Electrodialysis with bipolar membranes: Principles, optimization, and applications. *Russ. J. Electrochem.* **2002**, *38*, 919–926. [CrossRef]
35. Jaroszek, H.; Dydo, P. Ion-exchange membranes in chemical synthesis-a review. *Open Chem.* **2016**, *14*, 1–19. [CrossRef]
36. Huang, C.; Xu, T. Electrodialysis with bipolar membranes for sustainable development. *Environ. Sci. Technol.* **2006**, *40*, 5233–5243. [CrossRef]
37. Mani, K.N.; Chlanda, F.P.; Byszewski, C.H. Aquatech membrane technology for recovery of acid/base values for salt streams. *Desalination* **1988**, *68*, 149–166. [CrossRef]
38. Mani, K.N. Electrodialysis water splitting technology. *J. Membr. Sci.* **1991**, *58*, 117–138. [CrossRef]
39. Zhang, Y.; Paepen, S.; Pinoy, L.; Meesschaert, B.; Van Der Bruggen, B. Selectrodialysis: Fractionation of divalent ions from monovalent ions in a novel electrodialysis stack. *Sep. Purif. Technol.* **2012**, *88*, 191–201. [CrossRef]
40. Alhéritière, C.; Ernst, W.R.; Davis, T.A. Metathesis of magnesium and sodium salt systems by electrodialysis. *Desalination* **1998**, *115*, 189–198. [CrossRef]
41. Chen, Q.-B.; Ren, H.; Tian, Z.; Sun, L.; Wang, J. Conversion and pre-concentration of SWRO reject brine into high solubility liquid salts (HSLS) by using electrodialysis metathesis. *Sep. Purif. Technol.* **2019**, *213*, 587–598. [CrossRef]
42. Alvarado, L.; Chen, A. Electrodeionization: Principles, strategies and applications. *Electrochim. Acta* **2014**, *132*, 583–597. [CrossRef]
43. Hakim, A.N.; Khoiruddin, K.; Ariono, D.; Wenten, I.G. Ionic Separation in Electrodeionization System: Mass Transfer Mechanism and Factor Affecting Separation Performance. *Sep. Purif. Rev.* **2019**, 1–23. [CrossRef]
44. Wood, J.; Gifford, J.; Arba, J.; Shaw, M. Production of ultrapure water by continuous electrodeionization. *Desalination* **2010**, *250*, 973–976. [CrossRef]
45. Dzyazko, Y.S.; Belyakov, V.N. Purification of a diluted nickel solution containing nickel by a process combining ion exchange and electrodialysis. *Desalination* **2004**, *162*, 179–189. [CrossRef]
46. Feng, X.; Wu, Z.; Chen, X. Removal of metal ions from electroplating effluent by EDI process and recycle of purified water. *Sep. Purif. Technol.* **2007**, *57*, 257–263. [CrossRef]
47. Mahmoud, A.; Hoadley, A.F.A. An evaluation of a hybrid ion exchange electrodialysis process in the recovery of heavy metals from simulated dilute industrial wastewater. *Water Res.* **2012**, *46*, 3364–3376. [CrossRef]
48. Souilah, O.; Akretche, D.E.; Amara, M. Water reuse of an industrial effluent by means of electrodeionisation. *Desalination* **2004**, *167*, 49–54. [CrossRef]
49. Spoor, P.B.; Koene, L.; ter Veen, W.R.; Janssen, L.J.J. Continuous deionization of a dilute nickel solution. *Chem. Eng. J.* **2002**, *85*, 127–135. [CrossRef]
50. Spoor, P.B.; Grabovska, L.; Koene, L.; Janssen, L.J.J.; Ter Veen, W.R. Pilot scale deionisation of a galvanic nickel solution using a hybrid ion-exchange/electrodialysis system. *Chem. Eng. J.* **2002**, *89*, 193–202. [CrossRef]
51. Park, S.; Kwak, R. Microscale electrodeionization: In situ concentration profiling and flow visualization. *Water Res.* **2020**, *170*, 115310. [CrossRef] [PubMed]
52. Pan, S.Y.; Snyder, S.W.; Ma, H.W.; Lin, Y.J.; Chiang, P.C. Energy-efficient resin wafer electrodeionization for impaired water reclamation. *J. Clean. Prod.* **2018**, *174*, 1464–1474. [CrossRef]
53. Mei, Y.; Tang, C.Y. Recent developments and future perspectives of reverse electrodialysis technology: A review. *Desalination* **2018**, *425*, 156–174. [CrossRef]

54. Tufa, R.A.; Pawlowski, S.; Veerman, J.; Bouzek, K.; Fontananova, E.; di Profio, G.; Velizarov, S.; Goulão Crespo, J.; Nijmeijer, K.; Curcio, E. Progress and prospects in reverse electrodialysis for salinity gradient energy conversion and storage. *Appl. Energy* **2018**, *225*, 290–331. [CrossRef]
55. Cipollina, A.; Micale, G.; Tamburini, A.; Tedesco, M.; Gurreri, L.; Veerman, J.; Grasman, S. Reverse electrodialysis: Applications. In *Sustainable Energy from Salinity Gradients*; Cipollina, A., Micale, G., Eds.; Woodhead Publishing: Cambridge, UK; Elsevier: Amsterdam, The Netherlands, 2016; pp. 135–180. ISBN 9780081003237.
56. Tamburini, A.; Cipollina, A.; Tedesco, M.; Gurreri, L.; Ciofalo, M.; Micale, G. The REAPower Project: Power Production From Saline Waters and Concentrated Brines. In *Current Trends and Future Developments on (Bio-) Membranes-Membrane Desalination Systems: The Next Generation*; Basile, A., Curcio, E., Inamuddin, I., Eds.; Elsevier: Amsterdam, The Netherlands, 2019; pp. 407–448.
57. Tian, H.; Wang, Y.; Pei, Y.; Crittenden, J.C. Unique applications and improvements of reverse electrodialysis: A review and outlook. *Appl. Energy* **2020**, *262*, 114482. [CrossRef]
58. Avci, A.H.; Tufa, R.A.; Fontananova, E.; Di Profio, G.; Curcio, E. Reverse Electrodialysis for energy production from natural river water and seawater. *Energy* **2018**, *165*, 512–521. [CrossRef]
59. Sata, T. *Ion. Exchange Membranes: Preparation, Characterization, Modification and Application*; Royal Society of Chemistry: Cambridge, UK, 2004; ISBN 978-0-85404-590-7.
60. Luo, T.; Abdu, S.; Wessling, M. Selectivity of ion exchange membranes: A review. *J. Membr. Sci.* **2018**, *555*, 429–454. [CrossRef]
61. Kontturi, K.; Murtomäki, L.; Manzanares, J.A. *Ionic Transport. Processes in Electrochemistry and Membrane Science*; Oxford University Press Inc.: New York, NY, USA, 2008; ISBN 978-0-19–953381–7.
62. Manzanares, J.A.; Vergara, G.; Mafé, S.; Kontturi, K.; Viinikka, P. Potentiometric Determination of Transport Numbers of Ternary Electrolyte Systems in Charged Membranes. *J. Phys. Chem. B* **1998**, *102*, 1301–1307. [CrossRef]
63. Kraaijeveld, G.; Sumberova, V.; Kuindersma, S.; Wesselingh, H. Modelling electrodialysis using the Maxwell-Stefan description. *Chem. Eng. J. Biochem. Eng. J.* **1995**, *57*, 163–176. [CrossRef]
64. Plntauro, P.N.; Bennion, D.N. Mass Transport of Electrolytes in Membranes. 1. Development of Mathematical Transport Model. *Ind. Eng. Chem. Fundam.* **1984**, *23*, 230–234. [CrossRef]
65. Wesselingh, J.A.; Vonk, P.; Kraaijeveld, G. Exploring the Maxwell-Stefan description of ion exchange. *Chem. Eng. J. Biochem. Eng. J.* **1995**, *57*, 75–89. [CrossRef]
66. Sata, T. Studies on ion exchange membranes with permselectivity for specific ions in electrodialysis. *J. Membr. Sci.* **1994**, *93*, 117–135. [CrossRef]
67. Balster, J.; Yildirim, M.H.; Stamatialis, D.F.; Ibanez, R.; Lammertink, R.G.H.; Jordan, V.; Wessling, M. Morphology and microtopology of cation-exchange polymers and the origin of the overlimiting current. *J. Phys. Chem. B* **2007**, *111*, 2152–2165. [CrossRef]
68. Długołecki, P.; Anet, B.; Metz, S.J.; Nijmeijer, K.; Wessling, M. Transport limitations in ion exchange membranes at low salt concentrations. *J. Membr. Sci.* **2010**, *346*, 163–171. [CrossRef]
69. Galama, A.H.; Vermaas, D.A.; Veerman, J.; Saakes, M.; Rijnaarts, H.H.M.; Post, J.W.; Nijmeijer, K. Membrane resistance: The effect of salinity gradients over a cation exchange membrane. *J. Membr. Sci.* **2014**, *467*, 279–291. [CrossRef]
70. Gohil, G.S.; Shahi, V.K.; Rangarajan, R. Comparative studies on electrochemical characterization of homogeneous and heterogeneous type of ion-exchange membranes. *J. Membr. Sci.* **2004**, *240*, 211–219. [CrossRef]
71. Mehdizadeh, S.; Yasukawa, M.; Abo, T.; Kakihana, Y.; Higa, M. Effect of spacer geometry on membrane and solution compartment resistances in reverse electrodialysis. *J. Membr. Sci.* **2019**, *572*, 271–280. [CrossRef]
72. Galama, A.H.; Hoog, N.A.; Yntema, D.R. Method for determining ion exchange membrane resistance for electrodialysis systems. *Desalination* **2016**, *380*, 1–11. [CrossRef]
73. Silva, R.F.; De Francesco, M.; Pozio, A. Tangential and normal conductivities of Nafion® membranes used in polymer electrolyte fuel cells. *J. Power Sources* **2004**, *134*, 18–26. [CrossRef]
74. Kamcev, J.; Sujanani, R.; Jang, E.S.; Yan, N.; Moe, N.; Paul, D.R.; Freeman, B.D. Salt concentration dependence of ionic conductivity in ion exchange membranes. *J. Membr. Sci.* **2018**, *547*, 123–133. [CrossRef]

75. Zhu, S.; Kingsbury, R.S.; Call, D.F.; Coronell, O. Impact of solution composition on the resistance of ion exchange membranes. *J. Membr. Sci.* **2018**, *554*, 39–47. [CrossRef]
76. Larchet, C.; Nouri, S.; Auclair, B.; Dammak, L.; Nikonenko, V. Application of chronopotentiometry to determine the thickness of diffusion layer adjacent to an ion-exchange membrane under natural convection. *Adv. Colloid Interface Sci.* **2008**, *139*, 45–61. [CrossRef]
77. Zabolotsky, V.I.; Nikonenko, V.V. Effect of structural membrane inhomogeneity on transport properties. *J. Membr. Sci.* **1993**, *79*, 181–198. [CrossRef]
78. Veerman, J. The Effect of the NaCl Bulk Concentration on the Resistance of Ion Exchange Membranes—Measuring and Modeling. *Energies* **2020**, *13*, 1946. [CrossRef]
79. Porada, S.; van Egmond, W.J.; Post, J.W.; Saakes, M.; Hamelers, H.V.M. Tailoring ion exchange membranes to enable low osmotic water transport and energy efficient electrodialysis. *J. Membr. Sci.* **2018**, *552*, 22–30. [CrossRef]
80. Kamcev, J.; Doherty, C.M.; Lopez, K.P.; Hill, A.J.; Paul, D.R.; Freeman, B.D. Effect of fixed charge group concentration on salt permeability and diffusion coefficients in ion exchange membranes. *J. Membr. Sci.* **2018**, *566*, 307–316. [CrossRef]
81. Kamcev, J.; Paul, D.R.; Manning, G.S.; Freeman, B.D. Predicting salt permeability coefficients in highly swollen, highly charged ion exchange membranes. *ACS Appl. Mater. Interfaces* **2017**, *9*, 4044–4056. [CrossRef]
82. Kamcev, J.; Paul, D.R.; Manning, G.S.; Freeman, B.D. Ion Diffusion Coefficients in Ion Exchange Membranes: Significance of Counterion Condensation. *Macromolecules* **2018**, *51*, 5519–5529. [CrossRef]
83. Ciofalo, M.; Di Liberto, M.; Gurreri, L.; La Cerva, M.; Scelsi, L.; Micale, G. Mass transfer in ducts with transpiring walls. *Int. J. Heat Mass Transf.* **2019**, *132*, 1074–1086. [CrossRef]
84. Spiegler, K.S. Polarization at ion exchange membrane-solution interfaces. *Desalination* **1971**, *9*, 367–385. [CrossRef]
85. Helfferich, F. *Ion. Exchange*; McGraw-Hill: New York, NY, USA, 1962.
86. Levich, V.G. *Physicochemical Hydrodynamics*; Prentice-Hall: Englewood Cliffs, NJ, USA, 1962.
87. Krol, J.J.; Wessling, M.; Strathmann, H. Concentration polarization with monopolar ion exchange membranes: Current-voltage curves and water dissociation. *J. Membr. Sci.* **1999**, *162*, 145–154. [CrossRef]
88. Kwak, R.; Guan, G.; Peng, W.K.; Han, J. Microscale electrodialysis: Concentration profiling and vortex visualization. *Desalination* **2013**, *308*, 138–146. [CrossRef]
89. Rubinstein, I.; Shtilman, L. Voltage against current curves of cation exchange membranes. *J. Chem. Soc. Faraday Trans. 2 Mol. Chem. Phys.* **1979**, *75*, 231–246. [CrossRef]
90. Lee, H.J.; Strathmann, H.; Moon, S.H. Determination of the limiting current density in electrodialysis desalination as an empirical function of linear velocity. *Desalination* **2006**, *190*, 43–50. [CrossRef]
91. Urtenov, M.K.; Uzdenova, A.M.; Kovalenko, A.V.; Nikonenko, V.V.; Pismenskaya, N.D.; Vasil'eva, V.I.; Sistat, P.; Pourcelly, G. Basic mathematical model of overlimiting transfer enhanced by electroconvection in flow-through electrodialysis membrane cells. *J. Membr. Sci.* **2013**, *447*, 190–202. [CrossRef]
92. La Cerva, M.; Gurreri, L.; Tedesco, M.; Cipollina, A.; Ciofalo, M.; Tamburini, A.; Micale, G. Determination of limiting current density and current efficiency in electrodialysis units. *Desalination* **2018**, *445*, 138–148. [CrossRef]
93. Cowan, D.A.; Brown, J.H. Effect of Turbulence on Limiting Current in Electrodialysis Cells. *Ind. Eng. Chem.* **1959**, *51*, 1445–1448. [CrossRef]
94. Ben Sik Ali, M.; Mnif, A.; Hamrouni, B. Modelling of the limiting current density of an electrodialysis process by response surface methodology. *Ionics (Kiel)* **2018**, *24*, 617–628. [CrossRef]
95. Forgacs, C.; Ishibashi, N.; Leibovitz, J.; Sinkovic, J.; Spiegler, K.S. Polarization at ion-exchange membranes in electrodialysis. *Desalination* **1972**, *10*, 181–214. [CrossRef]
96. Kharkats, Y.I. Mechanism of "supralimiting" currents at ion-exchange mebrane/electrolyte interfaces. *Sov. Electrochem.* **1985**, *21*, 917–920.
97. Simons, R. The origin and elimination of water splitting in ion exchange membranes during water demineralisation by electrodialysis. *Desalination* **1979**, *28*, 41–42. [CrossRef]
98. Simons, R. Water splitting in ion exchange membranes. *Electrochim. Acta* **1985**, *30*, 275–282. [CrossRef]
99. Nikonenko, V.; Urtenov, M.; Mareev, S. Pourcelly Mathematical Modeling of the Effect of Water Splitting on Ion Transfer in the Depleted Diffusion Layer Near an Ion-Exchange Membrane. *Membranes* **2020**, *10*, 22. [CrossRef]

100. Uzdenova, A. 2D Mathematical Modelling of Overlimiting Transfer Enhanced by Electroconvection in Flow-Through Electrodialysis Membrane Cells in Galvanodynamic Mode. *Membranes* **2019**, *9*, 39. [CrossRef]
101. Uzdenova, A.; Urtenov, M. Potentiodynamic and Galvanodynamic Regimes of Mass Transfer in Flow-Through Electrodialysis Membrane Systems: Numerical Simulation of Electroconvection and Current-Voltage Curve. *Membranes* **2020**, *10*, 49. [CrossRef]
102. Nikonenko, V.V.; Pismenskaya, N.D.; Belova, E.I.; Sistat, P.; Huguet, P.; Pourcelly, G.; Larchet, C. Intensive current transfer in membrane systems: Modelling, mechanisms and application in electrodialysis. *Adv. Colloid Interface Sci.* **2010**, *160*, 101–123. [CrossRef]
103. Nikonenko, V.V.; Kovalenko, A.V.; Urtenov, M.K.; Pismenskaya, N.D.; Han, J.; Sistat, P.; Pourcelly, G. Desalination at overlimiting currents: State-of-the-art and perspectives. *Desalination* **2014**, *342*, 85–106. [CrossRef]
104. Mareev, S.A.; Nebavskiy, A.V.; Nichka, V.S.; Urtenov, M.K.; Nikonenko, V.V. The nature of two transition times on chronopotentiograms of heterogeneous ion exchange membranes: 2D modelling. *J. Membr. Sci.* **2019**, *575*, 179–190. [CrossRef]
105. Nikonenko, V.; Nebavsky, A.; Mareev, S.; Kovalenko, A.; Urtenov, M.; Pourcelly, G. Modelling of Ion Transport in Electromembrane Systems: Impacts of Membrane Bulk and Surface Heterogeneity. *Appl. Sci.* **2018**, *9*, 25. [CrossRef]
106. Andersen, M.B.; Wang, K.M.; Schiffbauer, J.; Mani, A. Confinement effects on electroconvective instability. *Electrophoresis* **2017**, *38*, 702–711. [CrossRef] [PubMed]
107. Pham, S.V.; Kwon, H.; Kim, B.; White, J.K.; Lim, G.; Han, J. Helical vortex formation in three-dimensional electrochemical systems with ion-selective membranes. *Phys. Rev. E* **2016**, *93*, 033114. [CrossRef] [PubMed]
108. Karatay, E.; Druzgalski, C.L.; Mani, A. Simulation of chaotic electrokinetic transport: Performance of commercial software versus custom-built direct numerical simulation codes. *J. Colloid Interface Sci.* **2015**, *446*, 67–76. [CrossRef]
109. Zaltzman, B.; Rubinstein, I. Electro-osmotic slip and electroconvective instability. *J. Fluid Mech.* **2007**, *579*, 173–226. [CrossRef]
110. Krol, J.J.; Wessling, M.; Strathmann, H. Chronopotentiometry and overlimiting ion transport through monopolar ion exchange membranes. *J. Membr. Sci.* **1999**, *162*, 155–164. [CrossRef]
111. Rubinstein, I. Electroconvection at an electrically inhomogeneous permselective interface. *Phys. Fluids A* **1991**, *3*, 2301–2309. [CrossRef]
112. Maletzki, F.; Rösler, H.W.; Staude, E. Ion transfer across electrodialysis membranes in the overlimiting current range: Stationary voltage current characteristics and current noise power spectra under different conditions of free convection. *J. Membr. Sci.* **1992**, *71*, 105–116. [CrossRef]
113. Rubinstein, I.; Staude, E.; Kedem, O. Role of the membrane surface in concentration polarization at ion-exchange membrane. *Desalination* **1988**, *69*, 101–114. [CrossRef]
114. Zabolotsky, V.I.; Nikonenko, V.V.; Pismenskaya, N.D.; Laktionov, E.V.; Urtenov, M.K.; Strathmann, H.; Wessling, M.; Koops, G.H. Coupled transport phenomena in overlimiting current electrodialysis. *Sep. Purif. Technol.* **1998**, *14*, 255–267. [CrossRef]
115. Dukhin, S.S. Electrokinetic phenomena of the second kind and their applications. *Adv. Colloid Interface Sci.* **1991**, *35*, 173–196. [CrossRef]
116. Rubinstein, I.; Zaltzman, B.; Kedem, O. Electric fields in and around ion-exchange membranes. *J. Membr. Sci.* **1997**, *125*, 17–21. [CrossRef]
117. Choi, J.-H.; Lee, H.-J.; Moon, S.-H. Effects of Electrolytes on the Transport Phenomena in a Cation-Exchange Membrane. *J. Colloid Interface Sci.* **2001**, *238*, 188–195. [CrossRef] [PubMed]
118. Ibanez, R.; Stamatialis, D.F.; Wessling, M. Role of membrane surface in concentration polarization at cation exchange membranes. *J. Membr. Sci.* **2004**, *239*, 119–128. [CrossRef]
119. Pismenskaia, N.; Sistat, P.; Huguet, P.; Nikonenko, V.; Pourcelly, G. Chronopotentiometry applied to the study of ion transfer through anion exchange membranes. *J. Membr. Sci.* **2004**, *228*, 65–76. [CrossRef]
120. Volodina, E.; Pismenskaya, N.; Nikonenko, V.; Larchet, C.; Pourcelly, G. Ion transfer across ion-exchange membranes with homogeneous and heterogeneous surfaces. *J. Colloid Interface Sci.* **2005**, *285*, 247–258. [CrossRef]

121. Gil, V.V.; Andreeva, M.A.; Jansezian, L.; Han, J.; Pismenskaya, N.D.; Nikonenko, V.V.; Larchet, C.; Dammak, L. Impact of heterogeneous cation-exchange membrane surface modification on chronopotentiometric and current–voltage characteristics in NaCl, CaCl2and MgCl2solutions. *Electrochim. Acta* **2018**, *281*, 472–485. [CrossRef]
122. Nebavskaya, K.A.; Sarapulova, V.V.; Sabbatovskiy, K.G.; Sobolev, V.D.; Pismenskaya, N.D.; Sistat, P.; Cretin, M.; Nikonenko, V.V. Impact of ion exchange membrane surface charge and hydrophobicity on electroconvection at underlimiting and overlimiting currents. *J. Membr. Sci.* **2017**, *523*, 36–44. [CrossRef]
123. Nikonenko, V.V.; Mareev, S.A.; Pis'menskaya, N.D.; Uzdenova, A.M.; Kovalenko, A.V.; Urtenov, M.K.; Pourcelly, G. Effect of electroconvection and its use in intensifying the mass transfer in electrodialysis (Review). *Russ. J. Electrochem.* **2017**, *53*, 1122–1144. [CrossRef]
124. Butylskii, D.; Moroz, I.; Tsygurina, K.; Mareev, S. Effect of Surface Inhomogeneity of Ion-Exchange Membranes on the Mass Transfer Efficiency in Pulsed Electric Field Modes. *Membranes* **2020**, *10*, 40. [CrossRef]
125. Titorova, V.; Sabbatovskiy, K.; Sarapulova, V.; Kirichenko, E.; Sobolev, V.; Kirichenko, K. Characterization of MK-40 membrane modified by layers of cation exchange and anion exchange polyelectrolytes. *Membranes* **2020**, *10*, 20. [CrossRef] [PubMed]
126. Zabolotsky, V.I.; Nikonenko, V.V.; Pismenskaya, N.D. On the role of gravitational convection in the transfer enhancement of salt ions in the course of dilute solution electrodialysis. *J. Membr. Sci.* **1996**, *119*, 171–181. [CrossRef]
127. Larchet, C.; Zabolotsky, V.I.; Pismenskaya, N.; Nikonenko, V.V.; Tskhay, A.; Tastanov, K.; Pourcelly, G. Comparison of different ED stack conceptions when applied for drinking water production from brackish waters. *Desalination* **2008**, *222*, 489–496. [CrossRef]
128. Isaacson, M.S.; Sonin, A.A. Sherwood Number and Friction Factor Correlations for Electrodialysis Systems, with Application to Process Optimization. *Ind. Eng. Chem. Process. Des. Dev.* **1976**, *15*, 313–321. [CrossRef]
129. Sonin, A.A.; Probstein, R.F. A hydrodynamic theory of desalination by electrodialysis. *Desalination* **1968**, *5*, 293–329. [CrossRef]
130. Malek, P.; Ortiz, J.M.; Richards, B.S.; Schäfer, A.I. Electrodialytic removal of NaCl from water: Impacts of using pulsed electric potential on ion transport and water dissociation phenomena. *J. Membr. Sci.* **2013**, *435*, 99–109. [CrossRef]
131. Tadimeti, J.G.D.; Chattopadhyay, S. Uninterrupted swirling motion facilitating ion transport in electrodialysis. *Desalination* **2016**, *392*, 54–62. [CrossRef]
132. Geraldes, V.; Afonso, M.D. Limiting current density in the electrodialysis of multi-ionic solutions. *J. Membr. Sci.* **2010**, *360*, 499–508. [CrossRef]
133. Sonin, A.A.; Isaacson, M.S. Optimization of Flow Design in Forced Flow Electrochemical Systems, with Special Application to Electrodialysis. *Ind. Eng. Chem. Process. Des. Dev.* **1974**, *13*, 241–248. [CrossRef]
134. Fidaleo, M.; Moresi, M. Optimal strategy to model the electrodialytic recovery of a strong electrolyte. *J. Membr. Sci.* **2005**, *260*, 90–111. [CrossRef]
135. Belfort, G.; Guter, G.A. An experimental study of electrodialysis hydrodynamics. *Desalination* **1972**, *10*, 221–262. [CrossRef]
136. Lee, H.J.; Sarfert, F.; Strathmann, H.; Moon, S.H. Designing of an electrodialysis desalination plant. *Desalination* **2002**, *142*, 267–286. [CrossRef]
137. Tanaka, Y. Limiting current density of an ion-exchange membrane and of an electrodialyzer. *J. Membr. Sci.* **2005**, *266*, 6–17. [CrossRef]
138. Gurreri, L.; Tamburini, A.; Cipollina, A.; Micale, G.; Ciofalo, M. Flow and mass transfer in spacer-filled channels for reverse electrodialysis: A CFD parametrical study. *J. Membr. Sci.* **2016**, *497*, 300–317. [CrossRef]
139. La Cerva, M.; Di Liberto, M.; Gurreri, L.; Tamburini, A.; Cipollina, A.; Micale, G.; Ciofalo, M. Coupling CFD with a one-dimensional model to predict the performance of reverse electrodialysis stacks. *J. Membr. Sci.* **2017**, *541*, 595–610. [CrossRef]

140. Gurreri, L.; Tamburini, A.; Cipollina, A.; Micale, G.; Ciofalo, M. Pressure drop at low Reynolds numbers in woven-spacer-filled channels for membrane processes: CFD prediction and experimental validation. *Desalin. Water Treat.* **2017**, *61*, 170–182. [CrossRef]
141. Kuroda, O.; Takahashi, S.; Nomura, M. Characteristics of flow and mass transfer rate in an electrodialyzer compartment including spacer. *Desalination* **1983**, *46*, 225–232. [CrossRef]
142. Winograd, Y.; Solan, A.; Toren, M. Mass transfer in narrow channels in the presence of turbulence promoters. *Desalination* **1973**, *13*, 171–186. [CrossRef]
143. Da Costa, A.R.; Fane, A.G.; Fell, C.J.D.; Franken, A.C.M. Optimal channel spacer design for ultrafiltration. *J. Membr. Sci.* **1991**, *62*, 275–291. [CrossRef]
144. Koutsou, C.P.; Yiantsios, S.G.; Karabelas, A.J. A numerical and experimental study of mass transfer in spacer-filled channels: Effects of spacer geometrical characteristics and Schmidt number. *J. Membr. Sci.* **2009**, *326*, 234–251. [CrossRef]
145. Campione, A.; Cipollina, A.; Bogle, I.D.L.; Gurreri, L.; Tamburini, A.; Tedesco, M.; Micale, G. A hierarchical model for novel schemes of electrodialysis desalination. *Desalination* **2019**, *465*, 79–93. [CrossRef]
146. Culcasi, A.; Gurreri, L.; Zaffora, A.; Cosenza, A.; Tamburini, A.; Cipollina, A.; Micale, G. Ionic shortcut currents via manifolds in reverse electrodialysis stacks. *Desalination* **2020**, *485*, 114450. [CrossRef]
147. Wagholikar, V.V.; Zhuang, H.; Jiao, Y.; Moe, N.E.; Ramanan, H.; Goh, L.M.; Barber, J.; Lee, K.S.; Lee, H.P.; Fuh, J.Y.H. Modeling cell pair resistance and spacer shadow factors in electro-separation processes. *J. Membr. Sci.* **2017**, *543*, 151–162. [CrossRef]
148. Kim, H.K.; Lee, M.S.; Lee, S.Y.; Choi, Y.W.; Jeong, N.J.; Kim, C.S. High power density of reverse electrodialysis with pore-filling ion exchange membranes and a high-open-area spacer. *J. Mater. Chem. A* **2015**, *3*, 16302–16306. [CrossRef]
149. Ciofalo, M.; La Cerva, M.; Di Liberto, M.; Gurreri, L.; Cipollina, A.; Micale, G. Optimization of net power density in Reverse Electrodialysis. *Energy* **2019**, *181*, 576–588. [CrossRef]
150. Barakat, M.A. New trends in removing heavy metals from industrial wastewater. *Arab. J. Chem.* **2011**, *4*, 361–377. [CrossRef]
151. Scarazzato, T.; Panossian, Z.; Tenório, J.A.S.; Pérez-Herranz, V.; Espinosa, D.C.R. A review of cleaner production in electroplating industries using electrodialysis. *J. Clean. Prod.* **2017**, *168*, 1590–1602. [CrossRef]
152. Arar, Ö.; Yüksel, Ü.; Kabay, N.; Yüksel, M. Various applications of electrodeionization (EDI) method for water treatment-A short review. *Desalination* **2014**, *342*, 16–22. [CrossRef]
153. Benvenuti, T.; García-Gabaldón, M.; Ortega, E.M.; Rodrigues, M.A.S.; Bernardes, A.M.; Pérez-Herranz, V.; Zoppas-Ferreira, J. Influence of the co-ions on the transport of sulfate through anion exchange membranes. *J. Membr. Sci.* **2017**, *542*, 320–328. [CrossRef]
154. Martí-Calatayud, M.; García-Gabaldón, M.; Pérez-Herranz, V. Mass Transfer Phenomena during Electrodialysis of Multivalent Ions: Chemical Equilibria and Overlimiting Currents. *Appl. Sci.* **2018**, *8*, 1566. [CrossRef]
155. Nemati, M.; Hosseini, S.M.; Shabanian, M. Novel electrodialysis cation exchange membrane prepared by 2-acrylamido-2-methylpropane sulfonic acid; heavy metal ions removal. *J. Hazard. Mater.* **2017**, *337*, 90–104. [CrossRef]
156. Martí-Calatayud, M.C.; García-Gabaldón, M.; Pérez-Herranz, V. Effect of the equilibria of multivalent metal sulfates on the transport through cation-exchange membranes at different current regimes. *J. Membr. Sci.* **2013**, *443*, 181–192. [CrossRef]
157. Sharma, P.; Shahi, V.K. Assembly of MIL-101(Cr)-sulphonated poly (ether sulfone) membrane matrix for selective electrodialytic separation of Pb2+ from mono-/bi-valent ions. *Chem. Eng. J.* **2020**, *382*, 122688. [CrossRef]
158. Vallois, C.; Sistat, P.; Roualdès, S.; Pourcelly, G. Separation of H+/Cu_2+cations by electrodialysis using modified proton conducting membranes. *J. Membr. Sci.* **2003**, *216*, 13–25. [CrossRef]
159. Chang, J.H.; Huang, C.P.; Cheng, S.F.; Shen, S.Y. Transport characteristics and removal efficiency of copper ions in the electrodialysis process under electroconvection operation. *Process. Saf. Environ. Prot.* **2017**, *112*, 235–242. [CrossRef]

160. Barros, K.S.; Scarazzato, T.; Espinosa, D.C.R. Evaluation of the effect of the solution concentration and membrane morphology on the transport properties of Cu (II) through two monopolar cation–exchange membranes. *Sep. Purif. Technol.* **2018**, *193*, 184–192. [CrossRef]
161. Mahmoud, A.; Muhr, L.; Vasiluk, S.; Aleynikoff, A.; Lapicque, F. Investigation of transport phenomena in a hybrid ion exchange-electrodialysis system for the removal of copper ions. *J. Appl. Electrochem.* **2003**, *33*, 875–884. [CrossRef]
162. Scarazzato, T.; Panossian, Z.; García-Gabaldón, M.; Ortega, E.M.; Tenório, J.A.S.; Pérez-Herranz, V.; Espinosa, D.C.R. Evaluation of the transport properties of copper ions through a heterogeneous ion-exchange membrane in etidronic acid solutions by chronopotentiometry. *J. Membr. Sci.* **2017**, *535*, 268–278. [CrossRef]
163. Aouad, F.; Lindheimer, A.; Gavach, C. Transport properties of electrodialysis membranes in the presence of Zn^{2+} complexes with Cl^{-}. *J. Membr. Sci.* **1997**, *123*, 207–223. [CrossRef]
164. Rodrigues, M.A.S.; Amado, F.D.R.; Bischoff, M.R.; Ferreira, C.A.; Bernardes, A.M.; Ferreira, J.Z. Transport of zinc complexes through an anion exchange membrane. *Desalination* **2008**, *227*, 241–252. [CrossRef]
165. Dalla Costa, R.F.; Antônio Siqueira Rodrigues, M.; Ferreira, J.Z. Transport of Trivalent and Hexavalent Chromium through Different Ion-Selective Membranes in Acidic Aqueous Media. *Sep. Sci. Technol.* **1998**, *33*, 1135–1143. [CrossRef]
166. Vallejo, M.E.; Persin, F.; Innocent, C.; Sistat, P.; Pourcelly, G. Electrotransport of Cr(VI) through an anion exchange membrane. *Sep. Purif. Technol.* **2000**, *21*, 61–69. [CrossRef]
167. Rodrigues, M.A.S.; Dalla Costa, R.F.; Bernardes, A.M.; Zoppas Ferreira, J. Influence of ligand exchange on the treatment of trivalent chromium solutions by electrodialysis. *Electrochim. Acta* **2001**, *47*, 753–758. [CrossRef]
168. Çengeloğlu, Y.; Tor, A.; Kir, E.; Ersöz, M. Transport of hexavalent chromium through anion-exchange membranes. *Desalination* **2003**, *154*, 239–246. [CrossRef]
169. Hosseini, S.M.; Sohrabnejad, S.; Nabiyouni, G.; Jashni, E.; Van der Bruggen, B.; Ahmadi, A. Magnetic cation exchange membrane incorporated with cobalt ferrite nanoparticles for chromium ions removal via electrodialysis. *J. Membr. Sci.* **2019**, *583*, 292–300. [CrossRef]
170. Jashni, E.; Hosseini, S.M. Promoting the electrochemical and separation properties of heterogeneous cation exchange membrane by embedding 8-hydroxyquinoline ligand: Chromium ions removal. *Sep. Purif. Technol.* **2020**, *234*, 116118. [CrossRef]
171. Hosseini, S.M.; Alibakhshi, H.; Jashni, E.; Parvizian, F.; Shen, J.N.; Taheri, M.; Ebrahimi, M.; Rafiei, N. A novel layer-by-layer heterogeneous cation exchange membrane for heavy metal ions removal from water. *J. Hazard. Mater.* **2020**, *381*, 120884. [CrossRef]
172. Barros, K.S.; Espinosa, D.C.R. Chronopotentiometry of an anion-exchange membrane for treating a synthesized free-cyanide effluent from brass electrodeposition with EDTA as chelating agent. *Sep. Purif. Technol.* **2018**, *201*, 244–255. [CrossRef]
173. Mohammadi, T.; Moheb, A.; Sadrzadeh, M.; Razmi, A. Modeling of metal ion removal from wastewater by electrodialysis. *Sep. Purif. Technol.* **2005**, *41*, 73–82. [CrossRef]
174. Sadrzadeh, M.; Razmi, A.; Mohammadi, T. Separation of different ions from wastewater at various operating conditions using electrodialysis. *Sep. Purif. Technol.* **2007**, *54*, 147–156. [CrossRef]
175. Itoi, S.; Nakamura, I.; Kawahara, T. Electrodialytic recovery process of metal finishing waste water. *Desalination* **1980**, *32*, 383–389. [CrossRef]
176. Benvenuti, T.; Krapf, R.S.; Rodrigues, M.A.S.; Bernardes, A.M.; Zoppas-Ferreira, J. Recovery of nickel and water from nickel electroplating wastewater by electrodialysis. *Sep. Purif. Technol.* **2014**, *129*, 106–112. [CrossRef]
177. Benvenuti, T.; Siqueira Rodrigues, M.A.; Bernardes, A.M.; Zoppas-Ferreira, J. Closing the loop in the electroplating industry by electrodialysis. *J. Clean. Prod.* **2017**, *155*, 130–138. [CrossRef]
178. Tzanetakis, N.; Taama, W.M.; Scott, K.; Jachuck, R.J.J.; Slade, R.S.; Varcoe, J. Comparative performance of ion exchange membranes for electrodialysis of nickel and cobalt. *Sep. Purif. Technol.* **2003**, *30*, 113–127. [CrossRef]
179. Li, C.L.; Zhao, H.X.; Tsuru, T.; Zhou, D.; Matsumura, M. Recovery of spent electroless nickel plating bath by electrodialysis. *J. Membr. Sci.* **1999**, *157*, 241–249. [CrossRef]

180. Peng, C.; Jin, R.; Li, G.; Li, F.; Gu, Q. Recovery of nickel and water from wastewater with electrochemical combination process. *Sep. Purif. Technol.* **2014**, *136*, 42–49. [CrossRef]
181. Lu, H.; Wang, Y.; Wang, J. Recovery of Ni2+ and pure water from electroplating rinse wastewater by an integrated two-stage electrodeionization process. *J. Clean. Prod.* **2015**, *92*, 257–266. [CrossRef]
182. Dzyazko, Y.S.; Ponomaryova, L.N.; Rozhdestvenskaya, L.M.; Vasilyuk, S.L.; Belyakov, V.N. Electrodeionization of low-concentrated multicomponent Ni2+-containing solutions using organic-inorganic ion-exchanger. *Desalination* **2014**, *342*, 43–51. [CrossRef]
183. Zhao, C.; Zhang, L.; Ge, R.; Zhang, A.; Zhang, C.; Chen, X. Treatment of low-level Cu(II) wastewater and regeneration through a novel capacitive deionization-electrodeionization (CDI-EDI) technology. *Chemosphere* **2019**, *217*, 763–772. [CrossRef]
184. Dermentzis, K. Removal of nickel from electroplating rinse waters using electrostatic shielding electrodialysis/electrodeionization. *J. Hazard. Mater.* **2010**, *173*, 647–652. [CrossRef] [PubMed]
185. Mohammadi, T.; Moheb, A.; Sadrzadeh, M.; Razmi, A. Separation of copper ions by electrodialysis using Taguchi experimental design. *Desalination* **2004**, *169*, 21–31. [CrossRef]
186. Korngold, E.; Kock, K.; Strathmann, H. Electrodialysis in advanced waste water treatment. *Desalination* **1978**, *24*, 129–139. [CrossRef]
187. Chiapello, J.M.; Gal, J.Y. Recovery by electrodialysis of cyanide electroplating rinse waters. *J. Membr. Sci.* **1992**, *68*, 283–291. [CrossRef]
188. Scarazzato, T.; Buzzi, D.C.; Bernardes, A.M.; Romano Espinosa, D.C. Treatment of wastewaters from cyanide-free plating process by electrodialysis. *J. Clean. Prod.* **2015**, *91*, 241–250. [CrossRef]
189. Scarazzato, T.; Panossian, Z.; Tenório, J.A.S.; Pérez-Herranz, V.; Espinosa, D.C.R. Water reclamation and chemicals recovery from a novel cyanide-free copper plating bath using electrodialysis membrane process. *Desalination* **2018**, *436*, 114–124. [CrossRef]
190. Zhelonkina, E.A.; Shishkina, S.V.; Mikhailova, I.Y.; Ananchenko, B.A. Study of electrodialysis of a copper chloride solution at overlimiting currents. *Pet. Chem.* **2017**, *57*, 947–953. [CrossRef]
191. Peng, C.; Liu, Y.; Bi, J.; Xu, H.; Ahmed, A.S. Recovery of copper and water from copper-electroplating wastewater by the combination process of electrolysis and electrodialysis. *J. Hazard. Mater.* **2011**, *189*, 814–820. [CrossRef]
192. Dong, Y.; Liu, J.; Sui, M.; Qu, Y.; Ambuchi, J.J.; Wang, H.; Feng, Y. A combined microbial desalination cell and electrodialysis system for copper-containing wastewater treatment and high-salinity-water desalination. *J. Hazard. Mater.* **2017**, *321*, 307–315. [CrossRef]
193. Song, Y.; Sun, T.; Cang, L.; Wu, S.; Zhou, D. Migration and transformation of Cu(II)-EDTA during electrodialysis accompanied by an electrochemical process with different compartment designs. *Electrochim. Acta* **2019**, *295*, 605–614. [CrossRef]
194. Nataraj, S.K.; Hosamani, K.M.; Aminabhavi, T.M. Potential application of an electrodialysis pilot plant containing ion-exchange membranes in chromium removal. *Desalination* **2007**, *217*, 181–190. [CrossRef]
195. Chen, S.-S.; Li, C.-W.; Hsu, H.-D.; Lee, P.-C.; Chang, Y.-M.; Yang, C.-H. Concentration and purification of chromate from electroplating wastewater by two-stage electrodialysis processes. *J. Hazard. Mater.* **2009**, *161*, 1075–1080. [CrossRef] [PubMed]
196. Dos Santos, C.S.L.; Miranda Reis, M.H.; Cardoso, V.L.; De Resende, M.M. Electrodialysis for removal of chromium (VI) from effluent: Analysis of concentrated solution saturation. *J. Environ. Chem. Eng.* **2019**, *7*, 103380. [CrossRef]
197. Alvarado, L.; Ramírez, A.; Rodríguez-Torres, I. Cr(VI) removal by continuous electrodeionization: Study of its basic technologies. *Desalination* **2009**, *249*, 423–428. [CrossRef]
198. Alvarado, L.; Torres, I.R.; Chen, A. Integration of ion exchange and electrodeionization as a new approach for the continuous treatment of hexavalent chromium wastewater. *Sep. Purif. Technol.* **2013**, *105*, 55–62. [CrossRef]
199. Xing, Y.; Chen, X.; Wang, D. Electrically regenerated ion exchange for removal and recovery of Cr(VI) from wastewater. *Environ. Sci. Technol.* **2007**, *41*, 1439–1443. [CrossRef]
200. Xing, Y.; Chen, X.; Yao, P.; Wang, D. Continuous electrodeionization for removal and recovery of Cr(VI) from wastewater. *Sep. Purif. Technol.* **2009**, *67*, 123–126. [CrossRef]

201. Xing, Y.; Chen, X.; Wang, D. Variable effects on the performance of continuous electrodeionization for the removal of Cr(VI) from wastewater. *Sep. Purif. Technol.* **2009**, *68*, 357–362. [CrossRef]
202. Jiang, C.; Chen, H.; Zhang, Y.; Feng, H.; Shehzad, M.A.; Wang, Y.; Xu, T. Complexation Electrodialysis as a general method to simultaneously treat wastewaters with metal and organic matter. *Chem. Eng. J.* **2018**, *348*, 952–959. [CrossRef]
203. Wu, X.; Zhu, H.; Liu, Y.; Chen, R.; Qian, Q.; Van der Bruggen, B. Cr(III) recovery in form of Na_2CrO_4 from aqueous solution using improved bipolar membrane electrodialysis. *J. Membr. Sci.* **2020**, *604*, 118097. [CrossRef]
204. Zhang, Z.; Liba, D.; Alvarado, L.; Chen, A. Separation and recovery of Cr(III) and Cr(VI) using electrodeionization as an efficient approach. *Sep. Purif. Technol.* **2014**, *137*, 86–93. [CrossRef]
205. Tor, A.; Büyükerkek, T.; Çengeloğlu, Y.; Ersöz, M. Simultaneous recovery of Cr(III) and Cr(VI) from the aqueous phase with ion-exchange membranes. *Desalination* **2005**, *171*, 233–241. [CrossRef]
206. Raghava Rao, J.; Prasad, B.G.S.; Narasimhan, V.; Ramasami, T.; Shah, P.R.; Khan, A.A. Electrodialysis in the recovery and reuse of chromium from industrial effluents. *J. Membr. Sci.* **1989**, *46*, 215–224.
207. Lambert, J.; Rakib, M.; Durand, G.; Avila-Rodríguez, M. Treatment of solutions containing trivalent chromium by electrodialysis. *Desalination* **2006**, *191*, 100–110. [CrossRef]
208. Lambert, J.; Avila-Rodriguez, M.; Durand, G.; Rakib, M. Separation of sodium ions from trivalent chromium by electrodialysis using monovalent cation selective membranes. *J. Membr. Sci.* **2006**, *280*, 219–225. [CrossRef]
209. Rodrigues, M.A.S.; Amado, F.D.R.; Xavier, J.L.N.; Streit, K.F.; Bernardes, A.M.; Ferreira, J.Z. Application of photoelectrochemical-electrodialysis treatment for the recovery and reuse of water from tannery effluents. *J. Clean. Prod.* **2008**, *16*, 605–611. [CrossRef]
210. Deghles, A.; Kurt, U. Treatment of tannery wastewater by a hybrid electrocoagulation/electrodialysis process. *Chem. Eng. Process. Process. Intensif.* **2016**, *104*, 43–50. [CrossRef]
211. Marder, L.; Sulzbach, G.O.; Bernardes, A.M.; Zoppas Ferreira, J. Removal of cadmium and cyanide from aqueous solutions through electrodialysis. *J. Braz. Chem. Soc.* **2003**, *14*, 610–615. [CrossRef]
212. Marder, L.; Bernardes, A.M.; Zoppas Ferreira, J. Cadmium electroplating wastewater treatment using a laboratory-scale electrodialysis system. *Sep. Purif. Technol.* **2004**, *37*, 247–255. [CrossRef]
213. Mehellou, A.; Delimi, R.; Benredjem, Z.; Saaidia, S.; Allat, L.; Innocent, C. Improving the efficiency and selectivity of Cd 2+ removal using a modified resin in the continuous electropermutation process. *Sep. Sci. Technol.* **2019**, *55*, 2049–2060.
214. Mohammadi, T.; Razmi, A.; Sadrzadeh, M. Effect of operating parameters on Pb^{2+} separation from wastewater using electrodialysis. *Desalination* **2004**, *167*, 379–385. [CrossRef]
215. Sadrzadeh, M.; Mohammadi, T.; Ivakpour, J.; Kasiri, N. Separation of lead ions from wastewater using electrodialysis: Comparing mathematical and neural network modeling. *Chem. Eng. J.* **2008**, *144*, 431–441. [CrossRef]
216. Abou-Shady, A.; Peng, C.; Almeria, O.J.; Xu, H. Effect of pH on separation of Pb (II) and NO^{3-} from aqueous solutions using electrodialysis. *Desalination* **2012**, *285*, 46–53. [CrossRef]
217. Abou-Shady, A.; Peng, C.; Bi, J.; Xu, H.; Almeria, O.J. Recovery of Pb (II) and removal of NO3- from aqueous solutions using integrated electrodialysis, electrolysis, and adsorption process. *Desalination* **2012**, *286*, 304–315. [CrossRef]
218. Gherasim, C.V.; Křivčík, J.; Mikulášek, P. Investigation of batch electrodialysis process for removal of lead ions from aqueous solutions. *Chem. Eng. J.* **2014**, *256*, 324–334. [CrossRef]
219. Barros, K.S.; Ortega, E.M.; Pérez-Herranz, V.; Espinosa, D.C.R. Evaluation of brass electrodeposition at RDE from cyanide-free bath using EDTA as a complexing agent. *J. Electroanal. Chem.* **2020**, *865*, 114129. [CrossRef]
220. Barros, K.S.; Scarazzato, T.; Pérez-Herranz, V.; Espinosa, D.C.R. Treatment of cyanide-free wastewater from brass electrodeposition with edta by electrodialysis: Evaluation of underlimiting and overlimiting operations. *Membranes* **2020**, *10*, 69. [CrossRef]
221. Min, K.J.; Choi, S.Y.; Jang, D.; Lee, J.; Park, K.Y. Separation of metals from electroplating wastewater using electrodialysis. *Energy Sourcespart. A Recover. Util. Environ. Eff.* **2019**, *41*, 2471–2480. [CrossRef]

222. Zuo, W.; Zhang, G.; Meng, Q.; Zhang, H. Characteristics and application of multiple membrane process in plating wastewater reutilization. *Desalination* **2008**, *222*, 187–196. [CrossRef]
223. Peng, C.; Meng, H.; Song, S.; Lu, S.; Lopez-Vaidivieso, A. Elimination of Cr(VI) from electroplating wastewater by electrodialysis following chemical precipitation. *Sep. Sci. Technol.* **2004**, *39*, 1501–1517. [CrossRef]
224. Babilas, D.; Dydo, P. Selective zinc recovery from electroplating wastewaters by electrodialysis enhanced with complex formation. *Sep. Purif. Technol.* **2018**, *192*, 419–428. [CrossRef]
225. Babilas, D.; Dydo, P. Zinc salt recovery from electroplating industry wastes by electrodialysis enhanced with complex formation. *Sep. Sci. Technol.* **2019**, 1–9. [CrossRef]
226. Frioui, S.; Oumeddour, R.; Lacour, S. Highly selective extraction of metal ions from dilute solutions by hybrid electrodialysis technology. *Sep. Purif. Technol.* **2017**, *174*, 264–274. [CrossRef]
227. Cherif, A.T.; Elmidaoui, A.; Gavach, C. Separation of Ag+, Zn2+ and Cu2+ ions by electrodialysis with monovalent cation specific membrane and EDTA. *J. Membr. Sci.* **1993**, *76*, 39–49. [CrossRef]
228. Cifuentes, L.; Crisóstomo, G.; Ibáñez, J.P.; Casas, J.M.; Alvarez, F.; Cifuentes, G. On the electrodialysis of aqueous H2SO4–CuSO4 electrolytes with metallic impurities. *J. Membr. Sci.* **2002**, *207*, 1–16. [CrossRef]
229. Cifuentes, L.; García, I.; Arriagada, P.; Casas, J.M. The use of electrodialysis for metal separation and water recovery from CuSO4-H2SO4-Fe solutions. *Sep. Purif. Technol.* **2009**, *68*, 105–108. [CrossRef]
230. Liu, Y.; Zhu, H.; Zhang, M.; Chen, R.; Chen, X.; Zheng, X.; Jin, Y. Cr(VI) recovery from chromite ore processing residual using an enhanced electrokinetic process by bipolar membranes. *J. Membr. Sci.* **2018**, *566*, 190–196. [CrossRef]
231. Reig, M.; Vecino, X.; Valderrama, C.; Gibert, O.; Cortina, J.L. Application of selectrodialysis for the removal of as from metallurgical process waters: Recovery of Cu and Zn. *Sep. Purif. Technol.* **2018**, *195*, 404–412. [CrossRef]
232. Zheng, Y.; Gao, X.; Wang, X.; Li, Z.; Wang, Y.; Gao, C. Application of electrodialysis to remove copper and cyanide from simulated and real gold mine effluents. *RSC Adv.* **2015**, *5*, 19807–19817. [CrossRef]
233. Yeon, K.H.; Song, J.H.; Moon, S.H. A study on stack configuration of continuous electrodeionization for removal of heavy metal ions from the primary coolant of a nuclear power plant. *Water Res.* **2004**, *38*, 1911–1921. [CrossRef]
234. Yeon, K.H.; Seong, J.H.; Rengaraj, S.; Moon, S.H. Electrochemical characterization of ion-exchange resin beds and removal of cobalt by electrodeionization for high purity water production. *Sep. Sci. Technol.* **2003**, *38*, 443–462. [CrossRef]
235. Zhang, Y.; Wang, L.; Xuan, S.; Lin, X.; Luo, X. Variable effects on electrodeionization for removal of Cs+ ions from simulated wastewater. *Desalination* **2014**, *344*, 212–218. [CrossRef]
236. Jiang, B.; Li, F.; Zhao, X. Removal of trace Cs(I), Sr(II), and Co(II) in aqueous solutions using continuous electrodeionization (CEDI). *Desalin. Water Treat.* **2019**, *155*, 175–182. [CrossRef]
237. Zahakifar, F.; Keshtkar, A.R.; Souderjani, E.Z.; Moosavian, M.A. Use of response surface methodology for optimization of thorium(IV) removal from aqueous solutions by electrodeionization (EDI). *Prog. Nucl. Energy* **2020**, *124*, 103335. [CrossRef]
238. Regel-Rosocka, M. A review on methods of regeneration of spent pickling solutions from steel processing. *J. Hazard. Mater.* **2010**, *177*, 57–69. [CrossRef] [PubMed]
239. Agrawal, A.; Sahu, K.K. An overview of the recovery of acid from spent acidic solutions from steel and electroplating industries. *J. Hazard. Mater.* **2009**, *171*, 61–75. [CrossRef]
240. Urano, K.; Ase, T.; Naito, Y. Recovery of acid from wastewater by electrodialysis. *Desalination* **1984**, *51*, 213–226. [CrossRef]
241. Pourcelly, G.; Tugas, I.; Gavach, C. Electrotransport of sulphuric acid in special anion exchange membranes for the recovery of acids. *J. Membr. Sci.* **1994**, *97*, 99–107. [CrossRef]
242. Jia, Y.X.; Li, F.J.; Chen, X.; Wang, M. Model analysis on electrodialysis for inorganic acid recovery and its experimental validation. *Sep. Purif. Technol.* **2018**, *190*, 261–267. [CrossRef]
243. Wang, L.; Li, Z.; Xu, Z.; Zhang, F.; Efome, J.E.; Li, N. Proton blockage membrane with tertiary amine groups for concentration of sulfonic acid in electrodialysis. *J. Membr. Sci.* **2018**, *555*, 78–87. [CrossRef]
244. Guo, R.Q.; Wang, B.B.; Jia, Y.X.; Wang, M. Development of acid block anion exchange membrane by structure design and its possible application in waste acid recovery. *Sep. Purif. Technol.* **2017**, *186*, 188–196. [CrossRef]

245. Bai, T.; Wang, M.; Zhang, B.; Jia, Y.; Chen, Y. Anion-exchange membrane with ion-nanochannels to beat trade-off between membrane conductivity and acid blocking performance for waste acid reclamation. *J. Membr. Sci.* **2019**, *573*, 657–667. [CrossRef]
246. Zhang, N.; Liu, Y.; Liu, R.; She, Z.; Tan, M.; Mao, D.; Fu, R.; Zhang, Y. Polymer inclusion membrane (PIM) containing ionic liquid as a proton blocker to improve waste acid recovery efficiency in electrodialysis process. *J. Membr. Sci.* **2019**, *581*, 18–27. [CrossRef]
247. Cong, M.Y.; Jia, Y.X.; Wang, H.; Wang, M. Preparation of acid block anion exchange membrane with quaternary ammonium groups by homogeneous amination for electrodialysis-based acid enrichment. *Sep. Purif. Technol.* **2020**, *238*, 116396. [CrossRef]
248. Bai, T.T.; Cong, M.Y.; Jia, Y.X.; Ma, K.K.; Wang, M. Preparation of self-crosslinking anion exchange membrane with acid block performance from side-chain type polysulfone. *J. Membr. Sci.* **2020**, *599*, 117831. [CrossRef]
249. Paquay, E.; Clarinval, A.M.; Delvaux, A.; Degrez, M.; Hurwitz, H.D. Applications of electrodialysis for acid pickling wastewater treatment. *Chem. Eng. J.* **2000**, *79*, 197–201. [CrossRef]
250. Chapotot, A.; Lopez, V.; Lindheimer, A.; Aouad, N.; Gavach, C. Electrodialysis of acid solutions with metallic divalent salts: Cation-exchange membranes with improved permeability to protons. *Desalination* **1995**, *101*, 141–153. [CrossRef]
251. Xu, T. Electrodialysis processes with bipolar membranes (EDBM) in environmental protection—A review. *Resour. Conserv. Recycl.* **2002**, *37*, 1–22.
252. Baltazar, V.; Harris, G.B.; White, C.W. The selective recovery and concentration of sulphuric acid by electrodialysis. *Hydrometallurgy* **1992**, *30*, 463–481. [CrossRef]
253. Tran, A.T.K.; Mondal, P.; Lin, J.; Meesschaert, B.; Pinoy, L.; Van der Bruggen, B. Simultaneous regeneration of inorganic acid and base from a metal washing step wastewater by bipolar membrane electrodialysis after pretreatment by crystallization in a fluidized pellet reactor. *J. Membr. Sci.* **2015**, *473*, 118–127. [CrossRef]
254. Jia, Y.; Chen, X.; Wang, M.; Wang, B. A win-win strategy for the reclamation of waste acid and conversion of organic acid by a modified electrodialysis. *Sep. Purif. Technol.* **2016**, *171*, 11–16. [CrossRef]
255. Song, P.; Wang, M.; Zhang, B.; Jia, Y.; Chen, Y. Fabrication of proton permselective composite membrane for electrodialysis-based waste acid reclamation. *J. Membr. Sci.* **2019**, *592*, 117366. [CrossRef]
256. Boucher, M.; Turcotte, N.; Guillemette, V.; Lantagne, G.; Chapotot, A.; Pourcelly, G.; Sandeaux, R.; Gavach, C. Recovery of spent acid by electrodialysis in the zinc hydrometallurgy industry: Performance study of different cation-exchange membranes. *Hydrometallurgy* **1997**, *45*, 137–160. [CrossRef]
257. Sistat, P.; Pourcelly, G.; Gavach, C.; Turcotte, N.; Boucher, M. Electrodialysis of acid effluents containing metallic divalent salts: Recovery of acid with a cation-exchange membrane modified in situ. *J. Appl. Electrochem.* **1997**, *27*, 65–70. [CrossRef]
258. Wang, M.; Liu, X.; Jia, Y.X.; Wang, X.L. The improvement of comprehensive transport properties to heterogeneous cation exchange membrane by the covalent immobilization of polyethyleneimine. *Sep. Purif. Technol.* **2015**, *140*, 69–76. [CrossRef]
259. He, Y.; Ge, L.; Ge, Z.J.; Zhao, Z.; Sheng, F.; Liu, X.; Ge, X.; Yang, Z.; Fu, R.; Liu, Z.; et al. Monovalent cations permselective membranes with zwitterionic side chains. *J. Membr. Sci.* **2018**, *563*, 320–325. [CrossRef]
260. Sheng, F.; Afsar, N.U.; Zhu, Y.; Ge, L.; Xu, T. PVA-based mixed matrix membranes comprising ZSM-5 for cations separation. *Membranes* **2020**, *10*, 114. [CrossRef] [PubMed]
261. Ge, L.; Wu, B.; Li, Q.; Wang, Y.; Yu, D.; Wu, L.; Pan, J.; Miao, J.; Xu, T. Electrodialysis with nanofiltration membrane (EDNF) for high-efficiency cations fractionation. *J. Membr. Sci.* **2016**, *498*, 192–200. [CrossRef]
262. Liu, Y.; Ke, X.; Zhu, H.; Chen, R.; Chen, X.; Zheng, X.; Jin, Y.; Van der Bruggen, B. Treatment of raffinate generated via copper ore hydrometallurgical processing using a bipolar membrane electrodialysis system. *Chem. Eng. J.* **2020**, *382*, 122956. [CrossRef]
263. Yuzer, B.; Aydin, M.I.; Hasançebi, B.; Selcuk, H. Application of an electrodialysis process to recover nitric acid from aluminum finishing industry waste. *Desalin. Water Treat.* **2019**, *172*, 199–205. [CrossRef]

264. Zhang, X.; Li, C.; Wang, X.; Wang, Y.; Xu, T. Recovery of hydrochloric acid from simulated chemosynthesis aluminum foils wastewater: An integration of diffusion dialysis and conventional electrodialysis. *J. Membr. Sci.* **2012**, *409–410*, 257–263. [CrossRef]
265. Zhuang, J.X.; Chen, Q.; Wang, S.; Zhang, W.M.; Song, W.G.; Wan, L.J.; Ma, K.S.; Zhang, C.N. Zero discharge process for foil industry waste acid reclamation: Coupling of diffusion dialysis and electrodialysis with bipolar membranes. *J. Membr. Sci.* **2013**, *432*, 90–96. [CrossRef]
266. Aydin, M.I.; Yuzer, B.; Hasancebi, B.; Selcuk, H. Application of electrodialysis membrane process to recovery sulfuric acid and wastewater in the chalcopyrite mining industry. *Desalin. Water Treat.* **2019**, *172*, 206–211. [CrossRef]
267. Heinonen, J.; Zhao, Y.; Van der Bruggen, B. A process combination of ion exchange and electrodialysis for the recovery and purification of hydroxy acids from secondary sources. *Sep. Purif. Technol.* **2020**, *240*, 116642. [CrossRef]
268. Li, M.; Sun, M.; Liu, W.; Zhang, X.; Wu, C.; Wu, Y. Quaternized graphene oxide modified PVA-QPEI membranes with excellent selectivity for alkali recovery through electrodialysis. *Chem. Eng. Res. Des.* **2020**, *153*, 875–886. [CrossRef]
269. Davis, J.R.; Chen, Y.; Baygents, J.C.; Farrell, J. Production of Acids and Bases for Ion Exchange Regeneration from Dilute Salt Solutions Using Bipolar Membrane Electrodialysis. *ACS Sustain. Chem. Eng.* **2015**, *3*, 2337–2342. [CrossRef]
270. Graillon, S.; Persin, F.; Pourcelly, G.; Gavach, C. Development of electrodialysis with bipolar membrane for the treatment of concentrated nitrate effluents. *Desalination* **1996**, *107*, 159–169. [CrossRef]
271. Ben Ali, M.A.; Rakib, M.; Laborie, S.; Viers, P.; Durand, G. Coupling of bipolar membrane electrodialysis and ammonia stripping for direct treatment of wastewaters containing ammonium nitrate. *J. Membr. Sci.* **2004**, *244*, 89–96.
272. Cherif, A.T.; Molenat, J.; Elmidaoui, A. Nitric acid and sodium hydroxide generation by electrodialysis using bipolar membranes. *J. Appl. Electrochem.* **1997**, *27*, 1069–1074. [CrossRef]
273. Monat, L.; Chaudhury, S.; Nir, O. Enhancing the Sustainability of Phosphogypsum Recycling by Integrating Electrodialysis with Bipolar Membranes. *ACS Sustain. Chem. Eng.* **2020**, *8*, 2490–2497. [CrossRef]
274. Li, Y.; Shi, S.; Cao, H.; Wu, X.; Zhao, Z.; Wang, L. Bipolar membrane electrodialysis for generation of hydrochloric acid and ammonia from simulated ammonium chloride wastewater. *Water Res.* **2016**, *89*, 201–209. [CrossRef] [PubMed]
275. Lv, Y.; Yan, H.; Yang, B.; Wu, C.; Zhang, X.; Wang, X. Bipolar membrane electrodialysis for the recycling of ammonium chloride wastewater: Membrane selection and process optimization. *Chem. Eng. Res. Des.* **2018**, *138*, 105–115. [CrossRef]
276. Van Linden, N.; Bandinu, G.L.; Vermaas, D.A.; Spanjers, H.; van Lier, J.B. Bipolar membrane electrodialysis for energetically competitive ammonium removal and dissolved ammonia production. *J. Clean. Prod.* **2020**, *259*, 120788. [CrossRef]
277. Trivedi, G.; Shah, B.; Adhikary, S.; Rangarajan, R. Studies on bipolar membranes: Part III: Conversion of sodium phosphate to phosphoric acid and sodium hydroxide. *React. Funct. Polym.* **1999**, *39*, 91–97. [CrossRef]
278. Wei, Y.; Wang, Y.; Zhang, X.; Xu, T. Treatment of simulated brominated butyl rubber wastewater by bipolar membrane electrodialysis. *Sep. Purif. Technol.* **2011**, *80*, 196–201. [CrossRef]
279. Wei, Y.; Wang, Y.; Zhang, X.; Xu, T. Comparative study on the treatment of simulated brominated butyl rubber wastewater by using bipolar membrane electrodialysis (BMED) and conventional electrodialysis (ED). *Sep. Purif. Technol.* **2013**, *110*, 164–169. [CrossRef]
280. Wang, D.; Meng, W.; Lei, Y.; Li, C.; Cheng, J.; Qu, W.; Wang, G.; Zhang, M.; Li, S. The novel strategy for increasing the efficiency and yield of the bipolar membrane electrodialysis by the double conjugate salts stress. *Polymers* **2020**, *12*, 343. [CrossRef]
281. Ghyselbrecht, K.; Huygebaert, M.; Van der Bruggen, B.; Ballet, R.; Meesschaert, B.; Pinoy, L. Desalination of an industrial saline water with conventional and bipolar membrane electrodialysis. *Desalination* **2013**, *318*, 9–18. [CrossRef]

282. Noguchi, M.; Nakamura, Y.; Shoji, T.; Iizuka, A.; Yamasaki, A. Simultaneous removal and recovery of boron from waste water by multi-step bipolar membrane electrodialysis. *J. Water Process. Eng.* **2018**, *23*, 299–305. [CrossRef]
283. Nagasawa, H.; Iizuka, A.; Yamasaki, A.; Yanagisawa, Y. Utilization of bipolar membrane electrodialysis for the removal of boron from aqueous solution. *Ind. Eng. Chem. Res.* **2011**, *50*, 6325–6330. [CrossRef]
284. Sun, M.; Li, M.; Zhang, X.; Wu, C.; Wu, Y. Graphene oxide modified porous P84 co-polyimide membranes for boron recovery by bipolar membrane electrodialysis process. *Sep. Purif. Technol.* **2020**, *232*, 115963. [CrossRef]
285. Reig, M.; Valderrama, C.; Gibert, O.; Cortina, J.L. Selectrodialysis and bipolar membrane electrodialysis combination for industrial process brines treatment: Monovalent-divalent ions separation and acid and base production. *Desalination* **2016**, *399*, 88–95. [CrossRef]
286. Liu, K.J.; Nagasubramanian, K.; Chlanda, F.P. Membrane electrodialysis process for recovery of sulfur dioxide from power plant stack gases. *J. Membr. Sci.* **1978**, *3*, 71–83. [CrossRef]
287. Liu, K.J.; Chlanda, F.P.; Nagasubramanian, K. Application of bipolar membrane technology: A novel process for control of sulfur dioxide from flue gases. *J. Membr. Sci.* **1978**, *3*, 57–70. [CrossRef]
288. Zhang, X.; Ye, C.; Pi, K.; Huang, J.; Xia, M.; Gerson, A.R. Sustainable treatment of desulfurization wastewater by ion exchange and bipolar membrane electrodialysis hybrid technology. *Sep. Purif. Technol.* **2019**, *211*, 330–339. [CrossRef]
289. Tian, W.; Wang, X.; Fan, C.; Cui, Z. Optimal treatment of hypersaline industrial wastewater via bipolar membrane electrodialysis. *ACS Sustain. Chem. Eng.* **2019**, *7*, 12358–12368. [CrossRef]
290. Luo, Z.; Wang, D.; Zhu, D.; Xu, J.; Jiang, H.; Geng, W.; Wei, W.; Lian, Z. Separation of fluoride and chloride ions from ammonia-based flue gas desulfurization slurry using a two-stage electrodialysis. *Chem. Eng. Res. Des.* **2019**, *147*, 73–82. [CrossRef]
291. Wang, Y.; Li, W.; Yan, H.; Xu, T. Removal of heat stable salts (HSS) from spent alkanolamine wastewater using electrodialysis. *J. Ind. Eng. Chem.* **2018**, *57*, 356–362. [CrossRef]
292. Meng, H.; Zhang, S.; Li, C.; Li, L. Removal of heat stable salts from aqueous solutions of N-methyldiethanolamine using a specially designed three-compartment configuration electrodialyzer. *J. Membr. Sci.* **2008**, *322*, 436–440. [CrossRef]
293. Chen, F.; Chi, Y.; Zhang, M.; Liu, Z.; Fei, X.; Yang, K.; Fu, C. Removal of heat stable salts from N-methyldiethanolamine wastewater by anion exchange resin coupled three-compartment electrodialysis. *Sep. Purif. Technol.* **2020**, *242*, 116777. [CrossRef]
294. Bazhenov, S.; Rieder, A.; Schallert, B.; Vasilevsky, V.; Unterberger, S.; Grushevenko, E.; Volkov, V.; Volkov, A. Reclaiming of degraded MEA solutions by electrodialysis: Results of ED pilot campaign at post-combustion CO_2 capture pilot plant. *Int. J. Greenh. Gas. Control.* **2015**, *42*, 593–601. [CrossRef]
295. Grushevenko, E.; Bazhenov, S.; Vasilevsky, V.; Novitsky, E.; Shalygin, M.; Volkov, A. Effect of Carbon Dioxide Loading on Removal of Heat Stable Salts from Amine Solvent by Electrodialysis. *Membranes* **2019**, *9*, 152. [CrossRef] [PubMed]
296. Iizuka, A.; Hashimoto, K.; Nagasawa, H.; Kumagai, K.; Yanagisawa, Y.; Yamasaki, A. Carbon dioxide recovery from carbonate solutions using bipolar membrane electrodialysis. *Sep. Purif. Technol.* **2012**, *101*, 49–59. [CrossRef]
297. Jiang, C.; Li, S.; Zhang, D.; Yang, Z.; Yu, D.; Chen, X.; Wang, Y.; Xu, T. Mathematical modelling and experimental investigation of CO_2 absorber recovery using an electro-acidification method. *Chem. Eng. J.* **2019**, *360*, 654–664. [CrossRef]
298. Wang, Q.; Yang, P.; Cong, W. Cation-exchange membrane fouling and cleaning in bipolar membrane electrodialysis of industrial glutamate production wastewater. *Sep. Purif. Technol.* **2011**, *79*, 103–113. [CrossRef]
299. Shen, J.; Huang, J.; Liu, L.; Ye, W.; Lin, J.; Van der Bruggen, B. The use of BMED for glyphosate recovery from glyphosate neutralization liquor in view of zero discharge. *J. Hazard. Mater.* **2013**, *260*, 660–667. [CrossRef]
300. Ye, W.; Huang, J.; Lin, J.; Zhang, X.; Shen, J.; Luis, P.; Van Der Bruggen, B. Environmental evaluation of bipolar membrane electrodialysis for NaOH production from wastewater: Conditioning NaOH as a CO_2 absorbent. *Sep. Purif. Technol.* **2015**, *144*, 206–214. [CrossRef]
301. Wang, Q.; Jiang, C.; Wang, Y.; Yang, Z.; Xu, T. Reclamation of Aniline Wastewater and CO_2 Capture Using Bipolar Membrane Electrodialysis. *ACS Sustain. Chem. Eng.* **2016**, *4*, 5743–5751. [CrossRef]

302. Loza, N.V.; Loza, S.A.; Romanyuk, N.A.; Kononenko, N.A. Experimental and Theoretical Studies of Electrodialysis of Model Solutions Containing Aniline and Sulfuric Acid. *Russ. J. Electrochem.* **2019**, *55*, 871–877. [CrossRef]
303. Peng, Z.; Sun, Y. Leakage circuit characteristics of a bipolar membrane electrodialyzer with 5 BP-A-C units. *J. Membr. Sci.* **2020**, *597*, 117762. [CrossRef]
304. Schlichter, B.; Mavrov, V.; Erwe, T.; Chmiel, H. Regeneration of bonding agents loaded with heavy metals by electrodialysis with bipolar membranes. *J. Membr. Sci.* **2004**, *232*, 99–105. [CrossRef]
305. Wei, Y.; Li, C.; Wang, Y.; Zhang, X.; Li, Q.; Xu, T. Regenerating sodium hydroxide from the spent caustic by bipolar membrane electrodialysis (BMED). *Sep. Purif. Technol.* **2012**, *86*, 49–54. [CrossRef]
306. Rohman, F.S.; Othman, M.R.; Aziz, N. Modeling of batch electrodialysis for hydrochloric acid recovery. *Chem. Eng. J.* **2010**, *162*, 466–479. [CrossRef]
307. Merkel, A.; Ashrafi, A.M.; Ondrušek, M. The use of electrodialysis for recovery of sodium hydroxide from the high alkaline solution as a model of mercerization wastewater. *J. Water Process. Eng.* **2017**, *20*, 123–129. [CrossRef]
308. Bailly, M. Production of organic acids by bipolar electrodialysis: Realizations and perspectives. *Desalination* **2002**, *144*, 157–162. [CrossRef]
309. Liu, J.; Wu, S.; Lu, Y.; Liu, Q.; Jiao, Q.; Wang, X.; Zhang, H. An integrated electrodialysis-biocatalysis-spray-drying process for efficient recycling of keratin acid hydrolysis industrial wastewater. *Chem. Eng. J.* **2016**, *302*, 146–154. [CrossRef]
310. Vertova, A.; Aricci, G.; Rondinini, S.; Miglio, R.; Carnelli, L.; D'Olimpio, P. Electrodialytic recovery of light carboxylic acids from industrial aqueous wastes. *J. Appl. Electrochem.* **2009**, *39*, 2051–2059. [CrossRef]
311. Wang, Q.; Cheng, G.; Sun, X.; Jin, B. Recovery of lactic acid from kitchen garbage fermentation broth by four-compartment configuration electrodialyzer. *Process. Biochem.* **2006**, *41*, 152–158. [CrossRef]
312. Zhang, Y.; Liu, R.; Lang, Q.; Tan, M.; Zhang, Y. Composite anion exchange membrane made by layer-by-layer method for selective ion separation and water migration control. *Sep. Purif. Technol.* **2018**, *192*, 278–286. [CrossRef]
313. Scoma, A.; Varela-Corredor, F.; Bertin, L.; Gostoli, C.; Bandini, S. Recovery of VFAs from anaerobic digestion of dephenolized Olive Mill Wastewaters by Electrodialysis. *Sep. Purif. Technol.* **2016**, *159*, 81–91. [CrossRef]
314. Pan, X.R.; Li, W.W.; Huang, L.; Liu, H.Q.; Wang, Y.K.; Geng, Y.K.; Kwan-Sing Lam, P.; Yu, H.Q. Recovery of high-concentration volatile fatty acids from wastewater using an acidogenesis-electrodialysis integrated system. *Bioresour. Technol.* **2018**, *260*, 61–67. [CrossRef] [PubMed]
315. Dai, K.; Wen, J.-L.; Wang, Y.-L.; Wu, Z.-G.; Zhao, P.-J.; Zhang, H.-H.; Wang, J.-J.; Zeng, R.J.; Zhang, F. Impacts of medium composition and applied current on recovery of volatile fatty acids during coupling of electrodialysis with an anaerobic digester. *J. Clean. Prod.* **2019**, *207*, 483–489. [CrossRef]
316. Yu, L.; Guo, Q.; Hao, J.; Jiang, W. Recovery of acetic acid from dilute wastewater by means of bipolar membrane electrodialysis. *Desalination* **2000**, *129*, 283–288. [CrossRef]
317. Yu, L.; Lin, T.; Guo, Q.; Hao, J. Relation between mass transfer and operation parameters in the electrodialysis recovery of acetic acid. *Desalination* **2003**, *154*, 147–152. [CrossRef]
318. Zhang, X.; Li, C.; Wang, Y.; Luo, J.; Xu, T. Recovery of acetic acid from simulated acetaldehyde wastewaters: Bipolar membrane electrodialysis processes and membrane selection. *J. Membr. Sci.* **2011**, *379*, 184–190. [CrossRef]
319. Ferrer, J.S.J.; Laborie, S.; Durand, G.; Rakib, M. Formic acid regeneration by electromembrane processes. *J. Membr. Sci.* **2006**, *280*, 509–516. [CrossRef]
320. Lameloise, M.L.; Lewandowski, R. Recovering l-malic acid from a beverage industry waste water: Experimental study of the conversion stage using bipolar membrane electrodialysis. *J. Membr. Sci.* **2012**, *403–404*, 196–202. [CrossRef]
321. Achoh, A.; Zabolotsky, V.; Melnikov, S. Conversion of water-organic solution of sodium naphtenates into naphtenic acids and alkali by electrodialysis with bipolar membranes. *Sep. Purif. Technol.* **2019**, *212*, 929–940. [CrossRef]
322. Fakhru'l-Razi, A.; Pendashteh, A.; Abdullah, L.C.; Biak, D.R.A.; Madaeni, S.S.; Abidin, Z.Z. Review of technologies for oil and gas produced water treatment. *J. Hazard. Mater.* **2009**, *170*, 530–551. [CrossRef]

323. Millar, G.J.; Couperthwaite, S.J.; Moodliar, C.D. Strategies for the management and treatment of coal seam gas associated water. *Renew. Sustain. Energy Rev.* **2016**, *57*, 669–691. [CrossRef]
324. Onishi, V.C.; Reyes-Labarta, J.A.; Caballero, J.A. Membrane Desalination in Shale Gas Industry: Applications and Perspectives. In *Current Trends and Future Developments on (Bio-) Membranes*; Basile, A., Curcio, E., Inamuddin, I., Eds.; Elsevier: Amsterdam, The Netherlands, 2019; pp. 243–267. ISBN 9780128135518.
325. Chang, H.; Li, T.; Liu, B.; Vidic, R.D.; Elimelech, M.; Crittenden, J.C. Potential and implemented membrane-based technologies for the treatment and reuse of flowback and produced water from shale gas and oil plays: A review. *Desalination* **2019**, *455*, 34–57. [CrossRef]
326. Hamawand, I.; Yusaf, T.; Hamawand, S.G. Coal seam gas and associated water: A review paper. *Renew. Sustain. Energy Rev.* **2013**, *22*, 550–560. [CrossRef]
327. Rezakazemi, M.; Khajeh, A.; Mesbah, M. Membrane filtration of wastewater from gas and oil production. *Environ. Chem. Lett.* **2018**, *16*, 367–388. [CrossRef]
328. Arthur, J.D.; Langhus, B.G.; Patel, C. *Technical Summary of Oil & Gas: Produced Water Treatment Technologies*; Tulsa World: Tulsa, OK, USA, 2005.
329. Sirivedhin, T.; McCue, J.; Dallbauman, L. Reclaiming produced water for beneficial use: Salt removal by electrodialysis. *J. Membr. Sci.* **2004**, *243*, 335–343. [CrossRef]
330. Hao, H.; Huang, X.; Gao, C.; Gao, X. Application of an integrated system of coagulation and electrodialysis for treatment of wastewater produced by fracturing. *Desalin. Water Treat.* **2014**, *55*, 2034–2043. [CrossRef]
331. McGovern, R.K.; Weiner, A.M.; Sun, L.; Chambers, C.G.; Zubair, S.M.; Lienhard, V.J.H. On the cost of electrodialysis for the desalination of high salinity feeds. *Appl. Energy* **2014**, *136*, 649–661. [CrossRef]
332. Peraki, M.; Ghazanfari, E.; Pinder, G.F.; Harrington, T.L. Electrodialysis: An application for the environmental protection in shale-gas extraction. *Sep. Purif. Technol.* **2016**, *161*, 96–103. [CrossRef]
333. McGovern, R.K.; Zubair, S.M.; Lienhard, V.J.H. The cost effectiveness of electrodialysis for diverse salinity applications. *Desalination* **2014**, *348*, 57–65. [CrossRef]
334. Hayes, T.D.; Severin, B.F. Electrodialysis of highly concentrated brines: Effects of calcium. *Sep. Purif. Technol.* **2017**, *175*, 443–453. [CrossRef]
335. Severin, B.F.; Hayes, T.D. Electrodialysis of concentrated brines: Effects of multivalent cations. *Sep. Purif. Technol.* **2019**, *218*, 227–241. [CrossRef]
336. Jing, G.L.; Xing, L.J.; Liu, Y; Du, W.T.; Han, C.J. Development of a four-grade and four-segment electrodialysis setup for desalination of polymer-flooding produced water. *Desalination* **2010**, *264*, 214–219. [CrossRef]
337. Guo, H.; You, F.; Yu, S.; Li, L.; Zhao, D. Mechanisms of chemical cleaning of ion exchange membranes: A case study of plant-scale electrodialysis for oily wastewater treatment. *J. Membr. Sci.* **2015**, *496*, 310–317. [CrossRef]
338. Jing, G.L.; Wang, X.Y.; Han, C.J. The effect of oilfield polymer-flooding wastewater on anion-exchange membrane performance. *Desalination* **2008**, *220*, 386–393. [CrossRef]
339. Guo, H.; Xiao, L.; Yu, S.; Yang, H.; Hu, J.; Liu, G.; Tang, Y. Analysis of anion exchange membrane fouling mechanism caused by anion polyacrylamide in electrodialysis. *Desalination* **2014**, *346*, 46–53. [CrossRef]
340. Zuo, X.; Wang, L.; He, J.; Li, Z.; Yu, S. SEM-EDX studies of SiO2/PVDF membranes fouling in electrodialysis of polymer-flooding produced wastewater: Diatomite, APAM and crude oil. *Desalination* **2014**, *347*, 43–51. [CrossRef]
341. Wang, T.; Yu, S.; Hou, L. Impacts of HPAM molecular weights on desalination performance of ion exchange membranes and fouling mechanism. *Desalination* **2017**, *404*, 50–58. [CrossRef]
342. Xia, Q.; Guo, H.; Ye, Y.; Yu, S.; Li, L.; Li, Q.; Zhang, R. Study on the fouling mechanism and cleaning method in the treatment of polymer flooding produced water with ion exchange membranes. *RSC Adv.* **2018**, *8*, 29947–29957. [CrossRef]
343. Sosa-Fernandez, P.A.; Post, J.W.; Bruning, H.; Leermakers, F.A.M.; Rijnaarts, H.H.M. Electrodialysis-based desalination and reuse of sea and brackish polymer-flooding produced water. *Desalination* **2018**, *447*, 120–132. [CrossRef]

344. Sosa-Fernandez, P.A.; Post, J.W.; Leermakers, F.A.M.; Rijnaarts, H.H.M.; Bruning, H. Removal of divalent ions from viscous polymer-flooding produced water and seawater via electrodialysis. *J. Membr. Sci.* **2019**, *589*, 117251. [CrossRef]
345. Sosa-Fernandez, P.A.; Miedema, S.J.; Bruning, H.; Leermakers, F.A.M.; Rijnaarts, H.H.M.; Post, J.W. Influence of solution composition on fouling of anion exchange membranes desalinating polymer-flooding produced water. *J. Colloid Interface Sci.* **2019**, *557*, 381–394. [CrossRef]
346. Sosa-Fernandez, P.A.; Post, J.W.; Ramdlan, M.S.; Leermakers, F.A.M.; Bruning, H.; Rijnaarts, H.H.M. Improving the performance of polymer-flooding produced water electrodialysis through the application of pulsed electric field. *Desalination* **2020**, *484*, 114424. [CrossRef]
347. Lopez, A.M.; Dunsworth, H.; Hestekin, J.A. Reduction of the shadow spacer effect using reverse electrodeionization and its applications in water recycling for hydraulic fracturing operations. *Sep. Purif. Technol.* **2016**, *162*, 84–90. [CrossRef]
348. AECOM Inc. *Petroleum Refining Water/Wastewater Use and Management*; IPIECA: London, UK, 2010.
349. Parkash, S. Refinery Water Systems. *Refin. Process. Handb.* **2007**, 242–269.
350. Mikhak, Y.; Torabi, M.M.A.; Fouladitajar, A. Refinery and petrochemical wastewater treatment. In *Sustainable Water and Wastewater Processing*; Elsevier: Amsterdam, The Netherlands, 2019; pp. 55–91. ISBN 9780128161708.
351. Gioli, P.; Silingardi, G.E.; Ghiglio, G. High quality water from refinery waste. *Desalination* **1987**, *67*, 271–282. [CrossRef]
352. Venzke, C.D.; Giacobbo, A.; Klauck, C.R.; Viegas, C.; Hansen, E.; Monteiro De Aquim, P.; Antônio, M.; Rodrigues, S.; Moura Bernardes, A. Integrated Membrane Processes (EDR-RO) for Water Reuse in the Petrochemical Industry. *J. Membr. Sci. Res.* **2018**, *4*, 218–226.
353. Hughes, M.; Raubenheimer, A.E.; Viljoen, A.J. Electrodialysis reversal at Tutuka power station, RSA—Seven years' design and operating experience. *Water Sci. Technol.* **1992**, *25*, 277–289. [CrossRef]
354. Turek, M.; Dydo, P. Electrodialysis reversal of calcium sulphate and calcium carbonate supersaturated solution. *Desalination* **2003**, *158*, 91–94. [CrossRef]
355. Turek, M. Electrodialytic desalination and concentration of coal-mine brine. *Desalination* **2004**, *162*, 355–359. [CrossRef]
356. Turek, M.; Laskowska, E.; Mitko, K.; Chorążewska, M.; Dydo, P.; Piotrowski, K.; Jakóbik-Kolon, A. Application of nanofiltration and electrodialysis for improved performance of a salt production plant. *Desalin. Water Treat.* **2017**, *64*, 244–250. [CrossRef]
357. Mitko, K.; Podleśny, B.; Jakóbik-Kolon, A.; Turek, M. Electrodialytic utilization of coal mine brines. *Desalin. Water Treat.* **2017**, *75*, 363–367. [CrossRef]
358. Turek, M.; Bandura, B.; Dydo, P. Power production from coal-mine brine utilizing reversed electrodialysis. *Desalination* **2008**, *221*, 462–466. [CrossRef]
359. Buzzi, D.C.; Viegas, L.S.; Rodrigues, M.A.S.; Bernardes, A.M.; Tenório, J.A.S. Water recovery from acid mine drainage by electrodialysis. *Min. Eng.* **2013**, *40*, 82–89. [CrossRef]
360. Martí-Calatayud, M.C.; Buzzi, D.C.; García-Gabaldón, M.; Bernardes, A.M.; Tenório, J.A.S.; Pérez-Herranz, V. Ion transport through homogeneous and heterogeneous ion-exchange membranes in single salt and multicomponent electrolyte solutions. *J. Membr. Sci.* **2014**, *466*, 45–57. [CrossRef]
361. Bisselink, R.; de Schepper, W.; Trampé, J.; van den Broek, W.; Pinel, I.; Krutko, A.; Groot, N. Mild desalination demo pilot: New normalization approach to effectively evaluate electrodialysis reversal technology. *Water Resour. Ind.* **2015**, *14*, 18–25. [CrossRef]
362. Irfan, M.; Ge, L.; Wang, Y.; Yang, Z.; Xu, T. Hydrophobic Side Chains Impart Anion Exchange Membranes with High Monovalent-Divalent Anion Selectivity in Electrodialysis. *ACS Sustain. Chem. Eng.* **2019**, *7*, 4429–4442. [CrossRef]
363. Irfan, M.; Xu, T.; Ge, L.; Wang, Y.; Xu, T. Zwitterion structure membrane provides high monovalent/divalent cation electrodialysis selectivity: Investigating the effect of functional groups and operating parameters. *J. Membr. Sci.* **2019**, *588*, 117211. [CrossRef]

364. Irfan, M.; Wang, Y.; Xu, T. Novel electrodialysis membranes with hydrophobic alkyl spacers and zwitterion structure enable high monovalent/divalent cation selectivity. *Chem. Eng. J.* **2020**, *383*, 123171. [CrossRef]
365. Van Der Bruggen, B.; Koninckx, A.; Vandecasteele, C. Separation of monovalent and divalent ions from aqueous solution by electrodialysis and nanofiltration. *Water Res.* **2004**, *38*, 1347–1353. [CrossRef]
366. Tufa, R.A.; Hnát, J.; Němeček, M.; Kodým, R.; Curcio, E.; Bouzek, K. Hydrogen production from industrial wastewaters: An integrated reverse electrodialysis—Water electrolysis energy system. *J. Clean. Prod.* **2018**, *203*, 418–426. [CrossRef]
367. Luo, K.; Jia, Y.X.; Liu, X.X.; Wang, M. On-line construction of electrodialyzer with mono-cation permselectivity and its application in reclamation of high salinity wastewater. *Desalination* **2019**, *454*, 38–47. [CrossRef]
368. Djouadi Belkada, F.; Kitous, O.; Drouiche, N.; Aoudj, S.; Bouchelaghem, O.; Abdi, N.; Grib, H.; Mameri, N. Electrodialysis for fluoride and nitrate removal from synthesized photovoltaic industry wastewater. *Sep. Purif. Technol.* **2018**, *204*, 108–115. [CrossRef]
369. Kabay, N.; Arar, Ö.; Samatya, S.; Yüksel, Ü.; Yüksel, M. Separation of fluoride from aqueous solution by electrodialysis: Effect of process parameters and other ionic species. *J. Hazard. Mater.* **2008**, *153*, 107–113. [CrossRef]
370. Wang, X.; Li, N.; Li, J.; Feng, J.; Ma, Z.; Xu, Y.; Sun, Y.; Xu, D.; Wang, J.; Gao, X.; et al. Fluoride removal from secondary effluent of the graphite industry using electrodialysis: Optimization with response surface methodology. *Front. Env. Sci. Eng.* **2019**, *13*. [CrossRef]
371. Kabay, N.; Arar, O.; Acar, F.; Ghazal, A.; Yuksel, U.; Yuksel, M. Removal of boron from water by electrodialysis: Effect of feed characteristics and interfering ions. *Desalination* **2008**, *223*, 63–72. [CrossRef]
372. Melnyk, L.; Goncharuk, V.; Butnyk, I.; Tsapiuk, E. Boron removal from natural and wastewaters using combined sorption/ membrane process. *Desalination* **2005**, *185*, 147–157. [CrossRef]
373. Turek, M.; Dydo, P.; Ciba, J.; Trojanowska, J.; Kluczka, J.; Palka-Kupczak, B. Electrodialytic treatment of boron-containing wastewater with univalent permselective membranes. *Desalination* **2005**, *185*, 139–145. [CrossRef]
374. Turek, M.; Dydo, P.; Trojanowska, J.; Bandura, B. Electrodialytic treatment of boron-containing wastewater. *Desalination* **2007**, *205*, 185–191. [CrossRef]
375. Jiang, B.; Zhang, X.; Zhao, X.; Li, F. Removal of high level boron in aqueous solutions using continuous electrodeionization (CEDI). *Sep. Purif. Technol.* **2018**, *192*, 297–301. [CrossRef]
376. Kozaderova, O.A.; Kim, K.B.; Gadzhiyeva, C.S.; Niftaliev, S.I. Electrochemical characteristics of thin heterogeneous ion exchange membranes. *J. Membr. Sci.* **2020**, *604*, 118081. [CrossRef]
377. Melnikov, S.S.; Mugtamov, O.A.; Zabolotsky, V.I. Study of electrodialysis concentration process of inorganic acids and salts for the two-stage conversion of salts into acids utilizing bipolar electrodialysis. *Sep. Purif. Technol.* **2020**, *235*, 116198. [CrossRef]
378. Zhang, Y.; Shi, Q.; Luo, M.; Wang, H.; Qi, X.; Hou, C.H.; Li, F.; Ai, Z.; Junior, J.T.A. Improved bauxite residue dealkalization by combination of aerated washing and electrodialysis. *J. Hazard. Mater.* **2019**, *364*, 682–690. [CrossRef] [PubMed]
379. Koivisto, E.; Zevenhoven, R. Energy use of flux salt recovery using bipolar membrane electrodialysis for a CO_2 mineralisation process. *Entropy* **2019**, *21*, 395. [CrossRef]
380. Iizuka, A.; Yamashita, Y.; Nagasawa, H.; Yamasaki, A.; Yanagisawa, Y. Separation of lithium and cobalt from waste lithium-ion batteries via bipolar membrane electrodialysis coupled with chelation. *Sep. Purif. Technol.* **2013**, *113*, 33–41. [CrossRef]
381. Lindstrand, V.; Jönsson, A.S.; Sundström, G. Organic fouling of electrodialysis membranes with and without applied voltage. *Desalination* **2000**, *130*, 73–84. [CrossRef]
382. Vanoppen, M.; Bakelants, A.F.A.M.; Gaublomme, D.; Schoutteten, K.V.K.M.; Van Den Bussche, J.; Vanhaecke, L.; Verliefde, A.R.D. Properties governing the transport of trace organic contaminants through ion-exchange membranes. *Environ. Sci. Technol.* **2015**, *49*, 489–497. [CrossRef]
383. Han, L.; Galier, S.; Roux-de Balmann, H. Transfer of neutral organic solutes during desalination by electrodialysis: Influence of the salt composition. *J. Membr. Sci.* **2016**, *511*, 207–218. [CrossRef]

384. Han, L.; Galier, S.; Roux-de Balmann, H. A phenomenological model to evaluate the performances of electrodialysis for the desalination of saline water containing organic solutes. *Desalination* **2017**, *422*, 17–24. [CrossRef]
385. Wang, Q.; Gao, X.; Zhang, Y.; He, Z.; Ji, Z.; Wang, X.; Gao, C. Hybrid RED/ED system: Simultaneous osmotic energy recovery and desalination of high-salinity wastewater. *Desalination* **2017**, *405*, 59–67. [CrossRef]
386. De Schepper, W.; Moraru, M.D.; Jacobs, B.; Oudshoorn, M.; Helsen, J. Electrodialysis of aqueous NaCl-glycerol solutions: A phenomenological comparison of various ion exchange membranes. *Sep. Purif. Technol.* **2019**, *217*, 274–283. [CrossRef]
387. Paltrinieri, L.; Huerta, E.; Puts, T.; Van Baak, W.; Verver, A.B.; Sudhölter, E.J.R.; De Smet, L.C.P.M. Functionalized Anion-Exchange Membranes Facilitate Electrodialysis of Citrate and Phosphate from Model Dairy Wastewater. *Environ. Sci. Technol.* **2019**, *53*, 2396–2404. [CrossRef] [PubMed]
388. Selvaraj, H.; Aravind, P.; Sundaram, M. Four compartment mono selective electrodialysis for separation of sodium formate from industry wastewater. *Chem. Eng. J.* **2018**, *333*, 162–169. [CrossRef]
389. Chao, Y.M.; Liang, T.M. A feasibility study of industrial wastewater recovery using electrodialysis reversal. *Desalination* **2008**, *221*, 433–439. [CrossRef]
390. Yen, F.C.; You, S.J.; Chang, T.C. Performance of electrodialysis reversal and reverse osmosis for reclaiming wastewater from high-tech industrial parks in Taiwan: A pilot-scale study. *J. Environ. Manag.* **2017**, *187*, 393–400. [CrossRef] [PubMed]
391. Rapp, H.J.; Pfromm, P.H. Electrodialysis for chloride removal from the chemical recovery cycle of a Kraft pulp mill. *J. Membr. Sci.* **1998**, *146*, 249–261. [CrossRef]
392. Nataraj, S.K.; Sridhar, S.; Shaikha, I.N.; Reddy, D.S.; Aminabhavi, T.M. Membrane-based microfiltration/electrodialysis hybrid process for the treatment of paper industry wastewater. *Sep. Purif. Technol.* **2007**, *57*, 185–192. [CrossRef]
393. Lafi, R.; Gzara, L.; Lajimi, R.H.; Hafiane, A. Treatment of textile wastewater by a hybrid ultrafiltration/electrodialysis process. *Chem. Eng. Process. Process Intensif.* **2018**, *132*, 105–113. [CrossRef]
394. Lin, J.; Lin, F.; Chen, X.; Ye, W.; Li, X.; Zeng, H.; Van Der Bruggen, B. Sustainable Management of Textile Wastewater: A Hybrid Tight Ultrafiltration/Bipolar-Membrane Electrodialysis Process for Resource Recovery and Zero Liquid Discharge. *Ind. Eng. Chem. Res.* **2019**, *58*, 11003–11012. [CrossRef]
395. Berkessa, Y.W.; Lang, Q.; Yan, B.; Kuang, S.; Mao, D.; Shu, L.; Zhang, Y. Anion exchange membrane organic fouling and mitigation in salt valorization process from high salinity textile wastewater by bipolar membrane electrodialysis. *Desalination* **2019**, *465*, 94–103. [CrossRef]
396. Tamersit, S.; Bouhidel, K.E.; Zidani, Z. Investigation of electrodialysis anti-fouling configuration for desalting and treating tannery unhairing wastewater: Feasibility of by-products recovery and water recycling. *J. Environ. Manag.* **2018**, *207*, 334–340. [CrossRef]
397. Valero, D.; García-García, V.; Expósito, E.; Aldaz, A.; Montiel, V. Application of electrodialysis for the treatment of almond industry wastewater. *J. Membr. Sci.* **2015**, *476*, 580–589. [CrossRef]
398. Kingsbury, R.S.; Liu, F.; Zhu, S.; Boggs, C.; Armstrong, M.D.; Call, D.F.; Coronell, O. Impact of natural organic matter and inorganic solutes on energy recovery from five real salinity gradients using reverse electrodialysis. *J. Membr. Sci.* **2017**, *541*, 621–632. [CrossRef]
399. Lee, H.J.; Oh, S.J.; Moon, S.H. Recovery of ammonium sulfate from fermentation waste by electrodialysis. *Water Res.* **2003**, *37*, 1091–1099. [CrossRef]
400. Luiz, A.; McClure, D.D.; Lim, K.; Leslie, G.; Coster, H.G.L.; Barton, G.W.; Kavanagh, J.M. Potential upgrading of bio-refinery streams by electrodialysis. *Desalination* **2017**, *415*, 20–28. [CrossRef]
401. Luiz, A.; Mcclure, D.D.; Lim, K.; Coster, H.G.L.; Barton, G.W.; Kavanagh, J.M. Towards a model for the electrodialysis of bio-refinery streams. *J. Membr. Sci.* **2019**, *573*, 320–332. [CrossRef]
402. Barros, L.B.M.; Andrade, L.H.; Drewes, J.E.; Amaral, M.C.S. Investigation of electrodialysis configurations for vinasse desalting and potassium recovery. *Sep. Purif. Technol.* **2019**, *229*, 115797. [CrossRef]
403. Milewski, A.; Czechowicz, D.; Jakóbik-Kolon, A.; Dydo, P. Preparation of Glycidol via Dehydrohalogenation of 3-Chloro-1,2-popanediol Using Bipolar Membrane Electrodialysis. *ACS Sustain. Chem. Eng.* **2019**, *7*, 18640–18646. [CrossRef]

404. Lu, H.; Zou, W.; Chai, P.; Wang, J.; Bazinet, L. Feasibility of antibiotic and sulfate ions separation from wastewater using electrodialysis with ultrafiltration membrane. *J. Clean. Prod.* **2016**, *112*, 3097–3105. [CrossRef]
405. Silva, V.; Poiesz, E.; Van Der Heijden, P. Industrial wastewater desalination using electrodialysis: Evaluation and plant design. *J. Appl. Electrochem.* **2013**, *43*, 1057–1067. [CrossRef]
406. Wang, X.; Wang, Y.; Zhang, X.; Feng, H.; Li, C.; Xu, T. Phosphate recovery from excess sludge by conventional electrodialysis (CED) and electrodialysis with bipolar membranes (EDBM). *Ind. Eng. Chem. Res.* **2013**, *52*, 15896–15904. [CrossRef]
407. Zhang, Y.; Desmidt, E.; Van Looveren, A.; Pinoy, L.; Meesschaert, B.; Van Der Bruggen, B. Phosphate separation and recovery from wastewater by novel electrodialysis. *Environ. Sci. Technol.* **2013**, *47*, 5888–5895. [CrossRef]
408. Abou-Shady, A. Recycling of polluted wastewater for agriculture purpose using electrodialysis: Perspective for large scale application. *Chem. Eng. J.* **2017**, *323*, 1–18. [CrossRef]
409. Besseris, G.J. Concurrent multiresponse multifactorial screening of an electrodialysis process of polluted wastewater using robust non-linear Taguchi profiling. *Chemom. Intell. Lab. Syst.* **2020**, *200*, 103997. [CrossRef]
410. Allison, R.P. Electrodialysis reversal in water reuse applications. *Desalination* **1995**, *103*, 11–18. [CrossRef]
411. Del Pino, M.P.; Durham, B. Wastewater reuse through dual-membrane processes: Opportunities for sustainable water resources. *Desalination* **1999**, *124*, 271–277. [CrossRef]
412. Gotor, A.G.; Pérez Baez, S.O.; Espinoza, C.A.; Bachir, S.I. Membrane processes for the recovery and reuse of wastewater in agriculture. *Desalination* **2001**, *137*, 187–192. [CrossRef]
413. Kim, J.O.; Jung, J.T.; Chung, J. Treatment performance of metal membrane microfiltration and electrodialysis integrated system for wastewater reclamation. *Desalination* **2007**, *202*, 343–350. [CrossRef]
414. Goodman, N.B.; Taylor, R.J.; Xie, Z.; Gozukara, Y.; Clements, A. A feasibility study of municipal wastewater desalination using electrodialysis reversal to provide recycled water for horticultural irrigation. *Desalination* **2013**, *317*, 77–83. [CrossRef]
415. Llanos, J.; Cotillas, S.; Cañizares, P.; Rodrigo, M.A. Novel electrodialysis-electrochlorination integrated process for the reclamation of treated wastewaters. *Sep. Purif. Technol.* **2014**, *132*, 362–369. [CrossRef]
416. Snyder, S.A.; Redding, A.M.; Yoon, Y.; Adham, S.; Wert, E.C.; Cannon, F.S.; Oppenheimer, J.; DeCarolis, J. Role of membranes and activated carbon in the removal of endocrine disruptors and pharmaceuticals. *Desalination* **2006**, *202*, 156–181. [CrossRef]
417. Guedes-Alonso, R.; Montesdeoca-Esponda, S.; Pacheco-Juárez, J.; Sosa-Ferrera, Z.; Santana-Rodríguez, J.J. A survey of the presence of pharmaceutical residues in wastewaters. Evaluation of their removal using conventional and natural treatment procedures. *Molecules* **2020**, *25*, 1639. [CrossRef]
418. Gally, C.R.; Benvenuti, T.; Da Trindade, C.D.M.; Rodrigues, M.A.S.; Zoppas-Ferreira, J.; Pérez-Herranz, V.; Bernardes, A.M. Electrodialysis for the tertiary treatment of municipal wastewater: Efficiency of ion removal and ageing of ion exchange membranes. *J. Environ. Chem. Eng.* **2018**, *6*, 5855–5869. [CrossRef]
419. Albornoz, L.L.; Marder, L.; Benvenuti, T.; Bernardes, A.M. Electrodialysis applied to the treatment of an university sewage for water recovery. *J. Environ. Chem. Eng.* **2019**, *7*, 102982. [CrossRef]
420. Zhang, Y.; Pinoy, L.; Meesschaert, B.; Van Der Bruggen, B. A natural driven membrane process for brackish and wastewater treatment: Photovoltaic powered ED and FO hybrid system. *Environ. Sci. Technol.* **2013**, *47*, 10548–10555. [CrossRef] [PubMed]
421. Lu, Y.; He, Z. Mitigation of Salinity Buildup and Recovery of Wasted Salts in a Hybrid Osmotic Membrane Bioreactor-Electrodialysis System. *Environ. Sci. Technol.* **2015**, *49*, 10529–10535. [CrossRef] [PubMed]
422. Zou, S.; He, Z. Electrodialysis recovery of reverse-fluxed fertilizer draw solute during forward osmosis water treatment. *Chem. Eng. J.* **2017**, *330*, 550–558. [CrossRef]
423. Mei, Y.; Tang, C.Y. Co-locating reverse electrodialysis with reverse osmosis desalination: Synergies and implications. *J. Membr. Sci.* **2017**, *539*, 305–312. [CrossRef]
424. Li, W.; Krantz, W.B.; Cornelissen, E.R.; Post, J.W.; Verliefde, A.R.D.; Tang, C.Y. A novel hybrid process of reverse electrodialysis and reverse osmosis for low energy seawater desalination and brine management. *Appl. Energy* **2013**, *104*, 592–602. [CrossRef]

425. Vanoppen, M.; Criel, E.; Walpot, G.; Vermaas, D.A.; Verliefde, A. Assisted reverse electrodialysis—principles, mechanisms, and potential. *npj Clean Water* **2018**, *1*, 9. [CrossRef]
426. La Cerva, M.; Gurreri, L.; Cipollina, A.; Tamburini, A.; Ciofalo, M.; Micale, G. Modelling and cost analysis of hybrid systems for seawater desalination: Electromembrane pre-treatments for Reverse Osmosis. *Desalination* **2019**, *467*, 175–195. [CrossRef]
427. Roman, M.; Van Dijk, L.H.; Gutierrez, L.; Vanoppen, M.; Post, J.W.; Wols, B.A.; Cornelissen, E.R.; Verliefde, A.R.D. Key physicochemical characteristics governing organic micropollutant adsorption and transport in ion-exchange membranes during reverse electrodialysis. *Desalination* **2019**, *468*, 114084. [CrossRef]
428. Nam, J.Y.; Hwang, K.S.; Kim, H.C.; Jeong, H.; Kim, H.; Jwa, E.; Yang, S.C.; Choi, J.; Kim, C.S.; Han, J.H.; et al. Assessing the behavior of the feed-water constituents of a pilot-scale 1000-cell-pair reverse electrodialysis with seawater and municipal wastewater effluent. *Water Res.* **2019**, *148*, 261–271. [CrossRef] [PubMed]
429. Higa, M.; Watanabe, T.; Yasukawa, M.; Endo, N.; Kakihana, Y.; Futamura, H.; Inoue, K.; Miyake, H.; Usui, J.; Hayashi, A.; et al. Sustainable hydrogen production from seawater and sewage treated water using reverse electrodialysis technology. *Water Pract. Technol.* **2019**, *14*, 645–651. [CrossRef]
430. Vanoppen, M.; van Vooren, T.; Gutierrez, L.; Roman, M.; Croué, L.-P.; Verbeken, K.; Philips, J.; Verliefde, A.R.D. Secondary treated domestic wastewater in reverse electrodialysis: What is the best pre-treatment? *Sep. Purif. Technol.* **2019**, *218*, 25–42. [CrossRef]
431. Mehdizadeh, S.; Yasukawa, M.; Suzuki, T.; Higa, M. Reverse electrodialysis for power generation using seawater/municipal wastewater: Effect of coagulation pretreatment. *Desalination* **2020**, *481*, 114356. [CrossRef]
432. Gómez-Coma, L.; Ortiz-Martínez, V.M.; Fallanza, M.; Ortiz, A.; Ibañez, R.; Ortiz, I. Blue energy for sustainable water reclamation in WWTPs. *J. Water Process. Eng.* **2020**, *33*, 101020. [CrossRef]
433. Luque Di Salvo, J.; Cosenza, A.; Tamburini, A.; Micale, G.; Cipollina, A. Long-run operation of a reverse electrodialysis system fed with wastewaters. *J. Environ. Manag.* **2018**, *217*, 871–887. [CrossRef] [PubMed]
434. Mercer, E.; Davey, C.J.; Azzini, D.; Eusebi, A.L.; Tierney, R.; Williams, L.; Jiang, Y.; Parker, A.; Tyrrel, S.; Cartmell, E.; et al. Hybrid membrane distillation reverse electrodialysis configuration for water and energy recovery from human urine: An opportunity for off-grid decentralised sanitation. *J. Membr. Sci.* **2019**, *584*, 343–352. [CrossRef] [PubMed]
435. Desmidt, E.; Ghyselbrecht, K.; Zhang, Y.; Pinoy, L.; Van der Bruggen, B.; Verstraete, W.; Rabaey, K.; Meesschaert, B. Global Phosphorus Scarcity and Full-Scale P-Recovery Techniques: A Review. *Crit. Rev. Environ. Sci. Technol.* **2015**, *45*, 336–384. [CrossRef]
436. Tran, A.T.K.; Zhang, Y.; De Corte, D.; Hannes, J.-B.; Ye, W.; Mondal, P.; Jullok, N.; Meesschaert, B.; Pinoy, L.; Van der Bruggen, B. P-recovery as calcium phosphate from wastewater using an integrated selectrodialysis/crystallization process. *J. Clean. Prod.* **2014**, *77*, 140–151. [CrossRef]
437. Tran, A.T.K.; Zhang, Y.; Lin, J.; Mondal, P.; Ye, W.; Meesschaert, B.; Pinoy, L.; Van Der Bruggen, B. Phosphate pre-concentration from municipal wastewater by selectrodialysis: Effect of competing components. *Sep. Purif. Technol.* **2015**, *141*, 38–47. [CrossRef]
438. Liu, R.; Wang, Y.; Wu, G.; Luo, J.; Wang, S. Development of a selective electrodialysis for nutrient recovery and desalination during secondary effluent treatment. *Chem. Eng. J.* **2017**, *322*, 224–233. [CrossRef]
439. Nur, H.M.; Yüzer, B.; Aydin, M.İ.; Aydin, S.; Öngen, A.; Selçuk, H. Desalination and fate of nutrient transport in domestic wastewater using electrodialysis membrane process. *Desalin. Water Treat.* **2019**, *172*, 323–329. [CrossRef]
440. Rotta, E.H.; Bitencourt, C.S.; Marder, L.; Bernardes, A.M. Phosphorus recovery from low phosphate-containing solution by electrodialysis. *J. Membr. Sci.* **2019**, *573*, 293–300. [CrossRef]
441. Rybalkina, O.; Tsygurina, K.; Melnikova, E.; Mareev, S.; Moroz, I.; Nikonenko, V.; Pismenskaya, N. Partial Fluxes of Phosphoric Acid Anions through Anion-Exchange Membranes in the Course of NaH_2PO_4 Solution Electrodialysis. *Int. J. Mol. Sci.* **2019**, *20*, 3593. [CrossRef] [PubMed]
442. Pismenskaya, N.; Sarapulova, V.; Nevakshenova, E.; Kononenko, N.; Fomenko, M.; Nikonenko, V. Concentration dependencies of diffusion permeability of anion-exchange membranes in sodium hydrogen carbonate, monosodium phosphate, and potassium hydrogen tartrate solutions. *Membranes* **2019**, *9*, 170. [CrossRef] [PubMed]

443. Cai, Y.; Han, Z.; Lin, X.; Duan, Y.; Du, J.; Ye, Z.; Zhu, J. Study on removal of phosphorus as struvite from synthetic wastewater using a pilot-scale electrodialysis system with magnesium anode. *Sci. Total Environ.* **2020**, *726*, 138221. [CrossRef]
444. Vineyard, D.; Hicks, A.; Karthikeyan, K.G.; Barak, P. Economic analysis of electrodialysis, denitrification, and anammox for nitrogen removal in municipal wastewater treatment. *J. Clean. Prod.* **2020**, *262*, 121145. [CrossRef]
445. Wang, X.; Zhang, X.; Wang, Y.; Du, Y.; Feng, H.; Xu, T. Simultaneous recovery of ammonium and phosphorus via the integration of electrodialysis with struvite reactor. *J. Membr. Sci.* **2015**, *490*, 65–71. [CrossRef]
446. Thompson Brewster, E.; Ward, A.J.; Mehta, C.M.; Radjenovic, J.; Batstone, D.J. Predicting scale formation during electrodialytic nutrient recovery. *Water Res.* **2017**, *110*, 202–210. [CrossRef]
447. Ward, A.J.; Arola, K.; Thompson Brewster, E.; Mehta, C.M.; Batstone, D.J. Nutrient recovery from wastewater through pilot scale electrodialysis. *Water Res.* **2018**, *135*, 57–65. [CrossRef]
448. Arola, K.; Ward, A.; Mänttäri, M.; Kallioinen, M.; Batstone, D. Transport of pharmaceuticals during electrodialysis treatment of wastewater. *Water Res.* **2019**, *161*, 496–504. [CrossRef] [PubMed]
449. Van Linden, N.; Spanjers, H.; van Lier, J.B. Application of dynamic current density for increased concentration factors and reduced energy consumption for concentrating ammonium by electrodialysis. *Water Res.* **2019**, *163*, 114856. [CrossRef]
450. Vecino, X.; Reig, M.; Gibert, O.; Valderrama, C.; Cortina, J.L. Integration of liquid-liquid membrane contactors and electrodialysis for ammonium recovery and concentration as a liquid fertilizer. *Chemosphere* **2020**, *245*, 125606. [CrossRef]
451. Gao, F.; Wang, L.; Wang, J.; Zhang, H.; Lin, S. Nutrient recovery from treated wastewater by a hybrid electrochemical sequence integrating bipolar membrane electrodialysis and membrane capacitive deionization. *Environ. Sci. Water Res. Technol.* **2020**, *6*, 383–391. [CrossRef]
452. Tao, B.; Passanha, P.; Kumi, P.; Wilson, V.; Jones, D.; Esteves, S. Recovery and concentration of thermally hydrolysed waste activated sludge derived volatile fatty acids and nutrients by microfiltration, electrodialysis and struvite precipitation for polyhydroxyalkanoates production. *Chem. Eng. J.* **2016**, *295*, 11–19. [CrossRef]
453. López-Gómez, J.P.; Alexandri, M.; Schneider, R.; Latorre-Sánchez, M.; Coll Lozano, C.; Venus, J. Organic fraction of municipal solid waste for the production of L-lactic acid with high optical purity. *J. Clean. Prod.* **2020**, *247*, 119165. [CrossRef]
454. Rose, C.; Parker, A.; Jefferson, B.; Cartmell, E. The characterization of feces and urine: A review of the literature to inform advanced treatment technology. *Crit. Rev. Environ. Sci. Technol.* **2015**, *45*, 1827–1879. [CrossRef]
455. Escher, B.I.; Pronk, W.; Suter, M.J.F.; Maurer, M. Monitoring the removal efficiency of pharmaceuticals and hormones in different treatment processes of source-separated urine with bioassays. *Environ. Sci. Technol.* **2006**, *40*, 5095–5101. [CrossRef] [PubMed]
456. Pronk, W.; Biebow, M.; Boller, M. Electrodialysis for recovering salts from a urine solution containing micropollutants. *Environ. Sci. Technol.* **2006**, *40*, 2414–2420. [CrossRef]
457. Pronk, W.; Zuleeg, S.; Lienert, J.; Escher, B.; Koller, M.; Berner, A.; Koch, G.; Boller, M. Pilot experiments with electrodialysis and ozonation for the production of a fertiliser from urine. *Water Sci. Technol.* **2007**, *56*, 219–227. [CrossRef]
458. Pronk, W.; Koné, D. Options for urine treatment in developing countries. *Desalination* **2009**, *248*, 360–368. [CrossRef]
459. De Paepe, J.; Lindeboom, R.E.F.; Vanoppen, M.; De Paepe, K.; Demey, D.; Coessens, W.; Lamaze, B.; Verliefde, A.R.D.; Clauwaert, P.; Vlaeminck, S.E. Refinery and concentration of nutrients from urine with electrodialysis enabled by upstream precipitation and nitrification. *Water Res.* **2018**, *144*, 76–86. [CrossRef]
460. Hjorth, M.; Christensen, K.V.; Christensen, M.L.; Sommer, S.G. Solid-liquid separation of animal slurry in theory and practice. *Sustain. Agric.* **2009**, *2*, 953–986.
461. Nasir, I.M.; Mohd Ghazi, T.I.; Omar, R. Anaerobic digestion technology in livestock manure treatment for biogas production: A review. *Eng. Life Sci.* **2012**, *12*, 258–269. [CrossRef]
462. FAO. *Food Outlook, Biannual Report on Global Food Markets*; FAO: Rome, Italy, 2017.

463. Mondor, M.; Masse, L.; Ippersiel, D.; Lamarche, F.; Massé, D.I. Use of electrodialysis and reverse osmosis for the recovery and concentration of ammonia from swine manure. *Bioresour. Technol.* **2008**, *99*, 7363–7368. [CrossRef]
464. Mondor, M.; Ippersiel, D.; Lamarche, F.; Masse, L. Fouling characterization of electrodialysis membranes used for the recovery and concentration of ammonia from swine manure. *Bioresour. Technol.* **2009**, *100*, 566–571. [CrossRef]
465. Ippersiel, D.; Mondor, M.; Lamarche, F.; Tremblay, F.; Dubreuil, J.; Masse, L. Nitrogen potential recovery and concentration of ammonia from swine manure using electrodialysis coupled with air stripping. *J. Environ. Manag.* **2012**, *95*, S165–S169. [CrossRef]
466. Shi, L.; Xie, S.; Hu, Z.; Wu, G.; Morrison, L.; Croot, P.; Hu, H.; Zhan, X. Nutrient recovery from pig manure digestate using electrodialysis reversal: Membrane fouling and feasibility of long-term operation. *J. Membr. Sci.* **2019**, *573*, 560–569. [CrossRef]
467. Shi, L.; Hu, Z.; Simplicio, W.S.; Qiu, S.; Xiao, L.; Harhen, B.; Zhan, X. Antibiotics in nutrient recovery from pig manure via electrodialysis reversal: Sorption and migration associated with membrane fouling. *J. Membr. Sci.* **2020**, *597*, 117633. [CrossRef]
468. Ye, Z.L.; Ghyselbrecht, K.; Monballiu, A.; Pinoy, L.; Meesschaert, B. Fractionating various nutrient ions for resource recovery from swine wastewater using simultaneous anionic and cationic selective-electrodialysis. *Water Res.* **2019**, *160*, 424–434. [CrossRef]
469. Shi, L.; Hu, Y.; Xie, S.; Wu, G.; Hu, Z.; Zhan, X. Recovery of nutrients and volatile fatty acids from pig manure hydrolysate using two-stage bipolar membrane electrodialysis. *Chem. Eng. J.* **2018**, *334*, 134–142. [CrossRef]
470. Duong, H.C.; Ansari, A.J.; Nghiem, L.D.; Cao, H.T.; Vu, T.D.; Nguyen, T.P. Membrane Processes for the Regeneration of Liquid Desiccant Solution for Air Conditioning. *Curr. Pollut. Rep.* **2019**, *5*, 308–318. [CrossRef]
471. Li, X.W.; Zhang, X.S. Photovoltaic-electrodialysis regeneration method for liquid desiccant cooling system. *Sol. Energy* **2009**, *83*, 2195–2204. [CrossRef]
472. Li, X.W.; Zhang, X.S.; Quan, S. Single-stage and double-stage photovoltaic driven regeneration for liquid desiccant cooling system. *Appl. Energy* **2011**, *88*, 4908–4917. [CrossRef]
473. Cheng, Q.; Zhang, X.S.; Li, X.W. Double-stage photovoltaic/thermal ED regeneration for liquid desiccant cooling system. *Energy Build.* **2012**, *51*, 64–72. [CrossRef]
474. Cheng, Q.; Xu, Y.; Zhang, X.S. Experimental investigation of an electrodialysis regenerator for liquid desiccant. *Energy Build.* **2013**, *67*, 419–425. [CrossRef]
475. Cheng, Q.; Zhang, X.; Jiao, S. Influence of concentration difference between dilute cells and regenerate cells on the performance of electrodialysis regenerator. *Energy* **2017**, *140*, 646–655. [CrossRef]
476. Cheng, Q.; Jiao, S. Experimental and theoretical research on the current efficiency of the electrodialysis regenerator for liquid desiccant air-conditioning system using LiCl solution. *Int. J. Refrig.* **2018**, *96*, 1–9. [CrossRef]
477. Guo, Y.; Ma, Z.; Al-Jubainawi, A.; Cooper, P.; Nghiem, L.D. Using electrodialysis for regeneration of aqueous lithium chloride solution in liquid desiccant air conditioning systems. *Energy Build.* **2016**, *116*, 285–295. [CrossRef]
478. Al-Jubainawi, A.; Ma, Z.; Guo, Y.; Nghiem, L.D.; Cooper, P.; Li, W. Factors governing mass transfer during membrane electrodialysis regeneration of LiCl solution for liquid desiccant dehumidification systems. *Sustain. Cities Soc.* **2017**, *28*, 30–41. [CrossRef]
479. Guo, Y.; Al-Jubainawi, A.; Ma, Z. Performance investigation and optimisation of electrodialysis regeneration for LiCl liquid desiccant cooling systems. *Appl. Therm. Eng.* **2019**, *149*, 1023–1034. [CrossRef]
480. Guo, Y.; Al-Jubainawi, A.; Peng, X. Modelling and the feasibility study of a hybrid electrodialysis and thermal regeneration method for LiCl liquid desiccant dehumidification. *Appl. Energy* **2019**, *239*, 1014–1036. [CrossRef]
481. Al-Jubainawi, A.; Ma, Z.; Guo, Y.; Nghiem, L.D. Effect of regulating main governing factors on the selectivity membranes of electrodialysis used for LiCl liquid desiccant regeneration. *J. Build. Eng.* **2020**, *28*, 101022. [CrossRef]
482. Pei, W.; Cheng, Q.; Jiao, S.; Liu, L. Performance evaluation of the electrodialysis regenerator for the lithium bromide solution with high concentration in the liquid desiccant air-conditioning system. *Energy* **2019**, *187*, 115928. [CrossRef]
483. Sun, B.; Zhang, M.; Huang, S.; Su, W.; Zhou, J.; Zhang, X. Performance evaluation on regeneration of high-salt solutions used in air conditioning systems by electrodialysis. *J. Membr. Sci.* **2019**, *582*, 224–235. [CrossRef]

484. International Desalination Association (IDA). *Desalination Yearbook 2016–2017*; International Desalination Association (IDA): Topsfield, MA, USA, 2017.
485. Jones, E.; Qadir, M.; van Vliet, M.T.H.; Smakhtin, V.; Kang, S. The state of desalination and brine production: A global outlook. *Sci. Total Environ.* **2019**, *657*, 1343–1356. [CrossRef]
486. Gude, V.G. Desalination and sustainability–An appraisal and current perspective. *Water Res.* **2016**, *89*, 87–106. [CrossRef]
487. Baker, R.W. *Membrane Technology and Applications*; John Wiley & Sons, Ltd.: Chichester, UK, 2012; ISBN 9781118359686.
488. Giwa, A.; Dufour, V.; Al Marzooqi, F.; Al Kaabi, M.; Hasan, S.W. Brine management methods: Recent innovations and current status. *Desalination* **2017**, *407*, 1–23. [CrossRef]
489. Mavukkandy, M.O.; Chabib, C.M.; Mustafa, I.; Al Ghaferi, A.; AlMarzooqi, F. Brine management in desalination industry: From waste to resources generation. *Desalination* **2019**, *472*, 114187. [CrossRef]
490. Panagopoulos, A.; Haralambous, K.J.; Loizidou, M. Desalination brine disposal methods and treatment technologies—A review. *Sci. Total Environ.* **2019**, *693*, 133545. [CrossRef]
491. Korngold, E.; Aronov, L.; Daltrophe, N. Electrodialysis of brine solutions discharged from an RO plant. *Desalination* **2009**, *242*, 215–227. [CrossRef]
492. Oren, Y.; Korngold, E.; Daltrophe, N.; Messalem, R.; Volkman, Y.; Aronov, L.; Weismann, M.; Bouriakov, N.; Glueckstern, P.; Gilron, J. Pilot studies on high recovery BWRO-EDR for near zero liquid discharge approach. *Desalination* **2010**, *261*, 321–330. [CrossRef]
493. Xu, X.; Lin, L.; Ma, G.; Wang, H.; Jiang, W.; He, Q.; Nirmalakhandan, N.; Xu, P. Study of polyethyleneimine coating on membrane permselectivity and desalination performance during pilot-scale electrodialysis of reverse osmosis concentrate. *Sep. Purif. Technol.* **2018**, *207*, 396–405. [CrossRef]
494. Yan, H.; Wang, Y.; Wu, L.; Shehzad, M.A.; Jiang, C.; Fu, R.; Liu, Z.; Xu, T. Multistage-batch electrodialysis to concentrate high-salinity solutions: Process optimisation, water transport, and energy consumption. *J. Membr. Sci.* **2019**, *570–571*, 245–257. [CrossRef]
495. Jiang, C.; Wang, Y.; Zhang, Z.; Xu, T. Electrodialysis of concentrated brine from RO plant to produce coarse salt and freshwater. *J. Membr. Sci.* **2014**, *450*, 323–330. [CrossRef]
496. Reig, M.; Casas, S.; Aladjem, C.; Valderrama, C.; Gibert, O.; Valero, F.; Centeno, C.M.; Larrotcha, E.; Cortina, J.L. Concentration of NaCl from seawater reverse osmosis brines for the chlor-alkali industry by electrodialysis. *Desalination* **2014**, *342*, 107–117. [CrossRef]
497. Tanaka, Y.; Reig, M.; Casas, S.; Aladjem, C.; Cortina, J.L. Computer simulation of ion-exchange membrane electrodialysis for salt concentration and reduction of RO discharged brine for salt production and marine environment conservation. *Desalination* **2015**, *367*, 76–89. [CrossRef]
498. Reig, M.; Farrokhzad, H.; Van der Bruggen, B.; Gibert, O.; Cortina, J.L. Synthesis of a monovalent selective cation exchange membrane to concentrate reverse osmosis brines by electrodialysis. *Desalination* **2015**, *375*, 1–9. [CrossRef]
499. Zhang, W.; Miao, M.; Pan, J.; Sotto, A.; Shen, J.; Gao, C.; Van der Bruggen, B. Separation of divalent ions from seawater concentrate to enhance the purity of coarse salt by electrodialysis with monovalent-selective membranes. *Desalination* **2017**, *411*, 28–37. [CrossRef]
500. Liu, J.; Yuan, J.; Ji, Z.; Wang, B.; Hao, Y.; Guo, X. Concentrating brine from seawater desalination process by nanofiltration-electrodialysis integrated membrane technology. *Desalination* **2016**, *390*, 53–61. [CrossRef]
501. McGovern, R.K.; Zubair, S.M.; Lienhard, V.J.H. The benefits of hybridising electrodialysis with reverse osmosis. *J. Membr. Sci.* **2014**, *469*, 326–335. [CrossRef]
502. Chung, H.W.; Nayar, K.G.; Swaminathan, J.; Chehayeb, K.M.; Lienhard, V.J.H. Thermodynamic analysis of brine management methods: Zero-discharge desalination and salinity-gradient power production. *Desalination* **2017**, *404*, 291–303. [CrossRef]
503. Chehayeb, K.M.; Farhat, D.M.; Nayar, K.G.; Lienhard, J.H. Optimal design and operation of electrodialysis for brackish-water desalination and for high-salinity brine concentration. *Desalination* **2017**, *420*, 167–182. [CrossRef]

504. Chehayeb, K.M.; Nayar, K.G.; Lienhard, J.H. On the merits of using multi-stage and counterflow electrodialysis for reduced energy consumption. *Desalination* **2018**, *439*, 1–16. [CrossRef]
505. Nayar, K.G.; Fernandes, J.; McGovern, R.K.; Dominguez, K.P.; McCance, A.; Al-Anzi, B.S.; Lienhard, J.H. Cost and energy requirements of hybrid RO and ED brine concentration systems for salt production. *Desalination* **2019**, *456*, 97–120. [CrossRef]
506. Nayar, K.G.; Fernandes, J.; McGovern, R.K.; Al-Anzi, B.S.; Lienhard, J.H. Cost and energy needs of RO-ED-crystallizer systems for zero brine discharge seawater desalination. *Desalination* **2019**, *457*, 115–132. [CrossRef]
507. Cappelle, M.; Walker, W.S.; Davis, T.A. Improving Desalination Recovery Using Zero Discharge Desalination (ZDD): A Process Model for Evaluating Technical Feasibility. *Ind. Eng. Chem. Res.* **2017**, *56*, 10448–10460. [CrossRef]
508. Reahl, E.R. Reclaiming reverse osmosis blowdown with electrodialysis reversal. *Desalination* **1990**, *78*, 77–89. [CrossRef]
509. Zhang, Y.; Ghyselbrecht, K.; Meesschaert, B.; Pinoy, L.; Van der Bruggen, B. Electrodialysis on RO concentrate to improve water recovery in wastewater reclamation. *J. Membr. Sci.* **2011**, *378*, 101–110. [CrossRef]
510. Zhang, Y.; Ghyselbrecht, K.; Vanherpe, R.; Meesschaert, B.; Pinoy, L.; Van der Bruggen, B. RO concentrate minimization by electrodialysis: Techno-economic analysis and environmental concerns. *J. Environ. Manag.* **2012**, *107*, 28–36. [CrossRef]
511. Tran, A.T.K.; Zhang, Y.; Jullok, N.; Meesschaert, B.; Pinoy, L.; Van der Bruggen, B. RO concentrate treatment by a hybrid system consisting of a pellet reactor and electrodialysis. *Chem. Eng. Sci.* **2012**, *79*, 228–238. [CrossRef]
512. Ghyselbrecht, K.; Van Houtte, E.; Pinoy, L.; Verbauwhede, J.; Van Der Bruggen, B.; Meesschaert, B. Treatment of RO concentrate by means of a combination of a willow field and electrodialysis. *Resour. Conserv. Recycl.* **2012**, *65*, 116–123. [CrossRef]
513. Ribera-Pi, J.; Badia-Fabregat, M.; Espí, J.; Clarens, F.; Jubany, I.; Martínez-Lladó, X. Decreasing environmental impact of landfill leachate treatment by MBR, RO and EDR hybrid treatment. *Environ. Technol. (UK)* **2020**. [CrossRef]
514. Zhang, Y.; Van der Bruggen, B.; Pinoy, L.; Meesschaert, B. Separation of nutrient ions and organic compounds from salts in RO concentrates by standard and monovalent selective ion-exchange membranes used in electrodialysis. *J. Membr. Sci.* **2009**, *332*, 104–112. [CrossRef]
515. Banasiak, L.J.; Van der Bruggen, B.; Schäfer, A.I. Sorption of pesticide endosulfan by electrodialysis membranes. *Chem. Eng. J.* **2011**, *166*, 233–239. [CrossRef]
516. Venzke, C.D.; Giacobbo, A.; Ferreira, J.Z.; Bernardes, A.M.; Rodrigues, M.A.S. Increasing water recovery rate of membrane hybrid process on the petrochemical wastewater treatment. *Process. Saf. Environ. Prot.* **2018**, *117*, 152–158. [CrossRef]
517. Zhao, D.; Lee, L.Y.; Ong, S.L.; Chowdhury, P.; Siah, K.B.; Ng, H.Y. Electrodialysis reversal for industrial reverse osmosis brine treatment. *Sep. Purif. Technol.* **2019**, *213*, 339–347. [CrossRef]
518. Van Linden, N.; Shang, R.; Stockinger, G.; Heijman, B.; Spanjers, H. Separation of natural organic matter and sodium chloride for salt recovery purposes in zero liquid discharge. *Water Resour. Ind.* **2020**, *23*, 100117. [CrossRef]
519. Xu, Y.; Sun, Y.; Ma, Z.; Wang, R.; Wang, X.; Wang, J.; Wang, L.; Gao, X.; Gao, J. Response surface modeling and optimization of electrodialysis for reclamation of RO concentrates in coal-fired power plants. *Sep. Sci. Technol.* **2019**, 1–11. [CrossRef]
520. Qiu, Y.; Ruan, H.; Tang, C.; Yao, L.; Shen, J.; Sotto, A. Study on Recovering High-Concentration Lithium Salt from Lithium-Containing Wastewater Using a Hybrid Reverse Osmosis (RO)–Electrodialysis (ED) Process. *ACS Sustain. Chem. Eng.* **2019**, *7*, 13481–13490. [CrossRef]
521. Vaudevire, E.; Radmanesh, F.; Kolkman, A.; Vughs, D.; Cornelissen, E.; Post, J.; van der Meer, W. Fate and removal of trace pollutants from an anion exchange spent brine during the recovery process of natural organic matter and salts. *Water Res.* **2019**, *154*, 34–44. [CrossRef]

522. Haddad, M.; Bazinet, L.; Barbeau, B. Eco-efficient treatment of ion exchange spent brine via electrodialysis to recover NaCl and minimize waste disposal. *Sci. Total Environ.* **2019**, *690*, 400–409. [CrossRef] [PubMed]
523. Ibáñez, R.; Pérez-González, A.; Gómez, P.; Urtiaga, A.M.; Ortiz, I. Acid and base recovery from softened reverse osmosis (RO) brines. Experimental assessment using model concentrates. *Desalination* **2013**, *309*, 165–170. [CrossRef]
524. Fernandez-Gonzalez, C.; Dominguez-Ramos, A.; Ibañez, R.; Chen, Y.; Irabien, A. Valorization of desalination brines by electrodialysis with bipolar membranes using nanocomposite anion exchange membranes. *Desalination* **2017**, *406*, 16–24. [CrossRef]
525. Herrero-Gonzalez, M.; Diaz-Guridi, P.; Dominguez-Ramos, A.; Ibañez, R.; Irabien, A. Photovoltaic solar electrodialysis with bipolar membranes. *Desalination* **2018**, *433*, 155–163. [CrossRef]
526. Herrero-Gonzalez, M.; Diaz-Guridi, P.; Dominguez-Ramos, A.; Irabien, A.; Ibañez, R. Highly concentrated HCl and NaOH from brines using electrodialysis with bipolar membranes. *Sep. Purif. Technol.* **2020**, *242*, 116785. [CrossRef]
527. Herrero-Gonzalez, M.; Admon, N.; Dominguez-Ramos, A.; Ibañez, R.; Wolfson, A.; Irabien, A. Environmental sustainability assessment of seawater reverse osmosis brine valorization by means of electrodialysis with bipolar membranes. *Environ. Sci. Pollut. Res.* **2020**, *27*, 1256–1266. [CrossRef]
528. Yang, Y.; Gao, X.; Fan, A.; Fu, L.; Gao, C. An innovative beneficial reuse of seawater concentrate using bipolar membrane electrodialysis. *J. Membr. Sci.* **2014**, *449*, 119–126. [CrossRef]
529. Reig, M.; Casas, S.; Gibert, O.; Valderrama, C.; Cortina, J.L. Integration of nanofiltration and bipolar electrodialysis for valorization of seawater desalination brines: Production of drinking and waste water treatment chemicals. *Desalination* **2016**, *382*, 13–20. [CrossRef]
530. Reig, M.; Casas, S.; Valderrama, C.; Gibert, O.; Cortina, J.L. Integration of monopolar and bipolar electrodialysis for valorization of seawater reverse osmosis desalination brines: Production of strong acid and base. *Desalination* **2016**, *398*, 87–97. [CrossRef]
531. Chen, B.; Jiang, C.; Wang, Y.; Fu, R.; Liu, Z.; Xu, T. Selectrodialysis with bipolar membrane for the reclamation of concentrated brine from RO plant. *Desalination* **2018**, *442*, 8–15. [CrossRef]
532. Badruzzaman, M.; Oppenheimer, J.; Adham, S.; Kumar, M. Innovative beneficial reuse of reverse osmosis concentrate using bipolar membrane electrodialysis and electrochlorination processes. *J. Membr. Sci.* **2009**, *326*, 392–399. [CrossRef]
533. Wang, M.; Wang, K.; Jia, Y.; Ren, Q. The reclamation of brine generated from desalination process by bipolar membrane electrodialysis. *J. Membr. Sci.* **2014**, *452*, 54–61. [CrossRef]
534. Yip, N.Y.; Brogioli, D.; Hamelers, H.V.M.; Nijmeijer, K. Salinity gradients for sustainable energy: Primer, progress, and prospects. *Environ. Sci. Technol.* **2016**, *50*, 12072–12094. [CrossRef]
535. Lee, S.; Choi, J.; Park, Y.G.; Shon, H.; Ahn, C.H.; Kim, S.H. Hybrid desalination processes for beneficial use of reverse osmosis brine: Current status and future prospects. *Desalination* **2019**, *454*, 104–111. [CrossRef]
536. Tufa, R.A.; Noviello, Y.; Di Profio, G.; Macedonio, F.; Ali, A.; Drioli, E.; Fontananova, E.; Bouzek, K.; Curcio, E. Integrated membrane distillation-reverse electrodialysis system for energy-efficient seawater desalination. *Appl. Energy* **2019**, *253*, 113551. [CrossRef]
537. Choi, J.; Oh, Y.; Chae, S.; Hong, S. Membrane capacitive deionization-reverse electrodialysis hybrid system for improving energy efficiency of reverse osmosis seawater desalination. *Desalination* **2019**, *462*, 19–28. [CrossRef]
538. Luo, F.; Wang, Y.; Jiang, C.; Wu, B.; Feng, H.; Xu, T. A power free electrodialysis (PFED) for desalination. *Desalination* **2017**, *404*, 138–146. [CrossRef]
539. Mei, Y.; Li, X.; Yao, Z.; Qing, W.; Fane, A.G.; Tang, C.Y. Simulation of an energy self-sufficient electrodialysis desalination stack for salt removal efficiency and fresh water recovery. *J. Membr. Sci.* **2020**, *598*, 117771. [CrossRef]
540. Kwon, K.; Han, J.; Park, B.H.; Shin, Y.; Kim, D. Brine recovery using reverse electrodialysis in membrane-based desalination processes. *Desalination* **2015**, *362*, 1–10. [CrossRef]
541. Tufa, R.A.; Curcio, E.; Brauns, E.; van Baak, W.; Fontananova, E.; Di Profio, G. Membrane Distillation and Reverse Electrodialysis for Near-Zero Liquid Discharge and low energy seawater desalination. *J. Membr. Sci.* **2015**, *496*, 325–333. [CrossRef]

542. Tufa, R.A.; Rugiero, E.; Chanda, D.; Hnàt, J.; van Baak, W.; Veerman, J.; Fontananova, E.; Di Profio, G.; Drioli, E.; Bouzek, K.; et al. Salinity gradient power-reverse electrodialysis and alkaline polymer electrolyte water electrolysis for hydrogen production. *J. Membr. Sci.* **2016**, *514*, 155–164. [CrossRef]
543. Mehdizadeh, S.; Yasukawa, M.; Kuno, M.; Kawabata, Y.; Higa, M. Evaluation of energy harvesting from discharge solutions in a salt production plant by reverse electrodialysis (RED). *Desalination* **2019**, *467*, 95–102. [CrossRef]
544. Tian, H.; Wang, Y.; Pei, Y. Energy capture from thermolytic solutions and simulated sunlight coupled with hydrogen peroxide production and wastewater remediation. *Water Res.* **2020**, *170*, 115318. [CrossRef]
545. Xu, P.; Zheng, D.; Xu, H. The feasibility and mechanism of reverse electrodialysis enhanced photocatalytic fuel cell-Fenton system on advanced treatment of coal gasification wastewater. *Sep. Purif. Technol.* **2019**, *220*, 183–188. [CrossRef]
546. D'Angelo, A.; Tedesco, M.; Cipollina, A.; Galia, A.; Micale, G.; Scialdone, O. Reverse electrodialysis performed at pilot plant scale: Evaluation of redox processes and simultaneous generation of electric energy and treatment of wastewater. *Water Res.* **2017**, *125*, 123–131. [CrossRef]
547. Ma, P.; Hao, X.; Galia, A.; Scialdone, O. Development of a process for the treatment of synthetic wastewater without energy inputs using the salinity gradient of wastewaters and a reverse electrodialysis stack. *Chemosphere* **2020**, *248*, 125994. [CrossRef]
548. Van Egmond, W.J.; Starke, U.K.; Saakes, M.; Buisman, C.J.N.; Hamelers, H.V.M. Energy efficiency of a concentration gradient flow battery at elevated temperatures. *J. Power Sources* **2017**, *340*, 71–79. [CrossRef]
549. Krakhella, K.W.; Morales, M.; Bock, R.; Seland, F.; Burheim, O.S.; Einarsrud, K.E. Electrodialytic energy storage system: Permselectivity, stack measurements and life-cycle analysis. *Energies* **2020**, *13*, 1247. [CrossRef]
550. Xia, J.; Eigenberger, G.; Strathmann, H.; Nieken, U. Acid-base flow battery, based on reverse electrodialysis with bi-polar membranes: Stack experiments. *Processes* **2020**, *8*, 99. [CrossRef]
551. Martí-Calatayud, M.C.; Buzzi, D.C.; García-Gabaldón, M.; Ortega, E.; Bernardes, A.M.; Tenório, J.A.S.; Pérez-Herranz, V. Sulfuric acid recovery from acid mine drainage by means of electrodialysis. *Desalination* **2014**, *343*, 120–127. [CrossRef]
552. Dara, S.; Bonakdarpour, A.; Ho, M.; Govindarajan, R.; Wilkinson, D.P. Conversion of saline waste-water and gaseous carbon dioxide to (bi)carbonate salts, hydrochloric acid and desalinated water for on-site industrial utilization. *React. Chem. Eng.* **2019**, *4*, 141–150. [CrossRef]
553. Wu, D.; Chen, G.Q.; Hu, B.; Deng, H. Feasibility and energy consumption analysis of phenol removal from salty wastewater by electro-electrodialysis. *Sep. Purif. Technol.* **2019**, *215*, 44–50. [CrossRef]
554. Magro, C.; Paz-Garcia, J.M.; Ottosen, L.M.; Mateus, E.P.; Ribeiro, A.B. Sustainability of construction materials: Electrodialytic technology as a tool for mortars production. *J. Hazard. Mater.* **2019**, *363*, 421–427. [CrossRef]
555. Liu, Z.; Zhang, L.; Li, L.; Zhang, S. Separation of olefin/paraffin by electrodialysis. *Sep. Purif. Technol.* **2019**, *218*, 20–24. [CrossRef]
556. Xia, A.; Wei, P.; Sun, C.; Show, P.L.; Huang, Y.; Fu, Q. Hydrogen fermentation of organic wastewater with high ammonium concentration via electrodialysis system. *Bioresour. Technol.* **2019**, *288*, 121560. [CrossRef]
557. Raschitor, A.; Llanos, J.; Rodrigo, M.A.; Cañizares, P. Is it worth using the coupled electrodialysis/electro-oxidation system for the removal of pesticides? Process modelling and role of the pollutant. *Chemosphere* **2020**, *246*, 125781. [CrossRef]
558. Liu, M.J.; Neo, B.S.; Tarpeh, W.A. Building an operational framework for selective nitrogen recovery via electrochemical stripping. *Water Res.* **2020**, *169*, 115226. [CrossRef]
559. Hara, K.; Kishimoto, N.; Kato, M.; Otsu, H. Efficacy of a two-compartment electrochemical flow cell introduced into a reagent-free UV/chlorine advanced oxidation process. *Chem. Eng. J.* **2020**, *388*, 124385. [CrossRef]
560. Cerrillo-Gonzalez, M.M.; Villen-Guzman, M.; Vereda-Alonso, C.; Gomez-Lahoz, C.; Rodriguez-Maroto, J.M.; Paz-Garcia, J.M. Recovery of Li and Co from LiCoO2 via hydrometallurgical-electrodialytic treatment. *Appl. Sci.* **2020**, *10*, 2367. [CrossRef]
561. Sadyrbaeva, T.Z. Removal of chromium(VI) from aqueous solutions using a novel hybrid liquid membrane—electrodialysis process. *Chem. Eng. Process. Process. Intensif.* **2016**, *99*, 183–191. [CrossRef]

562. Wang, B.; Li, Z.; Lang, Q.; Tan, M.; Ratanatamskul, C.; Lee, M.; Liu, Y.; Zhang, Y. A comprehensive investigation on the components in ionic liquid-based polymer inclusion membrane for Cr(VI) transport during electrodialysis. *J. Membr. Sci.* **2020**, *604*, 118016. [CrossRef]
563. Meng, X.; Li, J.; Lv, Y.; Feng, Y.; Zhong, Y. Electro-membrane extraction of cadmium(II) by bis(2-ethylhexyl) phosphate/kerosene/polyvinyl chloride polymer inclusion membrane. *J. Hazard. Mater.* **2020**, *386*, 121990. [CrossRef] [PubMed]
564. Pan, Y.; Zhu, T.; He, Z. Minimizing effects of chloride and calcium towards enhanced nutrient recovery from sidestream centrate in a decoupled electrodialysis driven by solar energy. *J. Clean. Prod.* **2020**, *263*, 121419. [CrossRef]
565. Alkhadra, M.A.; Conforti, K.M.; Gao, T.; Tian, H.; Bazant, M.Z. Continuous Separation of Radionuclides from Contaminated Water by Shock Electrodialysis. *Environ. Sci. Technol.* **2020**, *45*, 527–536. [CrossRef]
566. Lee, J.B.; Park, K.K.; Eum, H.M.; Lee, C.W. Desalination of a thermal power plant wastewater by membrane capacitive deionization. *Desalination* **2006**, *196*, 125–134. [CrossRef]
567. Xu, P.; Drewes, J.E.; Heil, D.; Wang, G. Treatment of brackish produced water using carbon aerogel-based capacitive deionization technology. *Water Res.* **2008**, *42*, 2605–2617. [CrossRef]
568. Liang, P.; Yuan, L.; Yang, X.; Zhou, S.; Huang, X. Coupling ion-exchangers with inexpensive activated carbon fiber electrodes to enhance the performance of capacitive deionization cells for domestic wastewater desalination. *Water Res.* **2013**, *47*, 2523–2530. [CrossRef]
569. Oren, Y. Capacitive deionization (CDI) for desalination and water treatment—Past, present and future (a review). *Desalination* **2008**, *228*, 10–29. [CrossRef]
570. Anderson, M.A.; Cudero, A.L.; Palma, J. Capacitive deionization as an electrochemical means of saving energy and delivering clean water. Comparison to present desalination practices: Will it compete? *Electrochim. Acta* **2010**, *55*, 3845–3856. [CrossRef]
571. Liu, P.; Yan, T.; Zhang, J.; Shi, L.; Zhang, D. Separation and recovery of heavy metal ions and salt ions from wastewater by 3D graphene-based asymmetric electrodes: Via capacitive deionization. *J. Mater. Chem. A* **2017**, *5*, 14748–14757. [CrossRef]
572. Choi, J.; Dorji, P.; Shon, H.K.; Hong, S. Applications of capacitive deionization: Desalination, softening, selective removal, and energy efficiency. *Desalination* **2019**, *449*, 118–130. [CrossRef]
573. Pawlowski, S.; Huertas, R.M.; Galinha, C.F.; Crespo, J.G.; Velizarov, S. On operation of reverse electrodialysis (RED) and membrane capacitive deionisation (MCDI) with natural saline streams: A critical review. *Desalination* **2020**, *476*, 114183. [CrossRef]
574. Folaranmi, G.; Bechelany, M.; Sistat, P.; Cretin, M.; Zaviska, F. Towards Electrochemical Water Desalination Techniques: A Review on Capacitive Deionization, Membrane Capacitive Deionization and Flow Capacitive Deionization. *Membranes* **2020**, *10*, 96. [CrossRef] [PubMed]
575. Zhou, Y.; Hu, C.; Liu, H.; Qu, J. Potassium-Ion Recovery with a Polypyrrole Membrane Electrode in Novel Redox Transistor Electrodialysis. *Environ. Sci. Technol.* **2020**, *54*, 4592–4600. [CrossRef]
576. Yang, E.; Chae, K.-J.; Choi, M.-J.; He, Z.; Kim, I.S. Critical review of bioelectrochemical systems integrated with membrane-based technologies for desalination, energy self-sufficiency, and high-efficiency water and wastewater treatment. *Desalination* **2019**, *452*, 40–67. [CrossRef]
577. Logan, B.E.; Rabaey, K. Conversion of wastes into bioelectricity and chemicals by using microbial electrochemical technologies. *Science* **2012**, *337*, 686–690. [CrossRef]
578. Srikanth, S.; Kumar, M.; Puri, S.K. Bio-electrochemical system (BES) as an innovative approach for sustainable waste management in petroleum industry. *Bioresour. Technol.* **2018**, *265*, 506–518. [CrossRef] [PubMed]
579. Wang, H.; Ren, Z.J. A comprehensive review of microbial electrochemical systems as a platform technology. *Biotechnol. Adv.* **2013**, *31*, 1796–1807. [CrossRef] [PubMed]
580. Cao, X.; Huang, X.; Liang, P.; Xiao, K.; Zhou, Y.; Zhang, X.; Logan, B.E. A new method for water desalination using microbial desalination cells. *Environ. Sci. Technol.* **2009**, *43*, 7148–7152. [CrossRef] [PubMed]
581. Saeed, H.M.; Husseini, G.A.; Yousef, S.; Saif, J.; Al-Asheh, S.; Abu Fara, A.; Azzam, S.; Khawaga, R.; Aidan, A. Microbial desalination cell technology: A review and a case study. *Desalination* **2015**, *359*, 1–13. [CrossRef]

582. Wang, Y.; Xu, A.; Cui, T.; Zhang, J.; Yu, H.; Han, W.; Shen, J.; Li, J.; Sun, X.; Wang, L. Construction and application of a 1-liter upflow-stacked microbial desalination cell. *Chemosphere* **2020**, *248*, 126028. [CrossRef] [PubMed]
583. Jafary, T.; Al-Mamun, A.; Alhimali, H.; Baawain, M.S.; Rahman, M.S.; Rahman, S.; Dhar, B.R.; Aghbashlo, M.; Tabatabaei, M. Enhanced power generation and desalination rate in a novel quadruple microbial desalination cell with a single desalination chamber. *Renew. Sustain. Energy Rev.* **2020**, *127*, 109855. [CrossRef]
584. Lan, J.; Ren, Y.; Lu, Y.; Liu, G.; Luo, H.; Zhang, R. Combined microbial desalination and chemical-production cell with Fenton process for treatment of electroplating wastewater nanofiltration concentrate. *Chem. Eng. J.* **2019**, *359*, 1139–1149. [CrossRef]
585. Li, X.; Jin, X.; Zhao, N.; Angelidaki, I.; Zhang, Y. Novel bio-electro-Fenton technology for azo dye wastewater treatment using microbial reverse-electrodialysis electrolysis cell. *Bioresour. Technol.* **2017**, *228*, 322–329. [CrossRef] [PubMed]
586. Kim, Y.; Logan, B.E. Microbial reverse electrodialysis cells for synergistically enhanced power production. *Environ. Sci. Technol.* **2011**, *45*, 5834–5839. [CrossRef]
587. Cusick, R.D.; Kim, Y.; Logan, B.E. Energy capture from thermolytic solutions in microbial reverse- electrodialysis cells. *Science* **2012**, *335*, 1474–1477. [CrossRef]